TRANSPORTATION RESEARCH
RECORD

No. 1303

Highway and Facility Design

Geometric Design Considerations 1991

A peer-reviewed publication of the Transportation Research Board

TRANSPORTATION RESEARCH BOARD
NATIONAL RESEARCH COUNCIL
WASHINGTON, D.C. 1991

Transportation Research Record 1303
Price: $20.00

Subscriber Category
IIA highway and facility design

TRB Publications Staff
Director of Publications: Nancy A. Ackerman
Senior Editor: Naomi C. Kassabian
Associate Editor: Alison G. Tobias
Assistant Editors: Luanne Crayton, Kathleen Solomon, Norman Solomon
Graphics Coordinator: Diane L. Ross
Production Coordinator: Karen S. Waugh
Office Manager: Phyllis D. Barber
Production Assistant: Betty L. Hawkins

Printed in the United States of America

Library of Congress Cataloging-in-Publication Data
National Research Council. Transportation Research Board.

Geometric design considerations, 1991.
p. cm.—(Transportation research record ; no. 1303)
Research papers from the 70th Annual Meeting of the Transportation Research Board held 1991 in Washington, D.C.
ISBN 0-309-05110-X
1. Roads—Design and construction. 2. Traffic engineering. I. National Research Council (U.S.). Transportation Research Board. Meeting (70th : 1991 : Washington, D.C.) II. Series: Transportation research record ; 1303.
TE7.H5 no. 1303
[TE175]
388 s—dc20
[625.7'25] 91-27382
CIP

Sponsorship of Transportation Research Record 1303

GROUP 2—DESIGN AND CONSTRUCTION OF TRANSPORTATION FACILITIES
Chairman: Raymond A. Forsyth, Sacramento, California

General Design Section
Chairman: Jarvis D. Michie, Dynatech Engineering Inc.

Committee on Geometric Design
Chairman: John C. Glennon, John C. Glennon Chartered
Secretary: George B. Pilkington II, Federal Highway Administration, U.S. Department of Transportation
James K. Cable, Paul D. Cribbins, William M. Dubose III, Daniel B. Fambro, Jerry L. Graham, Dennis A. Grylicki, David L. Guell, John C. Hayward, Milton L. Johnson, Frank J. Koepke, Ruediger Lamm, Joel P. Leisch, John M. Mason, Jr., John R. McLean, Thomas E. Meyer, Thomas E. Mulinazzi, Timothy R. Neuman, Abishai Polus, John L. Sanford, Seppo I. Sillan, Bob L. Smith, Peter R. Stefaniak, Jess E. Truby, Jr., Ross J. Walker, Keith M. Wolhuter, Joseph M. Yourno

GROUP 3—OPERATION, SAFETY, AND MAINTENANCE OF TRANSPORTATION FACILITIES
Chairman: H. Douglas Robertson, University of North Carolina–Charlotte

Facilities and Operations Section
Chairman: Lyle Saxton, Federal Highway Administration

Committee on Operational Effects of Geometrics
Chairman: Jerome W. Hall, University of New Mexico
Secretary: Douglas W. Harwood, Midwest Research Institute
Jack W. Anderson, Myung-Soon Chang, Ronald W. Eck, Daniel B. Fambro, Don Jay Gripne, Richard P. Kramer, Mark A. Marek, Robert P. Morris, Ronald C. Pfefer, Abishai Polus, Ramey O. Rogness, Rudolph Kenneth Shearin, Jr., Justin True, Daniel S. Turner, Stephen N. Van Winkle, Walter E. Witt, Paul H. Wright

Frank R. McCullagh and Richard A. Cunard, Transportation Research Board staff

Sponsorship is indicated by a footnote at the end of each paper. The organizational units, officers, and members are as of December 31, 1990.

Transportation Research Record 1303

Contents

Foreword

This Record contains 12 papers dealing with geometric design. Two papers deal with geometrics and trucks, four with sight distance, two with passing lanes, two with intersections, and two with design and safety.

Glauz and Harwood present research showing how the presence of superelevation contributes to offtracking of large trucks and also how truck body roll affects offtracking. Lamm et al. evaluate AASHTO's 1984 *Policy on Geometric Design of Highways and Streets* regarding the dynamic safety of driving for new design, redesign, and rehabilitation at curved sites. They concluded that interaction among three geometric criteria—achieving consistency in horizontal alignment, harmonizing design speed and operating speed, and providing adequate dynamic safety of driving—would improve overall safety. Easa derives the exact formulas that relate the available sight distance to the circular curve parameters, lateral clearance of the obstacle, its location along the curve, and the location of the observer and object. He also provides minimum sight distance and maximum lateral clearance values for a typical range of curve parameters, lateral clearances, and obstacle locations. Gattis discusses sight distance problems associated with residential streets in newer subdivisions, which often incorporate elements of discontinuity and curvilinear alignment.

In two papers, Easa develops sight distance models for unsymmetrical crest curves and unsymmetrical sag curves. May summarizes the results and conclusion of a research study concerned with traffic performance and design of passing lanes on two-lane, two-way rural highways. St. John and Harwood show how data on the speed profiles of trucks on sustained upgrades can be combined with safety estimates to quantify the increased accident rates due to slow-moving trucks and the changes in accident rates with distance up the grade.

Taylor and Jain use the simulation model TWOPAS to study the operational benefits gained by providing passing lanes on two-lane highways. Benekohal and Lee compare the cost-effectiveness of roadside versus road improvements on two-lane rural highways in Illinois by determining the accident reductions due to improvements on 17 resurfacing, restoration, and rehabilitation projects and comparing these to the improvement costs. The cost-effectiveness approach and benefit-cost analysis indicate that roadside and road improvements provided similar benefits.

Fitzpatrick identifies gap acceptance values at stop-controlled intersections available in the literature and from a field study for both truck and passenger car drivers. Poppe et al. evaluate the operation of the single-point diamond interchange (SPDI) through field data collected on 10 approaches at 3 interchanges. The data indicate that the large turning radii found at the SPDI tend to cause the left-turn movement to operate much like a through movement in terms of capacity and that long clearance intervals translate directly into increased cost time per cycle.

Superelevation and Body Roll Effects on Offtracking of Large Trucks

WILLIAM D. GLAUZ AND DOUGLAS W. HARWOOD

Past research has shown that vehicles, especially large trucks, offtrack on curves and turns; at low speeds the rear axles track inside the front axle (negative offtracking), and at sufficiently high speeds the reverse is true. New research shows that typical amounts of superelevation tend to increase low-speed, negative offtracking of trucks by 10 to 20 percent. Superelevation also tends to reduce the amount of high-speed outward offtracking. The magnitude of the superelevation effect is independent of speed. The superelevation effect is greater with more heavily loaded trucks, trucks with newer tires, and trucks with larger roll steer coefficients. This research also shows that body roll affects both high-speed offtracking and the superelevation contribution to total offtracking. Trucks with softer suspensions are more affected. The net effect is to increase outward offtracking at normal and high speeds and to slightly increase negative offtracking at very low speeds.

When any vehicle makes a turn, its rear wheels do not follow the same path as its front wheels. The magnitude of this difference in paths, known as offtracking, generally increases with the spacing between the axles of the vehicle and decreases for larger-radius turns. Offtracking of passenger cars is minimal because they have relatively short wheelbases; however, many trucks offtrack substantially. The most appropriate descriptor of offtracking for use in highway design is the "swept path width," shown in Figure 1 as the difference in paths between the outside front tractor tire and the inside rear trailer tire.

The AASHTO Green Book (*1,2*) notes two distinct types of offtracking: low-speed and high-speed. Low-speed offtracking is a purely geometrical phenomenon wherein the rear axles of a truck track toward the inside of a horizontal curve, relative to the front axle. Figure 1 illustrates low-speed offtracking. Because considerable research has been performed concerning low-speed offtracking, as a function of truck and roadway geometrics, it is well understood on level surfaces. However, pavement cross-slope, including superelevation on horizontal curves, has an effect on low-speed offtracking that has not been documented in previous research.

High-speed offtracking, on the other hand, is a dynamic, speed-dependent phenomenon. It is caused by the tendency of the rear of the vehicle to move outward because of the lateral acceleration of the vehicle as it negotiates a horizontal curve at higher speeds. High-speed offtracking is less well understood than low-speed offtracking; it is a function not only of truck and roadway geometrics, but also of the vehicle speed and the vehicle's suspension, tire, and loading characteristics.

Midwest Research Institute, 425 Volker Blvd., Kansas City, Mo. 64110.

Current AASHTO criteria for intersection and channelization geometrics and for pavement widening on horizontal curves consider only low-speed offtracking. The design of intersection and channelization geometrics is properly a function only of low-speed offtracking, because truck operations at intersections usually occur at low speeds. Pavement cross-slope effects on offtracking can generally be ignored in the design of intersection and channelization geometrics because normal pavement cross-slopes are small. Turning roadways at channelized intersections do not require much superelevation because operations there usually occur at low speeds. However, pavement widening at horizontal curves should consider both low-speed and high-speed offtracking, as well as superelevation effects.

LOW-SPEED OFFTRACKING WITHOUT SUPERELEVATION

Low-speed offtracking has been researched extensively and is considered in current AASHTO design criteria. An offtracking model for the Apple microcomputer was developed for FHWA in 1983 (*3*), and an IBM PC version of this model was subsequently developed (*4*). The user specifies the turning path to be followed by the front axles of the truck, and the models plot the path of the rear axle and other specified points on the truck. The Apple and IBM PC models provide plotted output but have no capability for numerical output. Recently the California Department of Transportation (Caltrans) enhanced the IBM PC version of the model to include numerical output of offtracking and swept path widths, as well as the turning plot (*5*). The Caltrans model runs on an IBM mainframe computer.

The Caltrans model was run as part of a recent study (*6*) to compare the offtracking performance of the design vehicles specified in Table 1. These vehicles are representative of those defined by the 1982 Surface Transportation Assistance Act (STAA). The offtracking performance of these vehicles was compared with those of a conventional tractor and 37-ft semitrailer (the AASHTO WB-50 design vehicle) and a conventional tractor and 45-ft semitrailer, the largest semitrailer in widespread use before the STAA.

As a truck proceeds into a 90-degree turn, the amount of offtracking increases (see Figure 1). As the truck negotiates the turn, the amount of offtracking reaches a maximum and then gradually decreases as the truck proceeds in the new direction. Figure 2 shows this maximum offtracking for various values of turn radius and total turning angle for the WB-50 design vehicle. Maximum offtracking does not continue to

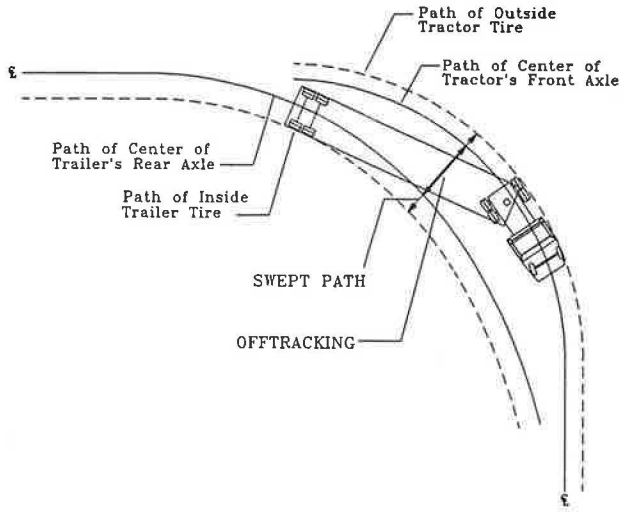

FIGURE 1 Swept path width and offtracking of a truck negotiating 90-degree intersection turn.

increase with turn angle, but reaches a constant value (becomes fully developed) after some angle that depends on the radius. For the WB-50, for example, at a turn radius of 100 ft, offtracking reaches about 6.5 ft for an angle of 90 degrees and does not increase further at larger angles, as shown in Figure 2. The turn angle required to fully develop offtracking is greater for smaller radii, and may exceed 180 degrees for very small radii.

The amount of offtracking depends most significantly on the distance between the kingpin and the center of the rear axles, which is dimension D in Table 1. The data shown in Figure 2, and elsewhere in this paper unless specified otherwise, assume that the rear axles are placed at the rear of the trailer, as indicated in Table 1. Many longer trailers are designed to allow these axles to be moved forward to decrease the low-speed offtracking. In fact, it is common for users of 53-ft trailers to slide the axles forward 5 ft, so their offtracking is essentially the same as the STAA single with a 48-ft trailer. Similar offtracking plots for the other design vehicles shown in Table 1 have been presented by Harwood et al. (*6*).

Swept path widths can be calculated directly by adding the effective truck width to the maximum offtracking values such as those shown in Figure 2. Because the Caltrans model calculates offtracking along the truck centerline and the swept path width is the difference in path between the front outside axle and the rear inside axle, the difference between offtracking and swept path width is one-half of the tractor axle width plus one-half of the rear trailer axle width. The front tractor axle is typically 6.66 ft wide, and the rear trailer axle is typically 8.5 ft wide, so half of their sum is 7.58 ft.

The maximum offtracking for all of the design vehicles considered for selected combinations of turn radius and turn angle is compared in Table 2. The data show that for the single-trailer configurations, the amount of offtracking increases nearly linearly with trailer length. For 90-degree turns, the offtracking of a 53-ft trailer, with axles in the furthest rear position, is almost double that of the WB-50 configuration. The offtracking of doubles is much less than that of STAA singles and is approximately the same as that of the WB-50.

MODEL FOR LOW-SPEED AND HIGH-SPEED OFFTRACKING INCLUDING SUPERELEVATION EFFECTS

Various models and formulas have been developed to estimate offtracking by trucks in turns so that turning plots, like

TABLE 1 DETAILED AXLE SPACINGS FOR LONGER DESIGN VEHICLES

Design vehicle	Dimension (ft)								
	A	B	C	D	E	F	G	H	Overall length
Single-unit truck	4.0	-	-	20.0	6.0	-	-	-	30.0
Single-trailer truck with 37-ft trailer (WB-50)	2.5	18.0	0.0-2.0	30.0	4.0	-	-	-	52.5-54.5
Single-trailer truck with 45-ft trailer	2.5	18.0	0.0-2.0	37.5	4.5	-	-	-	60.5-62.5
STAA single with 48-ft trailer and conventional tractor	2.5	18.0	0.0-2.0	40.5	4.5	-	-	-	63.5-65.5
STAA single with 48-ft trailer and long tractor	2.5	20.0	0.0-2.0	40.5	4.5	-	-	-	65.5-67.5
Long single with 53-ft trailer	2.5	18.0	0.0-2.0	45.5	4.5	-	-	-	68.5-70.5
STAA double with cab-over-engine tractor	2.5	10.0	0.0-2.0	22.5	2.5	6.0	22.5	2.5	66.5-68.5
STAA double with cab-behind-engine tractor	2.5	13.0	0.0-2.0	22.5	2.5	6.0	22.5	2.5	69.5-71.5

Note: Dimensions A through H are defined below.

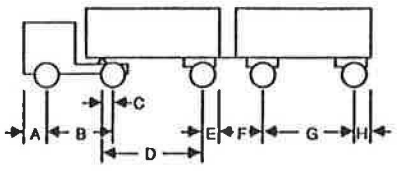

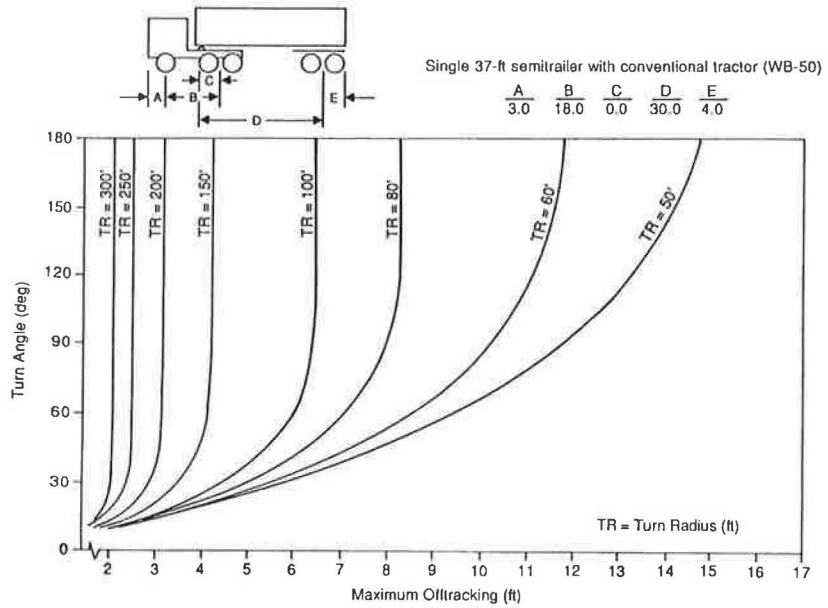

FIGURE 2 Offtracking plot for single 37-ft semitrailer truck with conventional tractor (WB-50).

TABLE 2 OFFTRACKING FOR SELECTED COMBINATIONS OF TURN RADIUS AND TURN ANGLE

	Maximum offtracking (ft)[a]								
Turn radius (ft)	50			100			300		
Turn angle:	60°	90°	120°	60°	90°	120°	60°	90°	120°
Single with 37-ft trailer (WB-50)	9.3	11.8	13.3	6.0	6.5	6.6	2.1	2.1	2.1
Single with 45-ft trailer	12.1	15.5	-	8.0	9.0	9.4	2.9	2.9	2.9
STAA single with 48-ft trailer and conventional tractor	13.0	16.9	-	8.8	10.0	10.5	3.3	3.3	3.3
STAA single with 48-ft trailer and long tractor	13.4	17.4	-	9.1	10.4	10.8	3.4	3.4	3.4
Long single with 53-ft trailer	14.4	19.5	23.4	10.3	12.1	12.8	4.1	4.1	4.1
STAA double with cab-over-engine tractor	9.2	11.3	12.6	5.8	6.1	6.2	1.9	1.9	1.9
STAA double with cab-behind-engine tractor	9.6	11.9	13.4	6.0	6.4	6.4	2.1	2.1	2.1

[a] Add 7.58 ft to entries in this table to get maximum swept path width.

Figure 1, need not be developed for every application. An early example is the Western Highway Institute (WHI) offtracking formula (*7*). Low-speed offtracking develops gradually as a truck traverses a turn, as shown in Figures 1 and 2. The WHI formula estimates the magnitude of fully developed low-speed offtracking, that is, the maximum offtracking that will occur for a given radius of turn if the turn angle is large enough.

In 1981, Bernard and Vanderploeg developed an offtracking model that includes both the low-speed and high-speed contributions to offtracking (*8*). However, their model applies only to vehicles on a level surface. The new model developed here extends the Bernard and Vanderploeg model by incorporating the added effect of superelevation on offtracking, as well as an explicit accounting for the roll of the truck body on its suspension relative to the axles. Both the Bernard and Vanderploeg model and the new model give values for fully developed offtracking. On shorter curves, the actual offtracking may be less than the fully developed offtracking indicated by turning templates (e.g., Figure 1) or computer models such as the Caltrans model (*5*).

The new model for offtracking of a second axle or axle set (i.e., tandem or triaxle), or hitch point, relative to a leading axle, and so forth, is

$$OT = -\frac{l^2}{R}\left[0.5 + \frac{\sum_i (a_i/l^2)}{n(1 + t/l)}\right] + \frac{lU^2}{R}\left[\frac{1}{\bar{C}_\alpha g(1 + t/l)} + S\right] - \frac{l\theta}{\bar{C}_\alpha(1 + t/l)} - Slg\theta \qquad (1)$$

where

OT = fully developed offtracking (ft), where offtracking to the inside of the turn is treated as negative, by convention;
l = distance between the two consecutive axles or centerlines of axle sets or hitch points (ft);
R = radius of curvature (ft);
a_i = distance from centerline of axle set to ith axle (ft) (for single axles, $a_1 = 0$; for tandem axles, $a_1 = a_2 = 2$ ft; for triaxles, $a_1 = a_3 = 2$ ft; $a_2 = 0$);
n = number of axles in set ($n = 1$ for single axle, $n = 2$ for tandem axle, $n = 3$ for triaxle);
t = pneumatic trail (ft) [for typical values, see Fancher et al. (*9*, p. 31)];
U = speed of vehicle (ft/sec);
g = acceleration of gravity (ft/sec^2) (equivalent to 32.2 ft/sec^2 or 9.8 m/sec^2);
$\overline{C}_\alpha$ = ratio of total cornering stiffness to total normal load (rad^{-1}) (see Equation 2);
S = roll steer angle (see Equation 3); and
θ = superelevation of curve (ft/ft).

All vehicle axle characteristics (a_i, n, t, $\overline{C}_\alpha$, and S) refer to the second axle set. The ratio of the total cornering stiffness to total normal load is determined as

$$\overline{C}_\alpha = \frac{n(C_\alpha/F_{zr})(F_{zr})(n_t)(57.296)}{W_a f} \tag{2}$$

where

C_α = cornering stiffness of tires (lb^{-1} deg^{-1}) [Fancher et al. (*9*, p. 29) indicate that C_α/F_{zr} is in the range from 0.1 to 0.2 deg^{-1}];
F_{zr} = rated load of tire (lb) [typical values are given by Fancher et al. (*9*, p. 27)];
n_t = number of tires per axle (usually four);
W_a = load (weight) carried by the tires for the axle set (lb); and
f = fraction of W_a supported by the suspension for the axle set ($W_a f$ is the sprung weight for the axle set).

The roll steer angle is determined as

$$S = \frac{M_a f s h}{k_r - M_a f g h} \tag{3}$$

where

$M_a f$ = sprung mass supported by axle set (lb-sec^2/ft) ($= W_a f/g$);
s = suspension roll steer coefficient (degrees of steer per degree of roll) [for typical values, see Fancher et al. (*9*, p. 66)];
k_r = composite roll stiffness for the axle set (ft-lb/rad) [for typical values, see Fancher et al. (*9*, p. 60); these values are given on a per-axle basis, so must be multiplied by n];
h = distance between load center of gravity and suspension roll center, $h_{CG} - h_{RC}$;
h_{CG} = height of center of gravity of load carried by the axle set (ft); and
h_{RC} = height of roll center of suspension system for the axle set (ft) [for typical values, see Fancher et al. (*9*, p. 65)].

Equation 1 consists of four terms. The first term represents the traditional low-speed offtracking, without superelevation. For a single axle ($a_i = 0$), the first term reduces to

$$OT = -\frac{0.5l^2}{R} \tag{4}$$

which is the WHI offtracking formula (*7*).

The second term in Equation 1 is the speed-dependent term and represents high-speed offtracking. The sign of the second term is positive, indicating that high-speed offtracking tends to offset the low-speed offtracking.

The third and fourth terms account for the effect of superelevation on offtracking. The third term represents the influence of the superelevation itself, and the fourth term is the contribution to offtracking of roll steer caused by the superelevation. The factor k_r accounts for the roll of the truck body and affects the second and fourth terms of the equation.

Equation 1 provides the offtracking for one axle, axle set, or hitch point relative to the preceding axle, axle set, or hitch point. To determine the offtracking for the entire vehicle, Equation 1 is applied successively to each pair of consecutive axles and the results are combined. Thus,

$$\text{Total } OT = \sum_j (X_j)(OT_j) \tag{5}$$

where

X_j = 1 for an axle or axle set,
X_j = -1 for a hitch point, and
OT_j = offtracking for axle, axle set, or hitch point determined from Equation 1.

The reason for the minus sign when the second "axle" is a hitch point is that it is normally located ahead of the axles it "follows," so all offsets are in the opposite direction to those given by the convention developed for Equation 1.

The derivation of this new offtracking model is presented in the next section. The following section examines the sensitivity of the offtracking model to typical ranges of the variables in Equations 1, 2, and 3.

DERIVATION OF OFFTRACKING MODEL

Several years ago, Bernard and Vanderploeg described the mathematics of offtracking, including both the commonly known low-speed offtracking and the less studied high-speed offtracking (*8*). They developed the basic equation of motion for a trailer as a function of the trailer characteristics and the motion of the hitch point. They then examined in detail the special case of most interest—the motion when the trailer is making a steady turn of radius R at speed U.

The present derivation follows that of Bernard and Vanderploeg, but is limited to the special case of constant R and U. However, it incorporates two added features. First, it explicitly includes the effects of superelevation. The superelevation directly reduces high-speed offtracking and interacts

with the roll steer behavior of the vehicle. Second, roll of the body of the trailer relative to the axles also contributes to roll steer. This derivation uses the basic nomenclature and derivation of Bernard and Vanderploeg, but with the noted changes. A fuller presentation has been given by Harwood et al. (*6*).

Figure 3 is a schematic of a trailer with its hitch point traveling at speed U on a circular path of radius R. The center of gravity of the trailer is a distance c from the hitch point, along the trailer centerline. From Figure 3, applying Newton's second law in the direction perpendicular to the trailer centerline gives

$$M(A_y) = H_f + \sum_i F_{ri} \tag{6}$$

where

M = trailer mass,
A_y = lateral acceleration,
H_f = lateral force on the trailer at hinge point, and
F_{ri} = lateral force at the tires on axle i.

From Figure 4

$$\sum_i F_{ri} = \sum_i F_{fi} \cos \theta + \sum_i F_{ni} \sin \theta \tag{7}$$

where $\Sigma_i F_{ri}$ is the horizontal component of the tire/pavement forces. The superelevation angle is θ. Also from Figure 4, summing forces in the vertical direction yields

$$\sum_i F_{ni} \cos \theta = \sum_i W_i + \sum_i F_{fi} \sin \theta \tag{8}$$

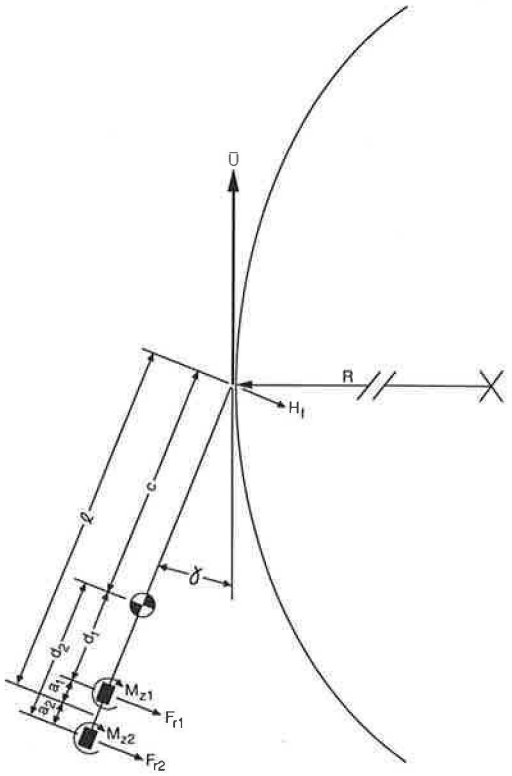

FIGURE 3 Forces and moments on trailer.

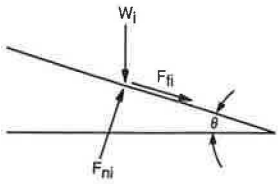

FIGURE 4 Tire/pavement forces with superelevation.

where W_i is the portion of the trailer weight on the tires of axle i. Eliminating $\Sigma_i F_{ni}$ between Equations 7 and 8 yields

$$\sum_i F_{ri} = \sum_i F_{fi} \cos \theta + \left(\sum_i W_i + \sum_i F_{fi} \sin \theta \right) \tan \theta \tag{9}$$

Next, consider the sum of moments in the horizontal plane about the trailer CG:

$$I(\dot{r} + \ddot{\gamma}) = H_f(c) - \sum_i F_{ri}(d_i) + \sum_i M_{zi} \tag{10}$$

where

I = trailer moment of inertia about its CG,
r = rotation rate of the velocity vector, $\overline{U}$, and
γ = angle between the trailer centerline and the velocity vector. (Note: $\dot{\gamma}$ and $\ddot{\gamma}$ are the first and second time derivatives, respectively, of γ, and $\dot{r}$ is the time derivative of r.)

The side friction force, F_{fi}, and aligning moment, M_{zi}, are defined by $F_{fi} = -C_{\alpha i}(\alpha_i)$ and $M_{zi} = K_i(\alpha_i)$, respectively. $C_{\alpha i}$ is the combined cornering stiffness for the tires on axle i, K_i is the combined aligning moment for those tires, and α_i is the slip angle [angle between the direction of motion of the trailer ($\overline{U}$) and the plane of the tire]. This can be shown to be (*8*)

$$\tan \alpha_i = -\tan \delta_i - \tan \gamma - \frac{(l + a_i)(r + \dot{\gamma})}{U \cos \gamma} \tag{11}$$

where δ_i is the steer angle of the axle (Figure 5).

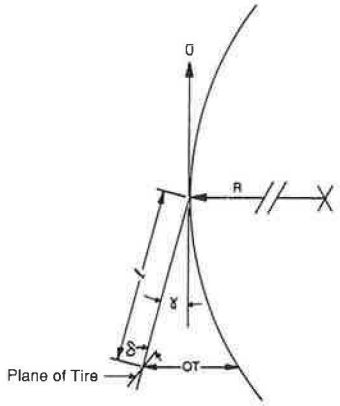

FIGURE 5 Slip and steer angles.

The lateral acceleration of the trailer CG is

$$A_y = Ur\cos\gamma - (\dot{r} + \ddot{\gamma})c \tag{12}$$

When the trailer tends to roll on its suspension, the rolling forces cause the tires to rotate (steer) slightly about a vertical axis. As such, they no longer track in the same direction as the axis of the trailer, as indicated in Figure 5. The amount of this steering depends on the rolling moment and the suspension characteristics.

Figure 6 shows the roll angle, ϕ, of the trailer negotiating a curve with superelevation, θ. The roll center (RC in Figure 6) is the point in space about which the trailer rolls. It is located a distance h below the center of gravity of the portion of the trailer $M_a f$ supported by the suspension. (M_a is the trailer mass supported by the tires of the axle set; f is the fraction that is suspended.) Now, summing moments about the roll center and making the usual small angle assumptions for θ and ϕ (e.g., $\sin\theta \simeq \theta$, $\cos\theta \simeq 1$), yields

$$\phi = M_a f h(A_y - g\theta)/(k_r - M_a f g h) \tag{13}$$

where k_r, the roll stiffness, is a property of the trailer suspension; $k_r\phi$ is the suspension-created restoring moment (clockwise in Figure 6). Then the steer angle, δ_i, is (by definition of s_i), $\delta_i = -s_i\phi$, where s_i is the suspension's roll steer coefficient. If we define

$$S_i \equiv M_a f s_i h/(k_r - M_a f g h) \tag{14}$$

then

$$\delta_i = -S_i(A_y - g\theta) \tag{15}$$

This equation compares with Bernard and Vanderploeg's equation (A-7) (*8*) except for the inclusion of the $g\theta$ term to denote the superelevation and a more inclusive definition of S_i to explicitly include the fact that the roll offsets the CG of the trailer, thus negating some of the suspension restoring moment.

Next, for a constant speed and radius turn, $\dot{r} = \dot{\gamma} = \ddot{\gamma} = 0$. Using Equations 6, 12, and 9 in Equation 10; using Equation 11 for α_i; noting from Figure 3 that $c + d_i = l + a_i$; and making the customary small angle assumptions for θ yields

$$\begin{aligned}\gamma = {} & \frac{cMUr}{\sum_i [C_{\alpha_i}(l + a_i) + K_i]} \\ & - \frac{r}{U}\frac{\sum_i [C_{\alpha_i}(l + a_i) + K_i](l + a_i)}{\sum_i [C_{\alpha_i}(l + a_i) + K_i]} \\ & - \frac{\sum_i [C_{\alpha_i}(l + a_i) + K_i]\delta_i}{\sum_i [c_{\alpha_i}(l + a_i) + K_i]} - \frac{\sum_i W_i(l + a_i)}{\sum_i [c_{\alpha_i}(l + a_i) + K_i]}\end{aligned} \tag{16}$$

At this point we simplify by setting all $K_i = K$, all $C_{\alpha_i} = C_\alpha$, and $W_i = W_a/n$, where n is the number of axles in the axle set and W_a is the total load on all tires of the axle set. We note that $\Sigma\alpha_i = 0$ and that $W_a = (c/l)Mg$ because some of the weight is carried by the hinge point. We also define the pneumatic trail t as K/C_α, and C_α as $nC_\alpha n_t/W_a f$. The number of tires per axle, n_t, is introduced because C_α is usually given on a per-tire basis. Finally, noting that for a steady turn the rotation rate r is U/R, Equation 16 becomes

$$\begin{aligned}\gamma = {} & -\frac{l}{R}\left[1 + \frac{\sum_i (a_i/l)^2}{n(1 + t/l)}\right] \\ & + \frac{U^2}{R}\left[\frac{1}{\bar{C}_\alpha g(+t/l)} + S\right] - S_g\theta - \frac{\theta}{\bar{C}_\alpha(1 + t/l)}\end{aligned} \tag{17}$$

where the definition of S_i in Equation 14 has also been used, and all $S_i = S$. Finally, defining the offtracking distance, OT, as $l\gamma + l^2/2R$ (see Figure 5), Equation 1 evolves.

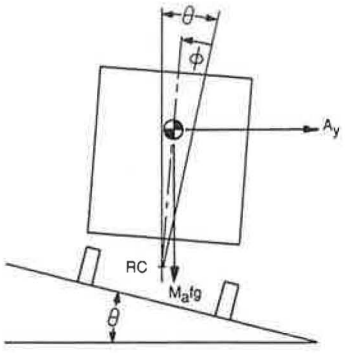

FIGURE 6 Trailer roll with superelevation.

SENSITIVITY OF OFFTRACKING TO TRUCK CHARACTERISTICS

Sensitivity analyses were conducted to determine the sensitivity of offtracking to truck characteristics using the new offtracking model. The sensitivity analyses used a simple computer program to exercise the model given by Equations 1, 2, and 3. The truck used for the sensitivity analyses was the STAA single with 48-ft trailer and conventional tractor described in Table 1. Both empty and loaded trucks were considered. The typical axle spacings, axle loads, and CG height assumed for empty and loaded trucks are given in Table 3. Table 4 shows both typical values and typical ranges for the other truck parameters in the offtracking model (*9*).

Vehicle Speed and Superelevation

Table 5 illustrates the sensitivity of offtracking to vehicle speed and superelevation for the loaded truck documented in Table 3 using the typical truck parameters presented in Table 4. The values in Table 5 are for a truck on a 500-ft (150-m) radius; shorter-radius turns, such as those made at intersections, are not addressed in this sensitivity analysis because

TABLE 3 ASSUMED CHARACTERISTICS FOR LOADED AND EMPTY TRUCKS USED IN OFFTRACKING SENSITIVITY ANALYSES

	Tractor drive axle		Rear trailer axle	
Parameter				
Type of axle set	Tandem (n = 2)		Tandem (n = 2)	
Distance from previous axle (ℓ) (ft)	18.0[a]		40.5[a]	
	Empty	Loaded	Empty	Loaded
Load (weight) carried by suspension for the axle set (W) (lb)	11,500	30,000	5,000	30,000
Height of center of gravity (in)	51	71.4	60	80

[a] Values of dimensions B and D for STAA 48-ft trailer truck from Table 1. Dimension C (fifth wheel offset) is assumed to be zero.

TABLE 4 TYPICAL VALUES OF PARAMETERS FOR OFFTRACKING MODEL (*8*)

Parameter	Typical value	Typical range
Cornering coefficient (C_a/F_{zr})	0.15 deg^{-1}	0.12 to 0.19
Rated load of tire (F_{zr})	6,040 lb for radial tires 5,150 lb for bias ply tires	
Number of tires per axle	4	2 to 4
Pneumatic trail (t)	0.179 ft	0.15 to 0.23
Suspension roll steer coefficient (s) (degrees of steer per degree of roll)	0.18	-0.04 to 0.213
Composite roll stiffness (k_r), per axle	0.158 x 10^6 in-lb/deg	0.070 to 0.165 x 10^6
Height of roll center (h_{RC})	22 in	21 to 33

speeds are lower and superelevation is less common for such turns. The 60-mph values in Table 5 are presented for illustrative purposes only; in accordance with AASHTO policies, the design speed for a 500-ft radius curve is less than 60 mph. For example, with a maximum superelevation of 0.06, a 500-ft radius curve would have a design speed of about 40 mph.

The data in Table 5 verify that the traditional low-speed component of offtracking, as defined, does not vary with either speed or superelevation. It is a function solely of the truck characteristics and the turning path. The negative sign of the low-speed offtracking component indicates that the rear trailer axle tracks inside the tractor steering axle. The value of the low-speed offtracking component, −1.98 ft, represents the maximum offtracking that could occur on a 500-ft radius curve (without superelevation) that is long enough for offtracking to fully develop; the Caltrans model could be used to determine the actual offtracking for any curve that is too short to develop that maximum.

Table 5 shows that because the high-speed component of offtracking increases with the square of speed, its value at 40

TABLE 5 COMPONENTS OF TOTAL OFFTRACKING ON 500-ft RADIUS CURVE

Truck speed (mi/h)	Superelevation (ft/ft)	Offtracking (ft)			
		Low-speed component	High-speed component	Superelevation component	Total
20	0.00	-1.98	0.28	0.00	-1.70
	0.02	-1.98	0.28	-0.10	-1.80
	0.04	-1.98	0.28	-0.21	-1.91
	0.06	-1.98	0.28	-0.31	-2.02
	0.08	-1.98	0.28	-0.43	-2.12
	0.10	-1.98	0.28	-0.53	-2.23
40	0.00	-1.98	1.13	0.00	-0.85
	0.02	-1.98	1.13	-0.10	-0.96
	0.04	-1.98	1.13	-0.21	-1.07
	0.06	-1.98	1.13	-0.31	-1.17
	0.08	-1.98	1.13	-0.43	-1.28
	0.10	-1.98	1.13	-0.53	-1.38
60	0.00	-1.98	2.53	0.00	0.55
	0.02	-1.98	2.53	-0.10	0.45
	0.04	-1.98	2.53	-0.21	0.34
	0.06	-1.98	2.53	-0.31	0.24
	0.08	-1.98	2.53	-0.43	0.13
	0.10	-1.98	2.53	-0.53	0.03

mph is four times its value at 20 mph. The positive sign of the high-speed offtracking term shows that it is in the opposite sense to the low-speed offtracking term, tending to move the rear trailer axle toward the outside of the turn. For the specific truck and radius of curvature shown in Table 5, the low-speed and high-speed offtracking terms would completely offset one another on a level surface (i.e., with no superelevation). At that speed, the rear trailer axle would exactly follow the tractor steering axle and there would be no offtracking. At higher speeds, the rear trailer axle would track outside the tractor steering axle. The values of the high-speed component of offtracking represent fully developed or steady state offtracking. However, there is no information in the literature about how the high-speed component develops as a truck enters a turn. This issue could be investigated with a computer simulation model of vehicle dynamics, such as the Phase-4 model (*10*).

Table 5 also shows that the effect of superelevation on offtracking increases linearly with the magnitude of the cross-slope and that this component of offtracking is in the same direction as the low-speed component. In addition, this superelevation effect is independent of speed, so it would contribute to offtracking in low-speed turns at intersections, as well as high-speed turns on horizontal curves, whenever there is a pavement cross-slope. Thus, the effect of superelevation is to increase the inside offtracking at low speeds and to reduce the outside offtracking at high speeds. This superelevation effect represents the fully developed offtracking. No information is available about how the superelevation effect develops as a truck enters a turn.

Empty Versus Loaded

The loading of a truck has an important effect on offtracking, which was investigated in a sensitivity analysis for standard test conditions, including a 500-ft radius curve with superelevation of 0.060, a truck travel speed of 40 mph, and the typical values of truck parameters given in Table 4. The analysis considered the empty and loaded conditions shown in Table 3. The added load does not affect the low-speed component of offtracking, but strongly increases the high-speed component and the (negative) superelevation component. The $1/\overline{C}_\alpha$ term is proportional to the axle load, and S is nearly so. The loaded condition has offtracking of -1.17 ft, as shown in Table 5. The empty or unloaded condition has offtracking of -1.80 ft. Thus, empty trucks have greater negative offtracking than loaded trucks.

Further sensitivity analyses for empty and loaded trucks were conducted using the standard test conditions and varying

the truck parameters in Table 4 one at a time over their typical ranges. The results are presented in Table 6.

Cornering Coefficient

The cornering coefficient (C_α/F_{zr} in Equation 2) is the ratio of the cornering stiffness to the rated load of the tire. The offtracking estimates in Table 5 were made using a cornering coefficient of 0.15 deg^{-1}, which represents a typical new radial tire. Cornering coefficients for radial tires typically range from 0.12 to 0.19 deg^{-1} depending on the tire model and the degree of wear (*9*).

The cornering coefficient has only a modest effect on offtracking. Increasing the cornering coefficient increases negative offtracking. Over the range from 0.12 to 0.19 deg^{-1}, total offtracking varies by only 0.07 ft for an empty truck and by 0.30 ft for a loaded truck for the defined standard test conditions. As tires wear, their cornering coefficient increases, causing the net offtracking to be more negative.

Rated Load of Tire

Variations over the typical range of rated load of the tires have very little effect on offtracking. Bias-ply tires have lower rated loads than radial tires and reduce negative offtracking by 0.03 ft for empty trucks and by 0.11 ft for loaded trucks. For all practical purposes, the rated load of the tire could be set to a constant value of 6,040 lb in the investigation of offtracking on horizontal curves.

Pneumatic Trail

The pneumatic trail of the tire determines the magnitude of the steering moment that is applied to the tire during cornering (*10*). Although the pneumatic trail theoretically influences offtracking (see Equation 1), this influence is so small—less than 0.01 ft for the standard test conditions—that for all practical purposes the pneumatic trail can be treated as a constant.

Suspension Roll Steer Coefficient

The suspension roll steer coefficient (degrees of roll per degree of steer) has very little effect on offtracking for empty trucks and has a moderately important effect for loaded trucks. An increase in the roll steer coefficient decreases the amount of negative offtracking. For the standard test conditions, variation of the roll steer coefficient over its typical range from −0.04 to 0.23 results in a variation in offtracking of 0.05 ft for empty trucks and 0.23 ft for loaded trucks.

Composite Roll Stiffness

The composite roll stiffness of a truck suspension system represents the relationship between the suspension roll angle and the restoring moment that tends to keep the truck body from rolling further. Increases in the composite roll stiffness result in increases in negative offtracking. For the standard test conditions, variation of the composite roll stiffness over its typical range, from 0.165 to 0.070 million in.-lb/deg, results in an increase in positive offtracking of 0.05 ft for empty trucks and 0.27 ft for loaded trucks. Thus, composite roll stiffness has a very small effect on offtracking for empty trucks and a moderate effect for loaded trucks.

Height of Roll Center

The height of the roll center has very little effect on offtracking over its typical range of variation. Negative offtracking in-

TABLE 6 OFFTRACKING RESULTS FROM SENSITIVITY ANALYSES

	Offtracking (ft)[a]			
	Empty truck		Loaded truck	
Parameter	High value	Low value	High value	Low value
Cornering coef.	-1.83	-1.76	-1.31	-1.01
Rated tire load	-1.80	-1.77	-1.17	-1.06
Pneumatic trail	-1.80	-1.80	-1.17	-1.17
Roll steer coef.	-1.79	-1.84	-1.14	-1.37
Roll stiffness	-1.80	-1.75	-1.18	-0.91
Roll center ht.	-1.80	-1.80	-1.21	-1.17
No. of axles[b]	-1.80	-1.53	-1.17	-0.48

[a] For 48 ft STAA semitrailer truck on 500 ft radius turn with 6 percent superelevation, at 40 mi/h.

[b] For 1 axle on rear of tractor and on trailer, truck weights and roll stiffnesses reduced appropriately.

creases as the roll center is raised. For the standard test conditions, variation in the height of the roll center from 21 to 33 in. changes offtracking by less than 0.01 ft for empty trucks and by 0.04 ft for loaded trucks. For all practical purposes, the height of the roll center can be set as a constant at its typical value of 22 in.

Number of Axles

The effect on offtracking of n, the number of axles, can be realistically addressed only by varying several related parameters. If the tractor and trailer have only one rear axle instead of two, the supported weight must be reduced in accordance with rated tire load and bridge-formula axle loads. The analysis used a maximum load of 20,000 lb on these axles. Also, the roll stiffness is generally much less for a single-axle suspension; 0.070×10^6 in.-lb/deg was used.

As shown in Table 6, the single-axle drive and trailer combination has significantly less negative offtracking than the tandem axle combination. This is primarily because the high-speed component is greater for the single-axle combination. This truck type will thus generate positive (outside) offtracking at lower speeds than tandem axle combinations.

CONCLUSIONS

The offtracking of vehicles, especially large trucks, is noticeably affected by the superelevation of the curve that the vehicle is traversing. This effect is proportional to the amount of superelevation and is independent of the vehicle speed.

At low speeds, the vehicle offtracking to the inside of the curve is made larger by the presence of superelevation. For a tractor with a 48-ft trailer, the low-speed offtracking on a 500-ft radius turn is increased by 20 percent with a superelevation of 8 percent. At high speed, where a truck might exhibit offtracking to the outside of the curve, the amount of offtracking is reduced or even canceled in the presence of superelevation.

The superelevation effect is dependent on the weight of the truck, the tire cornering coefficient, and the roll steer coefficient. Superelevation influences loaded trucks more than empty trucks; the effect is nearly proportional to the truck weight. The offtracking of trucks with worn tires, which have larger cornering coefficients, is less influenced by superelevation, especially at higher weights. Trucks with larger roll steer coefficients are more influenced by superelevation, although the effect is less than the opposite, high-speed effect, which is also a function of the roll steer coefficient.

A truck's suspension allows the truck body to roll toward the outside of the curve, relative to the axles. This body roll increases the high-speed offtracking. The amount of the increase depends on the stiffness of the suspension, being greater with softer suspensions, heavier loads, and larger roll steer coefficients. This body roll also increases (negatively) the amount of superelevation-related offtracking, although this effect is not as large as the high-speed effect. For a tractor with a 48-ft trailer traveling at 40 mph on a 500-ft radius turn with a 6 percent superelevation, the net effect on offtracking can be as much as +0.27 ft for a realistically rigid suspension.

Finally, it was found that lighter tractor-semitrailers, with only a single drive axle and trailer axle, are more subject to high-speed offtracking than heavier trucks when both are loaded close to their capacities.

ACKNOWLEDGMENTS

The work reported in this paper was conducted under the sponsorship of FHWA. The authors gratefully acknowledge the assistance provided by the California Department of Transportation in applying their offtracking model to the design vehicles presented in this paper, and the review and comments provided by Andrew D. St. John.

REFERENCES

1. *A Policy on Geometric Design for Highways and Streets.* AASHTO, Washington, D.C., 1984.
2. *A Policy on Geometric Design for Highways and Streets.* AASHTO, Washington, D.C., 1990.
3. M. Sayers. *FHWA/UMTRI Vehicle Offtracking Model and Computer Simulation—User's Guide, Version 1.00.* University of Michigan Transportation Research Institute, Ann Arbor, June 1984.
4. Analysis Group, Inc. *FHWA Vehicle Offtracking Model—IBM PC Version 1.0: Program Documentation and User's Guide.* FHWA, U.S. Department of Transportation, July 20, 1986.
5. *Truck Offtracking Model, Program Documentation and User's Guide.* Division of Transportation Planning, California Department of Transportation, Sacramento, 1985.
6. D. W. Harwood, J. M. Mason, W. D. Glauz, B. T. Kulakowski, and K. Fitzpatrick. *Truck Characteristics for Use in Highway Design and Operation.* Reports FHWA-RD-89-226 and -227, FHWA, U.S. Department of Transportation, Dec. 1989.
7. *Offtracking Characteristics of Trucks and Truck Combinations.* Research Committee Report No. 3. Western Highway Institute, San Bruno, Calif., Feb. 1970.
8. J. E. Bernard and M. Vanderploeg. *Static and Dynamic Offtracking of Articulated Vehicles.* Paper 800151. SAE, Warrendale, Pa., 1981.
9. P. S. Fancher, R. D. Ervin, C. B. Winkler, and T. D. Gillespie. *A Factbook of the Mechanical Properties of the Components of Single Unit and Articulated Heavy Vehicles.* Report DOT HS 807 125. NHTSA, U.S. Department of Transportation, Dec. 1986.
10. C. C. MacAdam, P. S. Fancher, G. T. Hu, and T. D. Gillespie. *A Computerized Dynamics Model of Trucks, Tractor Semi-Trailers, Doubles, and Triples Combinations.* Report UM-HSRI-80-58. Highway Safety Research Institute, University of Michigan, Ann Arbor, Sept. 1980.

The findings and conclusions in the paper are those of the authors and do not necessarily represent the views of FHWA.

Publication of this paper sponsored by Committee on Operational Effects of Geometrics.

Side Friction Demand Versus Side Friction Assumed for Curve Design on Two-Lane Rural Highways

RUEDIGER LAMM, ELIAS CHOUEIRI, AND THEODORE MAILAENDER

With the objective of exploring whether AASHTO's existing *Policy on Geometric Design of Highways and Streets* provides adequate dynamic safety of driving for new designs, redesigns, and rehabilitation strategies at curved sites, side friction factors on curved sections of two-lane rural highways were investigated. The study was based on geometric design, operating speed, and accident data for 197 curved roadway sections in New York State. To achieve this objective, a comparative analysis of side friction demand versus side friction assumed was carried out. With respect to the independent variable degree of curve, it was determined that (a) friction increases as degree of curve increases; (b) side friction assumed is higher than side friction demand on curves up to about 6.5 degrees; (c) for curves greater than 6.5 degrees, side friction demand is higher than side friction assumed; and (d) the gap between friction assumed and demand increases with increasing degree of curve. With respect to the independent variable operating speed, it was determined that (a) friction decreases as operating speed increases; (b) side friction assumed is lower than side friction demand up to operating speeds of 50 mph; (c) the gap between side friction assumed and demand increases with decreasing operating speeds; and (d) for operating speeds greater than 50 mph, side friction assumed is higher than side friction demand. With respect to the independent variable accident rate, it was determined that (a) side friction demand begins to exceed side friction assumed when the accident rate is about six or seven accidents per million vehicle-miles and (b) the gap between side friction assumed and demand increases with increasing accident rates. In general, analyses indicated that, especially in the lower design speed classes, which are combined with higher maximum allowable degree of curve classes, there exists the possibility that (a) friction demand exceeds friction assumed and (b) a high accident risk results, because at lower design speed levels the danger exists that design speeds and operating speeds are not well balanced. Thus, it is apparent that driving dynamic safety aspects have an important impact on geometric design, operating speed, and accident experience on curved roadway sections of two-lane rural highways.

One of the main safety goals in developing recommendations for the design of rural highways is the enhancement of traffic safety by increasing friction supply wherever possible.

A study of accidents on curved roadway sections in New York State (*1*) determined that

1. More than 70 percent of accidents on curves were fatal or injury accidents;
2. About 50 percent of accidents on curves were the result of wet or icy road conditions even though vehicle mileage driven under these conditions is far lower than that on dry pavements; and
3. About 65 percent of accidents on curves were single-vehicle accidents, mostly run-off-the-road accidents.

In summary, the study (*1*) concluded that a high risk of fatal or injury accidents does exist on curves, especially on wet or icy road surfaces and at night, with an accident type represented mainly by run-off-the-road accidents.

In this connection, the safety considerations of most countries are centered on improving highway geometric characteristics, not on improving skid resistance (tangential and side friction factors), although sufficient friction supply had been reported to be an important safety issue (*2*).

Several research investigations have indicated that skid resistance (friction) should be a main safety consideration in designing, redesigning, or resurfacing roadways (*3,4*). For instance, Brinkman (*3*) found that resurfacing alone did not have a significant effect on the mean skid number. He indicated that skid resistance should be a main safety issue. Glennon et al. (*4*) argued that accident studies indicate that pavement skid resistance is a safety consideration. They indicated that the probability of a highway curve becoming an accident black spot increases with decreasing pavement skid resistance. This finding supports the recommendation that the AASHTO policy should more clearly delineate the need for providing adequate friction between tire and roadway surface, for example, as on highway curves.

The upward trend of vehicle speeds and traffic densities will undoubtedly continue throughout this decade, and the skidding problem will become more serious, potentially becoming a major limitation to safe high-speed travel, especially on wet two-lane rural highways (*5*).

The objective of this research was to explore whether AASHTO's 1984 *Policy on Geometric Design of Highways and Streets* (*6*), provides adequate dynamic safety of driving for new designs, redesigns, and rehabilitation strategies at curved sites.

REVIEW

Research studies conducted during the past two decades have shown that highway geometric designs should address three design issues in order to gain direct or indirect safety advan-

R. Lamm, Institute of Highway and Railroad Engineering, University of Karlsruhe, D-7500 Karlsruhe 1, Kaiserstrasse 12, Federal Republic of Germany. E. Choueiri, North Country Community College, Route 1, Box 12, Potsdam, N.Y. 13676. T. Mailaender, Mailaender Ingenieur Consultant, D-7500 Karlsruhe 1, Mathystrasse 13, Federal Republic of Germany.

tages. These issues are (1) achieving consistency in horizontal alignment; (2) harmonizing design speed and operating speed, especially on wet pavements; and (3) providing adequate dynamic safety of driving (*7–14*).

Criteria 1 and 2 have been the subject of several reports, publications, and presentations (*1,15–23*). These investigations included (a) processes for evaluating horizontal design consistency and inconsistency, (b) processes for evaluating design speed and operating speed differences, (c) relationships between geometric design parameters and operating speeds and/or accident rates, and (d) recommendations for achieving good and fair design practices, as well as recommendations for detecting poor designs (see Table 1).

For example, Figure 1 shows the relationships between degree of curve and operating speeds, as well as between degree of curve and accidents rates for individual lane widths, as derived from the analysis of data on 322 two-lane rural highway sections in New York State (*15*). The studies demonstrated that (a) the most successful parameter in explaining much of the variability in operating speeds and accident rates was degree of curve, and (b) the relationship between degree of curve and operating speed is valid for both dry and wet pavements, as long as visibility is not appreciably affected by heavy rain (*24*).

Criterion 3 was the subject of a comparative analysis of tangential and side friction factors in the highway design

TABLE 1 RECOMMENDED RANGES FOR GOOD, FAIR, AND POOR DESIGN PRACTICES BETWEEN SUCCESSIVE DESIGN ELEMENTS (*15,16,20,22*)

CONSISTENCY CRITERIA

CASE 1 (GOOD DESIGN):
Range of change in degree of curve: $\Delta DC \leq 5^{o}$.
Range of change in operating speed: $\Delta V85 \leq 6$ mph (10km/h).
For these road sections, consistency in horizontal alignment exists between successive design elements, and the horizontal alignment does not create inconsistencies in vehicle operating speeds.

CASE 2 (FAIR DESIGN):
Range of change in degree of curve: $5^{o} < \Delta DC \leq 10^{o}$.
Range of change in operating speed: 6 mph < $\Delta V85 \leq 12$ mph (20 km/h).
These road sections may represent at least minor inconsistencies in geometric design between successive design elements. Normally, they would warrant traffic warning devices, but no redesigns.

CASE 3 (POOR DESIGN):
Range of change in degree of curve: $\Delta DC > 10^{o}$.
Range of change in operating speed: $\Delta V85 > 12$ mph (20km/h).
These road sections have strong inconsistencies horizontal geometric design between successive design elements combined with those breaks in the speed profile that may lead to critical driving maneuvers. Normally redesigns are recommended.

DESIGN SPEED CRITERIA

CASE 1 (GOOD DESIGN):

$V85 - V_d^* \leq 6$ mph (10 km/h).
No adaptions or corrections are necessary.

CASE 2 (FAIR DESIGN):

$6 \text{ mph} < V85 - V_d \leq 12$ mph (20 km/h).
Superelevation rates and stopping sight distances must be related to V85 to ensure that friction assumed will accomodate to friction demand.

CASE 3 (POOR DESIGN):

$V85 - V_d > 12$ mph (20 km/h).
Normally redesigns are recommended.

$^*V_d$ = Design Speed

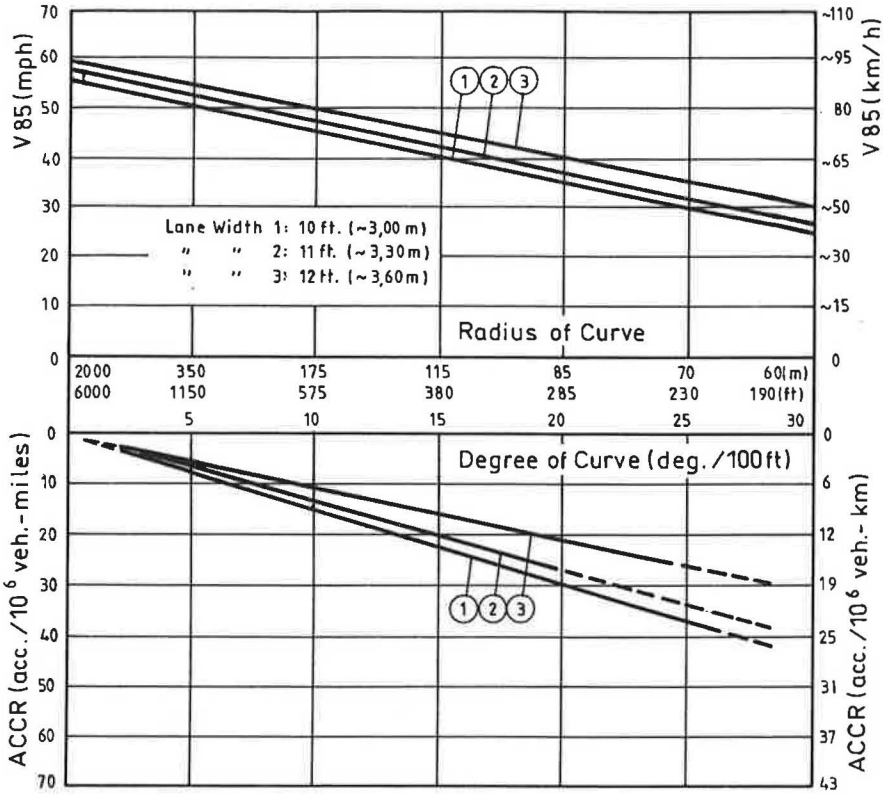

FIGURE 1 Nomogram for evaluating operating speeds and accident rates as related to degree of curve (radius of curve) for individual lane widths.

guidelines of four Western European countries—Federal Republic of Germany, France, Sweden, and Switzerland—and the United States, which (a) determined the type of the relationships that exist between friction factors and design speed and (b) developed overall relationships between friction factors and design speed. The resulting overall relationships were then compared to actual pavement friction inventories in New York State and the Federal Republic of Germany (*25,26*). Analyses indicated that the friction factors derived from the New York 95th-percentile level distribution curve (that is, 95 percent of wet pavements could be covered by using the 95th-percentile level distribution curve as a driving dynamic basis for design purposes) coincided with the friction factors derived from the German 95th-percentile level distribution curve (see Figure 2). Based on these results, recommendations were provided for minimum stopping sight distances and minimum radii of curve (*26*). It is estimated that by applying the proposed tangential and side friction factors, 95 percent of wet pavements will be covered in the United States and Europe. In this respect, Figure 2 shows the maximum allowable side friction factors versus design speed for AASHTO (*6*), AASHO (*27*), and the German Design Standard (*12*) and the overall relationship recommended by Lamm et al. (*26*). This figure clearly indicates that AASHO/AASHTO values exceed the recommended values already at design speeds $V_d \geq 30$ mph.

In contrast to the design friction factors of AASHO/AASHTO (*6,27*), using lower maximum allowable friction factors will certainly lead to a higher driving dynamic safety supply and could reduce the number and severity of accidents. It will also support maintenance personnel by easing the problems of maintaining high tangential and side friction factors for lower design speed classes where operating speeds often exceed design speeds decisively. Therefore, new designs, redesigns, and rehabilitation strategies are recommended to relate minimum stopping sight distances and minimum radii of curve to the proposed tangential and side friction factors, which cover 95 percent of wet pavements (see Figure 2) (*26*).

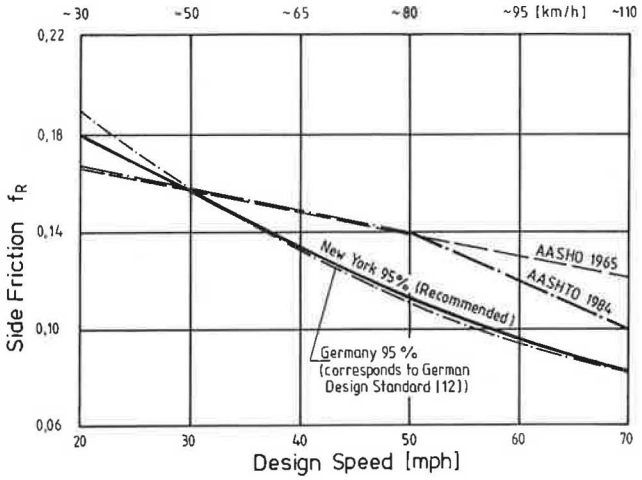

FIGURE 2 Maximum allowable side friction factors versus design speed for AASHTO 1984 (*6*), AASHO 1965 (*27*), Germany, and recommended relationships (*26*).

It may be concluded that by regarding all three design issues, mainly in relation to speed, a safer highway geometric design could be expected.

To prove that these statements are of great importance in enhancing traffic safety, the primary objective of this study was to determine to what extent friction assumed for curve design (*6,27*) corresponds to friction demand on existing curved sections of two-lane rural highways. In particular, regression analysis was used to obtain a quantitative estimate of the effect on the side friction factor produced by the following independent variables: degree of curve, 85th-percentile speed, and accident rate.

DRIVING DYNAMIC BASICS

With wide variation in vehicle speeds on curves, there usually is an unbalanced force whether or not the curve is superelevated. This force results in tire side thrust, which is counterbalanced by friction between tire and surface. The counterforce of friction is developed by distortion of the contact path area of the tire (*6,27*).

The coefficient of side friction (f_R) is the friction force divided by the weight perpendicular to the pavement and is expressed as the following simplified curve formula:

$$f_R = (V^2/15R) - e \quad (1)$$

where

V = constant speed in curve (mph),
R = radius of curve (ft),
e = superelevation rate (ft/ft), and
f_R = side friction factor.

This coefficient has been called *lateral ratio*, *cornering ratio*, *unbalanced centrifugal ratio*, *friction factor*, and *side friction factor*. Because of its widespread use, the last term is used here. The upper limit of this factor is that at which the tire is skidding, or at the point of impending skid. Because highway curves are designed to avoid skidding conditions with a margin of safety, the f_R-values should be substantially less than the coefficient of friction of impending skid (*6,27*).

However, this simplified curve formula is based on the assumption that the vehicle is considered a rigid body and that the dynamic forces are imagined acting in the center of gravity (*6,9,12*). In this assumption, the vehicle is idealized as a point of mass. However, it is easy to realize that such an explanation will not be able to determine the actual forces acting on each wheel of the vehicle and the strains of the resulting friction. Therefore, to overcome previous driving dynamic deficiencies and to enhance traffic safety, new principles for tangential and side friction factors were developed for the highway design guidelines of the Federal Republic of Germany (*12*) and were proposed for the United States in (*26*). The goal was to reduce the driving dynamic safety risk that may be caused by selecting improper design elements and sequences in horizontal and vertical alignments.

The side friction factor at which side skidding is imminent depends on a number of factors, most important of which are the speed of the vehicle, the type and condition of the roadway surface, and the type and condition of the tires (*25*).

The minimum safe radius (R_{min}) can be calculated directly from the following formula:

$$R_{min} = V^2/[15(e + f_{Rmax})] \quad (2)$$

where f_{Rmax} is the maximum allowable side friction factor.

On the basis of this formula, a safer minimum radius could be determined by introducing the recommended maximum allowable side friction factors of Figure 2 (*26*) than by applying the AASHO/AASHTO values for design speed classes $V_d \geq 30$ mph.

The degree of curve of a given circular curve is the angle (or number of degrees) subtended at the center by a 100-ft arc (*6*). It is defined as degrees per 100 ft. Many countries consider radius of curve an important design parameter, but U.S. highway geometric design is mainly related to the design parameter *degree of curve* (DC) (*6*). The relationship between degree of curve and radius of curve is given by DC = 5,729.6/R. The simplified curve formula (Equation 1) then becomes

$$DC_{max} = 85{,}660(e + f_{Rmax})/V^2 \quad (3)$$

where DC_{max} is the maximum degree of curve (degree/100 ft).

DATA COLLECTION AND REDUCTION

The data collection process for this investigation was broken down into four steps. The first step was the selection of road sections that were appropriate for the study. The second step was the collection of as much field data about the road sections as possible. The third step was the measurement of operating free speeds at each section. The fourth step was the collection of accident data for each section.

The sites selected for this research investigation were on two-lane rural highways in New York State. A total of 197 curved roadway sections, with degrees of curve ranging from 1 degree to 23 degrees, was selected from a data base of 322 roadway sections (*15,28,29*). The grades were level or nearly so at the curved sites and for a considerable distance before and after. Site selection was limited to sections with the following features:

1. Removed from the influence of intersections;
2. No physical features adjacent to or in the course of the roadway, such as narrow bridges, that may create abnormal hazards;
3. Delineated and with paved shoulders;
4. No changes in pavement or shoulder widths;
5. Protected by guardrails when the height of the embankment exceeded 5 ft;
6. Grades less than or equal to 5 percent; and
7. Average annual daily traffic (AADT) between 400 and 5,000 vehicles per day (vpd).

The design data for the curves under study were collected in the field and from the regional offices of the New York State Department of Transportation (NYSDOT). Degree of curve and superelevation rate, two of the most important geometric design parameters considered in the study, were collected in the field and later checked against the latest design plans of NYSDOT.

The basic method used for speed data collection involved the measurement of the time required for a vehicle to traverse

a measured course laid out in the center of the curved site. The length of the course for this study was 150 ft. The measurement of time over the measured distance involved the use of transverse pavement markings placed at each end of the course and an observer who started and stopped an electronic stop watch as a vehicle passed the markings. The observer was placed at least 15 ft from the pavement edge of the road to ensure that his presence would not influence the speeds of passing vehicles, but not too far away to minimize the cosine effect. By applying this procedure, satisfactory speed data, which were occasionally substantiated by the use of radar devices, were obtained for both directions of travel. About 120 to 140 passenger cars under free-flow conditions were sampled at each site for both directions of traffic (*1,15,28,29*).

To ensure that the speeds measured in this study represented the free speeds desired by the driver under a set of road conditions and were not affected by other traffic on the road, only the speeds of isolated vehicles (time gap of about 6 sec) or those heading a platoon of vehicles were measured in this study. Speed measurements were made during daytime hours, on weekdays, under dry pavement conditions.

After the data were collected, they were displayed in frequency distribution spot speed tables. The data from the spot speed tables were then used to obtain the operating speed, expressed as the 85th-percentile speeds (mph) (speed below which 85 percent of the vehicles travel). The observed operating speeds were shown to be valid for both dry and wet pavements, as long as visibility was not appreciably affected by heavy rain (*24*).

For each of the curved sites under study, accident data from January 1983 to December 1985 were obtained for all vehicle types from the New York State Accident Surveillance System (SASS) accident description file.

Because the amount of accident data (569 accidents) was not large enough to allow disaggregation into several categories, only the total number of accidents was analyzed. To assess the quality of the road, the accident rate was defined as the number of accidents per 1 million vehicle-mi. The accident rate for each of the investigated road sections was calculated from the following formula:

$$\text{ACCR} = [(\text{no. acc.} \times 10^6)/(365 \times \text{no. years} \times \text{LC} \times \text{AADT})]$$

where

ACCR = number of accidents per 1 million vehicle-mi,
no. acc. = number of accidents in the curved section related to all vehicle types,
no. years = number of years investigated (i.e., 3 years),
LC = length of curve or curved section (mi), and
AADT = average annual daily traffic (vpd, both directions).

The average curve length for 90 percent of the curves investigated was 1,230 ft. For the remaining 10 percent, the average curve length was 410 ft. For these curved sections, a length of 0.1 mile (528 ft) was used in the ACCR equation to calculate the accident rate. The 0.1-mi length was considered an appropriate value to use (a) because the New York SASS accident description file is based on a reference marker system of 0.1 mi and (b) to account for those accidents that may have occurred directly before and beyond short curves.

In general, nearly two-thirds of the accidents were fatal or injury accidents, attributed mostly to run-off-the-road accidents.

Other publications include detailed discussions of the data collection and reduction process (*1,15,28,29*). Table 2 shows a typical example of geometric design, speed, accident, and side friction data for some of the roadway sections under study.

SIDE FRICTION ASSUMED AND SIDE FRICTION DEMAND

The maximum allowable side friction factors ($f_{R_{max}}$) assumed for curve design by AASHTO are given in Table III-6 of the 1984 *Policy on Geometric Design of Highways and Streets* (*6*). This table reveals that

1. There is a one-to-one relationship between side friction factor (f_R) and design speed (V_d) ranging from 20 to 70 mph.
2. The assumed values of the side friction factors are held constant for superelevation rates ranging from 4 to 10 percent.
3. The assumed value of the side friction factor at a certain curved section in the field can be determined by the method of linear interpolation by simply knowing degree of curve and superelevation rate of that section, in case the design speed is not known.

For this investigation, Table III-6 (*6*) was extended to include superelevation rates between 2 and 12 percent, using increments of 0.5 percent to account for the actual superelevation rates collected in the field or obtained from NYSDOT for the 197 curved roadway sections under study. Table 3 shows a typical example of this extension for superelevation rates between 6.5 and 7.5 percent.

For the majority of the investigated curved roadway sections, design speed was not known, but degree of curve and superelevation rate were known from field observations (see Table 2). Therefore, on the basis of degree of curve and superelevation rate from Table 3, and in accordance with item 3, the assumed side friction factor (f_R) for curve design was determined for each of the curved sites under study by the method of linear interpolation. The resulting interpolated values are also given in Table 2.

It is well known that the design speed for a curved section often does not reflect the actual driving behavior. For example, at low and intermediate design speed levels, the portion of relatively flat alignments interspersed between the controlling portions of the highway tends to produce increases in operating speeds that may substantially exceed the design speeds on which the original designs of the road sections were based (*8*). This could lead to a higher side friction demand as compared with the side friction assumed for curve design.

On the basis of observed operating speeds, expressed by the 85th-percentile speeds, the actual side friction demand in this study was calculated for each curve site directly from the following formula:

$$f_{RD} = [(V85)^2 \times (\text{DC})/85{,}660] - e \quad (4)$$

TABLE 2 EXAMPLES OF COLLECTED GEOMETRIC DESIGN, SPEED, ACCIDENT, AND SIDE FRICTION DATA FOR INVESTIGATED CURVED SECTIONS

Section Number	Degree of Curve	Accident Rate (ACCR)	Superelevation Rate (e)	Assumed Side Friction Factor (f_R)	85th-Percentile Speed	Side Friction Demand (f_{RD})
3-5	16.1	18.6	0.065	0.155	43.3	0.287
3-9	7.8	9.6	0.065	0.145	48.0	0.145
3-11	2.5	2.9	0.030	0.100	57.6	0.067
3-15	1.8	0.0	0.025	0.100	59.3	0.049
3-19	1.0	0.0	0.020	0.100	58.0	0.019
11-1	3.50	0.7	0.050	0.110	56.5	0.080
11-3	20.00	25.7	0.065	0.160	39.3	0.296
11-5	2.30	2.3	0.030	0.100	59.0	0.063
11-7	1.40	0.0	0.020	0.100	59.8	0.038
19-1	11.00	18.8	0.075	0.150	46.9	0.207
20A-1	6.00	3.6	0.050	0.140	51.4	0.135
20A-3	22.40	24.3	0.050	0.160	33.7	0.247
28-3	3.20	5.3	0.035	0.120	57.3	0.088
28-7	19.00	23.0	0.095	0.155	41.0	0.278
30-1	21.60	19.6	0.085	0.160	36.9	0.258
31-1	5.30	6.1	0.060	0.130	52.9	0.113
31-3	4.20	6.8	0.050	0.120	55.5	0.101
31-5	4.20	4.1	0.035	0.130	55.0	0.113
37-1	4.20	2.6	0.050	0.120	57.2	0.110
37-3	4.60	2.0	0.040	0.130	54.7	0.121
58-1	3.00	0.0	0.040	0.110	58.0	0.078
68-3	4.50	4.8	0.060	0.120	57.9	0.116
86-1	6.80	6.3	0.065	0.140	51.0	0.141
96A-1	6.80	4.2	0.065	0.140	56.6	0.189
104-1	5.80	3.5	0.060	0.130	52.9	0.129
104-5	3.00	1.2	0.035	0.110	53.4	0.065

where f_{RD} equals side friction demand, and $V85$ equals 85th-percentile speed (mph).

In this manner, the side friction demand was calculated for each of the curved roadway sections under study.

RELATIONSHIPS BETWEEN VARIABLES

Regression analysis was used to obtain quantitative estimates of the effects produced by the independent variables—degree of curve, 85th-percentile speed, and accident rate—on side friction assumed and side friction demand. The following stipulations were used to terminate the regression process and to determine the final regression equation:

1. The selected equation must have a multiple regression coefficient R^2 that is significant at the 0.05 level.
2. Each of the independent variables included in the regression equation must have a regression coefficient that is significantly different from 0 at the 0.05 level.

The selected regression equation had to fulfill both stipulations.

The results of the regression analyses are discussed in the following order:

1. Relationship between side friction assumed/demand and degree of curve.
2. Relationship between side friction assumed/demand and operating speed.
3. Relationship between side friction assumed/demand and accident rate.

Relationship Between Side Friction Assumed/Demand and Degree of Curve

The relationships of side friction assumed/demand and degree of curve are quantified by the following regression models:

$$f_R = 0.092 + 8.104 * 10^{-3}\,DC - 2.3 * 10^{-4}\,(DC)^2$$

$$R^2 = 0.887 \qquad \text{SEE} = 0.006 \tag{5}$$

where

f_R = side friction assumed for curve design,
R^2 = coefficient of determination, and
SEE = standard error of the estimate.

This small standard error (0.006) and large R^2-value (0.887) suggest that the relationship represented by Equation 5 is a strong one.

$$f_{RD} = 0.014 + 2.248 * 10^{-2}\,DC - 5.7 * 10^{-4}\,(DC)^2$$

$$R^2 = 0.864 \qquad \text{SEE} = 0.021 \tag{6}$$

Again, the large coefficient of determination (0.864) and the small standard error (0.021) suggest that the relationship represented by Equation 6 is also strong.

Equations 5 and 6 are shown schematically in Figure 3, in which the side friction assumed is higher than the side friction demand on curves up to about 6.5 degrees. For degrees of

TABLE 3 EXAMPLES OF EXTENSION OF TABLE III-6 OF AASHTO 1984 (*6*) FOR SUPERELEVATION RATES BETWEEN 6.5 AND 7.5 PERCENT

DESIGN SPEED	MAXIMUM SUPER ELEVATION	ASSUMED SIDE FRICTION	TOTAL	MAXIMUM DEGREE OF CURVE
V_d (mph)	e	f_R	$[e+f_R]$	DC °
20	0.065	0.170	0.235	50.325
25	0.065	0.165	0.230	31.523
30	0.065	0.160	0.225	21.415
35	0.065	0.155	0.220	15.384
40	0.065	0.150	0.215	11.511
45	0.065	0.145	0.210	8.883
50	0.065	0.140	0.205	7.024
55	0.065	0.130	0.195	5.522
60	0.065	0.120	0.185	4.402
65	0.065	0.110	0.175	3.548
70	0.065	0.100	0.165	2.884
75	0.065	0.100	0.165	2.513
20	0.070	0.170	0.240	51.396
25	0.070	0.165	0.235	32.208
30	0.070	0.160	0.230	21.891
35	0.070	0.155	0.225	15.733
40	0.070	0.150	0.220	11.778
45	0.070	0.145	0.215	9.095
50	0.070	0.140	0.210	7.195
55	0.070	0.130	0.200	5.663
60	0.070	0.120	0.190	4.521
65	0.070	0.110	0.180	3.649
70	0.070	0.100	0.170	2.972
75	0.070	0.100	0.170	2.589
20	0.075	0.170	0.245	52.467
25	0.075	0.165	0.240	32.893
30	0.075	0.160	0.235	22.367
35	0.075	0.155	0.230	16.083
40	0.075	0.150	0.225	12.046
45	0.075	0.145	0.220	9.306
50	0.075	0.140	0.215	7.367
55	0.075	0.130	0.205	5.805
60	0.075	0.120	0.195	4.640
65	0.075	0.110	0.185	3.751
70	0.075	0.100	0.175	3.059
75	0.075	0.100	0.175	2.665

curve greater than 6.5, Figure 3 reveals that (a) the side friction demand is higher than the side friction assumed and (b) the gap between friction assumed and demand increases with increasing degree of curve. That means that, from a driving dynamic safety point of view, beginning with the point where the two curves intersect, the probability of critical driving maneuvers increases with increasing degree of curve. On the basis of the recommendations for good, fair, and poor design practices (see Table 1), it is clear that the point of intersection at 6.5 degrees, as related to degree of curve, falls into the range of fair design practices, for example, in a sequence from a tangent to a curve. In the case of good design practices ($\Delta DC \leq 5$ degrees) side friction assumed exceeds side friction demand, whereas the case of poor design practices ($\Delta DC > 10$ degrees) side friction demand exceeds side friction assumed.

Thus, it may be concluded that for higher degree of curve classes, the side friction values assumed for design by AASHO (*27*) and AASHTO (*6*) appear to be rather inadequate for their adaptation to actual curve designs as observed in the field. Therefore, these values should be further evaluated, with particular reference to operating speeds. The consequences of this will be discussed later in the section that discusses the relationship between side friction assumed/demand and accident rate.

Relationship Between Side Friction Assumed/Demand and Operating Speed

The relationships of side friction assumed/demand and operating speed are quantified by the following regression models:

$$f_R = 0.082 + 4.692 * 10^{-3} V85 - 7.0 * 10^{-5} (V85)^2$$

$$R^2 = 0.742 \quad \text{SEE} = 0.009 \tag{7}$$

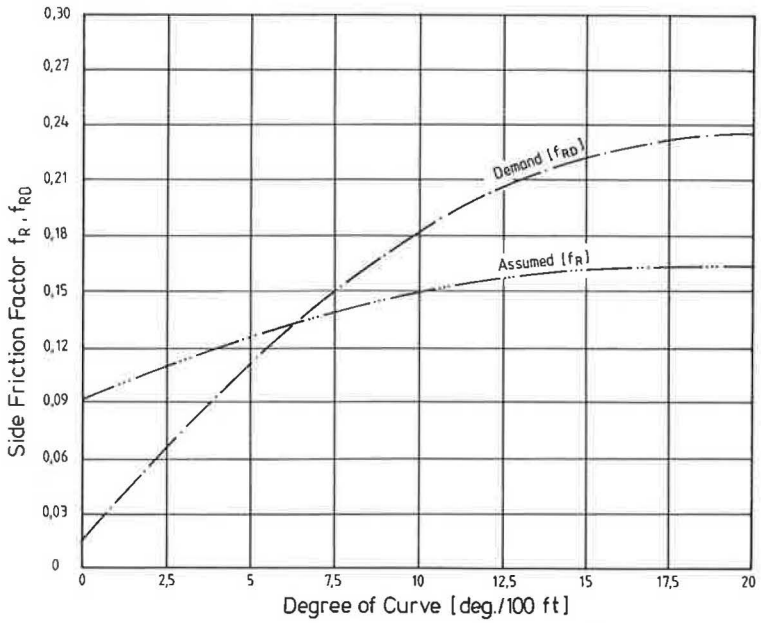

FIGURE 3 Relationship between side friction assumed/demand and degree of curve.

This small standard error (0.009) and large R^2-value (0.742) suggest that the relationship represented by Equation 7 is a strong one.

$$f_{RD} = 0.253 + 2.330 * 10^{-3} V85 - 9.0 * 10^{-5} (V85)^2$$

$$R^2 = 0.557 \qquad (8)$$
$$\text{SEE} = 0.038$$

The moderately large coefficient of determination (0.557) and small standard error (0.038) suggest that the relationship represented by Equation 8 is a moderate one.

Equations 7 and 8 are shown schematically in Figure 4, which reveals that (a) side friction assumed/demand decrease as operating speed increases and (b) the point of intersection corresponds to an operating speed of about 50 mph. This finding is not surprising because for higher design speed classes (for example $V_d \geq 60$ mph), degrees of curve ≤ 5 degrees are normally suggested by AASHTO (*6*) and AASHO (*27*) for geometric highway design. Tuning the horizontal alignment in such a way—whenever the changes in degree of curve (ΔDC) between successive design elements are less than or equal to 5 degrees—generally results in gentle curvilinear horizontal alignments that can be evaluated as good design practices (see Table 1).

Furthermore, operating speeds, which are influenced by the nationwide speed limit of 55 mph on two-lane rural (non-Interstate) roads, often do not reach the design speed levels on which the horizontal alignment is based. Thus, it should not be surprising that beginning at about 50 mph, side friction assumed is definitely higher than side friction demand. From a driving dynamic point of view, safe designs could be expected in these cases.

In contrast, for lower design speed levels, which are mostly combined with higher degrees of curve up to maximum values of about 50 degrees [see Table III-6, AASHTO (*6*)] operating speeds often substantially exceed design speeds (*2,4,7–14*). These operating speeds create substantially higher side friction demands than those assumed for highway design (*6,27*) (see Figure 4), at least based on the analysis of data for the 197 curved roadway sections under study.

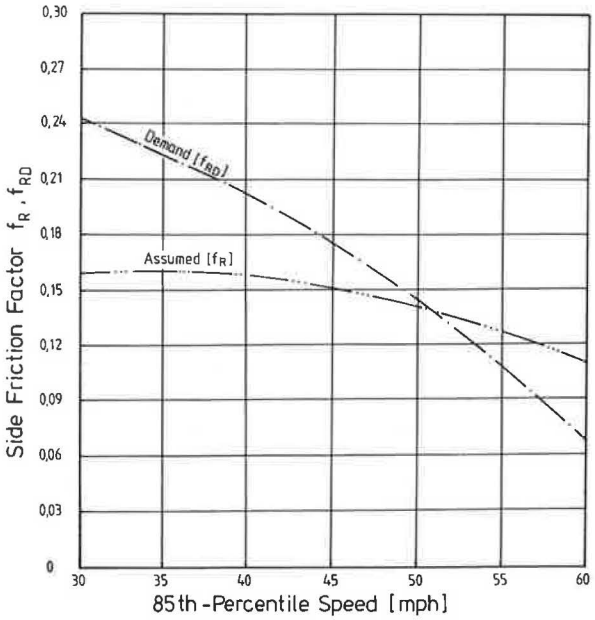

FIGURE 4 Relationship between side friction assumed/demand and operating speed.

Relationship Between Side Friction Assumed/Demand and Accident Rate

The relationships of side friction assumed/demand and accident rate are quantified by the following regression models:

$$f_R = 0.121 + 1.860 * 10^{-3}\,\text{ACCR} - 2.0 * 10^{-5}\,(\text{ACCR})^2$$

$$R^2 = 0.406 \quad \text{SEE} = 0.013 \tag{9}$$

and

$$f_{RD} = 0.097 + 6.041 * 10^{-3}\,\text{ACCR} - 7.0 * 10^{-5}\,(\text{ACCR})^2$$

$$R^2 = 0.401 \quad \text{SEE} = 0.045 \tag{10}$$

The relatively small coefficients of determination (R^2) of Equations 9 and 10 are not at all surprising because accident research relationships are not simple and direct, but often complex, and changes in frequency of accidents are often the result of many factors other than the driving dynamic aspects, expressed by side friction assumed and side friction demand.

Equations 9 and 10 are shown schematically in Figure 5. Side friction demand begins to exceed side friction assumed when the accident rate is about six or seven accidents per 1 million vehicle-mi. To understand the meaning of this outcome as related to highway geometric design and the accident situation, Table 4 was developed (*15,22,29*). On the basis of these studies, degree of curve was found to be the most successful parameter in explaining the variability in accident rates. As shown in Table 4, the results indicate significant increases (at the 95 percent level of confidence) in the average accident rates among the different degree of curve classes compared. In other words, the results of Table 4 indicate that gentle curvilinear horizontal alignments consisting of tangents or transition curves combined with curves up to 5 degrees showed the lowest average accident risk. These observations agree with the findings of some European guidelines (*12,14*) and the statements of AASHTO (*6*, pp. 248ff.).

For horizontal alignments with changes of curve between 5 and 10 degrees between successive design elements, the mean accident rate in Table 4 is already twice as high as for those between 1 and 5 degrees. For changes between 10 and 15 degrees of curve, the mean accident rate is four times the rate associated with curves between 1 and 5 degrees. For greater changes in degree of curve, the mean accident rate is even higher. This confirms that changes in curve that exceed 10 degrees between successive design elements should be interpreted as poor designs while those in the range between 5 and 10 degrees can still be judged as fair designs.

On the basis of the results of Table 4, and in addition to investigations about geometric design parameters and operating speed changes between successive design elements (*15,16,20,22*), recommendations for good, fair, and poor design practices were developed (see Table 1).

A comparison of the results clearly shows that the point of intersection at which side friction demand begins to exceed side friction assumed in Figure 5 nearly corresponds to the average accident rate for fair design in Table 4. In the range of good design, Figure 5 shows that the side friction assumed is higher than the side friction demand. On the other hand, in the range of poor design, Figure 5 shows that the side friction demand is higher than the side friction assumed. These results clearly support the opinions expressed by several researchers who argue that, in recognition of safety considerations, insufficient dynamic safety of driving has a direct impact on accident rate. Similar results are obvious from Figure 3 and Table 4 with respect to degree of curve.

These results clearly contradict the opinion of many practitioners and researchers who argue that the margin of safety against skidding (especially for passenger cars), that is, the difference between assumed friction and available actual pavement friction, is large enough to provide an adequate dynamic safety of driving. Related to good skid resistant pavements, this margin of safety may reach a factor of 2 for wet

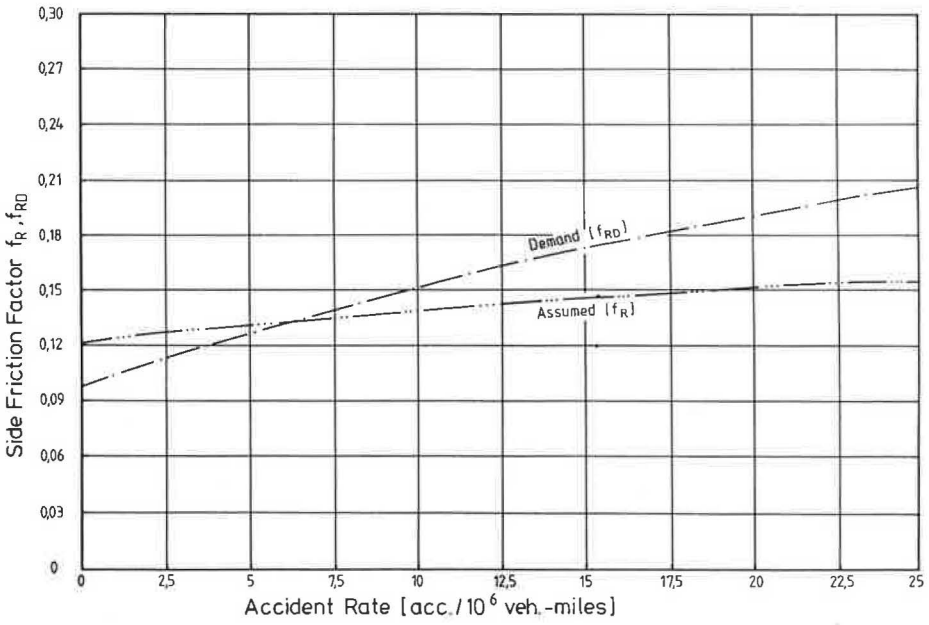

FIGURE 5 Relationship between side friction assumed/demand and accident rate.

TABLE 4 T-TEST RESULTS OF ACCIDENT RATES FOR CHANGES IN DEGREE OF CURVE CLASSES BETWEEN SUCCESSIVE DESIGN ELEMENTS (*15,22,29*)

Degree of Curve Classes (degrees per 100 ft)	Average Acc. Rate (acc./million veh. - miles)	t calc.	t crit.	Signi-ficance	Remarks
tangent 0°	1.87				Consider
		4.00	1.96	Yes	
1°- 5°	3.66				---- GD
		7.03	1.96	Yes	
> 5°- 10°	8.05				---- FD
		6.06	1.99	Yes	
> 10°- 15°	17.55				---- PD
		3.44	1.99	Yes	
> 15°- 26.9°	26.41				---- PD

Legend: GD = Good Design; FD = Fair Design; PD = Poor Design.

pavements and a factor of 4 or higher for dry pavements. Related to vehicular and human aspects, there may be another margin of safety against skidding. This additional margin is based on the fact that in nearly all highway design guidelines, assumed friction values are derived from locked-wheel friction measurements. These assumed friction values are lower than the peak friction coefficients that may be reached by experienced drivers, or with the presence of an antilock braking system. However, even those margins of safety do not alter the fact that higher accident risks do exist on poorly designed roadways, which exhibit inconsistencies in horizontal alignment and disharmony between design speeds and operating speeds, as compared to those roadways exhibiting fair designs or even good designs that are based on conditions in the real world.

CONCLUSIONS

The objective of this research was to explore whether the side friction assumed in the policies on geometric design (*6,27*) corresponds to friction demand on existing curved sections of two-lane rural highways. A total of 197 curved roadway sections was selected for the study. For each of the selected roadway sections, geometric design, operating speed, and accident data were collected. Side friction was determined from the available data. Regression analysis was used to obtain a quantitative estimate of the effect on side friction assumed and side friction demand produced by

- Roadway geometry (expressed by degree of curve),
- Operating speed (expressed by the 85th-percentile speed), and
- Accidents (expressed by the accident rate).

The resulting regression equations (see Figures 3 to 5) clearly reveal points of intersection in the relationships between side friction assumed and demand and degree of curve (DC), 85th-percentile speed ($V85$), and accident rate (ACCR). In other words, the figures show that there are ranges for the independent variables (DC, $V85$, ACCR) where side friction demand exceeds side friction assumed and vice versa.

On the basis of prior research (see Tables 1 and 4), this study has shown that, in relation to degree of curve and accident rate, (a) side friction assumed exceeded side friction demand, especially in the range of good design practices and (b) side friction demand exceeded side friction assumed, especially in the range of poor design practices. The points of intersection in Figures 3 and 5 lie somewhere into the range of fair design practices, as related to degree of curve and accident rate.

With respect to side friction, analyses of Figures 3 to 5 indicate that the points of intersection correspond to side friction factors of f_R, $f_{RD} \simeq 0.13$. AASHTO Table III-6 (*6*) indicates that this side friction factor corresponds to a design speed between 50 and 60 mph and to a degree of curve between 5 and 7 degrees.

These findings mean that, especially in the lower design speed classes, which are combined with higher maximum allowable degree of curve classes, (a) the danger exists that friction demand exceeds friction assumed (see Figure 3) and (b) a high accident risk results (see Figure 5 and Table 4). These statements are fully supported by the relationships shown in Figure 4, which reveals that side friction demand exceeds side friction assumed for operating speeds $V85 < 50$ mph, where (a) lower design speed levels could be expected and (b) the danger exists that design speeds and operating speeds are not well balanced. Thus, it is apparent that driving dynamic safety aspects have an important impact on geometric design, operating speed, and accident experience on curved roadway sections of two-lane rural highways.

However, previous research (*1,15–24*) demonstrated that adequate dynamic safety of driving is only one safety related criterion in modern geometric highway design. Thus, overall safety improvement, which would, for example, lead to a better harmony between friction assumed and friction demand, would result only through an interaction among the three geometric criteria:

- Achieving consistency in horizontal alignment (Table 1),
- Harmonizing design speed and operating speed (Table 1), and
- Providing adequate dynamic safety of driving (Figure 2).

By regarding only one safety related criterion, for example, adopting the recommended side friction factors of Figure 2 for new geometric design, only a partial success would result.

The relationships provided in this study demonstrated that changes in the AASHTO geometric design policy are war-

ranted in order to fulfill these three geometric criteria. Specific recommendations for those changes have already been discussed and have been provided elsewhere (*16,17,26*). Because the research is primarily based on data collected in New York State, further research in other areas of the United States may be warranted.

In summary, these three safety related issues should be of prime concern to state agencies as they carry out new designs, redesigns, and rehabilitation strategies in order to enhance traffic safety.

ACKNOWLEDGMENT

This study is based on data bases that were sponsored by the National Science Foundation and by the New York State Governor's Traffic Safety Committee, Albany, New York (State University of New York Research Foundation).

REFERENCES

1. R. Lamm and E. M. Choueiri. *A Design Procedure to Determine Critical Dissimilarities in Horizontal Alignment and Enhance Traffic Safety by Appropriate Low-Cost or High-Cost Projects.* Final Report. National Science Foundation, Washington, D.C., March 1987.
2. J. M. Mason and J. C. Peterson. Survey of States' R-R-R Practices and Safety Considerations. In *Transportation Research Record 960*, TRB, National Research Council, Washington, D.C., 1984.
3. C. P. Brinkman. Safety Studies Related to RRR Projects. *Transportation Journal of ASCE*, Vol. 108, July 1983.
4. J. C. Glennon, T. R. Neuman, and J. P. Leisch. *Safety and Operational Considerations for Design of Rural Highway Curves: Final Report.* Report DOT-FH-11-9575. U.S. Department of Transportation, Aug. 1983.
5. H. W. Kummer and W. E. Meyer. *NCHRP Report 37: Tentative Skid-Resistance Requirements for Main Rural Highways.* HRB, National Research Council, Washington, D.C., 1967.
6. *A Policy on Geometric Design of Highways and Streets.* AASHTO, Washington, D.C., 1984.
7. J. Hayward, R. Lamm, and A. Lyng. *Survey of Current Geometric and Pavement Design Practices in Europe: Geometric Design.* International Road Federation, Washington, D.C., July 1985.
8. J. E. Leisch and J. P. Leisch. New Concepts in Design Speed Application. In *Transportation Research Record 631*, TRB, National Research Council, Washington, D.C., 1977.
9. R. Lamm. *Driving Dynamics and Road Characteristics—A Contribution for Highway Design under Special Consideration of Operating Speeds*, Vol. 11. Institute for Highway and Railroad Engineering, University of Karlsruhe, Federal Republic of Germany, 1973.
10. J. C. Hayward. Highway Alignment and Superelevation: Some Design-Speed Misconceptions. In *Transportation Research Record 757*, TRB, National Research Council, Washington, D.C., 1980.
11. G. Koeppel and H. Bock. Operating Speed as a Function of Curvature Change Rate. *Research Road Construction and Traffic Technique*, Vol. 269, Federal Republic of Germany, Minister of Transport, 1979.
12. *Guidelines for the Design of Roads.* RAS-L-1, German Road and Transportation Research Association, Committee 2.3, Geometric Design Standards, 1984.
13. *Standard Specifications for Geometric Design of Rural Roads.* National Swedish Road Administration, Borlenge, 1982.
14. *Highway Design, Fundamentals, Speed as a Design Element.* Swiss Association of Road Specialists, Swiss Norm SN 640080a, 1981.
15. R. Lamm and E. M. Choueiri. *Rural Roads Speed Inconsistencies Design Methods.* Final Report, State University of New York Research Foundation, Contract No. RF320-PN72350, Albany, Part I, July 1987, and Part II, Oct. 1987.
16. R. Lamm, E. M. Choueiri, J. C. Hayward, and A. Paluri. Possible Design Procedure to Promote Design Consistency in Highway Geometric Design on Two-Lane Rural Roads. In *Transportation Research Record 1195*, TRB, National Research Council, Washington, D.C., 1988.
17. R. Lamm, E. M. Choueiri, and J. C. Hayward. Tangent as an Independent Design Element. In *Transportation Research Record 1195*, TRB, National Research Council, Washington, D.C., 1988.
18. R. Lamm, J. C. Hayward, and J. G. Cargin. Comparison of Different Procedures for Evaluating Speed Consistency. In *Transportation Research Record 1100*, TRB, National Research Council, Washington, D.C., 1986.
19. R. Lamm and E. M. Choueiri. Recommendations for Evaluating Horizontal Design Consistency, Based on Investigations in the State of New York. In *Transportation Research Record 1122*, TRB, National Research Council, Washington, D.C., 1987.
20. R. Lamm, E. M. Choueiri, T. Mailaender, and A. Paluri. A Logical Approach to Geometric Design consistency of Two-Lane Rural Roads in the U.S.A. *Proc., 11th IRF (International Road Federation) World Meeting*, Seoul, Korea, Vol. II, April 16–21, 1989, pp. 8–11.
21. R. Lamm, T. Mailaender, and E. M. Choueiri. New Ideas for the Design of Two-Lane Rural Roads in the U.S.A. *International Technical Journal: Road and Construction*, Federal Republic of Germany, Vol. 5, pp. 18–25, May 1989, and Vol. 6, pp. 13–18, June 1989.
22. R. Lamm, E. M. Choueiri, and T. Mailaender. Accident Rates on Curves as Influenced by Highway Design Elements—An International Review and an In-Depth Study. *Proc., Road Safety in Europe*, Gothenburg, Sweden, VTIrapport 344 A, Swedish Road and Traffic Research Institute, Linkoeping, Sweden, 1989, pp. 33–54.
23. R. Lamm and E. M. Choueiri. Investigations about Driver Behavior and Accident Experiences at Curved Sites (Including Black Spots) of Two-Lane Rural Highways in the U.S.A. *Proc., Roads and Traffic 2000*, Berlin, Federal Republic of Germany, Volume 4/2, Traffic Engineering and Safety, Sept. 6–9, 1988, pp. 153–158.
24. R. Lamm, E. M. Choueiri, and T. Mailaender. Comparison of Operating Speeds on Dry and Wet Pavements of Two-Lane Rural Highways. In *Transportation Research Record 1280*, TRB, National Research Council, Washington, D.C., 1990.
25. P. B. Goyal. *Friction Factors for Highway Design Regarding Driving Dynamic Safety Concerns in the State of New York.* Master's thesis. Clarkson University, Potsdam, N.Y., 1987.
26. R. Lamm, E. M. Choueiri, P. Goyal, and T. Mailaender. Design Friction Factors of Different Countries Versus Actual Pavement Friction Inventories. In *Transportation Research Record 1260*, TRB, National Research Council, Washington, D.C., 1990.
27. *A Policy on the Geometric Design of Rural Highways.* AASHO, Washington, D.C., 1965.
28. A. Paluri. *Relationships Between Design Parameters, Operating Speeds, Side Friction Factors, and Accident Rates for Future Highway Design Consideration, on Two-Lane Rural Curved Road Sections.* Master's thesis. Clarkson University, Potsdam, N.Y., 1987.
29. E. M. Choueiri. *Statistical Analysis of Operating Speeds and Accident Rates on Two-Lane Rural Highways.* Ph.D. dissertation. Clarkson University, Potsdam, N.Y., 1987.

The views expressed in this paper are those of the authors and not necessarily those of the sponsoring agencies.

Publication of this paper is sponsored by Committee on Geometric Design.

Lateral Clearance to Vision Obstacles on Horizontal Curves

SAID M. EASA

Evaluation of the sight distance adequacy on highway horizontal curves with single or multiple obstacles requires determination of the minimum sight distance on the curve. The current method of establishing such a minimum is to plot the sight distance profile for the given curve and obstacle. Approximate relationships have been developed for establishing the sight distance profile. However, there is no explicit, exact solution available for determining the minimum sight distance on the curve. Exact formulas have been derived to relate the available sight distance to the circular curve parameters, lateral clearance of the obstacle, its location along the curve, and the locations of observer and object. These relationships are then used to derive closed-form solutions of the minimum sight distance, S_m. To facilitate practical use, values of S_m are established for typical ranges of the curve parameters, lateral clearance, and obstacle location. Values of the maximum lateral clearance, which is required in design, are also provided. The methodology and results should be valuable in the operational and cost-effectiveness analysis of highway locations with restricted sight distances.

The sight distance on highway horizontal curves may be restricted by such physical features as longitudinal barriers, cut slopes, foliage, and other structures. For safe operations, the available sight distance at any point on the traveled way must be greater than the sight distance needed for stopping, passing, or decision at complex locations. The available sight distance is a function of the horizontal curve parameters, locations of the observer and object, and the location of the vision-limiting obstacle inside the curve.

The stopping sight distance (SSD), presented by AASHTO (*1–4*), is one of the basic considerations in the design of highways. Design values for SSD applicable to all highways are presented by AASHTO. A new approach to SSD that considers the functional classifications of highways was recently presented by Neuman (*5*). Design values for passing sight distance (PSD) involving passenger cars on two-lane highways are presented in AASHTO's 1984 *Policy on Geometric Design of Highways and Streets* (Green Book) (*4*). Design values for PSD for all combinations of passing involving a passenger car and a truck have been developed by Harwood and Glennon (*6*). These design values are based on a model developed by Glennon (*7*) that logically accounts for the kinematic relationships among the passing, passed, and opposing vehicles and explicitly contains vehicle-length variables. Design values for decision sight distance (DSD) are presented by AASHTO (*4*) and Neuman (*5*), and their usefulness and application have been evaluated by McGee (*8*).

A number of models exist that relate the available sight distance and the lateral clearance on horizontal curves. AASHTO presents a model that relates the sight distance, S_m, and maximum lateral clearance, M, for $S_m \leq L$, where L is the length of the curve (*4*). The case $S_m > L$ is not presented by AASHTO. When either the vehicle or vision obstacle is situated near the ends of the curve, the less clearance is needed. The studies by Olson et al. (*9*), Neuman and Glennon (*10*), and Glennon (*11*) show that when the vehicle is on the tangent within a distance S from the point of curvature, PC, the maximum lateral clearance needed varies from 0 to M (when the vehicle is at PC). The required lateral clearance for all points within $S/2$ beyond PC is also less than M. For these situations, AASHTO recommends the use of a graphical procedure or the curves empirically developed by Raymond (*12*).

To eliminate the need for the graphical procedure, Waissi and Cleveland (*13*), on the basis of the results of the NCHRP report by Olson et al. (*9*), derived approximate relationships that relate the available sight distance to the horizontal curve parameters, locations of observer and road object, location of obstacle, and lateral clearance to a single obstacle to vision located inside the curve. Relationships for determining the maximum lateral clearance for $S_m > L$ are also presented.

For a given obstacle on the curve, the available sight distance varies as the observer moves along the tangent and curve. Clearly, there is a minimum value of sight distance on the traveled path that determines the adequacy of sight distance on the curve. There is no explicit, exact solution available for determining this minimum sight distance. The purpose of this paper is threefold:

1. To derive exact relationships for determining the available sight distance for arbitrary locations of the observer and obstacle,
2. On the basis of the preceding, to develop relationships for determining the minimum sight distance, and
3. To establish evaluation and design values for practical use.

THEORETICAL DEVELOPMENT

Relationships for determining the minimum sight distance, S_m, are developed for a single obstacle located on the inside of a simple horizontal curve between PC and PT (point of tangency). Both the observer and object are assumed to be located on the centerline of the inside lane. Three cases are considered:

- Case 1: Observer before PC and object beyond PT,

Department of Civil Engineering, Lakehead University, Thunder Bay, Ontario, Canada P7B 5E1.

- Case 2: Observer before PC and object on curve, and
- Case 3: Observer and object on curve.

Case 1: Observer Before PC and Object Beyond PT

The geometry of this case is shown in Figure 1. As the observer moves toward PC, the available sight distance decreases, reaches a minimum value, and then increases again. The lateral clearance requirements should be based on this minimum value. In Figure 1, x_1 is the distance from the observer to PC, and x_2 is the distance from the object to PT.

Available Sight Distance

The available sight distance is given by

$$S = L + x_1 + x_2 \tag{1}$$

where S equals available sight distance, and L equals curve length.

With the law of sines for triangles *abPT* and *acPC*, x_1 and x_2 can be expressed in terms of the angles θ_1 and θ_2, shown in Figure 1, as

$$x_1 = m_1 \sin\theta_1/\sin(\theta_1 + \alpha) \tag{2}$$

$$x_2 = m_2 \sin\theta_2/\sin(\theta_2 + \beta) \tag{3}$$

where

m_1 = distance from the obstacle to PC,
m_2 = distance from the obstacle to PT,
α = angle at PC between the tangent and the line to the obstacle, and
β = angle at PT between the tangent and the line to the obstacle.

Note that in Equation 2, $\sin(\theta_1 + \alpha) = \sin(180 - \theta_1 - \alpha)$, and similarly for Equation 3. These four elements, which are constant for a given curve and obstacle, are computed using triangles *oaPC* and *oaPT* as follows:

$$m_1 = [R^2 + (R - m)^2 - 2R(R - m)\cos I_1]^{1/2} \tag{4}$$

$$m_2 = [R^2 + (R - m)^2 - 2R(R - m)\cos(I - I_1)]^{1/2} \tag{5}$$

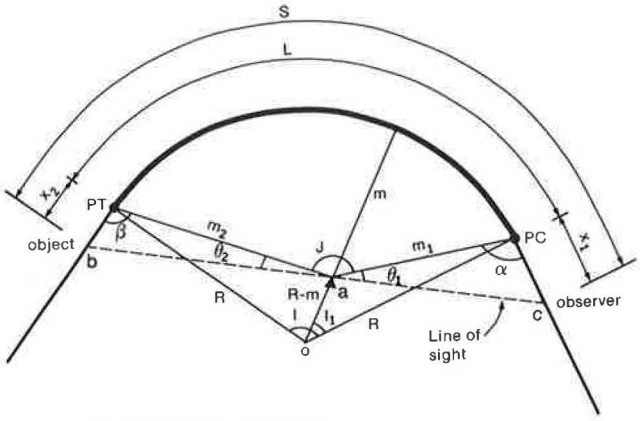

FIGURE 1 Case 1: Observer before PC and object beyond PT.

$$\alpha = 90° + \cos^{-1}\{[-(R - m)^2 + R^2 + m_1^2]/2Rm_1\} \tag{6}$$

$$\beta = 90° + \cos^{-1}\{[-(R - m)^2 + R^2 + m_2^2]/2Rm_2\} \tag{7}$$

where

R = curve radius,
m = lateral clearance between the centerline of the inside lane and obstacle,
I_1 = central angle from PC to the obstacle, and
I = central angle from PC to PT.

The angles θ_1 and θ_2 are related by

$$\theta_2 = 180° - \theta_1 - J \tag{8}$$

Since $\angle\, aPCo = \alpha - 90°$ and $\angle\, aPTo = \beta - 90°$, the angle J is obtained as follows:

$$J = \alpha + \beta + I - 180° \tag{9}$$

Substituting θ_2 of Equation 8 into Equation 3, the available sight distance of Equation 1 can be written as

$$S = L + [m_1 \sin\theta_1/\sin(\theta_1 + \alpha)] + [m_2 \sin(\theta_1 + J)/\sin(\theta_1 + J - \beta)] \tag{10}$$

in which the curve length L equals $R\pi I/180$.

Condition for S_m

Differentiating Equation 10 with respect to θ_1 and equating $dS/d\theta_1$ to zero gives

$$\sin(\theta_1^* + \alpha)/\sin(\theta_1^* + J - \beta) = (m_1 \sin\alpha/m_2 \sin\beta)^{1/2} \tag{11}$$

in which θ_1^* is the critical angle corresponding to the minimum sight distance, S_m. The derivation of Equation 11 is included in Appendix A. A successive approximation method for solving Equation 11 to determine θ_1^* is given in Appendix B. Note that Equation 11 implies that θ_1^* must be greater than $(\beta - J)$. For equal or smaller values, the line of sight from the observer to the obstacle does not intersect with the tangent beyond PT. After determining θ_1^*, S_m is computed by substituting θ_1^* into Equation 10.

If the obstacle lies at the midpoint of the curve ($I_1/I = 0.5$), then $m_1 = m_2$ and $\alpha = \beta$. With these values, Equation 11 yields $\theta_1^* + \alpha = 180 - (\theta_1^* + J - \beta)$ (note that $\alpha \neq J - \beta$ is based on Equation 9). Thus,

$$\theta_1^* = (180° - J)/2 \quad \text{for} \quad I_1/I = 0.5 \tag{12}$$

which implies that $x_1 = x_2$, as expected.

Case 2: Observer Before PC and Object on Curve

In this case, the observer is on the tangent at a distance x_1 from PC, and the object is on the curve at a distance L_1 from PC (Figure 2).

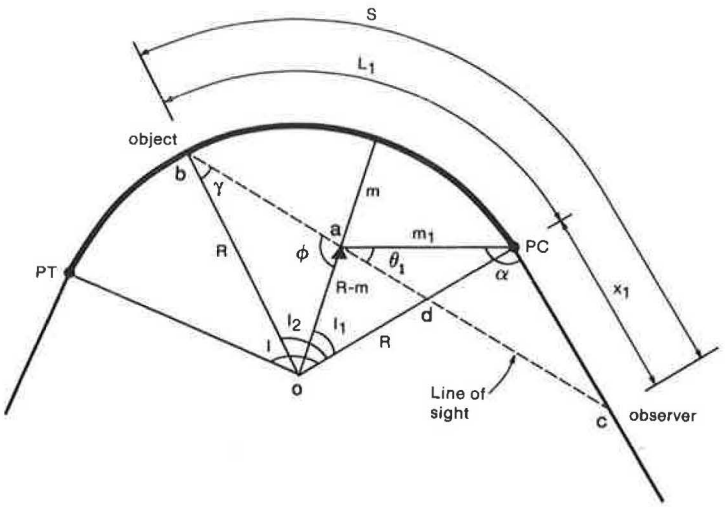

FIGURE 2 Case 2: Observer before PC and object on curve ($I_1/I \leq 0.5$).

Available Sight Distance

The available sight distance is given by

$$S = L_1 + x_1 \tag{13}$$

where L_1, the distance from PC to the object, is given by

$$L_1 = RI_2 \tag{14}$$

and x_1 is given by Equation 2 (m_1 and α are given by Equations 4 and 6). I_2 is the central angle between PC and the object (in radians). The angle $oda = \theta_1 + \alpha - 90°$. Therefore, using triangle *obd*, I_2 is obtained:

$$I_2 = 270° - \gamma - \alpha - \theta_1 \tag{15}$$

Using triangles *oab* and *oad*, respectively, γ and ϕ are obtained:

$$\gamma = \sin^{-1}[(R - m)\sin\phi/R] \tag{16}$$

$$\phi = I_1 + \alpha + \theta_1 - 90° \tag{17}$$

Now Equation 13 can be written as follows:

$$S = RI_2 + [m_1 \sin\theta_1/\sin(\theta_1 + \alpha)] \tag{18}$$

Condition for S_m

Differentiating Equation 18 with respect to θ_1 and equating $dS/d\theta_1$ to zero give (Appendix A)

$$\frac{m_1 \sin\alpha}{R \sin^2(\theta_1^* + \alpha)} - \frac{(R - m)\sin(\theta_1^* + \alpha + I_1)}{[R^2 - (R - m)^2 \cos^2(\theta_1^* + \alpha + I_1)]^{1/2}} = 1 \tag{19}$$

Solving Equation 19 by successive approximations gives the critical angle θ_1^* (Appendix B). S_m is then computed by substituting θ_1^* into Equation 18.

Because of the symmetry of the horizontal curve, Case 2 may occur only when I_1/I is less than 0.5. For I_1/I greater than 0.5, the minimum sight distance occurs when the observer is on the curve and the object is beyond PT. The solution of this situation is also given by Equations 13–19 after switching the positions of PC and PT, and of the observer and object.

Case 3: Observer and Object on Curve

In Case 3, both observer and object are on the curve. Figure 3 shows the geometry of this case. Let I_3 denote the central angle from the observer to the obstacle and I_4 the central angle from the obstacle to the perpendicular line *od*. Using triangle *ace*, $\tan I_4 = ae/ec$. But $ae = (R - m) - oe$. From triangle *oec*, $ec = R \sin I_3$ and $oe = R \cos I_3$. Thus,

$$I_4 = \tan^{-1}[(R - m - R\cos I_3)/(R \sin I_3)] \tag{20}$$

where I_3, which equals $I_1 - \angle\, coPC$, is given by

$$I_3 = I_1 - (180x_1/\pi R) \tag{21}$$

and x_1 is the distance along the curve between the observer and PC

Available Sight Distance

The available sight distance is given by (Figure 3)

$$S = 2R(I_3 - I_4) \tag{22}$$

where I_3 and I_4 are in radians. Substituting for I_4 from Equation 20 into Equation 22 gives

$$S = 2R\{I_3 - \tan^{-1}[(R - m - R\cos I_3)/(R \sin I_3)]\} \tag{23}$$

Condition for S_m

Differentiating Equation 23 with respect to I_3 and equating dS/dI_3 to zero gives (Appendix A)

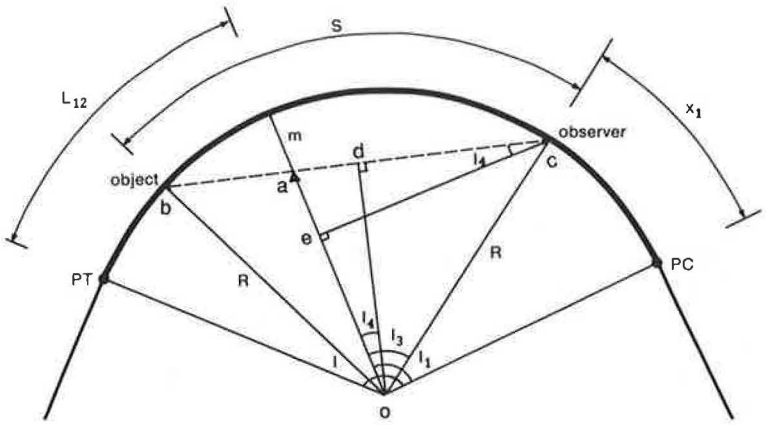

FIGURE 3 Case 3: Observer and object on curve.

$$[R(1 - \cos I_3^*) - m](R - m) = 0 \quad (24)$$

from which

$$m = R(1 - \cos I_3^*) \quad (25)$$

Substituting for m into Equation 20 gives $I_4 = 0$, which implies that S_m occurs when the observer and object are at equal distances from the obstacle. Thus, from Equation 22, $S_m = \pi R I_3^*/90$ or $I_3^* = 90S_m/\pi R$ (where I_3^* is in degrees). Substituting for I_3^* into Equation 25 gives

$$m = R[1 - \cos(90S_m/\pi R)] \quad (26)$$

which is the formula presented by AASHTO (*4*). It is clear that for Case 3, S_m is independent of the location of the obstacle for any given value of m.

Conditions for Case Determination

The geometry of the conditions for different cases is shown in Figure 4. Line *oc* is a radial line passing through the obstacle. The line from PC to *d* is perpendicular to this radial line. If m is less than *cb*, this is Case 3. If m is greater than *cb* but less than *ca*, this is Case 2. If m is equal to or greater than *ca*, this may be Case 1 or 2.

Given R, I, m, and I_1, the following steps are used to determine the respective case and the minimum sight distance:

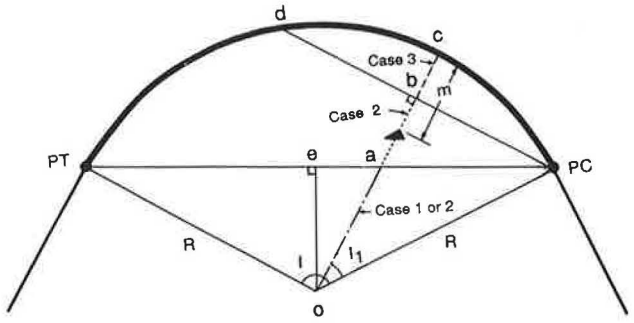

FIGURE 4 Geometry of the conditions for case determination.

1. S_m corresponds to Case 3 if the following condition is satisfied:

$$m \leq R[1 - \cos I'] \quad I' = \min\{I_1, I - I_1\} \quad (27)$$

The right-hand side equals *cb* in Figure 4. If this condition is not satisfied, go to the next step.

2. S_m corresponds to Case 2 if the following condition is satisfied:

$$m < R\{1 - [\cos(I/2)/\cos(I/2 - I_1]\} \quad (28)$$

The right-hand side of Equation 28 equals *ca* in Figure 4. This is the radial distance from the curve center to the line of sight when the observer is at PC and object is at PT. If this condition is not satisfied, S_m may correspond to Case 1 or 2. Go to the next step.

3. To determine whether S_m corresponds to Case 1 or 2, first calculate θ_1^*, x_1, and x_2 for Case 1. If x_1 and x_2 are positive or zero, then S_m corresponds to Case 1. Otherwise, S_m corresponds to Case 2.

The following numerical example illustrates these steps. Suppose that R = 1,500 ft, I = 38.2°, m = 30 ft, and I_1 = 7.64°. In Step 1, the right-hand side of Equation 27 equals 13.32 ft and Equation 27 is not satisfied. Therefore, this is not Case 3. In Step 2, the right-hand side of Equation 28 equals 53.74 ft. Therefore, Equation 28 is satisfied and S_m corresponds to Case 2. For Case 2, calculate m_1 = 200.12 ft (Equation 4) and α = 167.58° (Equation 6). Solving Equation 19 by successive approximations (Appendix B) gives θ_1^* = 3.25°. Then, ϕ = 88.47° (Equation 17), γ = 78.42° (Equation 16), I_2 = 20.75° (Equation 15), and S_m = 614 ft (Equation 18).

PRACTICAL ASPECTS

The minimum sight distance on a horizontal curve must be determined to know whether the required sight distance (stopping, decision, or passing) is satisfied. The sight distance profile is a necessary input to the cost-effectiveness analysis of locations with restricted sight distances. In this section the

sight distance profile, the application of the presented methodology to multiple obstacles, and a comparison with the NCHRP method are discussed.

Sight Distance Profile

The sight distance profile for a given obstacle for different values of the lateral clearance is shown in Figure 5. The obstacle is located at $I_1/I = 0.3$. The horizontal axis shows the location of the observer at various points of the tangent and curve. The PC is designated as the reference point, with the locations before it being negative and the locations beyond it being positive. The vertical axis shows the available sight distance for any given location of the observer. For example, for $m = 15$ ft, the minimum sight distance (435 ft) occurs when the observer is about 90 ft beyond PC. The sight distance profile is established using the developed relationships by computing the available sight distance for successive values of x_1. Unlike vertical curves, the minimum sight distance on a horizontal curve with a single obstacle occurs at a specific point on the traveled way rather than through a section of the traveled way.

For locations with restricted sight distances, the sight distance profile provides the length of the road within which the sight distance is restricted. This length is required for the operational and cost-effectiveness analysis developed by Neuman et al. (*14*). The probability that a critical event will occur at the location is directly proportional to the length of restricted sight distance. For example, if the required sight distance in Figure 5 is 600 ft and $m = 15$ ft, the SD profile shows that the length with a restricted sight distance is about 400 ft.

Application to Multiple Obstacles

For a horizontal curve with multiple obstacles, the sight distance profile of one obstacle interferes with the profiles of other obstacles. The actual sight distance profile is an envelope of the individual profiles, as shown in Figure 6. The horizontal curve has four obstacles with the indicated lateral clearances and locations on the curve. It is clear that Obstacle 2 is critical because it gives the least value of S_m (430 ft). The minimum sight distances can be determined using the developed relationships by considering each obstacle as a single obstacle (note that some obstacles may not have their minimum values on the sight distance envelope).

The interface among the profiles of various obstacles is an important element that should be considered in improving the sight distance on the curve. As noted in Figure 6, S_m on the curve can be improved by increasing the lateral clearance at Obstacle 2, but only to $S_m = 450$, which corresponds to Obstacle 4. Any further improvement in sight distance would require increasing the lateral clearances at both Obstacles 2 and 4, and so on. Thus, an obstacle that is currently not critical may become critical as other obstacles are displaced.

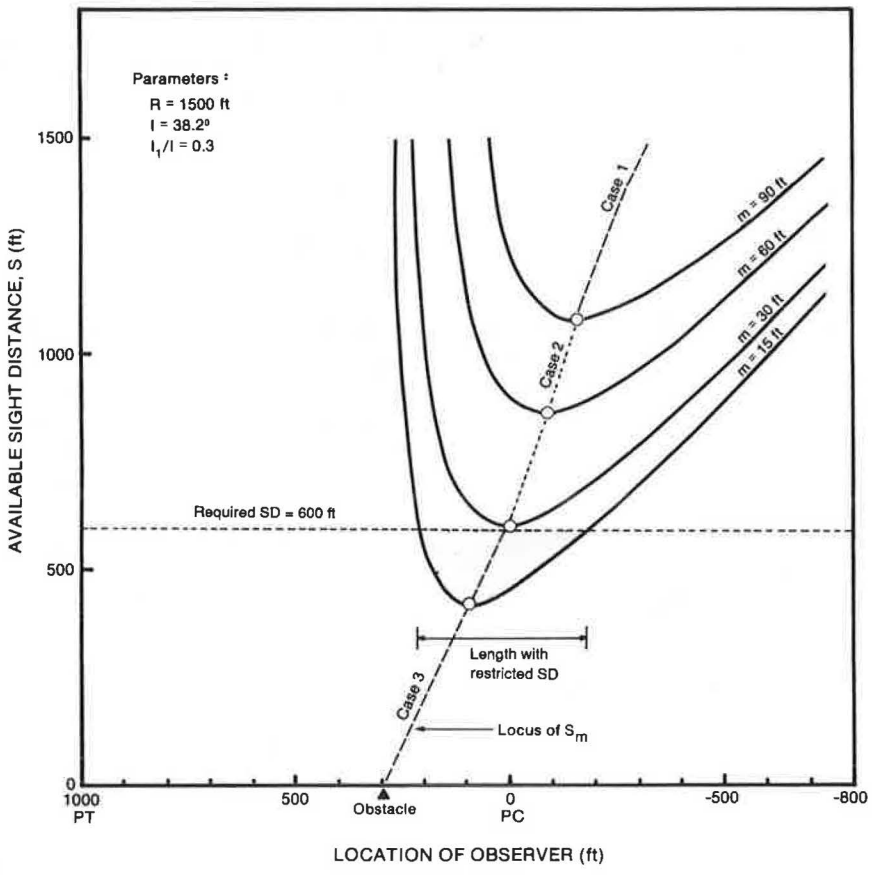

FIGURE 5 Sight distance profile on horizontal curve for different lateral clearances.

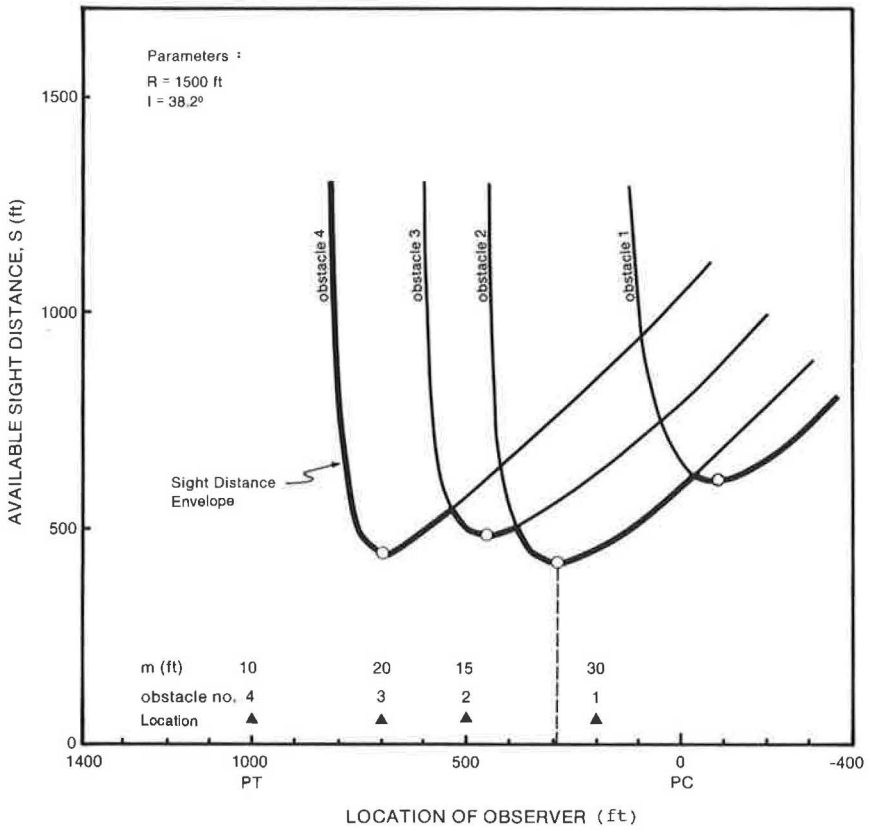

FIGURE 6 Sight distance envelope on horizontal curve with multiple obstacles.

Comparison with NCHRP Method

As previously indicated, the geometric relationships of the NCHRP report give the available sight distance for different locations of observer, object, and obstacle (*9,13*). Using these relationships, the available sight distance was computed for consecutive locations of the observer, and the sight distance profile was plotted as shown in Figure 7 (R = 1,000 ft, m = 80 ft, and I_1/I = 0.1). The sight distance profile based on the relationships presented in this paper is also shown. The S_m values of the NCHRP and presented methods are 1,020 ft and 950 ft, respectively. Thus, the NCHRP method overestimates S_m by about 7 percent. The differences in S_m were found to be much larger for I_1/I = 0 and smaller radii. However, the differences decrease as I_1/I approaches 0.5. The two methods give almost identical results of S_m for I_1/I = 0.5 in Case 1 and for any value of I_1/I in Case 3.

Although the difference between the minimum sight distances of the two methods is not large, the respective sight distance profiles are considerably different. If the required sight distance at the location is 1,100 ft, for example, the lengths of the restricted sight distance provided by the NCHRP and presented methods will be about 250 ft and 400 ft, respectively. Such a difference may affect the operational and cost-effectiveness analysis of restricted locations (*10,14*).

The difference between the two methods is caused by an assumption in the NCHRP relationships. The relationships implicitly assume that the lines connecting the observer and object to the curve center form equal angles with a perpendicular line drawn from the center to the line of sight. This assumption is not generally valid for computing the available sight distance. In addition, for computing S_m, this assumption is exact only for Case 1 (when I_1/I = 0.5) and Case 3.

EVALUATION AND DESIGN VALUES

To facilitate evaluation of the sight distance adequacy on horizontal curves, the developed relationships were used to establish values of the minimum sight distance for different characteristics of the curve and obstacle. The values are given in Tables 1 and 2, which are applicable to stopping, decision, and passing sight distances. Tables 1 and 2 can be used to

1. Determine the minimum sight distance on an existing curve and obstacles,
2. Determine the required lateral clearances to maintain a required minimum sight distance, and
3. Determine the critical lateral clearance (for design) that maintains a required minimum sight distance.

The critical lateral clearance, M, is the largest value of m for given S_m, R, and I. For $S_m \leq L$, the critical value is presented by AASHTO (*4*). For $S_m > L$, a formula and a nomograph for determining M were presented by Waissi and Cleveland (*13*). In Tables 1 and 2, the critical lateral clearance for $S_m \leq L$ or $S_m > L$ is the lateral clearance for I_1/I = 0.5. Figure 8 illustrates the results for R = 1,500 ft and I = 40°. As noted, there is a great difference between the lateral clearance requirements when the obstacle lies at PC (or PT) and

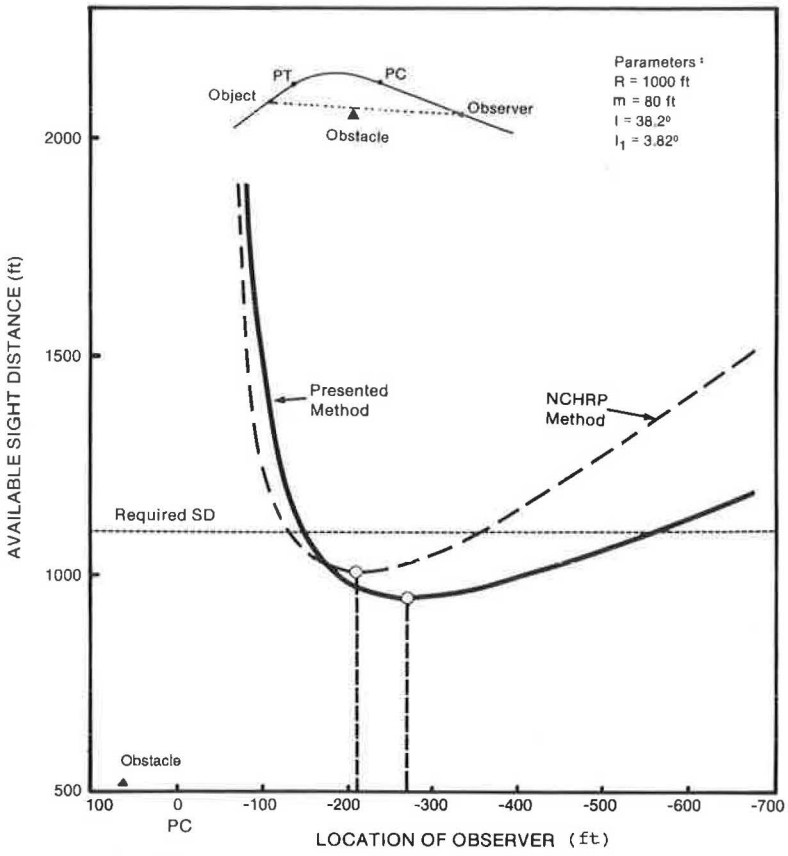

FIGURE 7 Comparison between sight distance profiles of presented and NCHRP methods.

TABLE 1 MINIMUM SIGHT DISTANCE ON HORIZONTAL CURVE WITH SINGLE OBSTACLE (R = 200 TO 800 ft)

Cent. Angle (deg)	Obst. Loc. (l_1/I)	Curve Radius (ft)																			
		200					400					600					800				
		m=20[a]	40	60	80	100	20	40	60	80	100	20	40	60	80	100	20	40	60	80	100
5	0.0	940	1850	2770	3690	4600	950	1870	2790	3700	4620	970	1890	2800	3720	4640	990	1910	2820	3740	4650
5	0.1	930	1850	2770	3680	4600	950	1870	2780	3700	4610	960	1880	2800	3710	4630	980	1890	2810	3730	4640
5	0.2	930	1850	2770	3680	4600	940	1860	2780	3690	4610	960	1870	2790	3710	4620	970	1880	2800	3720	4630
5	0.3	930	1850	2760	3680	4600	940	1860	2770	3690	4610	950	1870	2790	3700	4620	960	1880	2800	3710	4630
5	0.4	930	1850	2760	3680	4600	940	1860	2770	3690	4610	950	1870	2780	3700	4620	960	1870	2790	3710	4630
5	0.5	930	1850	2760	3680	4600	940	1860	2770	3690	4610	950	1860	2780	3700	4620	960	1870	2790	3710	4620
10	0.0	500	950	1410	1870	2320	530	990	1440	1900	2360	560	1020	1480	1940	2390	590	1050	1510	1970	2430
10	0.1	490	950	1410	1860	2320	520	980	1430	1890	2350	540	1000	1460	1920	2380	570	1030	1490	1950	2410
10	0.2	490	940	1400	1860	2320	510	970	1430	1880	2340	530	990	1450	1910	2370	550	1010	1470	1930	2390
10	0.3	480	940	1400	1860	2320	500	960	1420	1880	2340	520	980	1440	1900	2360	540	1000	1460	1920	2380
10	0.4	480	940	1400	1860	2320	500	960	1420	1880	2330	520	980	1430	1890	2350	540	990	1450	1910	2370
10	0.5	480	940	1400	1860	2320	500	960	1420	1870	2330	520	970	1430	1890	2350	530	990	1450	1910	2370
20	0.0	300	530	750	980	1210	360	590	820	1050	1280	410	650	880	1110	1340	470	710	950	1180	1410
20	0.1	290	520	750	970	1200	340	570	800	1030	1260	390	620	850	1080	1310	430	670	910	1140	1370
20	0.2	280	510	740	970	1200	320	550	780	1010	1240	360	600	830	1060	1290	410	640	870	1100	1340
20	0.3	270	500	730	960	1190	310	540	770	1000	1230	350	580	810	1040	1270	390	620	850	1080	1310
20	0.4	270	500	730	960	1190	310	540	770	1000	1230	340	570	800	1030	1260	380	610	840	1070	1300
20	0.5	270	500	730	960	1190	300	530	760	1000	1230	340	570	800	1030	1260	370	600	830	1060	1300
30	0.0	250	400	550	700	850	330	490	650	800	950	410	580	740	890	1050	470	660	820	980	1140
30	0.1	230	390	540	690	850	300	470	620	770	930	370	540	700	850	1010	420	610	770	930	1080
30	0.2	220	380	530	690	840	290	440	600	750	910	340	510	660	820	970	390	570	730	880	1040
30	0.3	220	370	530	680	830	270	430	580	740	890	320	490	640	800	950	370	540	700	850	1010
30	0.4	210	370	520	680	830	270	420	570	730	880	320	470	630	780	940	360	530	680	840	990
30	0.5	210	370	520	670	830	260	420	570	730	880	310	470	620	780	930	360	520	680	830	980
40	0.0	240	350	470	580	690	330	470	590	700	820	410	570	700	820	940	470	660	800	930	1050
40	0.1	220	340	450	570	680	300	430	550	670	790	360	520	650	770	890	400	590	740	860	980
40	0.2	210	320	440	550	670	280	410	530	640	760	330	480	610	730	850	370	550	690	810	930
40	0.3	200	310	430	550	660	260	390	510	620	740	320	460	580	700	820	360	520	660	770	890
40	0.4	190	310	430	540	660	260	380	500	610	730	310	450	570	680	800	360	510	640	750	870
40	0.5	190	310	420	540	660	260	380	490	610	730	310	450	560	680	800	360	510	630	750	870

[a] Lateral clearance (ft)

Note: minimum sight distances are expressed in feet.

TABLE 2 MINIMUM SIGHT DISTANCE ON HORIZONTAL CURVE WITH SINGLE OBSTACLE (R = 1,000 TO 3,000 ft)

Cent. Angle (deg)	Obst. Loc. (I_1/I)	Curve Radius (ft)																			
		1000					1500					2000					3000				
		m=20[a]	40	60	80	100	20	40	60	80	100	20	40	60	80	100	20	40	60	80	100
5	0.0	1010	1920	2840	3760	4670	1050	1970	2880	3800	4710	1090	2010	2920	3840	4760	1170	2090	3010	3930	4840
5	0.1	990	1910	2820	3740	4660	1030	1940	2860	3780	4690	1060	1980	2890	3810	4730	1130	2050	2960	3880	4800
5	0.2	980	1900	2810	3730	4650	1010	1930	2840	3760	4680	1040	1950	2870	3790	4710	1090	2010	2930	3850	4760
5	0.3	970	1890	2810	3720	4640	1000	1910	2830	3750	4660	1020	1940	2860	3770	4690	1070	1990	2910	3820	4740
5	0.4	970	1880	2800	3720	4630	990	1910	2820	3740	4660	1010	1930	2850	3760	4680	1060	1970	2890	3810	4730
5	0.5	960	1880	2800	3720	4630	990	1900	2820	3740	4650	1010	1930	2840	3760	4680	1050	1970	2890	3800	4720
10	0.0	620	1090	1550	2000	2460	700	1170	1630	2090	2550	770	1240	1710	2170	2630	910	1390	1860	2330	2790
10	0.1	600	1060	1520	1980	2430	660	1130	1590	2050	2500	720	1190	1650	2110	2570	840	1320	1780	2250	2710
10	0.2	580	1040	1500	1950	2410	630	1090	1550	2010	2470	680	1150	1610	2070	2530	790	1260	1720	2180	2640
10	0.3	560	1020	1480	1940	2400	610	1070	1530	1990	2450	660	1120	1580	2040	2500	750	1220	1680	2140	2600
10	0.4	550	1010	1470	1930	2390	600	1060	1520	1980	2430	640	1100	1560	2020	2480	730	1190	1650	2110	2570
10	0.5	550	1010	1470	1930	2390	590	1050	1510	1970	2430	640	1100	1560	2010	2470	720	1180	1640	2100	2560
20	0.0	520	770	1010	1240	1470	640	910	1150	1390	1620	740	1040	1290	1540	1770	900	1280	1560	1810	2060
20	0.1	480	720	960	1190	1420	570	840	1080	1320	1550	650	950	1200	1440	1670	780	1140	1430	1670	1920
20	0.2	450	680	920	1150	1380	530	790	1020	1260	1490	600	890	1130	1360	1600	720	1060	1330	1570	1810
20	0.3	420	660	890	1120	1350	510	750	990	1220	1450	580	850	1080	1310	1550	700	1010	1270	1500	1740
20	0.4	410	640	870	1100	1340	500	730	960	1190	1420	570	820	1050	1280	1510	700	990	1230	1460	1690
20	0.5	410	640	870	1100	1330	490	730	960	1190	1420	570	810	1040	1270	1500	700	980	1220	1450	1680
30	0.0	520	740	910	1070	1230	640	900	1100	1270	1440	740	1040	1270	1470	1640	900	1280	1560	1800	2010
30	0.1	460	670	840	1000	1160	550	810	1000	1170	1340	620	920	1140	1340	1510	740	1100	1370	1610	1820
30	0.2	420	620	790	950	1100	510	750	940	1100	1260	580	850	1060	1250	1410	700	1010	1270	1490	1690
30	0.3	410	600	750	910	1070	490	710	890	1050	1210	570	810	1010	1190	1350	700	990	1220	1420	1610
30	0.4	400	580	730	890	1040	490	700	870	1020	1180	570	810	990	1150	1310	700	980	1210	1390	1570
30	0.5	400	570	730	880	1040	490	700	860	1010	1170	570	810	990	1140	1300	700	980	1210	1390	1560
40	0.0	520	740	900	1040	1160	640	900	1100	1270	1420	740	1040	1270	1470	1640	900	1280	1560	1800	2010
40	0.1	450	650	810	950	1070	530	780	980	1140	1290	600	890	1110	1300	1470	720	1060	1330	1560	1770
40	0.2	410	600	760	890	1010	500	720	900	1060	1200	570	820	1020	1200	1360	700	990	1230	1440	1630
40	0.3	400	580	720	850	970	490	700	870	1010	1150	570	810	990	1150	1300	700	980	1210	1390	1570
40	0.4	400	570	710	820	940	490	700	860	990	1120	570	810	990	1140	1280	700	980	1210	1390	1560
40	0.5	400	570	700	820	930	490	700	860	990	1110	570	810	990	1140	1270	700	980	1210	1390	1560

[a] Lateral clearance (ft)

Note: minimum sight distances are expressed in feet.

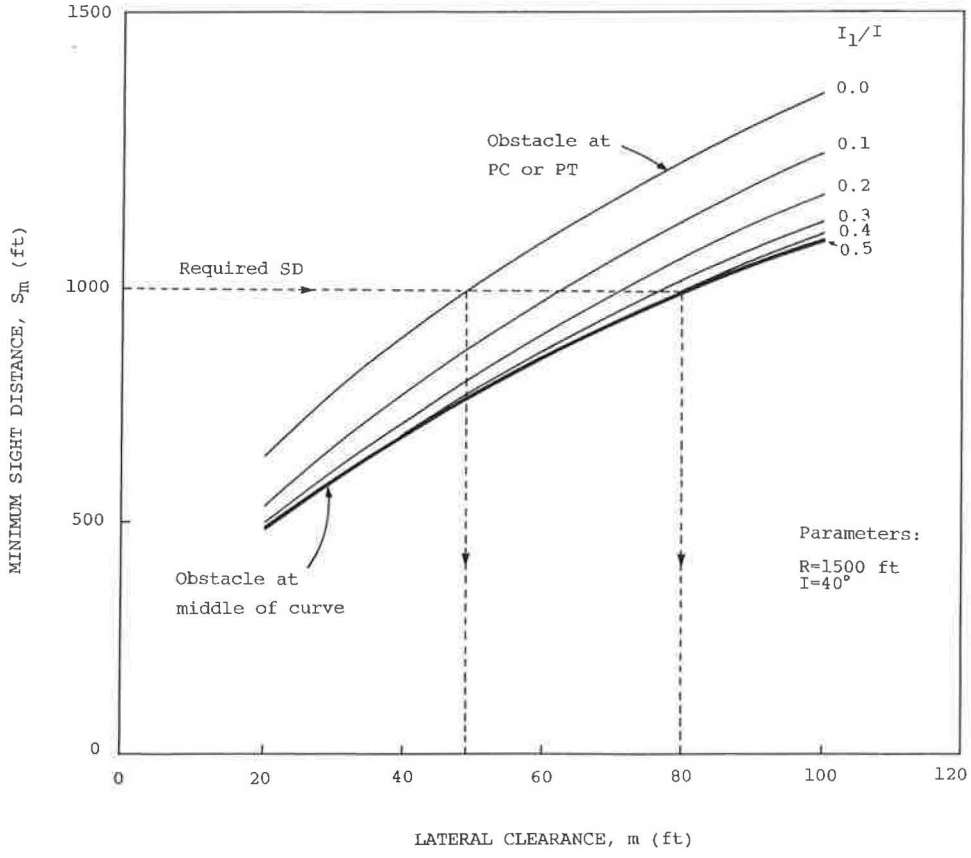

FIGURE 8 Comparison of lateral clearance requirements for different obstacle locations.

the middle of the curve; for example, for a sight distance of 1,000 ft, the lateral clearances needed are 49 ft and 80 ft, respectively.

Example

The following example illustrates the application of Tables 1 and 2. Given a horizontal curve with a single obstacle, R = 1,300 ft, m = 40 ft, I = 35°, and I_1 = 9.5°. The ratio I_1/I = 0.27. Then,

1. Determine S_m: Using Table 2, interpolate the values of S_m for R = 1,000 ft and 1,500 ft and I_1/I = 0.2 and 0.3 at I = 30° to obtain S_m = 682 ft. Repeat the interpolation for I = 40° to obtain S_m = 664 ft. Therefore, for I = 35°, S_m = 673 ft (the exact value of S_m computed by the presented relationships is 661 ft).
2. Determine m if the required sight distance is 800 ft: Using Table 2, the corresponding lateral clearance can be interpolated in a similar manner as m = 70 ft. The exact value of S_m (computed by the presented relationships) corresponding to this lateral clearance is 803 ft, which is very close to the required value.
3. Determine the critical lateral clearance: For S_m = 800 ft, M is determined from Table 2 as 75 ft (for I_1/I = 0.5). Using the Waissi and Cleveland formula (*13*), M is computed as 76 ft.

DISCUSSION OF RESULTS

Application of the AASHTO sight distance model for $S_m \leq L$ to situations in which $S_m > L$ results in overestimation of the maximum required lateral clearance M. Situations in which the sight distance is greater than the curve length may arise because of the following factors:

1. AASHTO policy (*4*) and NCHRP research (*9*) have presented increased values of SSD. In addition, Neuman (*5*) recommends greater SSD values than those of AASHTO for most of the highway classifications.
2. At locations with special geometry or conditions, the DSD should be provided. The AASHTO design values of DSD (*4*) and those recommended by Neuman (*5*) and McGee (*8*) are twice to three times the SSD design values.
3. Where AASHTO PSDs are provided, these distances will in most cases be greater than the curve length.

Even when $S_m \leq L$, the vision obstacle on the horizontal curve may lie near the ends of the curve so that the needed lateral clearance is less than the maximum value M. For these cases ($S_m \leq L$, $S_m > L$), the developed relationships provide exact values of the minimum sight distance or the lateral clearance that satisfy sight distance needs. Application of the presented method should result in cost savings from roadside clearing and perhaps land acquisition.

SUMMARY

Exact relationships for establishing the sight distance profiles for highway horizontal curves with a single obstacle or multiple obstacles on the inside of the curve are presented. Closed-form solutions of the minimum sight distance are also presented for any location of the obstacle, and design values for practical use are established. These values can be used to determine the adequacy of sight distance at a particular location. It is no longer necessary to plot the entire sight distance profile to determine whether the location has a restricted sight distance. Only for restricted locations is the sight distance profile plotted to determine the length of the road with restricted sight distance and to evaluate alternative improvements. The results of this research should be useful for the design, operation, and safety of critical highway locations.

ACKNOWLEDGMENT

This work was supported by the Natural Sciences and Engineering Research Council of Canada.

APPENDIX A
Derivation of the Formulas for S_m

CASE 1

Differentiating Equation 10 with respect to θ_1, then

$$\frac{dS}{d\theta_1} = m_1[\sin(\theta_1 + \alpha)\cos\theta_1 - \sin\theta_1\cos(\theta_1 + \alpha)] \div \sin^2(\theta_1 + \alpha) + m_2[\sin(\theta_1 + J - \beta)\cos(\theta_1 + J) - \sin(\theta_1 + J)\cos(\theta_1 + J - \beta)]/\sin^2(\theta_1 + J - \beta) \quad (29)$$

Consider the following identity (*15*):

$$\sin(x - y) = \sin x \cos y - \cos x \sin y \quad (30)$$

Based on this identity, the first and second expressions in brackets equal $\sin\alpha$ and $\sin(-\beta)$, respectively. Thus,

$$\frac{dS}{d\theta_1} = \frac{m_1 \sin\alpha}{\sin^2(\theta_1 + \alpha)} + \frac{m_2 \sin(-\beta)}{\sin^2(\theta_1 + J - \beta)} \quad (31)$$

Equating Equation 31 to zero and noting that $\sin(-\beta) = -\sin\beta$,

$$\frac{\sin(\theta_1^* + \alpha)}{\sin(\theta_1^* + J - \beta)} = \left(\frac{m_1 \sin\alpha}{m_2 \sin\beta}\right)^{1/2} \quad (32)$$

in which θ_1^* is the angle corresponding to the minimum sight distance. Equation 32 is the same as Equation 11.

CASE 2

Substituting for γ from Equation 16 into Equation 15 and then substituting for ϕ from Equation 17 gives

$$I_2 = 270° - \sin^{-1}(f) - \alpha - \theta_1 \quad (33)$$

where f is a function of θ_1 given by

$$f = \left(\frac{R - m}{R}\right) \sin(I_1 + \alpha + \theta_1 - 90°) \quad (34)$$

Substituting for I_2 from Equation 33 into Equation 18 and differentiating Equation 18 with respect to θ_1,

$$\frac{dS}{d\theta_1} = \frac{-f'}{(1 - f^2)^{1/2}} + \frac{m_1 \sin(\theta_1 + \alpha)\cos\theta_1}{\sin^2(\theta_1 + \alpha)} - \frac{m_1 \sin\theta_1 \cos(\theta_1 + \alpha)}{\sin^2(\theta_1 + \alpha)} - 1 \quad (35)$$

where f' equals $df/d\theta_1$, which is given by

$$f' = \left(\frac{R - m}{R}\right) \sin(\theta_1 + \alpha + I_1) \quad (36)$$

The expression in brackets in Equation 35 equals $\sin\alpha$ based on the identity of Equation 30. Substituting for f and f' from Equations 34 and 36 into Equation 35 and equating $dS/d\theta_1$ to zero gives

$$\frac{m_1 \sin\alpha}{R \sin^2(\theta_1^* + \alpha)} - \frac{(R - m)\sin(\theta_1^* + \alpha + I_1)}{[R^2 - (R - m)^2 \cos^2(\theta_1^* + \alpha + I_1)]^{1/2}} = 1 \quad (37)$$

which is Equation 19.

CASE 3

Equation 23 is written as

$$S = 2R[I_3 - \tan^{-1}(f)] \quad (38)$$

where f is a function of I_3 given by

$$f = [R(1 - \cos I_3) - m]/(R \sin I_3) \quad (39)$$

Differentiating Equation 38 with respect to I_3,

$$\frac{dS}{dI_3} = 2R\left[1 - \frac{f'}{(1 + f^2)}\right] \quad (40)$$

where $f' = df/dI_3$, which is given by

$$f' = \frac{(R \sin I_3)^2 - [R(1 - \cos I_3) - m]R \cos I_3}{R^2 \sin^2 I_3} \quad (41)$$

Substituting for f and f' from Equations 39 and 41 into Equation 40 and equating dS/dI_3 to zero gives

$$[R(1 - \cos I_3^*) - m]^2 + [R(1 - \cos I_3^*) - m]R \cos I_3^* = 0 \quad (42)$$

After rearranging, Equation 42 becomes

$$[R(1 - \cos I_3^*) - m](R - m) = 0 \quad (43)$$

which is Equation 24.

APPENDIX B
Numerical Solution of Equations 11 and 19

The critical angle θ_1^* of Equations 11 and 19 can be obtained by successive approximations using the method of linear interpolation (*16*). Equation 11 or 19 is written as

$$f(u) = 0 \quad (44)$$

where u is used instead of θ_1^*. To determine the root of Equation 44, select two values u_1 and u_2 for which $f(u_1)$ and $f(u_2)$ have opposite signs. The following steps are then performed:

1. Set

$$u_3 = u_2 - f(u_2)\frac{u_2 - u_1}{f(u_2) - f(u_1)}$$

2. If $f(u_3)$ has an opposite sign to $f(u_1)$, set $u_2 = u_3$. Otherwise, set $u_1 = u_3$
3. Repeat Steps 1 and 2 until

$$|u_2 - u_1| \leq \varepsilon_1$$

$$|f(u_3)| \leq \varepsilon_2$$

where ε_1 and ε_2 are specified tolerance values.

This method guarantees convergence. A modified linear interpolation method, which converges faster, may also be used (*16*).

REFERENCES

1. *A Policy on Sight Distance for Highways, Policies on Geometric Highway Design.* AASHO, Washington, D.C., 1940.
2. *A Policy on Geometric Design of Rural Highways.* AASHO, Washington, D.C., 1965.
3. *A Policy on Design Standards for Stopping Sight Distance.* AASHO, Washington, D.C., 1971.
4. *A Policy on Geometric Design of Highways and Streets.* AASHTO, Washington, D.C., 1984.
5. T. R. Neuman. New Approach to Design for Stopping Sight Distance. In *Transportation Research Record 1208*, TRB, National Research Council, Washington, D.C., 1989, pp. 14–22.
6. D. W. Harwood and J. C. Glennon. Passing Sight Distance Design for Passenger Cars and Trucks. In *Transportation Research Record 1208*, TRB, National Research Council, Washington, D.C., 1989, pp. 59–69.
7. J. C. Glennon. New and Improved Model of Passing Sight Distance on Two-Lane Highways. In *Transportation Research Record 1195*, TRB, National Research Council, Washington, D.C., 1988, pp. 132–137.
8. H. W. McGee. Reevaluation of the Usefulness and Application of Decision Sight Distance. In *Transportation Research Record 1208*, TRB, National Research Council, Washington, D.C., 1989, pp. 85–89.

9. P. L. Olson, D. E. Cleveland, P. S. Fancher, L. P. Kostyniuk, and L. W. Schneider. *NCHRP Report 270: Parameters Affecting Stopping Sight Distance*. TRB, National Research Council, Washington, D.C., 1984.
10. T. R. Neuman and J. C. Glennon. Cost-Effectiveness of Improvements to Stopping Sight Distance. In *Transportation Research Record 923*, TRB, National Research Council, Washington, D.C., 1984, pp. 26–34.
11. J. C. Glennon. Effects of Sight Distance on Highway Safety. In *State-of-the-Art Report 6*, TRB, National Research Council, Washington, D.C., 1987, pp. 64–77.
12. W. L. Raymond. Offsets to Sight Obstructions Near the Ends of Horizontal Curves. *Civil Engineering*, Vol. 42, No. 1, 1972, pp. 71–72.
13. G. R. Waissi and D. E. Cleveland. Sight Distance Relationships Involving Horizontal Curves. In *Transportation Research Record 1122*, TRB, National Research Council, Washington, D.C., 1987, pp. 96–107.
14. T. R. Neuman, J. C. Glennon, and J. E. Leish. *Stopping Sight Distance—An Operational and Cost Effectiveness Analysis*. Report FHWA/RD-83/067. FHWA, U.S. Department of Transportation, Washington, D.C., 1982.
15. S. I. Grossman. *Calculus*. Academic Press, New York, N.Y. 1981.
16. C. F. Gerald and P. O. Wheatley. *Applied Numerical Analysis*. Addison-Wesley Publishing Company, London, England, 1985.

Publication of this paper sponsored by Committee on Geometric Design.

Effects of Design Criteria on Local Street Sight Distance

J. L. GATTIS

Of the three roadway functional classes (arterial, collector, and local), the local road is the one intended to provided access. Local street design criteria interact to affect the available sight distance. Urban residential streets of the type often found in newer subdivisions tend not to be laid out in the traditional grid pattern, but rather in a more free-form pattern incorporating elements of discontinuity and curvilinear alignment. In these settings, on-street parking, whether on both sides of the street or only on one side, forces vehicles traveling in opposite directions to operate in the same lane. The presence of vegetation or other objects at the curbside can also limit the available head-on sight distance. Where two lanes of traffic moving in opposite directions operate in one lane, the amount of sight distance needed is greater than under normal conditions. The design needed is analogous to one that permits two locomotives to approach head-on on a single track and to stop before colliding. Roadway designers should recognize situations that require adequate head-on sight distance and provide a sight distance sufficient for the two approaching vehicles to react and stop before colliding.

Of the three roadway functional classes (arterial, collector, and local), and local road is the one intended to provide access. Desirable attributes of local streets serving residential lots include safety, efficiency, and enhancement of the "livability" (*1*) of the residential area. In addition, they must be built with a recognition of economic considerations.

Certain local street design criteria act in concert to affect the available sight distance. Included is a brief review of certain design guidelines for residential streets and observations about the actual applications of these criteria. This is followed by a discussion of the interactions of various criteria when they are incorporated into a design and resulting deficiencies that may not be specifically addressed by current design practices.

The local roads discussed are the type of urban residential streets often found in newer subdivisions. These streets tend not to be laid out in the traditional grid pattern, but rather in a more free-form pattern that includes elements of discontinuity and curvilinear alignment.

SELECTED LOCAL STREET DESIGN CRITERIA

The function of the local or residential street is to furnish access to abutting properties, not to provide high levels of movement. The recommended design criteria for residential streets reflect these needs. Although not all published design guidelines agree on all aspects of residential area layout and street design (*2*), certain perspectives and attributes seem to be predominant.

Oklahoma Transportation and Infrastructure Center, University of Oklahoma, 202 W. Boyd, Room 334, Norman, Okla. 73019.

Sight Distance

Sight distance refers to a distance along the roadway ahead of the driver for which the driver has a specified needed visibility. Three types of sight distance are stopping sight distance (SSD), passing sight distance (PSD), and decision sight distance (DSD). The AASHTO Green Book states, "The minimum sight distance available on a roadway should be sufficiently long to enable a vehicle traveling at or near the design speed to stop before reaching a stationary object in its path" (*3*). Furthermore, it states that "it is normally of little practical value to provide passing sight distance on two-lane urban streets" (*3*). If adequate SSD is to be available on a residential street, then the available sight distance (S) must exceed the needed SSD (*4*).

SSD has two components. The initial component, the distance traveled while the driver recognizes the need to stop and activate the brake pedal, has been called the perception, identification, emotion, and volition (PIEV) time (*5*), or the perception-reaction time (PRT). The second component is the actual braking distance over which the vehicle decelerates. The sum of the two distances, or the SSD, is

$$SSD = 1.467 * V * t_{PR} + V^2/[30 * (f \pm G)] \quad (1)$$

where

V = initial velocity (mph),
t_{PR} = perception-reaction time (sec),
f = braking friction coefficient, or friction factor, and
G = grade in decimal form.

Minimum acceptable residential street sight distances are in the range of 110 ft or more (*1,6*).

Even after the velocity and grade are defined for a given situation, the calculated SSD will vary according to the chosen t_{PR}- and f-values. The current t_{PR} design value is 2.5 sec, or 1.0 sec for reacting to traffic signal changes. Use of the lesser value for reactions to signal change intervals is based on the presumption that the driver approaching a signal is more prepared to react to a change from green to yellow. A review by Taoka (*7*) showed the mean signal change t_{PR}-values found by other researchers to range from 1.1 to 1.3 sec. Investigations of the response times of older or impaired drivers or of the braking capabilities of newer vehicles may eventually lead

to changes in the current t_{PR}- and f-values, which will in turn affect SSD values.

Layout and Length

The street layouts in many newer residential areas are influenced by the concept of functional hierarchy. Although this concept may be misunderstood by some who attempt to use it, the concept dictates the setting of certain objectives. Two such objectives are to discourage excessive volumes and to provide a discontinuous internal-local street system that discourages through traffic (*8*). The length of a continuous residential street can influence the degree to which these objectives are met.

Some recommended design criteria set a maximum length for residential streets. One publication (*8*) suggests maximum lengths of 750 ft for cul-de-sacs and 1,300 ft for other local streets. Others would allow longer maximum lengths (*1*,*9*).

The maximum residential street length should be a function of the intensity of development. With more intense development, more traffic can be expected per unit of length. Therefore, the maximum length should decrease when higher development intensities exist, assuming that other factors, such as street width, remain constant.

Width

Commonly recommended design widths for residential streets, face of curb to face of curb, range from 26 ft (*3*) to 28 ft (*8*), although lesser (*1*,*9*) and greater values can be found (*6*). The common residential street widths are not intended to accommodate vehicles parked on both sides nor two lanes of traffic moving in opposite directions. Rather, the width is sufficient to accommodate automobiles parked on both sides of the street with one moving lane between them (*3*), which is acceptable because traffic volumes are light.

The street right-of-way should be wide enough to accommodate not only the traveled way, but also sidewalks and utilities. A commonly recommended right-of-way width for residential streets is 50 ft (*3*), with some sources listing values of 60 ft (*1*,*6*,*8*).

Design Speed

Recommended residential street design speeds range from 25 to 30 mph (*1*). These low design speeds permit alignment with greater horizontal and vertical curvature than would be allowed on roadways with higher design speeds. Table 1 presents combinations of design speeds, needed SSDs, and minimum allowable radii based on speed and superelevation or crossfall. Calculations are presented for both the standard 2.5-sec PRT and an assumed 1.2-sec PRT for alerted-driver situations. The 1.2-sec PRT calculations are included to show the sensitivity of the formula to a less conservative PRT value.

APPLICATIONS OF CURRENT CRITERIA

A review of how the various design criteria are applied in actual practice helps to identify design criteria interactions. The street system that results from interactions of design elements should not compromise the safety levels intended for the individual elements. Such a system should function well from the perspective of both the driver and the area residents. One author stated, "Elements in the local circulation system should not have to rely on extensive traffic regulations in order to function efficiently and safely" (*1*).

Sight Distance

The amount of sight distance available is not a design input, but rather a result of other inputs. Combinations of horizontal and vertical alignment, vegetation, parked cars, and fences limit the sight distance along some streets. In a local residential street setting, a limited sight distance that restricts passing maneuvers is acceptable.

TABLE 1 SELECTED RESIDENTIAL STREET DESIGN CRITERIA

Assumed Speed (mph)	Perception-reaction time (sec)	Distance during P-R (ft)	Wet[1] braking distance (ft)	Stopping sight distance (ft)	Minimum[2] allowable radius (ft)
25	1.2	44.0	54.8	99	114
25	2.5	91.7	54.8	146	114
30	1.2	52.8	85.7	139	179
30	2.5	110.0	85.7	196	179

[1] Braking distance calculated assuming 0 grade.

[2] Minimum allowable radius assumes -3/16 inch/ft crossfall, side f=0.252 for 25 mph, side f=0.221 for 30 mph

When using the SSD formula, the engineer measures or estimates the velocity and grade for each situation because these variables are site specific and relatively easily determined. However, for PRT and friction factors the engineer would probably rely on values obtained from a table, in effect conclusions of published research or engineering practice guidelines.

Layout and Length

The combination of short lengths and a hierarchical layout, which directs residential neighborhood traffic onto collector streets, should lower the possibility that two vehicles traveling in opposite directions will encounter each other on a residential street. However, if the subdivision layout does not provide true collectors, some residentially designed streets are forced to function as collectors. Under such conditions, the frequency with which vehicles traveling in opposite directions may meet at or near parked cars may increase.

Many residential streets are longer than the recommended minimums. A review of street layouts in place shows that some designers are either unaware of or have ignored the hierarchical layout concept. Some of the subdivision streets built to residential design criteria are functioning as collectors.

Width

Within the confines of the allocated residential street width, cars may be parked at irregular intervals on one or both sides. A vehicle traveling on the street will stay on the right side except when encountering a vehicle parked on the right side; the moving vehicle will then use the center portion of the road to, in effect, pass the parked vehicle.

The amount of parking on the street will vary according to the density of the development, amount of space provided for off-street parking on each lot (e.g., single or double driveways), and social patterns of the residents. A vehicle parked along the curb "takes up space and blocks views and sight lines" (*6*).

The residential street right-of-way may or may not include sidewalks or utility poles. The rights-of-way of some neighborhoods contain liberal amounts of shrubs and trees. One author (*2*) called for steady rows of trees in a residential area, going on to state, "Since the tree canopies must be clear of the building line . . . the trees must be placed as close as possible to the curb." Other studies may lead to a different view of the urban clear-zone issue (*10*). In any event, there are plenty of tree-lined urban streets, some with vegetation of sufficient size and density to create the effect of a wall beside the traveled way.

Design Speed

Anyone who has worked as a city traffic engineer has probably received calls from citizens complaining about speeders on their street. An investigation of the situation will reveal that most drivers are driving close to the speed limit; only a few vehicles significantly exceed the speed limit.

In other situations, higher speeds may occur, especially on those streets designed as local residential but functioning as collectors. For the purposes of the following illustrations, design speed operation is assumed.

COMBINED EFFECTS

Consider the effects of these design criteria when combined in a residential street setting:

1. The length of some residential streets or the layout of the subdivision will cause a higher traffic volume on some parts of the local street system.
2. Within the street and right-of-way widths provided, cars will be parked intermittently on both sides of the street, effectively creating one-lane operation on some stretches. Trees, shrubs, or fences may be along or even in the right-of-way.
3. The roadway design speeds will be 25 to 30 mph, with expected operating speeds in this same range.

These combined factors can create the following scenario. Two vehicles traveling in opposite directions at 25 mph approach each other on a horizontal curve with a 150-ft radius. Parked cars line both sides of the street. The curve length is 220 ft. As the two vehicles enter their respective ends of the curve, the two drivers cannot see each other approaching. There is adequate SSD. How safe is the situation?

Figures 1 and 2 show residential streets with sharp horizontal curvature. In Figure 1, cars are parked along the curbs, leaving only the middle of the street available for moving traffic; vegetation in the margin blocks the view on the inside of the curve. In Figure 2, an oncoming moving vehicle is traveling in the center of the street, threading its way among cars parked on both sides of the street. Both photographs show how design element interactions in a real-world environment can limit the sight distance around the curve.

NEEDED SIGHT DISTANCE AND DESIGN CONTROLS

The practice of permitting parking on both sides of a residential street, combined with a 26- to 28-ft-wide paved sec-

FIGURE 1 Parked cars and vegetation limit sight distance.

FIGURE 2 Vehicles traveling in center of residential street.

tion, will occasionally cause the street to operate as a one-lane street with two-way traffic. The resulting effect is that normal SSD may not always be an adequate design control. Adequate SSD permits a vehicle to stop before colliding with a stationary object in its path. The "one lane street with two-way traffic' phenomenon necessitates that sight distance be adequate to permit two vehicles moving toward each other to be able to stop before colliding. Designing for normal SSD is analogous to permitting two locomotives approaching head-on, on a single track, to stop before colliding.

Table 2 contrasts the sight distance needed for these head-on situations with the currently recommended SSD values.

Using an approach that complements the concept contained in "Sight Distance on Horizontal Curves" in the AASHTO Green Book (*3*), Figure 3 shows schematically the geometric considerations on a residential street horizontal curve. The following factors are assumed:

1. Face-to-face residential street width is 28 ft;
2. Cars parked along the curb have an effective "view-blocking" width of 8 ft, so a clear line of sight that passes (28/2) − 8 = 6 ft from the centerline is needed;

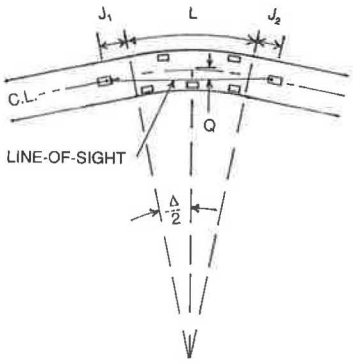

FIGURE 3 Geometric layout.

3. Vehicles and drivers are positioned so that needed head-on sight distance (HSD) is measured along the centerline;
4. Vehicles approaching the curve of length L are the same distance away from the middle of the horizontal curve (i.e., $j_1 = j_2 = j$); and
5. Vehicles are parked along both curbs, particularly on the inside of the middle of the curve.

For a given design speed, there is a minimum allowable HSD. This HSD equals $2 * j + L$. For a given radius, the central angle Δ must be limited so that the resulting offset distance (Q) from the curve centerline to the line of sight is no more than 6 ft. Said another way, if certain limits are exceeded, a horizontal curve will "bend out of sight" and result in a deficient HSD.

The offset distance from the centerline to the line of sight can be expressed as

$$Q = R * (1 - \cos \Delta/2) + j * \sin \Delta/2 \quad (2)$$

Substituting,

$$Q = R * (1 - \cos \Delta/2) + [(\text{HSD} - 100 * \Delta * R/5729.578)/2] * \sin \Delta/2 \quad (3)$$

TABLE 2 SIGHT DISTANCE COMPARISON

Assumed Speed (mph)	Perception-reaction time (sec)	Distance during P-R (ft)	Wet[1] braking distance (ft)	Needed total S for two approaching vehicles (ft)	Currently[2] recommended SSD (ft)
25	1.2	44.0	54.8	198	146
25	2.5	91.7	54.8	293	146
30	1.2	52.8	85.7	277	196
30	2.5	110.0	85.7	391	196

[1] Braking distance calculated assuming 0 grade.

[2] Currently recommended per Green Book Table III-1, using t_{PR} = 2.5 sec

By establishing the maximum or limiting value of Q and the needed value of HSD, one may solve for Δ.

Using the criteria from this example, Table 3 provides example limiting design values. The radius and design speed are assumed, and from them an HSD value and then a maximum allowable Δ are found. Using a PRT longer than the 1.2 sec used in Table 3 would result in smaller values of maximum Δ.

DESIGN CONSIDERATIONS

The probabilities of a potential HSD problem need to be evaluated when design controls are set. Certain design and operational considerations should also be studied before design criteria are established for situations with two-way operation in one lane.

Probability of Encounter

Even though a theoretical geometric deficiency exists, the various contributing factors must be present simultaneously before adverse results become a reality. The probability of experiencing operating problems caused by deficient HSD will vary from location to location. Given the lower volumes on the residential street, many of the vehicles that enter a curve will not simultaneously encounter wet pavement, cars parked on both sides creating a one-lane segment, parked cars or vegetation restricting sight distance, and a vehicle coming from the opposite direction. A low probability of encounter may justify less conservative design assumptions.

Driver Perception-Reaction Time

For short lengths of two-way in one-lane operation, the driver should be alerted to the potentially precarious situation, which should lower the driver's reaction time.

On the other hand, the driver is faced with an object contrast problem (*11*) in which he must search out and identify the front parts of an oncoming vehicle from the row of parked cars along the curb. This may tend to increase the amount of t_{PR} needed.

TABLE 3 MAXIMUM ALLOWABLE CENTRAL ANGLE FOR GIVEN RADIUS

Radius (ft)	Design Speed (mph)	Head-on Sight Distance[1] (feet)	Maximum Δ (degrees)
150	25	198	7.30
300	25	198	7.74
450	25	198	8.33
450	30	277	5.38
600	30	277	5.55

[1] Head-on sight distance calculated using t_{PR} = 1.2 sec

Speed

Some motorists may slow down when encountering short lengths of one-lane operation between parked cars on residential streets. If so, the design V used in the stopping equation can be decreased. If studies find that other motorists travel through small-radius horizontal curves at higher than design speeds, then a higher speed should be entered into the equation. Perhaps drivers are more likely to exceed design speed on a 25-mph local residential street than they are on a 30-mph section.

Appropriate Friction Factors

Friction values used in the SSD formula tend toward a worst-case scenario—tires with minimal tread on a wet, slick pavement. With two approaching vehicles, is the probability that both will have minimal tread great enough to justify using near-worst-case f-values?

Another friction issue is decreased available deceleration on a horizontal curve (*11*). A vector analysis of braking on a curve (*12*) suggests a longer stopping distance for horizontal curves than for tangents:

$$f_H^2 = f^2 - [V^2/(15 * R) - e]^2 \quad (4)$$

where

f_H = braking friction coefficient available on a horizontal curve,
f = braking friction coefficient available on a tangent,
V = velocity (mph),
R = radius (ft), and
e = superelevation rate.

Using the values from the previous case and calculating for a vehicle on the inside of the curve (positive superelevation or crossfall),

$$f_H^2 = 0.38^2 - [25^2/(15 * 150) - 0.015625]^2$$
$$= 0.1444 - (625/2{,}250 - 0.015625)^2 = 0.075675$$
$$f = 0.275092 \quad (5)$$

This methodology finds an available friction of 0.275092/0.38 = 0.724, or 72.4 percent of the original. This would increase the calculated stopping distance of one car from 99 to 119.7 ft. The combined stopping distance for two oncoming vehicles, or the HSD, would change from 198 to 239 ft. The calculated sight distance deficiency becomes greater than indicated by the initial analysis, which used f = 0.38 for 25-mph urban operation.

Vertical Curvature

In addition to problems associated with local residential street horizontal curves, there are potential problems at vertical curves (VCs). Crest vertical curves at intersections of steep grades may have adequate SSD, but inadequate HSD. Three

mitigating factors work to counteract limited HSD over crest curves:

1. Vehicles traveling uphill require shorter stopping distances.
2. In the design of a VC for SSD in accordance with the Green Book (*3*), the driver's eye height is taken to be 3.5 ft and an object on the road, 0.5 ft high. A VC designed for HSD would instead use the 4.25-ft PSD object height.
3. A t_{PR} of less than 2.5 sec may be acceptable if drivers are more alert while maneuvering through short sections on local residential streets with inadequate HSD.

One would not expect a properly designed sag vertical curve to have inadequate HSD.

SUMMARY AND RECOMMENDATIONS

Where two lanes of traffic moving in opposite directions operate in one lane, as happens on many residential streets, an amount of sight distance greater than SSD is needed. Approaching motorists must be able to react and stop before colliding.

Design standards should recognize the need for and provide sufficient HSD for the two approaching vehicles to react and stop before colliding on both horizontal and vertical curves. The need may exist when parking occurs on both sides of a residential street, or even when parking exists on only one side of more narrow streets. The presence of vegetation or other large fixed objects at the side of the curb may obstruct the driver's view and can help create these situations.

If a simple horizontal curve is short (curve length much less than SSD) and has only a slight deflection, the head-on sight deficiencies would be less likely to occur. The driver's view ahead would include the forward tangent, so the roadway would not continue to curve until it is out of the sight line.

Where HSD is deficient on local residential streets, parking restrictions may provide a remedy. Removing view-obstructing objects along the roadway may also be in order. Each agency responsible for roadways must be empowered with suitable ordinances and effective enforcement in order to remove sight-blocking vegetation, fences, and other obstacles.

More study is needed to determine the proper PRT for certain local residential street situations. For short lengths of two-way-in-one-lane operation, perhaps an alerted reaction time of less than the standard 2.5 sec would be appropriate, although the current 1.0 sec used for traffic signal timing may be too short. Other parameters, such as the proper tire friction values at lower speeds on a curve, the amount of sight clearance around a parked car needed to perceive another moving car, and the suitable assumed lateral position of the driver's eye (from the row of parked cars or inside curb) will need definition in order to design for these situations.

REFERENCES

1. *Recommended Guidelines for Subdivision Streets*. Institute of Transportation Engineers, Washington, D.C., 1984.
2. F. Spielberg. The Traditional Neighborhood Development: How Will Traffic Engineers Respond? *ITE Journal*, Vol. 59, No. 9, Sept. 1989, pp. 17–18.
3. *A Policy on Geometric Design of Highways and Streets*. AASHTO, Washington, D.C., 1984.
4. G. R. Waissi and D. E. Cleveland. Sight Distance Relationships Involving Horizontal Curves. In *Transportation Research Record 1122*, TRB, National Research Council, Washington, D.C., 1987, pp. 96–107.
5. L. J. Pignataro. *Traffic Engineering*. Prentice Hall, Inc., Englewood Cliffs, N.J., 1973.
6. W. S. Homburger, E. A. Deakin, P. C. Bosselman, D. T. Smith, and B. Beukers. *Residential Street Design and Traffic Control*. Institute of Transportation Engineers, Washington, D.C., 1989.
7. G. T. Taoka. Brake Reaction Times of Unalerted Drivers. *ITE Journal*, Vol. 59, No. 3, March 1989, pp. 19–21.
8. V. G. Stover and F. J. Koepke. *Transportation and Land Development*. Prentice Hall, Inc., Englewood Cliffs, N.J., 1988.
9. Summary of Proposed Revisions–Guidelines for Residential Subdivision Street Design. *ITE Journal*, Vol. 60, No. 5, May 1990, pp. 35–36.
10. D. S. Turner and E. R. Mansfield. Urban Trees and Roadside Safety. *Journal of Transportation Engineering*, Vol. 116, No. 1, Jan. 1990, pp. 90–103.
11. D. E. Cleveland et al. Stopping Sight Distance Parameters. In *Transportation Research Record 1026*, TRB, National Research Council, Washington, D.C., 1985, pp. 13–23.
12. T. R. Neuman, J. C. Glennon, and J. E. Leisch. Functional Analysis of Stopping-Sight Distance Relationships. In *Transportation Research Record 923*, TRB, National Research Council, Washington, D.C., 1983, pp. 57–64.

Publication of this paper sponsored by Committee on Geometric Design.

Sight Distance Model for Unsymmetrical Crest Curves

SAID M. EASA

In the AASHTO geometric design policy, the need for using unsymmetrical vertical curves because of clearance restrictions and other design controls is pointed out. Formulas for laying out these curves are presented in the highway engineering literature. However, no relationships are available concerning sight distance characteristics on these curves. A sight distance model for unsymmetrical crest curves has been developed to relate the available sight distance to the curve parameters, driver and object heights, and their locations along the curve. These relationships are used in a procedure for determining the available minimum sight distance. The model is used to explore the distinct features of sight distance profiles on unsymmetrical crest curves. To facilitate practical use, the model is used to establish design length requirements of unsymmetrical crest curves based on the stopping, decision, and passing sight distance needs presented by recent innovative approaches and by AASHTO. The model should prove useful in the design and safety evaluation of critical highway locations.

Three types of sight distances are considered on highways and streets: (a) stopping sight distance (SSD), applicable to all highways; (b) passing sight distance (PSD), applicable only to two-lane highways; and (c) decision sight distance (DSD), needed at complex locations [AASHTO (*1–4*), Neuman and Glennon (*5*), Olson et al. (*6*)]. Sight distance is one of the most fundamental criteria affecting the design of horizontal and vertical curves and their construction cost and safety. The effect of sight distance on highway safety has been addressed by Glennon (*7*) and Urbanik et al. (*8*). To meet this criterion, the available sight distance at any point on the curve must be greater than the required sight distance. For vertical crest curves, the available sight distance depends on the curve design parameters, the driver's eye height, the height of the road object, and the positions of the driver and the object.

The AASHTO sight distance models for crest (and sag) vertical curves (*1–4*) are based on a parabolic curve with an equivalent vertical axis centered on the vertical point of intersection (PVI). For simplicity, this symmetrical curve, which has equal horizontal projections of the tangents, is usually used in roadway profile design. In AASHTO's *Policy on Geometric Design of Highways and Streets* (Green Book) (*4*) it is pointed out that on certain occasions, because of critical clearance or other controls, the use of unsymmetrical curves may be required. Because the need for these curves is infrequent, no information on them has been included in the Green Book; for limited instances, this information is available in highway engineering texts.

A number of existing highway and surveying engineering texts (*9–11*) derive or present the formulas required for laying out an unsymmetrical curve (which consists of two unequal parabolic arcs with a common tangent). These formulas relate the rates of change in grade of the two arcs to the total curve length, the algebraic difference in grade, and the lengths of the arcs. Apparently, however, no information has been presented in the literature concerning the relationships between sight distance and the parameters of an unsymmetrical curve. These relationships are needed to design the curve length that satisfies a required sight distance or to evaluate the adequacy of sight distance on existing unsymmetrical curves.

A sight distance model for unsymmetrical crest curves has been developed and used to establish design length requirements for these curves based on SSD, DSD, and PSD. Before the model is presented, it is useful to describe the characteristics of an unsymmetrical curve.

The unsymmetrical vertical curve connects two tangents of the grade line and consists of two parabolic arcs with a common tangent point, PCC, located at PVI as shown in Figure 1. The first and second tangents have grades g_1 and g_2 (in decimals) and intersect at PVI. The grade is positive if it is upward to the right and negative if it is downward to the right. The beginning and end points of the curve are BVC (beginning of vertical curve) and EVC (end of vertical curve). The length of the vertical curve is L and the lengths of its first and second parabolic arcs are L_1 and L_2. The algebraic difference in grade of the vertical curve, A, equals $(g_1 - g_2)$.

The formulas for the rates of change in grade of the first and second parabolic arcs, r_1 and r_2, are given by Hickerson (*9*):

$$r_1 = AL_2/LL_1 \tag{1}$$

$$r_2 = AL_1/LL_2 \tag{2}$$

The ratio (A/L) is the rate of change in grade for the vertical curve if it were symmetrical $(L_1 = L_2 = L/2)$. Therefore, if $L_1 > L_2$ for an unsymmetrical curve, r_1 would be smaller than the rate of change in grade of the respective symmetrical curve and r_2 would be greater. This means that the parabolic arc with a smaller length is sharper and the arc with a larger length is flatter. For this reason, the minimum sight distance on an unsymmetrical curve would be smaller than that of a symmetrical curve of the same length.

GEOMETRIC RELATIONSHIPS

Suppose that the second parabolic arc of the unsymmetrical curve has a shorter length. To determine the minimum sight

Department of Civil Engineering, Lakehead University, Thunder Bay, Ontario, Canada P7B 5E1.

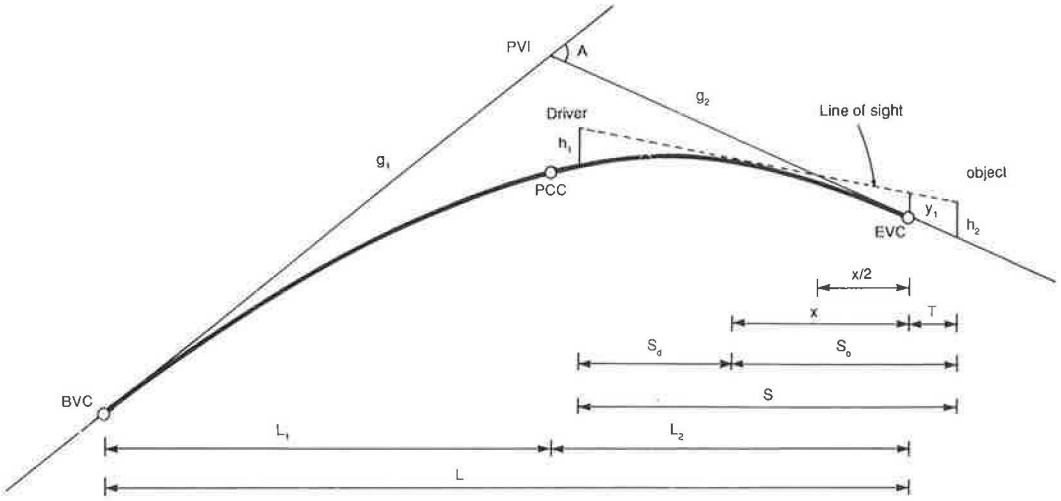

FIGURE 1 Case 1: Object beyond EVC and driver on second arc.

distance, S_m, on the curve, the following five cases are considered:

- Case 1: Object beyond EVC and driver on second arc,
- Case 2: Object beyond EVC and driver on first arc,
- Case 3: Object beyond EVC and driver before BVC,
- Case 4: Object before EVC and driver on first arc, and
- Case 5: Object before EVC and driver before BVC.

The relationships between the available sight distance S and the vertical curve length are derived for each of these cases for a specified location of the object. These relations are used later to determine S_m. The derivation is divided into the following three parts:

1. Derivation of the distance between the object and the tangent point of the line of sight, S_o;
2. Derivation of the distance between the driver and the tangent point of the line of sight, S_d; and
3. Obtaining the sight distance, $S = S_o + S_d$.

Case 1: Object Beyond EVC and Driver on Second Arc

In Case 1, the object lies beyond (or at) EVC and the driver is on the second arc. The distance between the object and EVC is denoted by T. Figure 1 shows the geometry of this case.

Component S_o

On the basis of the property of a parabola, the vertical distance from EVC to the line of sight, y_1, is given by

$$y_1 = r_2x^2/2 \tag{3}$$

where x is the distance from EVC to the tangent point of the line of sight. Based on the similarity of the two triangles with bases h_2 and y_1, a quadratic equation in x is formed and the following relationship can be obtained:

$$x = -T + [T^2 + (2h_2/r_2)]^{1/2} \tag{4}$$

The distance S_o, which equals $T + x$, becomes

$$S_o = [T^2 + (2h_2/r_2)\ ]\ 1/2 \tag{5}$$

Component S_d

On the basis of the property of a parabola, S_d is given by

$$S_d = (2h_1/r_2)^{1/2} \tag{6}$$

Sight Distance S

The sight distance S is the sum of the components of Equations 5 and 6, which gives

$$S = [T^2 + (2h_2/r_2)]^{1/2} + (2h_1/r_2)^{1/2} \tag{7}$$

If the object is at EVC ($T = 0$), Equation 7 indicates that S will be constant and will remain so even if the object is before EVC, as long as both the driver and object are on the second arc.

Case 2: Object Beyond EVC and Driver on First Arc

The geometry of Case 2 is shown in Figure 2. Assume for now that the line of sight is tangent to the second arc. (The situation when the line of sight is tangent to the first arc is addressed later.)

Component S_o

The derivation of S_o is similar to Case 1. Thus,

$$S_o = [T^2 + (2h_2/r_2)]^{1/2} \tag{8}$$

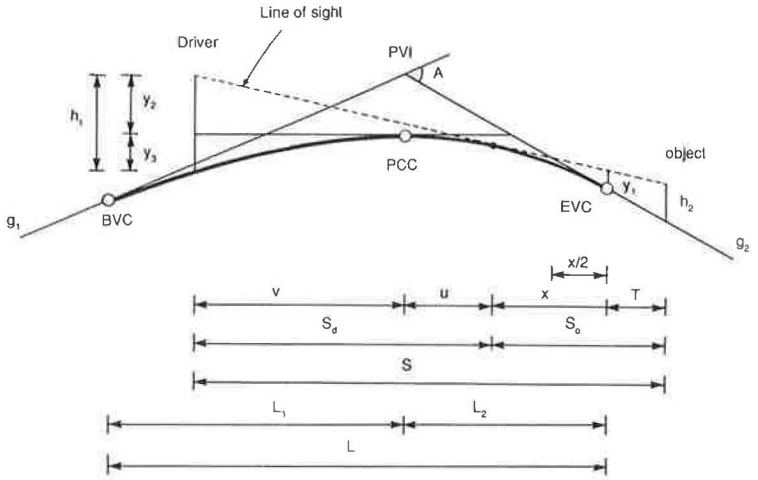

FIGURE 2 Case 1: Object beyond EVC and driver on first arc.

Components S_d

The distance S_d consists of two components, u and v. The distance u equals $(L_2 - x)$, which after substituting for x from Equation 4 becomes

$$u = L_2 + T - [T^2 + (2h_2/r_2)]^{1/2} \tag{9}$$

The component v can be derived by equating h_1 to its two parts, y_2 and y_3, shown in Figure 2. These parts are given by

$$y_2 = r_2u[(u/2) + v] \tag{10}$$

$$y_3 = r_1v^2/2 \tag{11}$$

The right-hand side of Equation 10 is the product of the difference in grade between the line of sight and the tangent at PCC, r_2u, and the respective horizontal distance, $(u/2) + v$. Thus,

$$h_1 = (r_2u^2/2) + r_2uv + (r_1v^2/2) \tag{12}$$

Solving Equation 12 for v and considering the positive root,

$$v = [-r_2u + (r_2^2u^2 - r_1r_2u^2 + 2r_1h_1)^{1/2}]/r_1 \tag{13}$$

Thus, the sight distance compound S_d is given by

$$S_d = u + [-r_2u + (r_2^2u^2 - r_1r_2u^2 + 2r_1h_1)^{1/2}]/r_1 \tag{14}$$

Sight Distance S

The available sight distance when the object is beyond EVC and the driver is on the first arc is the sum of the components of Equations 8 and 14. Thus,

$$S = L_2 + T + [- r_2u + (r_2^2u^2 - r_1r_2u^2 + 2r_1h_1)^{1/2}]/r_1 \tag{15}$$

where u is a function of T given by Equation 9.

Case 3: Object Beyond EVC and Driver Before BVC

The geometry of Case 3 is shown in Figure 3. Assume again that the line of sight is tangent to the second arc. The distance from the object to EVC is T.

Component S_o

The component S_o is derived, as it was for Case 2, as

$$S_o = [T^2 + (2h_2/r_2)]^{1/2} \tag{16}$$

Component S_d

As shown in Figure 3, the component S_d consists of three parts, u, v, and w. The distance u is given by Equation 9, and the derivation of v and w follows. The distance from PVI to the line of sight, y_2, equals the distance from PVI to PCC minus the distance from PCC to the line of sight. Thus,

$$y_2 = r_2(L_2^2 - u^2)/2 \tag{17}$$

The horizontal distance v equals y_2 divided by the difference in grade between the line of sight and the first tangent, $A - r_2(L_2 - u)$. Thus,

$$v = r_2(L_2^2 - u^2)/2\,[A - r_2(L_2 - u)] \tag{18}$$

Similarly, the distance w equals h_1 divided by the difference in grade between the line of sight and the first tangent. Thus,

$$w = h_1/[A - r_2(L_2 - u)] \tag{19}$$

The sight distance component, S_d, equals the sum of u, v, and w, giving

$$S_d = u + \{[r_2(L_2^2 - u^2)/2] + h_1\}/[A - r_2(L_2 - u)\,] \tag{20}$$

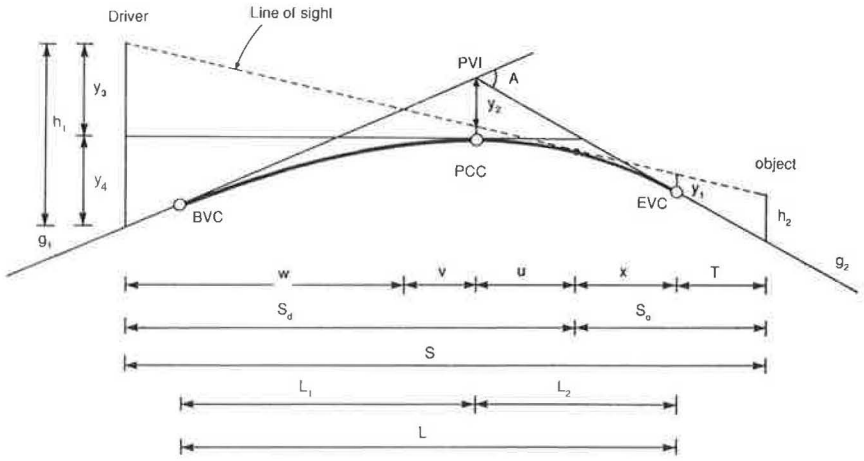

FIGURE 3 Case 1: Object beyond EVC and driver before bvc.

Sight Distance S

The available sight distance when the object is beyond EVC and the driver is before BVC is the sum of the components of Equations 16 and 20. Thus,

$$S = T + L_2 + \{[r_2(L_2^2 - u^2)/2] + h_1\}/[A - r_2(L_2 - u)] \quad (21)$$

where u is a function of T given by Equation 9.

Case 4: Object Before EVC and Driver on First Arc

The geometry of Case 4 is similar to that of Case 2, except that the object is on the second arc at a distance T' from EVC. The component S_o is given by Equation 8 for T equals zero, and S_d is given by Equation 14. Thus, the sight distance can be obtained as

$$S = L_2 - T' + [- r_2u + (r_2^2u^2 - r_1r_2u^2 + 2r_1h_1)^{1/2}]/r_1 \quad (22)$$

in which u is given by

$$u = L_2 - T' - (2h_2/r_2)^{1/2} \quad (23)$$

Case 5: Object Before EVC and Driver Before BVC

The geometry of Case 5 is similar to that of Case 3, except that the object is on the second arc at a distance T'. Again, the component S_o is given by Equation 8 for $T = 0$ and S_d is given by Equation 20. Thus, the sight distance becomes

$$S = L_2 - T' + \{[r_2(L_2^2 - u^2)/2] + h_1\}/[A - r_2(L_2 - u)] \quad (24)$$

in which u is given by Equation 23.

SIGHT DISTANCE CHARACTERISTICS

The minimum sight distance can occur only for Case 1, 2, or 3. For Case 1, the minimum value occurs when the object is at EVC ($T = 0$). For Cases 2 and 3 the object generally would be somewhere beyond EVC. For Cases 4 and 5, the available sight distance decreases as the driver and object move toward EVC, because the second arc is sharper than the first arc. S_m then occurs when the object is beyond EVC, which corresponds to Case 2 or 3.

Cases 4 and 5, however, are considered if the line of sight for Cases 2 and 3 is tangent to the first arc, which occurs when u of Equation 9 is negative. This situation is handled by defining T as the distance between the driver and BVC and applying the relationships of the five cases after replacing h_1 by h_2, L_1 by L_2, and r_1 by r_2 (and vice versa). A comparison of the sight distance characteristics for symmetrical and unsymmetrical curves and a procedure for determining S_m follow.

Comparison with Symmetrical Curves

For symmetrical crest curves, the sight distance relationships have been developed for $S \leq L$ and $S \geq L$ (*6*). The relationships of Cases 1, 2, and 3 are reduced to the known relationships for symmetrical crest curves for $r_1 = r_2 = A/L$ and $L_1 = L_2 = L/2$. Substituting these values into Equations 7 and 15 of Cases 1 and 2 (for $T = 0$) yields the relationship for $S \leq L$. Similarly, substituting these values into Equation 21 of Case 3, expressing u and T in terms of x, the known relationship for $S \geq L$ is obtained.

The sight distance profile for an unsymmetrical curve differs from that of a symmetrical curve (with the same length) in several respects, as shown in Figure 4. Note that R denotes the ratio of the shorter arc to the total curve length, L_2/L. For the unsymmetrical curve, the available sight distance varies along the curve even when both the driver and object are on the curve. The sight distance profile for the unsymmetrical curve also varies with the direction of travel, unlike that for the symmetrical curve. This significant aspect of sight dis-

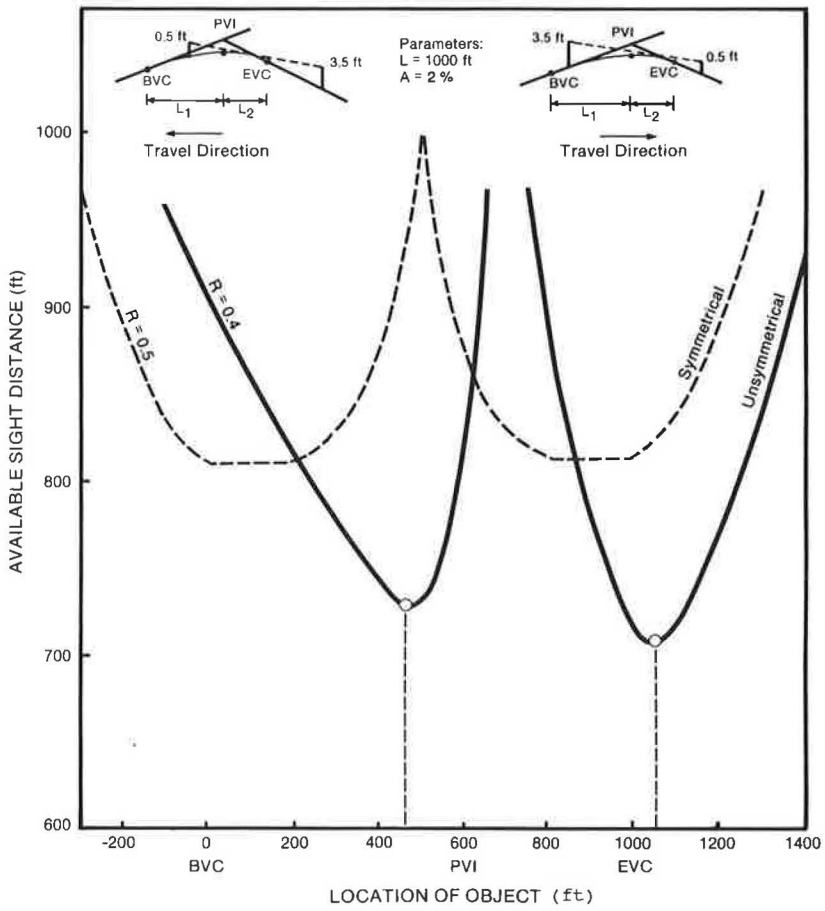

FIGURE 4 Sight distance profile of an unsymmetrical crest curve.

tances on unsymmetrical crest curves has implications for the operational and cost-effectiveness analysis of critical locations [Neuman and Glennon (*5*), Neuman et al. (*12*)]. As noted in Figure 4, the minimum sight distance is less when the driver travels from the flatter to the sharper arc of the unsymmetrical curve (S = 710 ft). This value is 13 percent less than the minimum sight distance of the symmetrical curve (815 ft).

Procedure for Calculating S_m

The minimum sight distance, S_m, can be determined by differentiating S (for Cases 2 and 3) with respect to T and equating the derivative to zero. The resulting expression, however, is too complicated to be useful. Therefore, a simple iterative procedure was used to determine the available sight distance for consecutive values of T until S_m is obtained (see Figure 5).

The procedure starts with an initial (sufficiently large) value of T along with an increment ΔT. For each T, the available sight distance S is computed and compared with the previously computed value, S'. The procedure continues until $S > S'$; at this point the minimum sight distance has just been reached ($S_m = S'$). If $u < 0$ (the line of sight is tangent to the first arc), the curve and sight distance variables are switched and all five cases are considered.

DESIGN CREST CURVE LENGTH FOR SSD

Design length requirements of unsymmetrical crest curves are developed based on the SSD design values, object height, and driver's eye height presented by Neuman (*13*) and AASHTO (*4*).

Neuman's Approach

Neuman's approach abandons the concept that a single design model of SSD is appropriate for all highway types under all conditions (*13*). It suggests a fresh approach that considers the functional highway classification in determining SSD design policy and values. The following five types of highways are considered:

1. Low-volume roads,
2. Two-lane primary rural highways,
3. Multilane urban arterials,
4. Urban freeways, and
5. Rural freeways.

SSD requirements by highway type were developed by Neuman on the basis of highway-related perception-reaction time and friction characteristics. The design values of the object

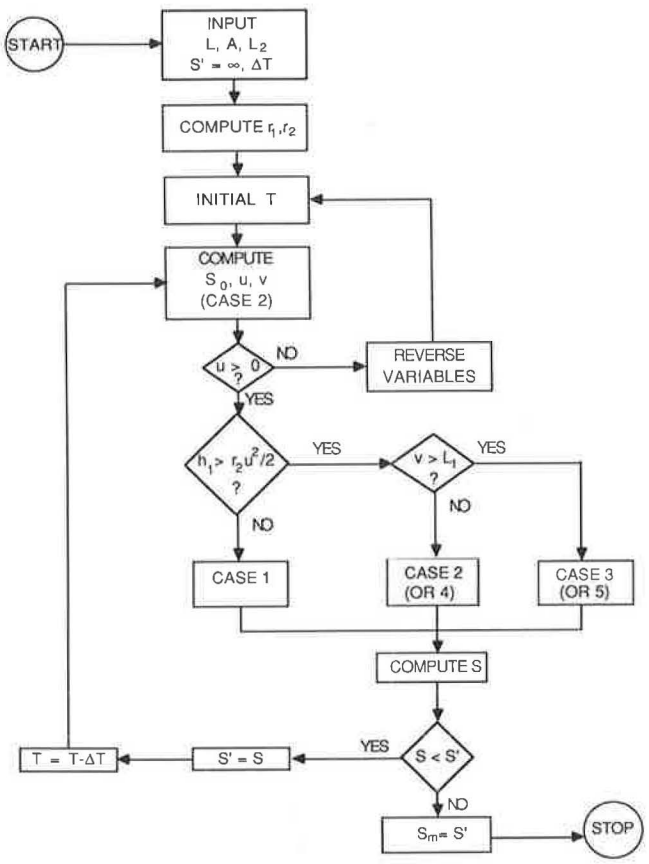

FIGURE 5 Calculating minimum sight distance on an unsymmetrical crest-curve–logical flow.

and driver eye heights also vary according to the highway type. These different values reflect the frequency of occurrence and severity of the consequences of events on various highways. The design values are based on the following critical events: (a) a single-vehicle encounter with a large object (1-ft high) for low-volume roads; (b) a single-vehicle encounter with a small object (6-in. high) for rural highways; and (c) vehicle-vehicle conflict (2-ft object height) for other highway types.

Length Requirements

Based on Neuman's Approach

Crest curve length requirements are calculated using the developed relationships. The crest curve length, L, is varied and the minimum sight distance is determined for each assumed value of L. The required design length is the one for which the minimum sight distance equals the required SSD.

Tables 1–5 show the length requirements of crest curves for $R = 0.3$, 0.4, and 0.5, where $R = L_2/L$ (L_2 is the length of the shorter parabolic arc and therefore $R \leq 0.5$). These requirements are based on Neuman's SSD values, which are shown in the column heads. The values for $R = 0.5$ are the same as those presented by Neuman for symmetrical curves (*13*). As noted, the length requirements of unsymmetrical curves can be more than twice those of symmetrical curves. For small SSD and A, the required curve length is generally small. A minimum value equal to three times the design speed in miles per hour is used. It is also noted that some length requirements are not practical.

Based on AASHTO Approach

Table 6 shows the length requirements based on the required SSD values of AASHTO, a driver's eye height of 3.5 ft, and an object height of 6 in. These requirements are applicable to all highways. The values for $R = 0.5$ correspond to symmetrical crest curves and are the same as those of AASHTO (*4*).

A comparison of the length requirements for symmetrical and unsymmetrical crest curves is shown in Figure 6. The length of the symmetrical curve is expressed as a percentage of the design length of the unsymmetrical curve. The solid curves correspond to the low-volume roads (Table 1) for $V = 50$ mph. For $R = 0.3$, the length of the symmetrical curve represents 69 percent of the required design length for $A = 3$ percent and only 43 percent for $A = 8$ to 10 percent. The results for $A = 8$ to 10 percent are the same because for these values $S < L_2$ and the ratio of L_s and L depends only on R. These results clearly show that the sight distance model for symmetrical curves would greatly underestimate the length

TABLE 1 DESIGN LENGTH REQUIREMENTS FOR UNSYMMETRICAL CREST CURVES ON LOW-VOLUME ROADS BASED ON SSD (IN FEET)[a]

Algeb. Diff. grade (%)	Design Speed											
	30 mph (SSD= 141 ft)			40 mph (SSD= 236 ft)			50 mph (SSD= 363 ft)			60 mph (SSD= 507 ft)		
	R=.3[b]	R=.4	R=.5	R=.3	R=.4	R=.5	R=.3	R=.4	R=.5	R=.3	R=.4	R=.5
2	90	90	90	120	120	120	150	150	150	280	220	190
4	90	90	90	120	120	120	560	370	320	1430	880	630
6	90	90	90	350	240	200	1120	700	480	2190	1410	940
8	120	90	90	600	370	280	1500	960	640	2920	1880	1250
10	210	140	120	790	500	340	1870	1200	800	3640	2340	1560

[a] Driver eye height = 3.5 ft
Object height = 1.0 ft
SSD values are based on Neuman (13)

[b] Ratio of shorter arc to total curve length

TABLE 2 DESIGN LENGTH REQUIREMENTS FOR UNSYMMETRICAL CREST CURVES ON TWO-LANE PRIMARY RURAL ROADS BASED ON SSD (IN FEET)[a]

Algeb. Diff. grade (%)	Design Speed											
	40 mph (SSD= 343 ft)			50 mph (SSD= 498 ft)			60 mph (SSD= 680 ft)			70 mph (SSD= 891 ft)		
	R=.3[b]	R=.4	R=.5	R=.3	R=.4	R=.5	R=.3	R=.4	R=.5	R=.3	R=.4	R=.5
2	120	120	120	150	150	150	390	320	290	1140	790	710
4	210	170	150	850	540	460	1970	1220	860	3440	2210	1480
6	630	400	330	1610	1010	690	3000	1930	1290	5150	3320	2210
8	1010	620	440	2150	1380	920	4000	2580	1720	6870	4420	2950
10	1280	820	550	2690	1730	1150	5000	3220	2150	8590	5520	3680

a Driver eye height = 3.5 ft
Object height = 2.0 ft
SSD values are based on Neuman (13)
b Ratio of shorter arc to total curve length

TABLE 3 DESIGN LENGTH REQUIREMENTS FOR UNSYMMETRICAL CREST CURVES FOR MULTILANE URBAN ARTERIALS BASED ON SSD (IN FEET)[a]

Algeb. Diff. grade (%)	Design Speed								
	30 mph (SSD= 189 ft)			40 mph (SSD= 304 ft)			50 mph (SSD= 452 ft)		
	R=.3[b]	R=.4	R=.5	R=.3	R=.4	R=.5	R=.3	R=.4	R=.5
2	90	90	90	120	120	120	150	150	150
4	90	90	90	120	120	120	610	420	370
6	90	90	90	420	290	250	1310	810	570
8	160	130	110	760	460	350	1770	1140	760
10	290	190	170	1000	630	430	2210	1420	950

a Driver eye height = 3.5 ft
Object height = 2.0 ft
SSD values are based on Neuman (13)
b Ratio of shorter arc to total curve length

TABLE 4 DESIGN LENGTH REQUIREMENTS FOR UNSYMMETRICAL CREST CURVES ON URBAN FREEWAYS BASED ON SSD (IN FEET)[a]

Algeb. Diff. grade (%)	Design Speed								
	50 mph (SSD= 518 ft)			60 mph (SSD= 726 ft)			70 mph (SSD= 989 ft)		
	R=.3[b]	R=.4	R=.5	R=.3	R=.4	R=.5	R=.3	R=.4	R=.5
2	150	150	150	520	420	380	1650	1060	900
4	960	600	500	2280	1420	980	4230	2720	1820
6	1750	1110	750	3420	2200	1470	6350	4080	2720
8	2330	1500	1000	4560	2940	1960	8460	5440	3630
10	2910	1870	1250	5700	3670	2450	10580	6800	4540

a Driver eye height = 3.5 ft
Object height = 2.0 ft
SSD values are based on Neuman (13)
b Ratio of shorter arc to total curve length

TABLE 5 DESIGN LENGTH REQUIREMENTS FOR UNSYMMETRICAL CREST CURVES ON RURAL FREEWAYS BASED ON SSD (IN FEET)[a]

Algeb. Diff. grade (%)	Design Speed								
	50 mph (SSD= 545 ft)			60 mph (SSD= 765 ft)			70 mph (SSD=1074 ft)		
	R=.3[b]	R=.4	R=.5	R=.3	R=.4	R=.5	R=.3	R=.4	R=.5
2	720	510	430	1970	1210	890	4050	2610	1740
4	2090	1350	900	4110	2650	1770	8100	5210	3480
6	3130	2020	1350	6170	3970	2650	12150	7820	5210
8	4180	2690	1790	8220	5290	3530	16200	10420	6950
10	5220	3360	2240	10280	6610	4410	20250	13020	8680

a Driver eye height = 3.5 ft
Object height = 0.5 ft
SSD values are based on Neuman (13)
b Ratio of shorter arc to total curve length

if it were used for unsymmetrical curves. The dashed curves, which correspond to Table 6 (based on AASHTO's SSD), exhibit similar characteristics.

DESIGN CREST CURVE LENGTH FOR DSD

For locations with special geometry or conditions, where DSD should be provided, object and eye heights of 0 and 3.5 ft, respectively, are used to develop the design length requirements from crest curves. The results are presented in Table 7 for DSD ranging from 200 to 800 ft. For larger values of DSD, the length requirements are generally impractical, except for very flat curves. It should be noted that Table 7 is applicable to all highway types. One need only specify the required DSD value [AASHTO (*4*), Neuman (*13*), McGee (*14*)] and interpolate the curve length from the table.

TABLE 6 DESIGN LENGTH REQUIREMENTS FOR UNSYMMETRICAL CREST CURVES ON ALL HIGHWAYS BASED ON SSD OF AASHTO[a]

Algeb. Diff. grade (%)	Design Speed																	
	20 mph (SSD= 125 ft)			30 mph (SSD= 200 ft)			40 mph (SSD= 275 ft)			50 mph (SSD= 400 ft)			60 mph (SSD= 525 ft)			70 mph (SSD= 625 ft)		
	R=.3[b]	R=.4	R=.5	R=.3	R=.4	R=.5	R=.3	R=.4	R=.5	R=.3	R=.4	R=.5	R=.3[b]	R=.4	R=.5	R=.3	R=.4	R=.5
2	60	60	60	90	90	90	120	120	120	210	160	150	630	460	390	1120	720	590
4	60	60	60	110	90	90	370	260	220	1100	680	490	1940	1250	830	2750	1770	1180
6	60	60	60	330	220	180	790	490	350	1690	1090	730	2910	1870	1250	4120	2650	1770
8	140	100	90	550	340	250	1070	690	460	2250	1450	970	3880	2490	1660	5490	3530	2360
10	230	150	120	710	450	310	1330	860	570	2810	1810	1210	4840	3120	2080	6860	4410	2940

[a] Driver eye height = 3.5 ft
Object height =0.5 ft

[b] Ratio of shorter arc to total curve length

Note: curve lengths are expressed in feet.

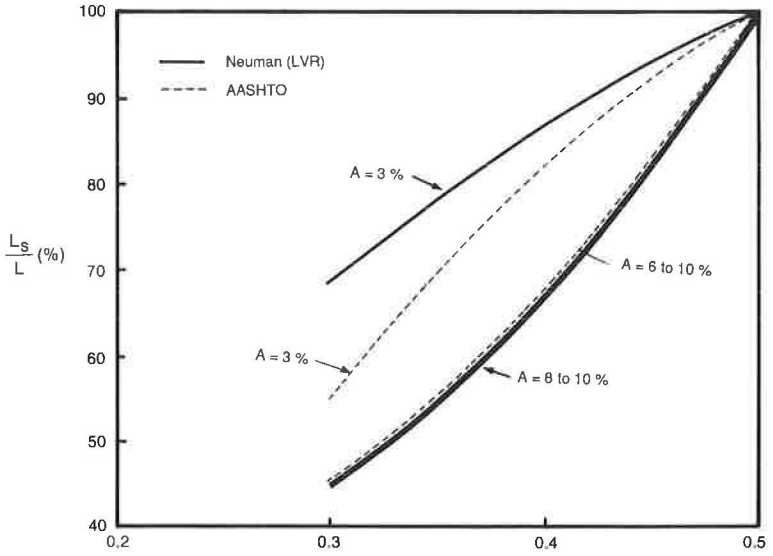

FIGURE 6 Comparison of length requirements of symmetrical and unsymmetrical crest curves (V = 50 mph).

TABLE 7 DESIGN LENGTH REQUIREMENTS FOR UNSYMMETRICAL CREST CURVES ON ALL HIGHWAYS BASED ON DSD[a]

Algeb. Diff. grade (%)	Decision Sight Distance (ft)											
	200			400			600			800		
	R=.3[b]	R=.4	R=.5	R=.3	R=.4	R=.5	R=.3	R=.4	R=.5	R=.3	R=.4	R=.5
2	90	70	50	1020	640	460	2400	1550	1030	4270	2750	1830
4	510	320	230	2140	1380	920	4800	3090	2060	8540	5490	3660
6	800	520	350	3200	2060	1380	7200	4630	3090	12800	8230	5490
8	1070	690	460	4270	2750	1830	9600	6180	4120	17070	10980	7320
10	1340	860	580	5340	3430	2290	12000	7720	5150	21340	13720	9150

[a] Driver eye height = 3.5 ft
Object height = 0 ft

[b] Ratio of shorter arc to total curve length

Note: curve lengths are expressed in feet.

TABLE 8 DESIGN LENGTH REQUIREMENTS FOR UNSYMMETRICAL CREST CURVES BASED ON PSD (IN FEET)[a]

Algeb. Diff. grade (%)	Design Speed																	
	20 mph			30 mph			40 mph			50 mph			60 mph			70 mph		
	R=.3[d]	R=.4	R=.5	R=.3	R=.4	R=.5	R=.3	R=.4	R=.5	R=.3	R=.4	R=.5	R=.3	R=.4	R=.5	R=.3	R=.4	R=.5
Passenger Car Passing Passenger Car[b]																		
	(PSD= 325 ft)			(PSD= 525 ft)			(PSD= 700 ft)			(PSD= 875 ft)			(PSD= 1025 ft)			(PSD= 1200 ft)		
2	60	60	60	90	90	90	120	120	120	260	220	200	650	540	500	1250	920	850
4	60	60	60	360	300	280	1120	710	630	2180	1320	1000	3160	1960	1360	4350	2790	1870
6	180	150	140	1090	660	540	2220	1380	960	3470	2230	1490	4760	3060	2040	6520	4200	2800
8	430	290	270	1660	1040	720	2960	1910	1270	4630	2980	1990	6350	4080	2720	8700	5590	3730
10	720	440	350	2080	1340	900	3700	2380	1590	5780	3720	2480	7930	5100	3400	10870	6990	4660
Passenger Car Passing Truck[b]																		
	(PSD= 350 ft)			(PSD= 575 ft)			(PSD= 800 ft)			(PSD= 1025 ft)			(PSD= 1250 ft)			(PSD= 1450 ft)		
2	60	60	60	90	90	90	120	120	120	650	540	500	1470	1030	950	2520	1570	1350
4	60	60	60	530	410	380	1710	1040	830	3160	1960	1360	4720	3030	2030	6350	4080	2720
6	240	200	190	1400	850	650	1900	1860	1250	4760	3060	2040	7080	4550	3040	9520	6120	4080
8	560	360	320	2000	1280	860	3870	2490	1660	6350	4080	2720	9440	6070	4050	12690	8160	5440
10	880	530	400	2500	1610	1070	4830	3110	2070	7930	5100	3400	11790	7580	5060	15870	10200	6800
Truck Passing Passenger Car[c]																		
	(PSD= 350 ft)			(PSD= 600 ft)			(PSD= 875 ft)			(PSD= 1125 ft)			(PSD= 1375 ft)			(PSD= 1625 ft)		
2	60	60	60	90	90	90	120	120	120	230	190	170	920	740	670	1770	1300	1170
4	60	60	60	220	180	160	1170	800	710	2610	1590	1220	4220	2620	1820	5930	3800	2540
6	60	60	60	870	580	510	2540	1570	1110	4260	2740	1830	6370	4090	2730	8890	5720	3810
8	250	200	180	1540	940	700	3440	2210	1480	5680	3650	2440	8490	5460	3640	11850	7620	5080
10	470	320	290	2020	1280	870	4300	2760	1840	7100	4570	3050	10610	6820	4550	14810	9520	6350
Truck Passing Truck[c]																		
	(PSD= 350 ft)			(PSD= 675 ft)			(PSD= 975 ft)			(PSD= 1275 ft)			(PSD= 1575 ft)			(PSD= 1875 ft)		
2	60	60	60	90	90	90	120	120	120	640	520	470	1570	1190	1070	2990	1930	1670
4	60	60	60	430	350	310	1710	1080	910	3570	2190	1570	5570	3560	2390	7890	5070	3380
6	60	60	60	1280	800	660	3200	2020	1380	5470	3520	2350	8350	5370	3580	11830	7610	5070
8	250	200	180	2030	1260	880	4270	2750	1830	7300	4690	3130	11130	7160	4770	15770	10140	6760
10	470	320	290	2560	1650	1100	5340	3430	2290	9120	5860	3910	13910	8950	5970	19720	12680	8450

[a] PSD values are based on Harwood and Glennon (15)

[b] Driver eye height = 3.5 ft
Object height = 4.25 ft

[c] Truck driver eye height = 6.25 ft
Object height = 4.25 ft

[d] Ratio of shorter arc to total curve length

DESIGN CREST CURVE LENGTH FOR PSD

Design length requirements of unsymmetrical crest curves for PSD are established based on the PSD design requirements presented by Harwood and Glennon (*15*) and AASHTO (*4*).

Harwood-Glennon Approach

Glennon (*16*) developed a model for estimating PSD that accounts for the kinematic relationships among the passing, passed, and opposing vehicles. The model not only involves a more logical formulation than the AASHTO and other similar models, it also explicitly contains vehicle length terms. The Glennon model was used by Harwood and Glennon (*15*) to develop sight distance requirements for passing in the following cases:

1. Passenger car passing passenger car,
2. Passenger car passing truck,
3. Truck passing passenger car, and
4. Truck passing truck.

The PSD requirements for these four cases are shown in parentheses in Table 8.

Length Requirements

Based on Harwood-Glennon Approach

The minimum length requirements of unsymmetrical crest curves, established using the developed relationships, are shown in Table 8. For any design or prevailing speed, the length requirements are given for $R = 0.3$, 0.4, and 0.5. The values for $R = 0.5$ are the length requirements for symmetrical crest curves.

Table 8 is based on a passenger car driver eye height of 42 in., truck driver eye height of 75 in., and object height of 51 in. These are the same values used by Harwood and Glennon (*15*). The use of 75 in. to represent truck driver eye height is conservative because the literature shows that truck driver eye height ranges from 71.5 to 112.5 in. (*17–19*). The object height of 51 in. suggested by AASHTO (*4*) corresponds to an opposing passenger car and therefore is also conservative.

Based on AASHTO Approach

Table 9 shows the length requirements based on the required PSD of AASHTO, a driver's eye height of 3.5 ft, and an object height of 4.25 ft (which corresponds to passenger cars).

TABLE 9 DESIGN LENGTH REQUIREMENTS FOR UNSYMMETRICAL CREST CURVES BASED ON PSD OF AASHTO (PASSENGER CARS)[a]

Algeb. Diff. grade (%)	Design Speed											
	20 mph (PSD= 800 ft)			30 mph (PSD=1100 ft)			40 mph (PSD=1500 ft)			50 mph (PSD=1800 ft)		
	R=.3[b]	R=.4	R=.5	R=.3	R=.4	R=.5	R=.3	R=.4	R=.5	R=.3	R=.4	R=.5
1	60	60	60	90	90	90	120	120	120	650	540	500
2	70	60	60	870	700	650	2810	1730	1450	4680	2840	2100
3	830	610	570	2480	1500	1180	5100	3230	2190	7340	4720	3150
4	1710	1040	830	3660	2310	1570	6800	4370	2920	9780	6290	4200
5	2400	1480	1040	4570	2940	1960	8490	5460	3640	12230	7860	5240
6	2900	1860	1250	5480	3530	2350	10190	6550	4370	14670	9430	6290

[a] Driver eye height = 3.5 ft, Object height = 4.25 ft

[b] Ratio of shorter arc to total curve length

Note: curve lengths are expressed in feet.

The values for $R = 0.5$ are the same as those obtained by the AASHTO equations (*4*). Table 9 includes only moderate values of algebraic difference in grades and design speeds up to 50 mph. Design for PSD may be feasible only for special combinations of high design speeds and very small grades, or low design speeds with moderate grades.

SUMMARY AND CONCLUSIONS

Unsymmetrical crest curves may be required because of vertical clearance and other design controls. No relationships are available concerning the available and minimum sight distances on these curves. Such relationships are derived here and are used to establish design length requirements of unsymmetrical crest curves based on the SSD, DSD, and PSD needs presented by recent innovative approaches (*13,15*) and by AASHTO (*4*). A computer program implementing these relationships was prepared and can be used to generate the sight distance profiles on both travel directions and the minimum sight distance. Such profiles are useful for evaluating the length of the road with restricted sight distances and the locations on the crest curve where the minimum sight distance occurs.

The developed model can be used to design or evaluate unsymmetrical crest curves to satisfy sight distance needs. The length requirements presented for SSD and DSD are based on passenger cars. In recent years, however, attention has been given to sight distance needs for large trucks (*20,21*). Crest curve lengths needed to provide SSD for trucks can be examined using the model.

The results show that, for a given sight distance, the length requirements of unsymmetrical curves are as great as twice or three times those of symmetrical curves. This finding strongly supports the use of the developed model in new design and in evaluating the adequacy of sight distance on existing unsymmetrical curves. Although the use of these curves in practice is infrequent, their design must satisfy sight distance needs to maintain or achieve safe operations.

ACKNOWLEDGMENT

This work was supported by the Natural Sciences and Engineering Research Council of Canada.

REFERENCES

1. *A Policy on Sight Distance for Highways, Policies on Geometric Highway Design*. AASHO, Washington, D.C., 1940.
2. *A Policy on Geometric Design of Rural Highways*, AASHO, Washington, D.C., 1965.
3. *A Policy on Design Standards for Stopping Sight Distance*. AASHO, Washington, D.C., 1971.
4. *A Policy on Geometric Design of Highways and Streets*. AASHTO, Washington, D.C., 1984.
5. T. R. Neuman and J. C. Glennon. Cost-Effectiveness of Improvements to Stopping Sight Distance. In *Transportation Research Record 923*, TRB, National Research Council, Washington, D.C., 1984, pp. 26–34.
6. P. L. Olson, D. E. Cleveland, P. S. Fancher, L. P. Kostyniuk, and L. W. Schneider. *NCHRP Report 270: Parameters Affecting Stopping Sight Distance*. TRB, National Research Council, Washington, D.C., 1984.
7. J. C. Glennon. Effects of Sight Distance on Highway Safety. In *State-of-the-Art Report 6*, TRB, National Research Council, Washington, D.C., 1987, pp. 64–77.
8. T. Urbanik II, W. Hinshaw, and D. B. Fambro. Safety Effects of Limited Sight Distance on Crest Vertical Curves. In *Transportation Research Record 1208*, TRB, National Research Council, Washington, D.C., 1989, pp. 23–35.
9. T. F. Hickerson. *Route Location and Design*. McGraw-Hill Book Company, New York, 1964.
10. C. F. Meyer. *Route Surveying and Design*. International Textbook Company, Scranton, Pa., 1971.
11. P. R. Wolf and R. C. Brinker. *Elementary Surveying*. Harper & Row, New York, 1989.
12. T. R. Neuman, J. C. Glennon, and J. E. Leish. *Stopping Sight Distance—An Operational and Cost Effectiveness Analysis*. Report FHWA/RD-83/067. FHWA, U.S. Department of Transportation, Washington, D.C., 1982.
13. T. R. Neuman. New Approach to Design for Stopping Sight Distance. In *Transportation Research Record 1208*, TRB, National Research Council, Washington, D.C., 1989, pp. 14–22.
14. H. W. McGee, Reevaluation of the Usefulness and Application of Decision Sight Distance. In *Transportation Research Record 1208*, TRB, National Research Council, Washington, D.C., 1989, pp. 85–89.
15. D. W. Harwood and J. C. Glennon. Passing Sight Distance Design for Passenger Cars and Trucks. In *Transportation Research Record 1208*, TRB, National Research Council, Washington, D.C., 1989, pp. 59–69.
16. J. C. Glennon. New and Improved Model of Passing Sight Distance on Two-Lane Highways. In *Transportation Research Record 1195*, TRB, National Research Council, Washington, D.C., 1988, pp. 132–137.
17. P. B. Middleton, M. Y. Wong, J. Taylor, H. Thompson, and J. Bennett. *Analysis of Truck Safety on Crest Vertical Curves*.

Report FHWA/RD-86/060. FHWA, U.S. Department of Transportation, Washington, D.C., 1983.
18. J. W. Burger and M. U. Mulholland. *Plane and Convex Mirror Sizes for Small to Large Trucks*. NHTSA, U.S. Department of Transportation, Washington, D.C., 1982.
19. Urban Behavioral Research Associates. *The Investigation of Driver Eye Height and Field of Vision*. FHWA, U.S. Department of Transportation, Washington, D.C., 1978.
20. P. S. Fancher. Sight Distance Problems Related to Large Trucks. In *Transportation Research Record 1052*, TRB, National Research Council, Washington, D.C., 1986, pp. 29–35.
21. D. W. Harwood, W. D. Glauz, and J. M. Mason, Jr. Stopping Sight Distance Design for Large Trucks. In *Transportation Research Record 1208*, TRB, National Research Council, Washington, D.C., 1989, pp. 36–46.

DISCUSSION

DAVID L. GUELL
Department of Civil Engineering, University of Missouri-Columbia, Columbia, Mo. 65211.

Easa has added to the knowledge of sight distance on vertical curves with this paper. The ability to develop sight distance profiles, as shown in Figure 4, will be valuable in assessing sight distance conditions on existing highways.

This discussion is concerned with the design requirements for unsymmetrical crest vertical curves, and in particular the length of curve necessary to provide a specified length of sight distance. In keeping with the nomenclature of the paper (Figure 1), an unsymmetrical vertical curve is made up of two symmetrical vertical curves of length L_1 and L_2 (where $L_1 > L_2$) with the common point PCC under the PVI. A line tangent to the curve at PCC is parallel to a line connecting BVC to EVC and has a grade g_3 given by

$$g_3 = \frac{g_1L_1 + g_2L_2}{L_1 + L_2} \tag{25}$$

The algebraic difference in grade for the unsymmetrical vertical curve is A equal to $g_2 - g_1$. Note that this is the negative of A as given in the paper. The algebraic differences in grades of the two symmetrical curves are given by

$$A_1 = g_3 - g_1 \tag{26}$$

and

$$A_2 = g_2 - g_3 \tag{27}$$

In this discussion, g and A are given in percent.

The symmetrical vertical curve of length L_2 is the critical one for sight distance because it is the shorter of the two. Therefore the length of this curve must satisfy the design requirement that

$$L_2 > K \cdot A_2 \tag{28}$$

where K is the rate of vertical curvature as given, for example, in Tables III-40 and III-41 of AASHTO (*1*) for stopping and passing sight distance. Substituting g_3 from Equation 25 into A_2 in Equation 27 and recognizing that L_1 plus L_2 is equal to L, the total length of the unsymmetrical curve, gives

$$A_2 = L_1 \cdot A/L = (L - L_2) \cdot A/L \tag{29}$$

Substituting $L = L_2/R$, as defined by the author, into Equation 29 and then substituting this A_2 into Equation 28 gives

$$L_2 > K \cdot A \cdot (1 - R) \tag{30}$$

Substitution into $L = L_2/R$ gives

$$L > K \cdot A \cdot (1 - R)/R \tag{31}$$

Equation 30 gives the required length of the shorter symmetrical vertical curve, and Equation 31 gives the required total length of the unsymmetrical curve in terms of parameters familiar to designers and the additional parameter R:

- A = algebraic difference in grade,
- K = required rate of vertical curvature as given in AASHTO tables (*1*), and
- R = ratio of length of shorter symmetrical curve to total length of the unsymmetrical curve.

It should be noted that when using the tabulated values of K as given by AASHTO (*1*) with small values of A, the calculated length of the vertical curve is greater than actually required for sight distance. This occurs when the sight distance is greater than the required length of the shorter symmetrical vertical curve. For this reason the values of L computed by Equation 31 will be greater than the values given in the paper in Tables 6 and 9 for small values of A. Also note that the author did not used the tabulated K-values in AASHTO (*1*) Tables III-40 and III-41 associated with the design speeds in the author's Tables 6 and 9. The corresponding K-values for the paper's sight distances can be determined from AASHTO

TABLE 10 DESIGN LENGTH REQUIREMENTS FOR UNSYMMETRICAL CREST CURVES AT 50-MPH DESIGN SPEED

	SSD = 400 ft				PSD = 1,800 ft			
	Paper, Table 6		Discussion, Equation 31[a]		Paper, Table 9		Discussion, Equation 31[b]	
A(%)	R = 0.3	R = 0.4	R = 0.3	R = 0.4	R = 0.3	R = 0.4	R = 0.3	R = 0.4
2	210	160	562	361	4,680	2,840	4,888	3,143
3			843	542	7,340	4,720	7,333	4,714
4	1,100	680	1,124	722	9,780	6,290	9,777	6,285
5			1,405	903	12,230	7,860	12,221	7,856
6	1,690	1,090	1,686	1,084	14,670	9,430	14,665	9,428
8	2,250	1,450	2,247	1,445				
10	2,810	1,810	2,809	1,805				

[a]With $K = S^2/1{,}329 = 120.4$
[b]With $K = S^2/3{,}093 = 1{,}047.5$.

Equation 3 for stopping sight distance ($K = S^2/1329$) (*1*, p. 283) and Equation 5 for passing sight distance ($K = S^2/3093$) (*1*, p. 288).

Table 10 compares the design length for unsymmetrical vertical curves as determined by the method of the paper and the method of this discussion for 50-mph design speed. The lengths are essentially the same except for small values of A.

REFERENCE

1. *A Policy on Geometric Design of Highways and Streets*. AASHTO, Washington, D.C., 1990.

AUTHOR'S CLOSURE

The author thanks Professor Guell for his interest in the paper and for his thoughtful comments regarding establishment of the design length requirements of unsymmetrical crest curves based on the shorter arc.

The formula derived in his discussion for establishing length requirements (Equation 31) assumes that both the driver and object are on the shorter arc, which corresponds to Case 1 of the paper. The discussion indicates that the lengths calculated using this formula will be greater than actually required when A is small. The purpose of this closure is twofold: (a) to derive a general expression for Equation 31 and the condition for applying it, and (b) to show that this equation may overestimate the length requirements even when A is large.

For Case 1, the minimum sight distance, S_m, occurs when the object is at EVC. Setting $T = 0$, substituting for r_2 from Equation 2 into Equation 7, and nothing that $L_1 = (1 - R)L$, one obtains

$$L_2 = A\,(1 - R)\left\{\frac{S_m^2}{[(2h_1)^{1/2} + (2h_2)^{1/2}]^2}\right\} \tag{32}$$

where the term in brackets equals the rate of vertical curvature K (Equation 32 is similar to Equation 30). Note that A is defined in the paper as $g_1 - g_2$, which always yields a positive value for crest curves. Since $L_2 = LR$, Equation 32 gives

$$L = A\,\frac{(1 - R)}{R}\left\{\frac{S_m^2}{[(2h_1)^{1/2} + (2h_2)^{1/2}]^2}\right\} \quad \text{(Case 1)} \tag{33}$$

which is a general expression for the length requirements for Case 1 (Equation 33 is similar to Equation 3). For Equation 33 to be valid, however, S_m must be less than or equal to L_2. That is,

$$S_m \le A\,(1 - R)\left\{\frac{S_m^2}{[(2h_1)^{1/2} + (2h_2)^{1/2}]^2}\right\} \tag{34}$$

from which

$$A \ge \frac{[(2h_1)^{1/2} + (2h_2)^{1/2}]^2}{(1 - R)S_m} \tag{35}$$

Equation 35 is the condition of A for which Equation 33 gives exact length requirements. For values of A less than those given by Equation 35, Equation 33 overestimates the length requirements.

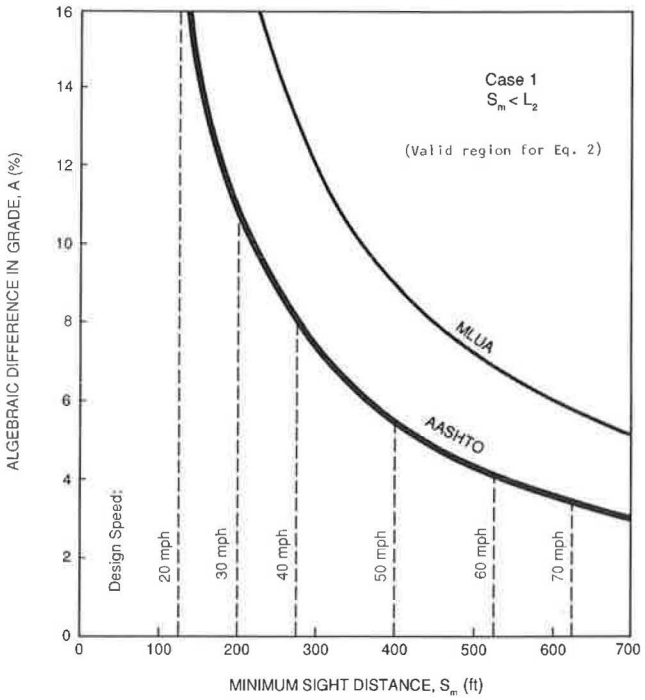

FIGURE 7 Range of A for which Equation 33 overestimates length requirements based on SSD ($R = 0.4$).

A graphical representation of Equation 35 using the AASHTO design parameters of SSD ($h_1 = 3.5$ ft, $h_2 = 0.5$ ft) and $R = 0.4$ is shown in Figure 7. For a given S_m, Equation 33 overestimates the length requirements for the values of A below the shaded region. For $S_m = 400$ ft (50-mph design speed), the length requirements are overestimated when $A < 5.5$ percent. The overestimation may be more than 100 percent, as noted from Table 10. For lower design speeds, the overestimation occurs for larger values of A. For example, the length requirements are overestimated when $A < 11.1$ percent for $S_m = 200$ ft (30 mph) and when $A < 17.7$ percent for $S_m = 125$ ft (20 mph). For other design parameters of SSD, the region of A for which overestimation occurs may be larger than that of AASHTO. This is illustrated in Figure 7 by the upper curve, which corresponds to the design parameters of multilane urban arterials (MLUA) of Table 3 ($h_1 = 3.5$ ft, $h_2 = 2.0$ ft). Applying Equation 35 using the AASHTO design parameters of PSD ($h_1 = 3.5$ ft, $h_2 = 4.25$ ft) shows that overestimation occurs when $A < 2$ percent for $S_m = 1{,}800$ ft (50 mph), as also noted in Table 10. For $S_m = 800$ ft (20 mph), overestimation occurs when A < 4.5 percent.

In summary, the length requirements of unsymmetrical crest curves may be computed using Equation 33 (which corresponds to Case 1) only if the condition of Equation 35 holds. If this condition does not hold, this means the analysis corresponds to other sight distance cases and the length requirements should be established using the procedure presented in the paper.

Publication of this paper sponsored by Committee on Geometric Design.

Sight Distance Models for Unsymmetrical Sag Curves

SAID M. EASA

Unsymmetrical sag (vertical) curves may be required at complex interchanges and other highway locations because of clearance and other controls. No relationships are available for designing or evaluating these curves on the basis of sight distance needs, so sight distance models for unsymmetrical sag curves are developed for headlight and overhead obstacle controls. For headlight control, the model relates the minimum sight distance (S_m), vertical curve parameters, and vehicle and object characteristics. For overhead control, the model relates the available sight distance, sag curve parameters, vertical clearance and location of overhead obstacle, and locations and heights of driver eye and object. A procedure for calculating S_m is presented. The distinct characteristics of sight distance on unsymmetrical sag curves are examined. To facilitate practical use, graphs and tables of the minimum sight distance for headlight and overhead controls are established. The length requirements and sight distance characteristics of symmetrical and unsymmetrical sag curves were found to be quite different. The developed models should be valuable in the evaluation of safety and operation of unsymmetrical sag curves.

The current AASHTO models for designing sag curves based on stopping sight distance (SSD) consider two cases: headlight control and overhead obstacle control (*1–4*). The headlight sight distance depends on the position of the headlights and the direction of the light beam. Generally, the headlight height is 2.0 ft and the upward divergence of the light beam from the longitudinal axis of the vehicle is 1 degree. The AASHTO model defines SSD as the distance between the eye of the driver and the point where the light beam intersects the road surface.

For overhead obstacle control, as in the case of a sag curve at an underpass, the structure may restrict the sight distance. The 1965 AASHO policy (*2*) presents formulas for checking the available sight distance or computing the required curve length assuming that the structure is centered over the vertical point of intersection (PVI). Derivation of these formulas can be found in work by Hickerson (*5*) and Ives and Kissam (*6*). The 1965 AASHO policy suggests a truck driver eye height of 6.0 ft and an object height of 1.5 ft, which may represent the vehicle taillight or a discernible portion of an oncoming vehicle. Olson et al. (*7*) evaluated the AASHO equations for a driver eye height of 9 ft, which is typical for cab-over-engine tractors, and an object height of 0.5 ft. They found that the resulting curves were about 10 percent longer than those found in the AASHO policy.

Sag curves are normally designed for headlight control based on SSD. The available sight distance at an undercrossing sag curve is then checked when special conditions exist; for example, at a two-lane undercrossing without ramps where passing sight distance (PSD) is desirable (*2*). In addition, at complex locations where information is difficult to perceive, the decision sight distance (DSD) should be provided. DSD values are presented in the AASHTO *Policy on Geometric Design of Highways and Streets* (Green Book) (*4*). Revised design values have been developed recently for SSD by Neuman (*8*) and Olson et al. (*7*); for PSD by Harwood and Glennon (*9*), based on a model by Glennon (*10*); and for DSD by Neuman (*8*) and McGee (*11*). A methodology for operational and cost-effectiveness analysis of locations with sight distance restriction has been presented by Neuman et al. (*12*) and Neuman and Glennon (*13*). The effects of sight distance on highway safety have been reviewed by Glennon (*14*).

Both the headlight and overhead control models assume that the sag curve is a symmetrical parabola whose tangents have equal horizontal projections. In some situations, such as at interchanges, an unsymmetrical curve may be required because of clearance or other design controls [AASHTO (*4*)]. The formulas for laying out unsymmetrical curves have been presented in a number of highway engineering texts (*5,15*); however, the available sight distance on these curves has not been addressed in the literature. Although the use of unsymmetrical curves in practice is infrequent, it is essential to ensure that they provide safe operations.

Sight distance models were developed for unsymmetrical sag curves for both headlight and overhead controls. For overhead control, the structure may lie at any point on the curve or tangent. The models can be used to design the required length of a new curve or to check the adequacy of the available sight distance on existing curves. A brief description of the unsymmetrical curve follows.

The unsymmetrical vertical curve consists of two parabolic arcs with a common tangent at the intersection point, PVI, of the initial and final tangents (Figure 1). The horizontal projections of the two arcs, which are unequal, are denoted by L_1 and L_2. The grades of these tangents are g_1 and g_2, respectively. The grade is positive if it is upward to the right and negative if it is downward to the right. The beginning point of the vertical curve (BVC) lies on the initial tangent with the adjacent arc designated as the first arc. The end point (EVC) lies on the final tangent with the adjacent arc designated as the second arc. The second arc represents the smaller arc. These vertical curve terminologies are used regardless of the travel direction. The rates of change in grade of the two parabolic arcs are given by Hickerson (*5*). Let the ratio of the length of the second arc to the length of the curve be denoted by R. That is,

Department of Civil Engineering, Lakehead University, Thunder Bay, Ontario, Canada P7B 5E1.

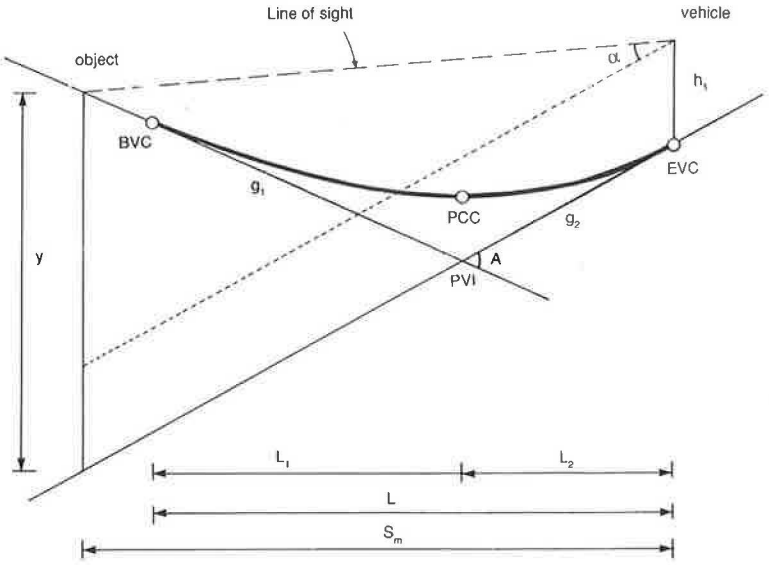

a) Case 1

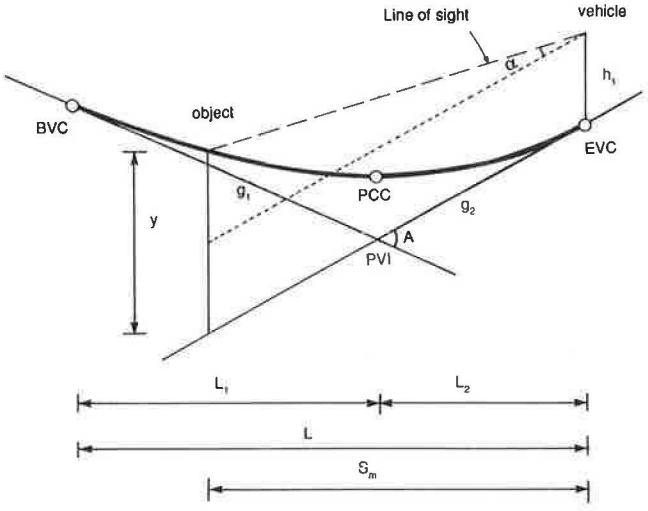

b) Case 2

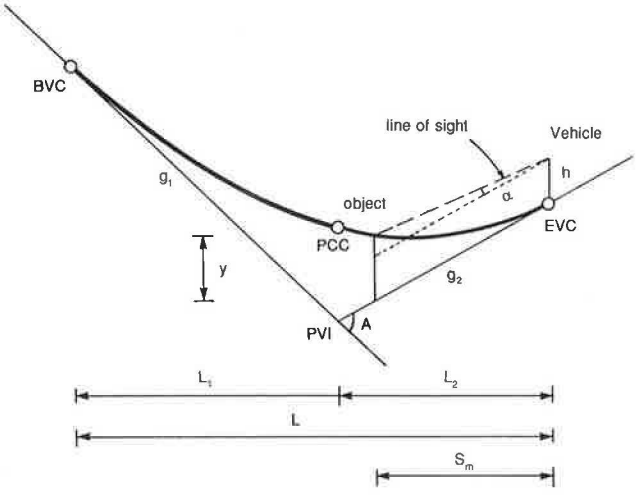

c) Case 3

FIGURE 1 Geometry of sight distance for headlight control on an unsymmetrical sag curve.

$$R = L_2/L \quad (1)$$

Then, Hickerson's formulas for the rates of change in grade can be written in terms of R as follows:

$$r_1 = (A/L)R/(1 - R) \quad (2)$$

$$r_2 = (A/L)(1 - R)/R \quad (3)$$

where

r_1, r_2 = rates of change in grade of the first and second parabolic arcs, respectively,
A = algebraic difference in grades ($g_2 - g_1$), and
L = length of the vertical curve.

For symmetrical curves, $L_1 = L_2$, R of Equation 1 equals 0.5, and Equations 2 and 3 yield equal rates of change in grade of A/L. The radius of vertical curvature (a measure of sharpness) equals the inverse of the rate of change in grade. Thus, for the unsymmetrical curve, the radius of the first and second arcs $K_1 = 1/r_1$ and $K_2 = 1/r_2$. The radius of vertical curvature of the symmetrical curve $K = 1/r = L/A$. Therefore, if L_2 is the smaller arc, the second arc will be sharper and the first arc will be flatter than a symmetrical curve with the same length. Note that the variables g_1, g_2, and A are assumed to be in decimals in the developed relationships.

HEADLIGHT CONTROL

The geometry of sight distance for headlight control on an unsymmetrical sag curve is shown in Figure 1. The critical direction of travel for headlight control is generally from the smaller to the longer arc. The minimum sight distance, S_m, occurs when the driver is at EVC. For some cases, however, S_m will be the same in both travel directions.

Geometric Relationships

Relationships for the minimum sight distance are developed for three cases:

- Case 1: Sight distance greater than curve length,
- Case 2: sight distance less than curve length but greater than length of the smaller arc, and
- Case 3: Sight distance less than length of the smaller arc.

In all cases, h_1 and α denote the headlight height and the upward divergence (in degrees) of the light beam from the longitudinal axis of the vehicle, respectively. The variable y is given by

$$y = h_1 + S_m \tan \alpha \quad (4)$$

Case 1: Sight Distance Greater Than Curve Length ($S_m \geq L$)

The geometry of Case 1 is shown in Figure 1a. The variable y is also written as

$$y = (S_m - L_2)A \quad (5)$$

Equating the right-hand sides of Equations 4 and 5 and substituting for L_2 from Equation 1 gives

$$L = (S_m/R) - (h_1 + S_m \tan\alpha)/RA \qquad S_m \geq L \quad (6)$$

Case 2: Sight Distance Less than Curve Length but Greater Than Length of Smaller Arc ($L_2 \leq S_m \leq L$)

The variable y in Figure 1b is written as

$$y = (S_m - L_2)A + r_1(L - S_m)^2/2 \quad (7)$$

Equating the right-hand sides of Equations 4 and 7 and substituting for L_2 and r_1 from Equations 1 and 2 gives

$$aL^2 + bL + c = 0 \quad (8)$$

where

$$a = (1 - 2R)RA \quad (9)$$

$$b = 2(1 - R)(h_1 + S_m \tan \alpha) - 2(1 - 2R)S_mA \quad (10)$$

$$c = -ARS_m^2 \quad (11)$$

The solution of Equation 8 is given by (considering the positive root)

$$L = [-b + (b^2 - 4ac)^{1/2}]/2a \qquad L_2 \leq S_m \leq L \quad (12)$$

Case 3: Sight Distance Less than Length of Smaller Arc ($S_m \leq L_2$)

The variable y in Figure 1c is written as

$$y = r_2S_m^2/2 \quad (13)$$

Equating the right-hand sides of Equations 4 and 13 and substituting for r_2 from Equation 3 gives

$$L = [(1 - R)/R]AS_m^2/2(h_1 + S_m \tan \alpha) \qquad S_m \leq L_2 \quad (14)$$

Comparison with Symmetrical Curves

For symmetrical sag curves, where $R = 0.5$, Equation 6 of Case 1 reduces to

$$L_s = 2S_m - 2(h_1 + S_m \tan \alpha)/A \qquad S_m \geq L_s \quad (15)$$

where L_s = length of the symmetrical curve. For Case 2, for $R = 0.5$, Equations 9–11 give $a = 0$, $b = h_1 + S_m \tan \alpha$, and $c = -0.5AS_m^2$. Substituting these variables into Equation 8 gives

$$L_s = AS_m^2/2(h_1 + S^m \tan \alpha) \qquad S_m \leq L_s \quad (16)$$

Equations 15 and 16 are the known formulas for symmetrical curves for $S_m \geq L_s$ and $S_m \leq L_s$, respectively (*6,16*). For Case 3, Equation 14 also reduces to Equation 16 for $R = 0.5$, as expected.

A comparison of the length requirements of symmetrical and unsymmetrical curves is shown in Figure 2. As noted, the ratio of the length of an unsymmetrical curve and that of a symmetrical curve (providing the same sight distance) is much greater than one for smaller values of R. The lower and upper bounds of this ratio are given by

$$(1/2R) \leq L/L_s \leq (1 - R)/R \quad (17)$$

The lower bound corresponds to Case 1 and the upper bound corresponds to Case 3.

Design Length Requirements

For headlight control, Figures 3 and 4 show the design length requirements of unsymmetrical sag curves for $R = 0.3$ and 0.4, respectively, based on SSD requirements of AASHTO. Figure 5, which is similar to that of AASHTO (*4*), shows the length requirements for symmetrical curves ($R = 0.5$). For other values of R, the length requirements can be interpolated from these figures. The vertical lines at the lower left of figures represent the minimum curve length, which equals three times the design speed in miles per hour. If the designer wishes to use other SSD design values [see, for example, Neuman (*8*)], the length requirements can be determined approximately from Figures 3–5. In this case, the speeds associated with the curves are ignored and the curve for the specified SSD value is interpolated using the adjacent curves.

There are drainage requirements for curbed pavements on symmetrical sag curves, whose first and second grades have different signs. The AASHTO policy requires a minimum grade of 0.3 percent at a point about 50 ft from the level point (*4*). This corresponds to a K value equal to 50/0.3 = 167. For unsymmetrical sag curves, the drainage requirements may be controlled by the first or second arc, depending on the location of the level point. The first arc controls if the level point lies on it, which occurs when the grade of the tangent at PCC is positive ($g_1 + r_1L_1 > 0$). The second arc controls if the grade of the tangent at PCC is negative ($g_1 + r_1L_1 < 0$).

When the first arc controls, K_1 equals 167. This yields a maximum curve length equal to 167 $AR/(1 - R)$, based on Equation 2. Similarly, when the second arc controls, K_2 equals 167 and the maximum curve length equals 167 $A(1 - R)/R$, based on Equation 3. These maximum values for drainage requirements are shown by dashed lines in Figures 3–5. All combinations above and to the left of the dashed line would satisfy the drainage criterion. For the combinations below and to the right of the line, pavement drainage must be carefully designed. For $R = 0.4$, for example, if the first arc controls, the maximum length for the drainage criterion is less than the minimum length for the headlight criterion for speeds of about 45 mph and greater. For symmetrical sag curves, the drainage criterion is not critical for almost all the speeds.

OVERHEAD OBSTACLE CONTROL

The geometry of sight distance for overhead control on an unsymmetrical sag curve is shown is Figure 6. Suppose that L_2 is smaller than L_1, so that the second arc is sharper. The

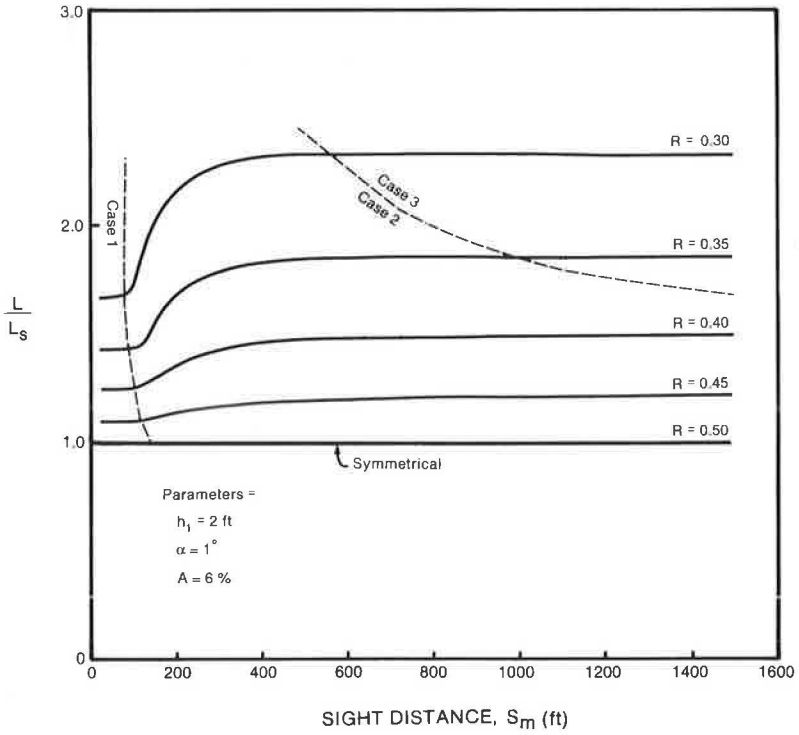

FIGURE 2 Comparison of symmetrical and unsymmetrical sag curves for headlight control.

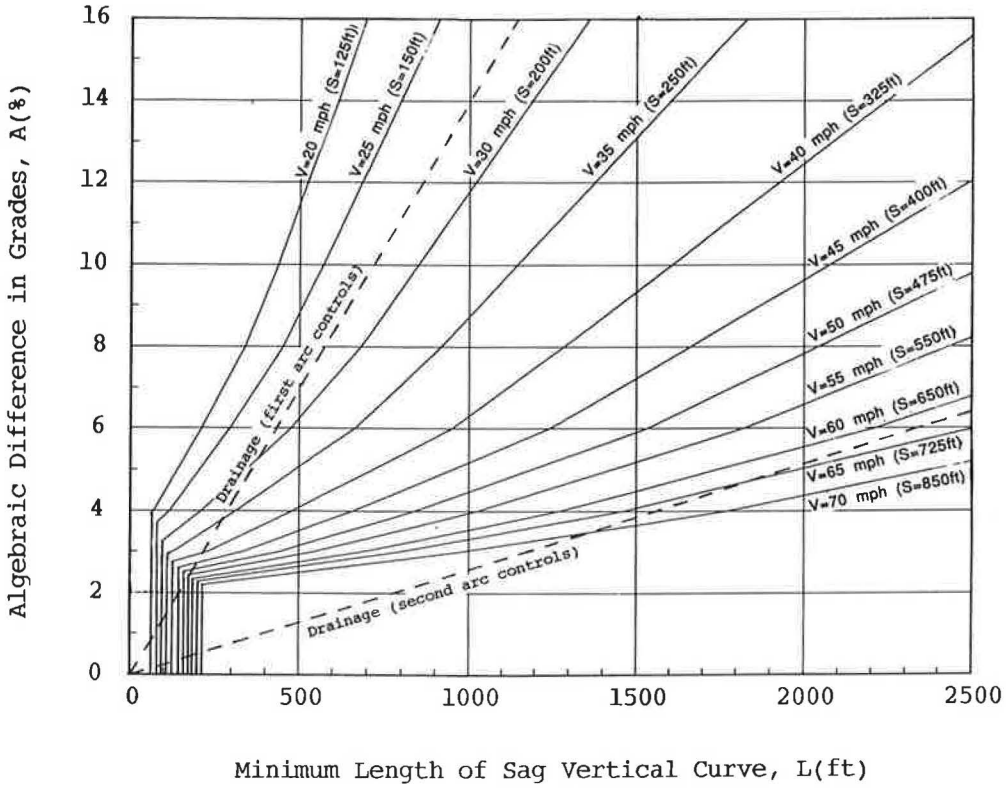

FIGURE 3 Design length requirements of unsymmetrical sag curves for headlight control (R = 0.3).

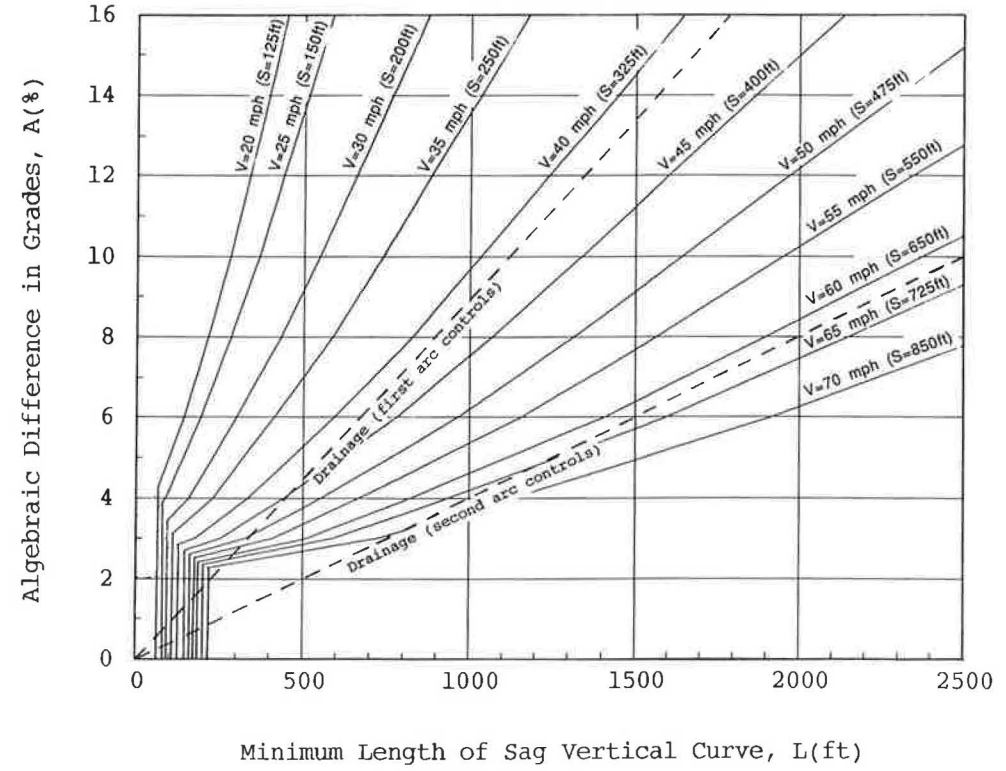

FIGURE 4 Design length requirements of unsymmetrical sag curves for headlight control (R = 0.4).

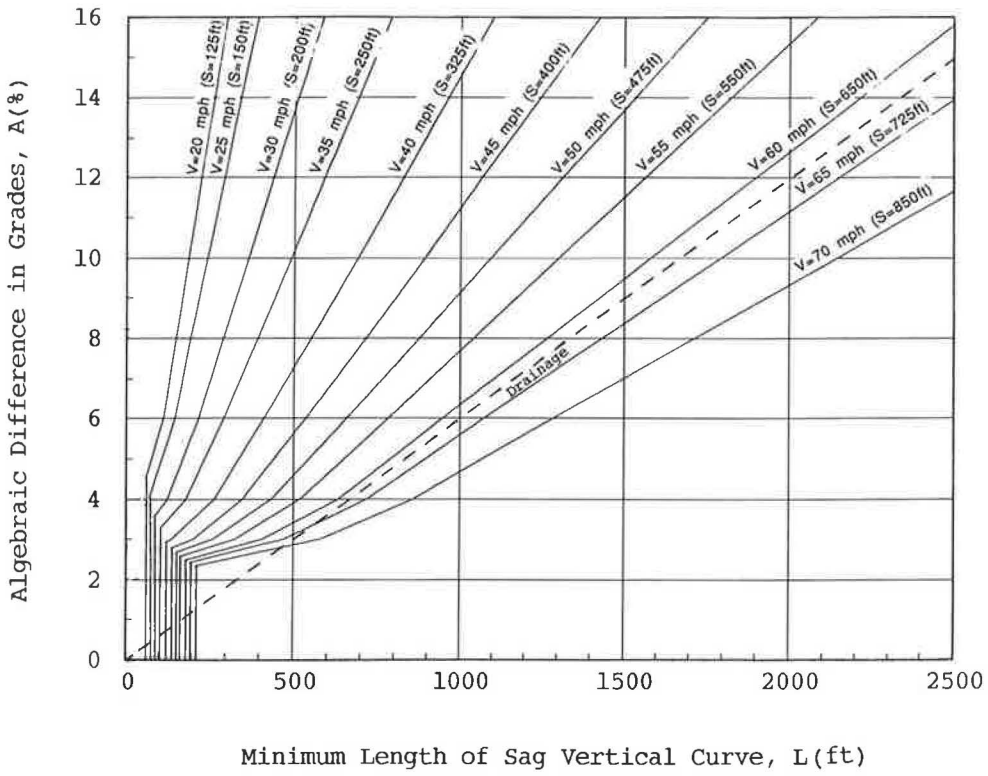

FIGURE 5 Design length requirements of symmetrical sag curves for headlight control (R = 0.5).

direction of travel with the minimum sight distance depends on the location of the obstacle, as will be shown later. Geometric relationships for the available sight distance are developed next, followed by a procedure for calculating the minimum sight distance and a comparison with symmetrical curves. In Figure 6, h_1 and h_2 may represent the driver eye or object height. However, to simplify the presentation these variables are considered to refer to the driver and object, respectively.

Geometric Relationships

Suppose for now that the overhead obstacle lies on the second arc or beyond EVC. The following six cases are considered:

- Case 1: Driver before BVC and object beyond EVC,
- Case 2: Driver before BVC and object on second arc,
- Case 3: Driver on first arc and object beyond EVC,
- Case 4: Driver on first arc and object on second arc,
- Case 5: Driver on second arc and object beyond EVC, and
- Case 6: Driver and object on second arc.

These cases are indicated by the numbers in circles in Figure 6. The height of obstacle above the first tangent in given by

$$y_3 = c + r_2(L - d)^2/2 + (d - L_1)A \qquad L \geq d \geq L_1 \tag{18a}$$

$$y_3 = c + (d - L_1)A \qquad d \geq L \tag{18b}$$

where

y_3 = height of obstacle above the first tangent,
c = height of obstacle above the sag curve, and
d = distance between obstacle and BVC.

The following relationship is also true for all cases:

$$y_3 = (y_1S_2 + y_2S_1)/(S_1 + S_2) \tag{19}$$

where

y_1 = height of driver eye above the first tangent,
y_2 = height of top of object above the first tangent,
S_1 = distance between the obstacle and driver, and
S_2 = distance between the obstacle and object.

The sight distance component, S_1 and S_2, are given by

$$S_1 = d - T \tag{20}$$

$$S_2 = w - z \tag{21}$$

where

T = distance between the driver and BVC [T is negative if the driver is before BVC (on tangent) and positive if the driver is beyond BVC (on curve)], and
z = distance between the obstacle and PVI.

The available sight distance, S, which is the sum of S_1 and S_2, is given by

$$S = L_1 + w - T \tag{22}$$

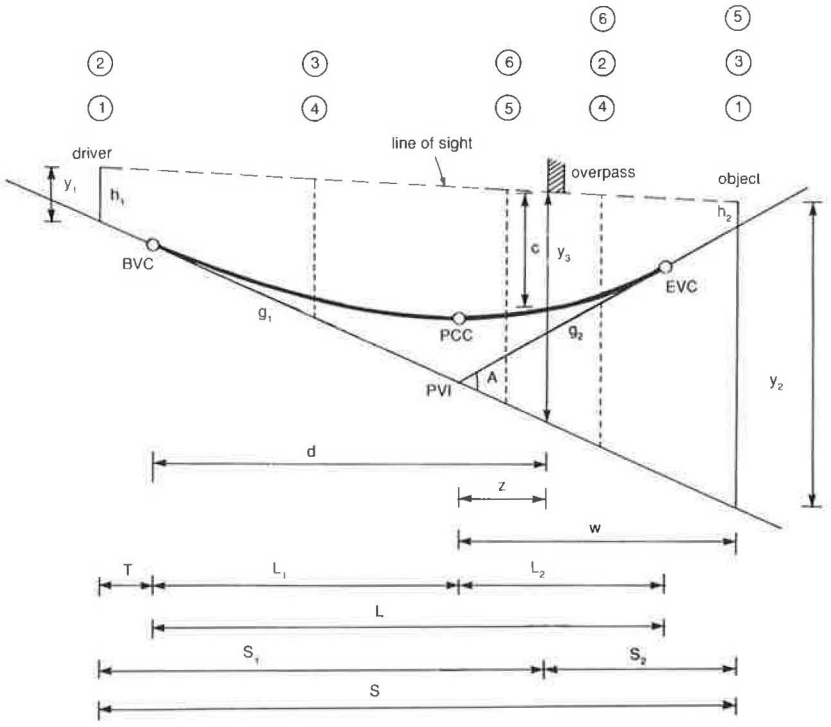

FIGURE 6 Geometry of sight distance for overhead control on an unsymmetrical sag curve (numbers in circles indicate various cases).

The variables y_1 and y_2 of Equation 19 are derived next for various cases and used along with Equations 18 and 19 to develop a relationship for w.

Case 1: Driver Before BVC and Object Beyond EVC

In this case, y_1 and y_2 are given by

$$y_1 = h_1 \tag{23}$$

$$y_2 = h_2 + wA \tag{24}$$

where

h_1 = height of driver eye above the sag curve,
h_2 = height of object above the sag curve, and
w = distance between the object and PVI.

Substituting for S_2 and y_2 (Equations 21 and 24) into Equation 19 and solving for w,

$$w = [y_3(z - S_1) - y_1 z + h_2 S_1]/(y_3 - y_1 - AS_1) \tag{25}$$

in which y_1 is given by Equation 23.

Case 2: Driver Before BVC and Object on Second Arc

In this case, y_1 is given by Equation 23, and y_2 is given by

$$y_2 = h_2 + r_2[L_2 - w]^2/2 + wA \tag{26}$$

Substituting for S_2 and y_2 (Equations 21 and 26) into Equation 19 and solving for w,

$$w = [-b + (b^2 - 4ac)^{1/2}]/2a \tag{27}$$

where

$$a = r_2 S_1/2 \tag{28}$$

$$b = y_1 - y_3 + S_1[A - r_2 L_2] \tag{29}$$

$$c = z(y_3 - y_1) + S_1[h_2 + r_2 L_2^2/2 - y_3] \tag{30}$$

in which r_2 and y_1 are given by Equations 2 and 23.

Case 3: Driver on First Arc and Object Beyond EVC

In this case, y_2 is obtained using Equation 24, and y_1 is given by

$$y_1 = h_1 + r_1 T^2/2 \tag{31}$$

This case is similar to Case 1. The relationship for w is given by Equation 25, where y_1 in this equation is obtained using Equation 31.

Case 4: Driver on First Arc and Object on Second Arc

In this case, y_1 and y_2 are given by Equations 31 and 26. Similar to Case 2, the relationship for w is given by Equation 27, where y_1 is obtained using Equation 31.

Case 5: Driver on Second Arc and Object Beyond EVC

In this case, y_2 is given by Equation 24, and y_1 is given by

$$y_1 = h_1 + r_2(L - T)^2/2 + A(T - L_1) \quad (32)$$

Similar to Case 1, the relationship for w is given by Equation 25, where y_1 is obtained using Equation 32.

Case 6: Driver and Object on Second Arc

In this case, y_1 and y_2 are given in Equations 32 and 26. Similar to Case 2, the relationship for w is given by Equation 27, where y_1 is obtained using Equation 32.

As previously indicated, the obstacle was assumed to lie on the second arc or beyond EVC. If the obstacle lies on the first arc or before BVC, y_3 of Equations 18a and 18b becomes

$$y_3 = c + r_1 d^2/2 \qquad 0 \leq d \leq L_1 \quad (33a)$$

$$y_3 = c \qquad d < 0 \quad (33b)$$

The relationships of Cases 1–4 are then applied using y_3 of Equations 33a and 33b. Cases 5 and 6 are not applicable in this situation, but two more cases need to be considered (when w of Equation 27 is negative). Case A has the driver before BVC and the object on the first arc, and Case B has the driver beyond BVC and the object on the first arc. The relationships for Cases A and B are the same as those for Cases 2 and 4, respectively, except that in Equations 28–30, r_2 and L_2 are replaced by r_1 and L_1, and A is set equal to zero. After w has been computed (Equation 27), S is computed using Equation 22, with w being negative.

Procedure for Calculating S_m

The minimum sight distance is determined using an iterative procedure. The available sight distance S is computed for consecutive values of T until the minimum value is reached. The computation steps are as follows:

1. Compute y_1 for Cases 1, 3, and 5 (Equations 23, 31, and 32).
2. Compute w for these three cases (Equation 25):
   a. If $w > L_2$, the object is beyond EVC. This corresponds to Case 1, 3, or 5 depending on whether the driver is before BVC, on first arc, or on second arc, respectively.
   b. If $w \leq L_2$, the object is on the second arc. This corresponds to Case 2, 4, or 6 depending on the driver's location. Compute the corresponding w (Equation 27).
   c. If $w < 0$, reverse the variables and set $A = 0$. Use Case 2 or 4, depending on the driver's location. Compute w (Equation 27).
3. Compute the available sight distance (Equation 22).

A computer program implementing this procedure was prepared, and its logical flow is shown in Figure 7. The geometric characteristics of the curve L, L_1 (or L_2), and A and the location and height of the obstacle, d and c, must be known or measured. The available sight distance, S, is computed for an initial negative value of T. The procedure is repeated for successively smaller values of T (using an increment ΔT) until $S < S'$, where S' is the available sight distance of the previous iteration. At this point, the minimum sight distance has just been reached and $S_m = S'$. The computer program can also be used to determine the required sag curve length that satisfies a desirable sight distance, given d, c, and other curve characteristics.

Sight Distance Characteristics

The sight distance for overhead control on unsymmetrical sag curves exhibits interesting characteristics. These are discussed in relation to a comparison with symmetrical curves and effect of obstacle location.

Comparison with Symmetrical Curves

As indicated, the relationships between the curve length and sight distance for symmetrical sag curves have been developed for situations in which the obstacle is located at PVI (*4*). These situations can be obtained by setting $L_2 = L/2$ in the developed relationships. Figure 8 shows the variations of the available sight distance along an unsymmetrical curve with an obstacle located at PVI. The variations of sight distance for a symmetrical curve ($R = 0.5$) with the same length are also shown.

The sight distance profile and minimum sight distance on the unsymmetrical curve vary with the direction of travel as shown in Figure 8. In this case, where the overpass lies at PVI, the minimum sight distance is smaller when the driver travels from the flatter to the sharper arc. For the symmetrical curve, the sight distance profile is the same in both directions of travel with $S_m = 1{,}450$ ft. For $R = 0.3$, $S_m = 1{,}167$ ft, which differs from that of the symmetrical curve by about −20 percent. This means that a larger length of the unsymmetrical curve is needed to satisfy a specific sight distance, under similar geometric and operating conditions.

Effect of Obstacle Location

The variations of minimum sight distance as the obstacle location changes are shown in Figure 9 for both travel directions on an unsymmetrical curve. As noted, if the overpass lies at PVI or on the first (flatter) arc, the critical travel direction is from the first to the second arc. If the overpass lies on the second arc, both travel directions may be critical depending on the overpass location. In Figure 9, the travel direction from the second to the first arc becomes critical when the overpass is on the second arc at about 300 ft or more from PVI. The circles in the figure are the points at which the driver or object is at the beginning or end of the curve, where a change in curvature in the sight distance profile occurs.

For the symmetrical curve, the minimum sight distance does not depend on the location of obstacle when both the driver

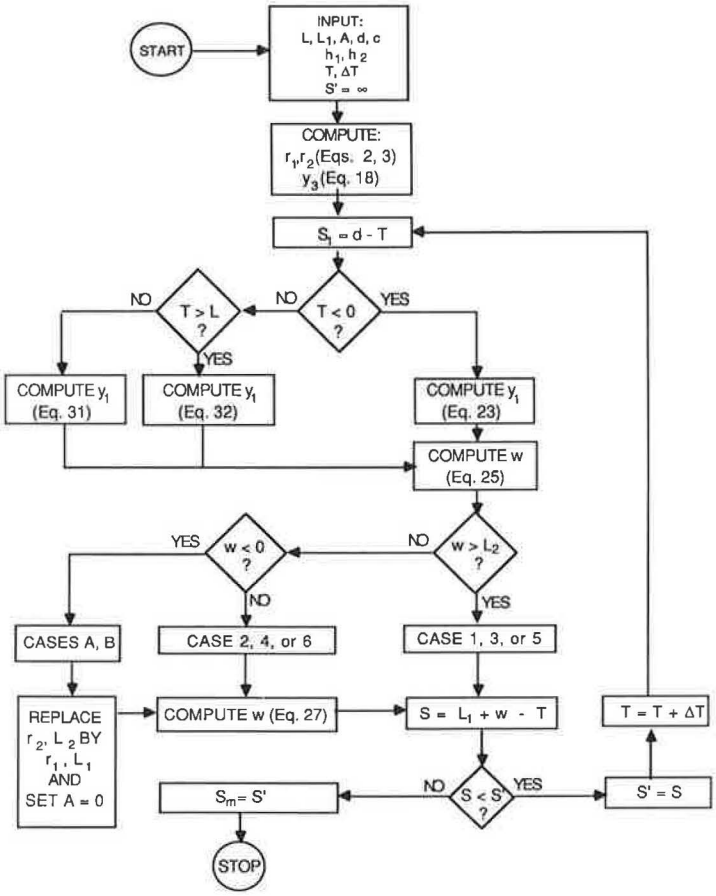

FIGURE 7 Calculating minimum sight distance for overhead control on unsymmetrical sag curves–logical flow.

and object are on the curve. For the unsymmetrical curve, the minimum sight distance occurs when the obstacle is somewhere on the sharper arc. The minimum sight distance exceeds that of the symmetrical curve when the obstacle is located on the flatter arc at a distance greater than about 200 ft from PVI.

Evaluation and Design Values

For overhead control, Table 1 shows the minimum sight distance for sag curve lengths ranging from 200 ft to 1,200 ft, for $R = 0.4$ and 0.5. The following five locations of the obstacle are considered:

1. $d = 0$ (obstacle at BVC),
2. $d = L_1/2$ (obstacle at the midpoint of first arc),
3. $d = L_1$ (obstacle at PVI),
4. $d = L_1 + L_2/2$ (obstacle at the midpoint of second arc), and
5. $d = L$ (obstacle at EVC).

Table 1, which is applicable to highways with trucks, is based on a truck driver eye height of 9 ft and an object height of 1.5 ft. This eye height is conservative because typically truck driver eye height ranges from 71.5 to 112.5 in. (*9,17–19*). The object height of 1.5 ft was suggested in the 1965 AASHO policy (*2*). This height may represent the taillight or a discernible portion of an oncoming vehicle. Table 1 is based on a vertical clearance of 14.5 ft, which is the minimum value suggested by AASHTO (*4*).

A comparison of the minimum sight distance for $A = 12$ percent is shown in Figure 10 for $R = 0.4$ and 0.5 for three locations of the obstacle. There is almost no difference in S_m between symmetrical and unsymmetrical curves when the overpass lies at PVI. However, the sight distance of the unsymmetrical curve increases when the overpass lies at BVC (near the flatter arc) and decreases when the overpass lies at EVC (near the sharper arc). For example, for $L = 1{,}200$ ft, the increase in S_m when the overpass lies at BVC is 25 percent and the decrease when it lies at EVC is 18 percent.

SUMMARY AND CONCLUSIONS

The AASHTO Green Book points out the need for using unsymmetrical vertical curves to accommodate clearance and other controls (*4*). For these curves, however, no relationships are available to relate the available sight distance to the curve parameters and other operating characteristics. Sight distance relationships for unsymmetrical sag curves are derived for both headlight and overhead obstacle controls. Simple design

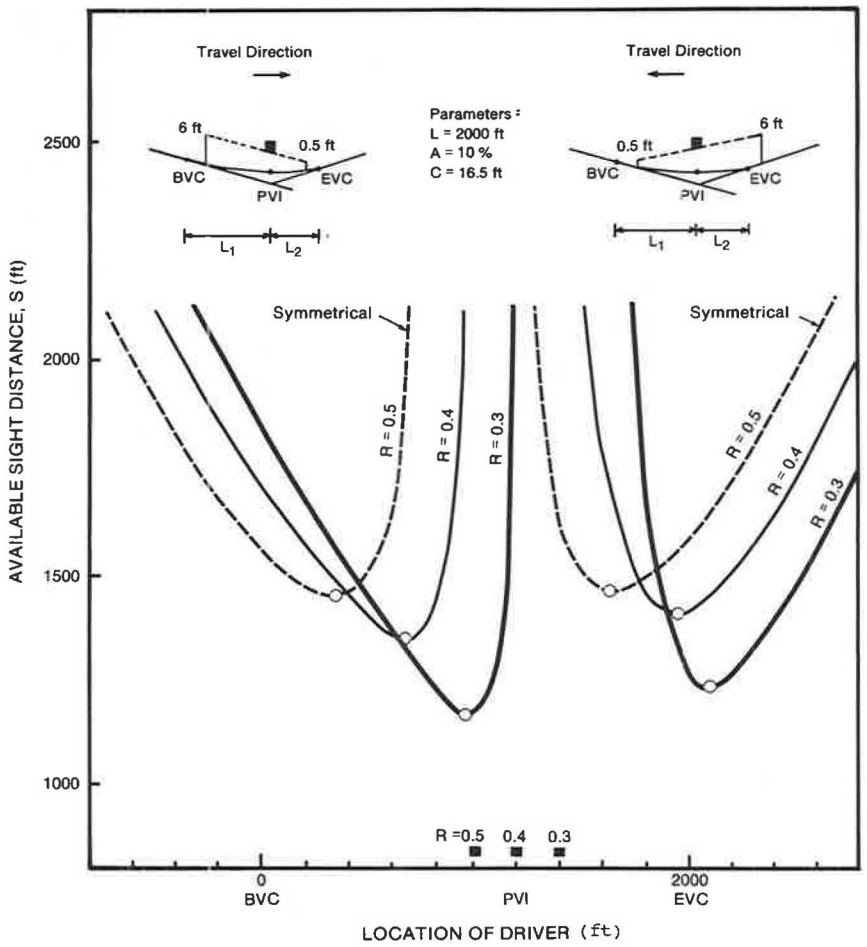

FIGURE 8 Sight distance profiles of symmetrical and unsymmetrical sag curves for overhead control (obstacle at PVI).

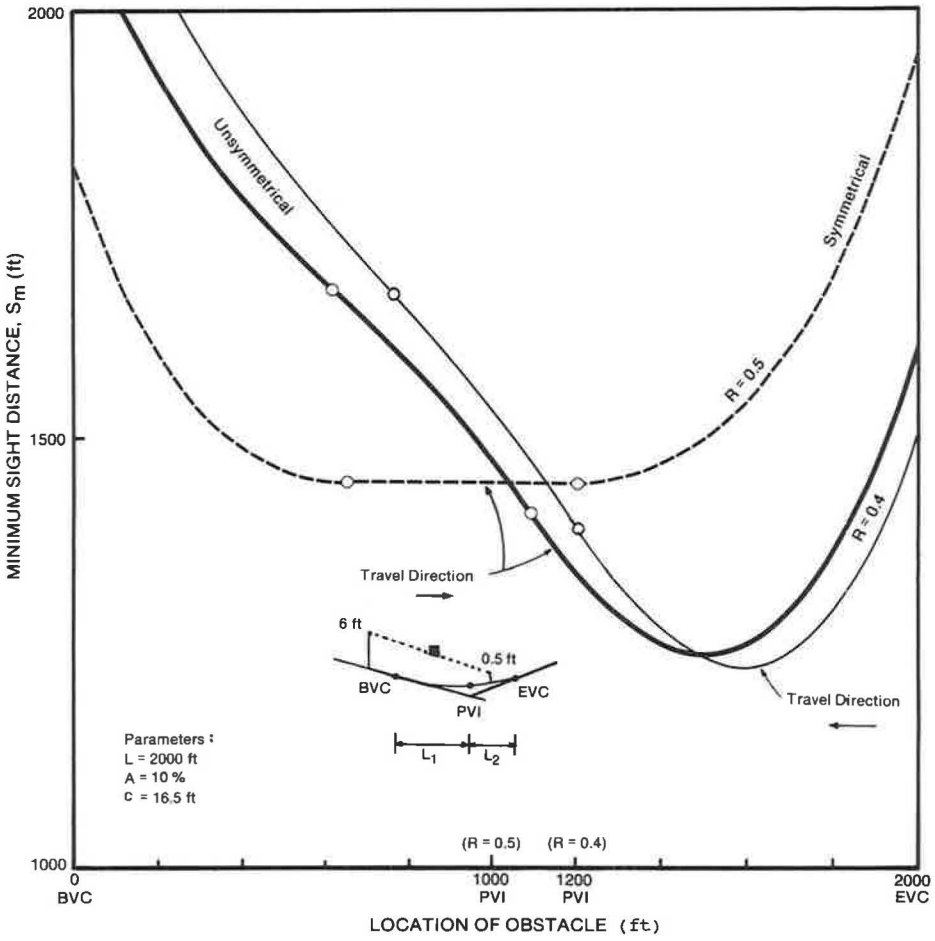

FIGURE 9 Variations of minimum sight distance with obstacle location.

TABLE 1 MINIMUM SIGHT DISTANCE FOR OVERHEAD CONTROL ON UNSYMMETRICAL SAG CURVES FOR HIGHWAYS WITH TRUCKS[a]

Algeb. Diff. Grade (%)	Overp. Loc.[c]	Length of sag curve (ft)											
		200		400		600		800		1000		1200	
		R=.4[b]	R=.5	R=.4	R=.5	R=.4	R=.5	R=.4	R=.5	R=.4	R=.5	R=.4	R=.5
6	1	780	750	960	900	1130	1050	1300	1190	1460	1320	1620	1450
6	2	720	700	840	810	950	910	1070	1020	1190	1120	1300	1220
6	3	700	700	800	800	900	900	1010	1010	1100	1110	1200	1200
6	4	680	700	770	810	860	910	950	1020	1030	1120	1100	1220
6	5	720	750	840	900	960	1050	1070	1190	1180	1320	1260	1450
8	1	630	600	810	750	970	890	1140	1030	1290	1150	1440	1260
8	2	570	550	690	660	800	760	920	870	1040	960	1150	1040
8	3	550	550	650	650	760	750	850	860	940	950	1030	1040
8	4	540	550	630	660	710	760	790	870	860	960	920	1040
8	5	570	600	690	750	810	890	910	1030	990	1150	1070	1260
10	1	540	510	710	660	880	800	1040	920	1180	1030	1320	1120
10	2	480	470	600	570	710	670	830	770	940	850	1050	930
10	3	460	460	560	560	660	670	750	760	840	850	920	930
10	4	450	470	540	570	620	670	690	770	750	850	800	930
10	5	480	510	600	660	710	800	790	920	870	1030	940	1120
12	1	480	450	650	600	810	730	960	840	1100	940	1220	1030
12	2	420	410	540	510	650	610	770	700	870	780	970	850
12	3	400	400	500	500	600	600	690	690	770	770	850	850
12	4	390	410	480	510	550	610	610	700	670	780	720	850
12	5	420	450	540	600	630	730	710	840	780	940	850	1030
14	1	440	410	600	550	760	670	900	780	1030	870	1150	950
14	2	380	360	490	470	610	560	720	640	820	720	910	780
14	3	360	360	460	460	550	560	640	640	720	720	790	780
14	4	350	360	430	470	500	560	560	640	610	720	660	780
14	5	380	410	490	550	580	670	650	780	720	870	780	950
16	1	410	380	570	520	720	630	860	730	980	810	1080	890
16	2	350	330	460	430	580	520	680	600	770	670	860	730
16	3	330	330	430	430	520	520	600	600	670	670	740	730
16	4	310	330	400	430	460	520	510	600	560	670	610	730
16	5	350	380	450	520	540	630	610	730	670	810	730	890

[a] Driver eye height = 9.0 ft; Object height = 1.5 ft

[b] Ratio of shorter arc to total curve length

[c] 1: Overpass at BVC; 2: Overpass at midpoint of first arc; 3: Overpass at PVI; 4: Overpass at midpoint of second arc; 5: Overpass at EVC

Note: minimum sight distances are expressed in feet. Vertical clearance = 14.5 ft.

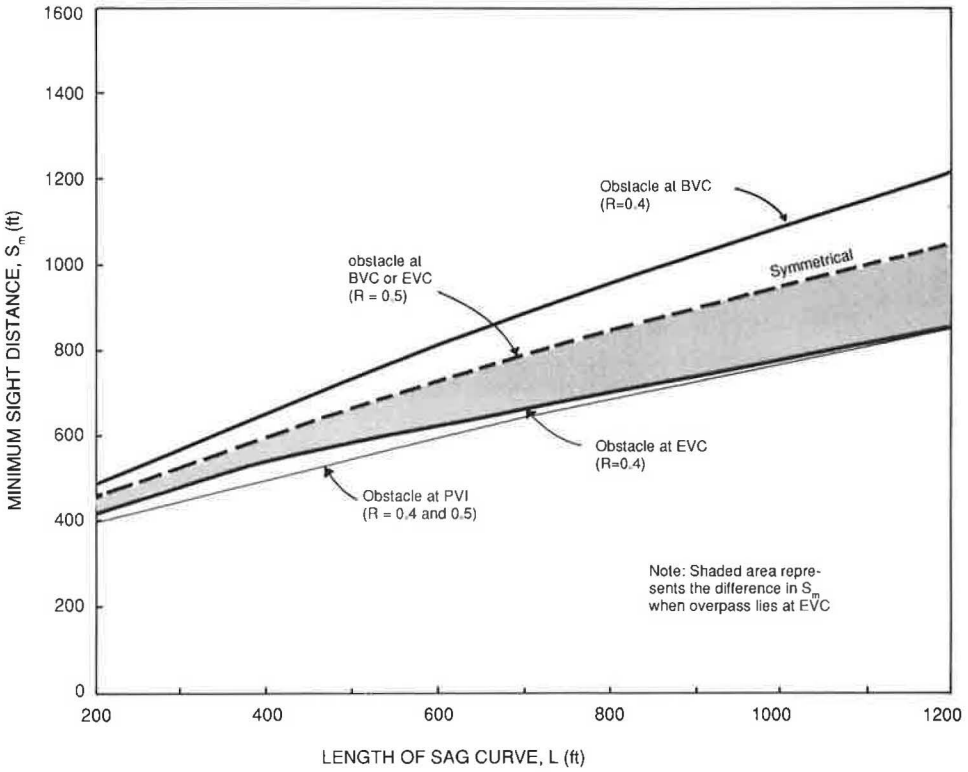

FIGURE 10 Comparison of the minimum sight distance for different obstacle locations for A = 12 percent (highways with trucks).

graphs and tables of the curve length requirements and minimum sight distance are established.

The results show that unsymmetrical sag curves must be much longer than symmetrical curves, under similar conditions. The sight distance profiles of unsymmetrical curves with overhead control exhibit certain characteristics that may have important design implications. This strongly supports the early use of the developed models in the design and evaluation of unsymmetrical sag curves. The models should be useful in maintaining or achieving adequate sight distances on unsymmetrical sag curves, and thus making highways safer.

ACKNOWLEDGMENT

This work was supported by the Natural Sciences and Engineering Research Council of Canada.

REFERENCES

1. *A Policy on Sight Distance for Highway, Policies on Geometric Highway Design*. AASHO, Washington, D.C., 1940.
2. *A Policy on Geometric Design of Rural Highways*, AASHO, Washington, D.C., 1965.
3. *A Policy on Design Standards for Stopping Sight Distance*. AASHO, Washington, D.C., 1971.
4. *A Policy on Geometric Design of Highways and Streets*. AASHTO, Washington, D.C., 1984.
5. T. F. Hickerson. *Route Location and Design*. McGraw-Hill Book Company, New York, 1964.
6. H. C. Ives and P. Kissam. *Highway Curves*. John Wiley & Sons, London, England, 1956.
7. P. F. Olson, D. E. Cleveland, P. S. Fancher, L. P. Kostyniuk, and L. W. Schneider. *NCHRP Report 270: Parameters Affecting Stopping Sight Distance*. TRB, National Research Council, Washington, D.C., 1984.
8. T. R. Neuman. New Approach to Design for Stopping Sight Distance. In *Transportation Research Record 1208*, TRB, National Research Council, Washington, D.C., 1989.
9. D. W. Harwood and J. C. Glennon. Passing Sight Distance Design for Passenger Cars and Trucks. In *Transportation Research Record 1208*, TRB, National Research Council, Washington, D.C., 1989.
10. J. C. Glennon. New and Improved Model of Passing Sight Distance on Two-Lane Highways. In *Transportation Research Record 1195*, TRB, National Research Council, Washington, D.C., 1988, pp. 132–137.
11. H. W. McGee. Reevaluation of the Usefulness and Application of Decision Sight Distance. In *Transportation Research Record 1208*, TRB, National Research Council, Washington, D.C., 1989, pp. 85–89.
12. T. R. Neuman, J. C. Glennon, and J. E. Leish. *Stopping Sight Distance—An Operational and Cost Effectiveness Analysis*. Report FHWA/RD-83/067. FHWA, U.S. Department of Transportation, Washington, D.C., 1982.
13. T. R. Neuman and J. C. Glennon. Cost-Effectiveness of Improvements to Stopping Sight Distance. In *Transportation Research Record 923*, TRB, National Research Council, Washington, D.C., 1984, pp. 26–34.
14. J. C. Glennon. Effects of Sight Distance on Highway Safety. In *State-of-the-Art Report 6*. TRB, National Research Council, Washington, D.C., 1987.
15. C. F. Meyer. *Route Surveying and Design*. International Textbook Company, Scranton, Pa., 1971.
16. C. J. Khisty. *Transportation Engineering: An Introduction*. Prentice Hall, Englewood Cliffs, New Jersey, 1990.
17. P. B. Middleton, M. Y. Wong, J. Taylor, H. Thompson, and J. Bennett. *Analysis of Truck Safety on Crest Vertical Curves*. Report FHWA/RD-86/060. FHWA, U.S. Department of Transportation, Washington, D.C., 1983.
18. J. W. Burger and M. U. Mulholland. *Plane and Convex Mirror Sizes for Small to Large Trucks*. NHTSA, U.S. Department of Transportation, Washington, D.C., 1982.
19. Urban Behavioral Research Associates. *The Investigation of Driver Eye Height and Field of Vision*. FHWA, U.S. Department of Transportation, Washington, D.C., 1978.

Publication of this paper sponsored by Committee on Geometric Design.

Traffic Performance and Design of Passing Lanes

ADOLF D. MAY

A study of traffic performance and design of passing lanes on two-lane, two-way rural highways emphasized four major research areas. Field studies of traffic performance and design of five California passing lanes provided an operational assessment and focused attention on the other three research efforts. A before-and-after field study of two passing-lane entrance designs demonstrated that the modified design significantly increased the proportion of traffic that would enter the passing-lane section in the basic lane. Field observations of passing maneuvers clearly indicated that the number of passes per passing-lane length was a good measure of effectiveness of passing lanes. Equations were developed for estimating the number of passes as a function of traffic flow level for each of the five data sets. A sensitivity analysis through simulation identified that passing lanes from 0.25 to 0.75 mi long appeared to be the most effective and that spacing of 2 to 5 mi between such passing lanes appeared appropriate depending on downstream roadway and traffic conditions. The number of passes that would likely occur at three of the field sites under various traffic flow levels and vehicle composition mixes was estimated.

During the past several years, the Institute for Transportation Studies has performed research on two-lane, two-way rural highways; particular attention has been given to the traffic performance and design of passing lanes. This research has been sponsored by the California Department of Transportation (Caltrans) and FHWA. A number of reports have been prepared, including a final project report (*1,2*). This paper summarizes the results and conclusions of this research project, emphasizing four major substudies.

Field studies at five passing-lane locations in northern California assessed traffic performance in passing lanes. These five locations included short, medium, and long passing lanes in level, rolling, and mountainous terrain. Traffic performance measures included lane flows, traffic composition, travel times, spot speeds, passing-lane use, percent time delay, time headway distribution, and platoon structure.

The results of the field studies drew attention to the design of the entrance to passing-lane sections and suggested a possible modification in which traffic would be directed to the rightmost lane rather than to the passing lane. A before-and-after study at one of the five field study locations assessed this type of entrance design modification. Traffic performance measures for this assessment included passing-lane use, spot speeds, percent time delay, time headway distribution, and platoon structure.

The results of the earlier field studies identified weaknesses in the traffic performance measures used to assess the effectiveness of passing lanes. Because the purpose of passing lanes is to permit faster vehicles to pass slower vehicles, the number of passes in the passing lane might be a good traffic performance measure. The video records permitted reanalysis so that the number of vehicle passes under different flow levels by type of vehicle could be obtained.

The previous analyses were limited to five passing-lane locations with specific passing-lane designs and under existing traffic conditions. A simulation permitted extensive sensitivity analysis for situations that were not studied in the field. The simulation assessed the effect of passing-lane length, the effect of passing lanes on downstream conditions, and the effect of flow level and vehicle composition. The TRARR simulation model was used for this assessment, and was calibrated for the existing field study conditions.

Institute of Transportation Studies, University of California, Berkeley, 109 McLaughlin Hall, Berkeley, Calif. 94720.

FIELD STUDY RESULTS

The field study assessed site characteristics and measured traffic performance measures for the five passing-lane locations. This information for all five sites is presented in Tables 1 and 2.

Short Passing Lane in Level Terrain

The short passing lane studied was on State Route 70 in level terrain with good horizontal and vertical alignment. The average hourly flow in the direction of the passing lane during the 6-hr study period was approximately 300 vehicles per hour (vph). The traffic stream consisted of 90 percent four-tire vehicles, 4 percent trucks, and 6 percent recreational vehicles. Spot speed studies revealed average speeds of 57, 62, and 58 mph in the opposing, passing, and basic lanes, respectively.

Traffic performance measures included percent time delay, time headway distribution, and platoon size distribution. The percent time delay was estimated in the field as the percentage of vehicles traveling at headways of 5 sec or less. The percent time delay actually increased from 47 to 48 percent when traffic entering was compared with traffic leaving the passing lane. Traffic with 2-sec headways actually increased from 20 to 23 percent. Single-vehicle platoons also increased from 58 to 60 percent. These traffic performance measures did not indicate user benefits from the passing lane.

Short Passing Lane in Rolling Terrain

The short passing lane studied was on State Route 41 in rolling terrain with good horizontal alignment and on a 5-percent

TABLE 1 FIELD STUDY RESULTS

Route Number	Passing Lane Length (miles)	Terrain (percent grade)	Directional Average Hourly Flow	Vehicle Composition (%)			Spot Speeds (mph)		
				Four-tired Vehicles	Trucks	Recreational Vehicles	Opposing Lane	Passing Lane	Basic Lane
70	short (0.5)	level (0-1)	300	90	4	6	57	62	58
41	short (0.5)	rolling (5)	200	88	5	7	59	57	54
49	short (0.4)	rolling (4)	150	96	1	3	N/A	58	55
140	medium (0.9)	rolling (4)	100	95	1	4	N/A	58	56
299	long (1.5)	mountain-ous (5-8)	150	87	1	12	54	59	53

N/A - Not Available

TABLE 2 FIELD STUDY PERFORMANCE MEASURES

Route Number	Passing Lane Length (miles)	Terrain (percent grade)	Percent Time Delay*		Percent Two-Second Headways		Percent One-Vehicle Platoons*	
			At Entrance	At Exit	At Entrance	At Exit	At Entrance	At Exit
70	short (0.5)	Level (0-1)	47	48	20	23	58	60
41	short (0.5)	Rolling (5)	52	49	26	19	58	63
49	short (0.4)	Rolling (4)	48	42	20	15	55	64
140	medium (0.9)	Rolling (4)	25	23	10	4	75	80
299	long (1.5)	Mountain-ous (5-8)	44	25	18	8	58	78

* Based on four second headway threshold value.

upgrade (*3*). The average hourly flow in the direction of the passing lane during the 6-hr study period was approximately 200 vph. The traffic stream consisted of 88 percent four-tire vehicles, 5 percent trucks, and 7 percent recreational vehicles. Spot speed studies revealed average speeds of 59, 57, and 54 mph in the opposing, passing, and basic lanes, respectively.

The percent time delay in the passing lane section decreased from 52 to 49 percent, and the percent of traffic with 2-sec headways decreased from 26 to 19 percent. Single-vehicle platoons increased from 58 to 63 percent. These traffic performance measures indicated slight improvements in user benefits due to the passing lane.

Short Passing Lane in Rolling Terrain

The short passing lane studied was on State Route 49 in rolling terrain with good horizontal alignment and on a 4-percent upgrade (*4*). The average hourly flow in the direction of the passing lane during the 6-hour study period was approximately 150 vph. The traffic stream consisted of 96 percent four-tire vehicles, 1 percent trucks, and 3 percent recreational vehicles. Spot speed studies revealed average lane speeds of 58 and 55 mph in the passing and basic lanes, respectively.

The percent time delay in the passing lane section decreased from 48 to 42 percent, and the percent of traffic with 2-sec headways decreased from 20 to 15 percent. Single-vehicle platoons increased from 55 to 64 percent. These traffic performance measures indicated slight improvements in user benefits due to the passing lane. These results were somewhat similar to those for State Route 41.

Medium-Length Passing Lane in Rolling Terrain

The medium-length passing lane studied was on State Route 140 in rolling terrain with good horizontal alignment and on a 4-percent upgrade. The average hourly flow in the direction of the passing lane during the 6-hour study period was approximately 100 vph. The traffic stream consisted of 95 percent four-tire vehicles, 1 percent trucks, and 4 percent recreational vehicles. Spot speed studies revealed average lane speeds of 58 and 56 mph in the passing and basic lanes, respectively.

The percent time delay in the passing lane section decreased from 25 to 23 percent, and the percent of traffic with 2-sec headways decreased from 10 to 4 percent. Single-vehicle platoons increased from 75 to 80 percent. These traffic performance measures indicated slight improvements in user benefits due to the passing lane. These results were somewhat similar to the results for the previous two passing lane sites. The increased potential benefits due to the longer passing lane, however, appeared to be offset by a lower hourly flow level.

Longer Passing Lane in Mountainous Terrain

The longer passing lane site studied was on US-299 in mountainous terrain on a grade varying from 5 to 8 percent. The average hourly flow in the direction of the passing lane during the 6-hour period was approximately 150 vph. The traffic stream consisted of 87 percent four-tire vehicles, 1 percent trucks, and 12 percent recreational vehicles. Spot speed stud-

ies revealed average lane speeds of 54, 59, and 53 mph in the opposing, passing, and basic lanes, respectively.

The percent time delay in the passing lane section decreased from 44 to 25 percent, and the percent of traffic with 2-sec headways decreased from 18 to 8 percent. Single-vehicle platoons increased from 58 to 78 percent. All of these measures of effectiveness indicated significant improvements and the largest improvement of all sites studied. The longer passing lane combined with the steeper grades and high percentage of recreational vehicles most likely accounted for these larger improvements.

Summary of Field Study Results

The results, particularly for the shorter passing lanes, raised three questions that shaped the later work on the project:

- What impact does entrance design have on the potential benefits derived from passing lanes, particularly short passing lanes in level terrain?
- What measures of traffic flow performance can best evaluate user benefit as affected by the passing lane?
- Where should measurements be taken in reference to the physical passing lane in order to best evaluate its effectiveness?

It was observed at the different sites that the entrance design and pavement markings did not encourage drivers to go immediately into the basic nonpassing lane. Hence, the effective length of the passing lane might be reduced. This reduction was most evident in the case of short passing lanes and where the differential speed between vehicles passing and being passed was small. After discussions with Caltrans engineers, it was decided to do a before-and-after study at the State Route 70 site; the change was restriping of the pavement markings to direct entering traffic into the basic nonpassing lane upon entrance to the passing-lane section.

Percent time delay, time headways, and percent of vehicles in single platoons were used in the field studies as measures of user benefits due to the passing lane. Results were inconclusive for short passing lanes, especially in level terrain. Several additional measures were considered, and those that could be expressed as a function of passing-lane length were preferred. It was decided that the number of passes per length of passing lane would be analyzed. Fortunately, the videotapes could be reanalyzed to obtain this measure of performance, although it was a tedious and time-consuming effort.

Almost all measurements obtained in the field study were taken within the passing-lane section. Further review of the results of this study, related references, and initial work with simulation models suggested that measurements some distance upstream and downstream of the passing-lane section might more completely indicate the user benefits as affected by the passing lane. Unfortunately, because of time and funding limitations, it was not possible to restudy upstream and downstream sections at the five field sites. Plans had already been developed to perform experiments with simulation, so this effort was shifted to computer simulation.

EFFECT OF PASSING-LANE ENTRANCE DESIGN

The field study of Route 70 with the existing passing-lane entrance design was conducted in October 1988. The pavement markings were modified in the early fall of 1989, and the field study of Route 70 with the modified passing-lane entrance design was conducted in November 1989.

The existing and modified passing-lane entrance design is shown in Figure 1. The lower sketch shows the existing design and pavement markings. The entrance flare widens at an approximate 1:25-ft ratio. Striping starts at the point where two full 11.5-ft lanes become available. The striping consists of a white dashed line that divides the passing section into two southbound lanes.

The upper sketch shows the modified design and pavement markings. Yellow striping was added at the entrance to the passing lane section with the intent of directing traffic into the basic lane. Neither the geometric design features nor the signing was changed. After the study area was restriped, drivers were given approximately 3 weeks to become familiar with the changes before the after study was initiated.

The after study was conducted under similar conditions of the before study. Both studies occurred on the same day of the week during almost identical daylight hours. Both days were sunny and roadway and traffic conditions were as similar as possible. The studies used identical field measurement techniques, including video cameras, tach vehicles, traffic counters, and radar speed guns.

The entrance design study results are summarized in Table 3 for both the before (existing design) and the after (modified design) studies. The traffic flow levels for the two studies were almost identical (305 versus 309 vph). There were slightly more trucks in the after study (4 to 5 percent) and fewer recreational vehicles (6 to 3 percent). The single most significant difference between the two studies was the lane distribution between the passing lane and the basic lane. Whereas 80 percent of the entering traffic in the before study moved directly into the passing lane, 80 percent of the entering traffic in the after study moved directly into the basic lane. The shift in this direction was expected, but the magnitude was far greater than expected. Unfortunately, this redirection of traffic into the basic lane was not accompanied by significant improvement in user benefits, at least considering the measures of effectiveness described in the following paragraph.

Lane speeds increased slightly, as expected, but not significantly. Changes in percent time delay within the passing-

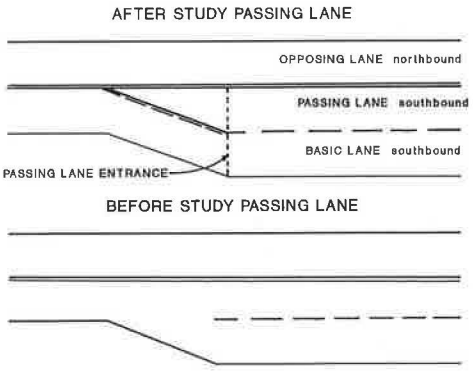

FIGURE 1 State Route 70 entrance design.

TABLE 3 ENTRANCE DESIGN STUDY RESULTS

RESULTS	Entrance Design	
	Existing	Modified
Flow Level		
- No. of Vehicles Observed	1828	1854
- Duration of Study (hrs)	6	6
- Hourly Flow (veh/hr)	305	309
Vehicle Composition (percent)		
- Four-tired Vehicles	90	92
- Trucks	4	5
- Recreation Vehicles	6	3
Lane Distribution (percent)		
- Passing Lane	80	20
- Basic Lane	20	80
Lane Speeds (mph)		
- Passing Lane	62	63
- Basic Lane	58	57
Percent Time Delay (percent)		
- At Entrance	53	50
- At Exit	54	52
1-2 Second Time Headways (%)		
- At Entrance	25	30
- At Exit	27	25
>10 Second Time Headways (%)		
- At Entrance	33	36
- At Exit	33	35
1-Vehicle Platoons (percent)		
- At Entrance	51	53
- At Exit	52	56
2-Vehicle Platoons (percent)		
- At Entrance	20	21
- At Exit	19	18

lane section were similar. The modified design did appear to reduce the percent of vehicles with small headways (1 to 2 sec), but large headways (more than 10 sec) were unaffected. There was a slightly greater increase in single-vehicle platoons and a slightly greater decrease in two-vehicle platoons with the modified entrance design, but neither difference was significant.

In summary, although the modified entrance design significantly changed the lane distribution at the beginning of the passing lane section, none of the measures of effectiveness showed significant improvements. Obviously this is an area for further research.

FIELD OBSERVATIONS OF PASSING MANEUVERS

A major conclusion from the field study results was the identification of the need for additional measures of effectiveness, particularly for short passing lanes in level terrain. Qualitative review of field study videotapes, review of the TRARR simulation model outputs, and discussions with Caltrans engineers led to the consideration of using the number of passes in the passing-lane section as a new measure of effectiveness. Another advantage of this measure of effectiveness is the ability to compare various lengths of passing lane by normalizing the number of passes by dividing by the length of the passing lane.

Videotapes of the field study sites were reanalyzed to determine levels of passing activity at each site. Each field site had been filmed for 6 hr, and approximately one-half of these films were analyzed. The quality of the film and the position of cameras at the Route 49 site did not permit the inclusion of this site in the study of passing activity. On the other hand, both the before and the after study tapes of the Route 70 site were included.

Assistants first matched a distinctive vehicle found in the passing-lane entrance videotape to the same vehicle in the videotape of the same passing-lane exit. From there, teams of two assistants noted the type and order of vehicles entering the passing lane. The order of the same vehicles was noted at the exit to the passing lane. The net number of passes occurring within the passing lane length was determined. The number of passes determined in this manner is considered the minimum number of passes that took place. Intermediate-type passes, such as one vehicle overtaking another but then being passed by the initially overtaken vehicle, are considered two passes and would have not been counted using this method. With this data collection scheme, it was possible to relate the number of passes to the entering traffic flow rate and to identify the types of vehicles passing and being passed. The next two subsections deal with these two issues, namely, the passing maneuver frequencies related to traffic flow levels and the passing maneuver frequencies related to vehicle types. This analysis included five data sites: Route 70 (existing design), Route 70 (modified design), Route 41, Route 140, and Route 299.

Passing Maneuver Frequencies Related to Traffic Flow Levels

The passing maneuver results related to traffic flow levels for the five data sets are summarized in Table 4. The passing-lane design features are again identified, and the traffic composition for each data set is given, with Route 41 having the highest percent of vehicles other than automobiles. The number of 5-min samples varied from 35 to 43, and the total number of vehicles observed and number of passes recorded are shown. The 5-min hourly flow levels for each data set varied from a low of 20 vph at the Route 140 site to a high of 530 vph at the Route 70 site (existing design). The 5-min hourly passing rates for each data set varied from a low of zero passes per hour at the Route 41, 140, and 299 sites to a high of 410 passes per hour at the Route 70 site (existing design).

The number of passes in the passing lane was plotted against the number of vehicles entering the passing lane. Inspection of these plots suggested that a linear fit was as appropriate as various nonlinear formulations. Linear regression analysis was performed with each of the five data sets, and the resulting linear relations are shown in Figure 2. The numerical results of the linear regression analysis are shown in Table 4.

The X-intercept values ranged from $+3.8$ to $+11.3$ vehicles in a 5-min period entering the passing lane. This range of

TABLE 4 PASSING MANEUVER FREQUENCY RELATED TO FLOW LEVELS

RESULTS	ROUTE NUMBER				
	70	70M	41	140	299
Passing Lane Design					
- General Length	short	short	short	medium	long
- Length (miles)	0.5	0.3	0.5	0.9	1.5
- Terrain	level	level	roll-ing	roll-ing	moun-tainous
- Percent Grade	1	1	5	4	5-8
- Entrance Design	exist-ing	modi-fied	exist-ing	exist-ing	exist-ing
Traffic Composition (%)					
- Four-tired Vehicles	94	92	87	96	95
- Trucks	2	4	5	0	1
- Recreation Vehicles	4	4	8	4	4
Sample Size					
- No. of 5-minute Intervals	39	39	35	43	39
- No. of Vehicles Observed	1059	1015	525	422	412
- No. of Passing Maneuvers	458	413	189	94	206
5-minute Hourly Flow					
- Lowest	190	180	50	20	40
- Average	330	310	180	120	130
- Highest	530	480	490	240	360
5-minute Hourly Passing Rate					
- Lowest	10	20	0	0	0
- Average	140	130	70	30	60
- Highest	410	330	310	120	310
Linear Regression Results					
- X-intercept	+7.7	+11.3	+5.5	+5.4	+3.8
- Y-intercept	-4.6	-8.0	-3.0	-2.7	-3.0
- Slope	+0.60	+0.71	+0.55	+0.50	+0.78
- R^2 Value	0.31	0.45	0.76	0.49	0.66

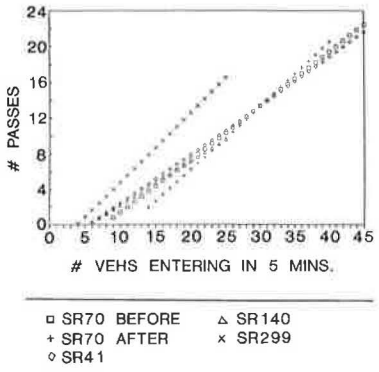

FIGURE 2 Passing activity: regression analysis comparison.

values indicates that when averaging time headways of vehicles entering the passing lane are about 1 min, the likelihood of vehicles passing is negligible. There appeared to be a pattern in that longer passing lanes had lower X-intercept values.

The Y-intercept values ranges from -8.0 to -2.7 passes in a 5-min period in the passing-lane section. This range of values indicates that the relationships are nonlinear and concave upward as traffic flow levels approach zero because the curve should go through the origin. Again a pattern appeared in that longer passing lanes had higher Y-intercept values. The no-intercept model and the nonlinear model were also considered for these data, but were not tested because of time constraints.

The slopes of the regression lines varied from $+0.50$ to $+0.78$. The slopes for the lines representing Routes 70 (existing design), 41, and 140 were quite similar; the slopes for the lines representing Routes 70 (modified design) and 299 had similar but higher values. A higher value might be expected for the Route 299 site because of its longer length, but the Route 70 site with the modified design would be expected to have a slope similar to Routes 70 (existing design), 41, and 140.

The regression correlation coefficients varied from 0.31 to 0.76. Although several of the higher valued coefficients might be considered to be in the acceptable range, the poor fit of Route 70 (existing design) (0.31) caused concern. The plot of data points for this data set revealed that six data points were significantly higher or lower than what the regression curve would indicate. In an attempt to explain the considerable variations, the videos for these six data points were reanalyzed to determine whether there had been a data analysis error.

Three situations contributed to significant changes in passing patterns:

- Vehicles entered the passing lane at uniform and large headways, and fewer passes were observed than expected;
- Vehicles in the sample were all passenger vehicles traveling at approximately the same speed, and although the flow level was high, fewer passes were observed than expected; and
- Vehicles entered in bunches with a nonauto as the platoon leader. Although the flow level was relatively low, there were more passes observed than expected.

Returning to Figure 2, the resulting linear regression lines for three of the five sites are almost identical. The Route 299 regression line is significantly different and shifted to the left. This difference is not unexpected because Route 299 had the longest passing lane and was located in the most mountainous terrain. In summary, for the shorter passing-lane locations in level to rolling terrain, the following observations were noted:

- The number of passes in a passing lane is negligible when the hourly 5-min rate of flow is less than 120 vph;
- The ratio of the number of passes to the number of vehicles entering (expressed as a percentage) increases from approximately 30 to 50 percent as the hourly 5-min rates of flow increase from 200 to 400 vph; and
- The ratio of the number of passes to the number of vehicles entering (expressed as a percentage) is about 50 percent when hourly 5-min rates of flow range from 400 to 600 vph.

Passing Maneuver Frequencies Related to Vehicle Types

The reanalysis of the videotapes for passing maneuvers also provided the opportunity to study passing maneuver frequency by vehicle types. Because the proportion of automobiles and nonautomobiles was measured, it was possible to predict an expected fraction of passes by combinations of vehicle types assuming random behavior. For example, if passing maneuvers are independent of vehicle type and 90 percent of the traffic was automobiles, then one would expect that 81 percent of the passes would be of automobiles passing automobiles.

The actual number of passes by four vehicle-type combinations was observed for each of the described five data sets: automobiles passing automobiles, automobiles passing nonautomobiles, nonautomobiles passing automobiles, and nonautomobiles passing nonautomobiles. Chi-square tests were performed to test for significant differences with these vehicle-type distributions. The results are summarized in Table 5.

Automobiles passing automobiles had highest frequency of passes. No significant difference was noted between the expected number and the observed number. The next highest frequency of passes was for automobiles passing nonautomobiles. In almost all cases, the observed frequency of passes was significantly higher than the expected frequency. In the case of nonautomobiles passing automobiles, the observed number of passes was always less, frequently significantly less, than the expected number of passes. The last case was that of nonautomobiles passing nonautomobiles. The frequencies of such passes were so small that it was difficult to assess differences. Overall, each of the data sets revealed a significant difference between expected and observed distributions of vehicle-type passing. Automobiles passing nonautomobiles were more prevalent than expected, and nonautomobiles passing automobiles were less prevalent than expected.

TABLE 5 PASSING MANEUVER FREQUENCY RELATED TO VEHICLE TYPES

RESULTS	ROUTE NUMBER				
	70	70M	41	140	299
Autos Passing Autos					
- Expected Number	371	343	146	82	150
- Observed Number	356	346	109	74	154
- Significant Difference	No	No	No	No	No
Autos Passing Non-autos					
- Expected Number	41	33	20	6	26
- Observed Number	83	64	69	5	52
- Significant Difference	Yes+	Yes+	Yes+	No	Yes+
Non-autos Passing Autos					
- Expected Number	41	33	20	6	26
- Observed Number	16	3	6	0	0
- Significant Difference	Yes-	Yes-	No	No	Yes-
Non-autos Passing Non-autos					
- Expected Number	5	4	3	0	4
- Observed Number	3	0	5	15	0
- Significant Difference	No	No	No	Yes+	No
Chi-square Results					
- Calculated Value	59.7	60.4	141.6	∞	56.1
- Table Value	11.3	11.3	11.3	11.3	11.3
- Significant Difference	Yes	Yes	Yes	Yes	Yes

SENSITIVITY ANALYSIS THROUGH SIMULATION

The research dealing with passing lanes on two-lane rural highways was directed to sensitivity analysis using the TRARR simulation model. The sensitivity analysis was designed to answer three questions:

- What effect does passing-lane length have on traffic performance within the passing lane?
- What effect do passing lanes and their lengths have on downstream traffic conditions?
- What effect do flow level and traffic composition have on traffic performance within the passing lane?

The TRARR model has been extensively used in Australia (*5*) and Canada (*6*), and was well suited to this research effort. This model is a stochastic microscopic simulation model with great versatility and is operational on IBM-compactible microcomputers.

The TRARR model was applied to existing conditions on three of the field study locations:

- Route 70—the short (0.5-mi) level terrain (0 to 1 percent) passing-lane site,
- Route 41—the short (0.5-mi) rolling terrain (5 percent) passing-lane site, and
- Route 299—the long (1.5-mi) mountainous terrain (5 to 8 percent) passing-lane site.

The predicted simulation model traffic performances were compared with the corresponding field measured traffic performances at the three sites. There were some relatively minor differences, but these were reduced by varying the vehicle performance characteristics and the standard deviations of vehicle speeds. Considerable effort was devoted to this calibration process before proceeding to the sensitivity analysis; this process is described in the project final report (*1*).

Effect of Passing-Lane Length on Traffic Performance

The model was applied to the three calibrated field data sets in which all input data were held constant except for passing-lane length. Passing-lane lengths of 0.25, 0.50, 0.75, 1.00, 1.50, and 2.00 mi were investigated. Three measures of effectiveness were used to assess the effect of passing-lane length on traffic performance within the passing lane. These measures were number of passes, reduction in percent time delay, and estimated annual travel time savings.

The results of the effect of passing-lane length on number of passes at the three sites are summarized in Figure 3. In the top diagram, the number of passes per hour is plotted as a function of passing-lane length. As expected, the number of passes increases with increased passing-lane length but at a decreasing rate. The resulting curve for Route 70 is the highest, followed by those for Routes 41 and 299. These differences are caused by site-specific characteristics, including existing flow level, vertical and horizontal alignment, and vehicle characteristics.

The results are normalized in the lower diagram of Figure 3 by dividing the number of passes by the passing-lane length. Passing-lane lengths less than 0.25 mi were not considered. Assuming that passing-lane costs are directly related to their lengths, short passing lanes from about 0.25 to 0.75 mi are most effective in terms of number of passes per mile. Due primarily to higher flow levels, the Route 70 curve is significantly higher than those for the other two sites.

The results of the effect of passing-lane length on reducing the percent time delay at the three sites are summarized in Figure 4. In the top diagram, the reductions in percent time delay are plotted as a function of passing-lane length. As expected, the reduction in percent time delay increases with longer passing-lane lengths but at a decreasing rate. The resulting curve is highest for Route 299, followed by Routes 70 and 41.

The results are normalized in the lower diagram of Figure 4 by dividing the reduction in percent time delay by passing-

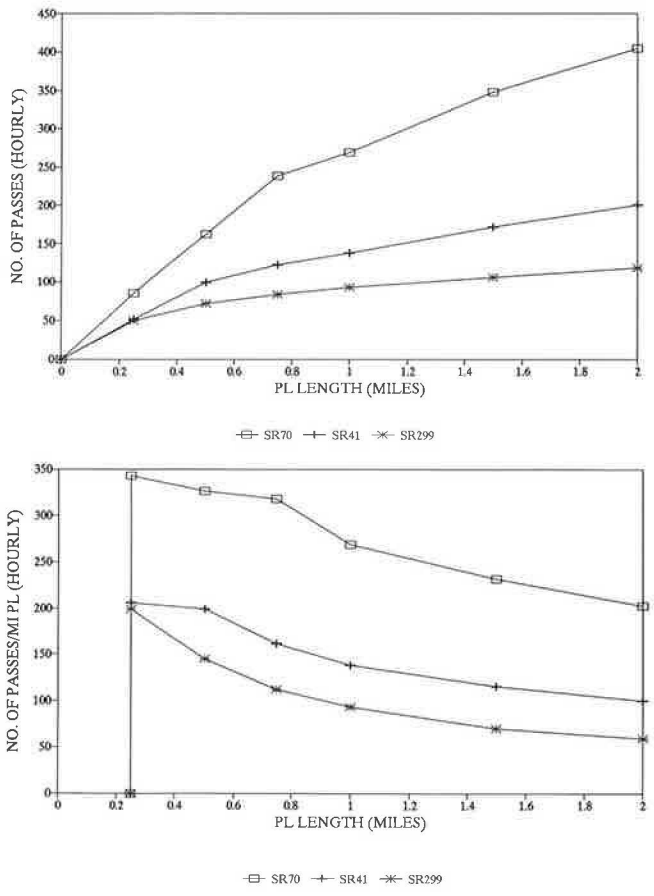

FIGURE 3 Effect of passing-lane length on number of passes.

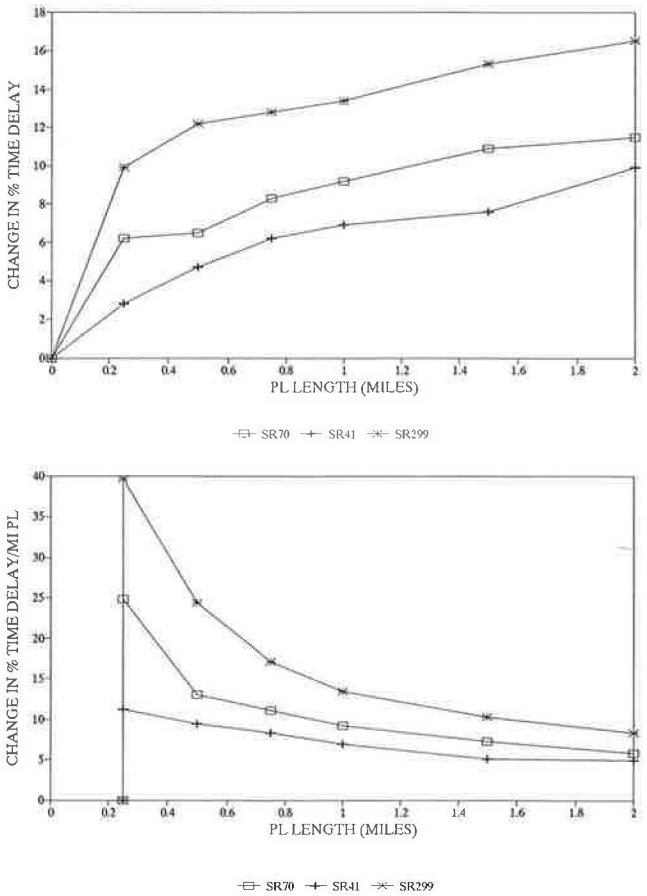

FIGURE 4 Effect of passing-lane length on reducing percent time delay.

lane length. Again, short passing lanes appear to be most effective in terms of reduction in percent time delay and are most effective under Route 299 conditions.

The results of the effect of passing-lane length on estimated annual travel time savings at the three sites are summarized in Figure 5. In the top diagram, estimated annual travel time savings are plotted as a function of passing-lane length. Again, as expected, the estimated savings increase with passing-lane length but at a decreasing rate. The resulting curves for Routes 70 and 41 are the highest.

The results are normalized in the lower diagram of Figure 5 by dividing the estimated savings by the passing-lane length. The results indicate that very short passing lanes are most effective for Routes 41 and 299, whereas slightly longer passing lanes are most effective for sites similar to Route 70. Savings of more than 3,000 vehicle hours per year per mile of passing lane are predicted for short passing lanes.

On the basis of these simulation results, the most effective passing-lane lengths for sites similar to the three study sites are 0.25 to 0.75 mi. Selecting the most effective site between the three study sites depends on the measure of effectiveness used. Route 70 is most effective in number of passes; Route 299 is most effective in reduction in percent time delay; and Route 41 is most effective in annual travel time savings.

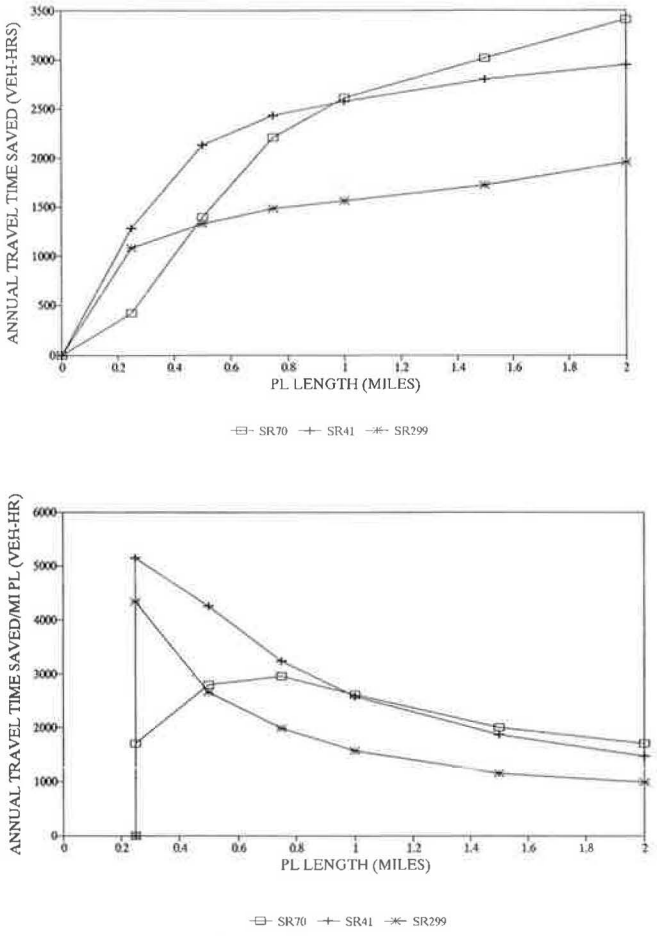

FIGURE 5 Effect of passing-lane length on annual travel time savings.

Effect of Passing-Lane Length on Downstream Conditions

The second set of investigations with the simulation model dealt with the effect on passing-lane lengths of downstream traffic conditions. More specifically, the investigations attempted to answer the question: At what distance downstream of the end of the passing lane does percent time delay return to the percent time delay value as measured at the beginning of the passing lane? A passing lane will normally reduce the percent time delay over its length, but downstream of the passing lane the percent time delay gradually increases and at some point returns to its initial value. One application of such results is the selection of spacing between passing lanes. In these investigations all input data except passing-lane length were kept constant at each of the three sites. Passing-lane lengths of 0.25, 0.50, 0.75, 1.00, 1.50, and 2.00 mi were investigated at each of the three sites.

Sample results are presented in Figure 6 for 0.5-mi (top diagram) and 2.00-mi (lower diagram) passing-lane lengths at the Route 70 site. The vertical scale is percent vehicles in car-following (equivalent to percent time delay), and the horizontal scale is distance in miles from the start of the passing lane. The proportion of vehicles in car-following at the start of the passing lane in both cases was 54 percent. With the 0.5-mi passing lane, the percent of vehicles in car-following

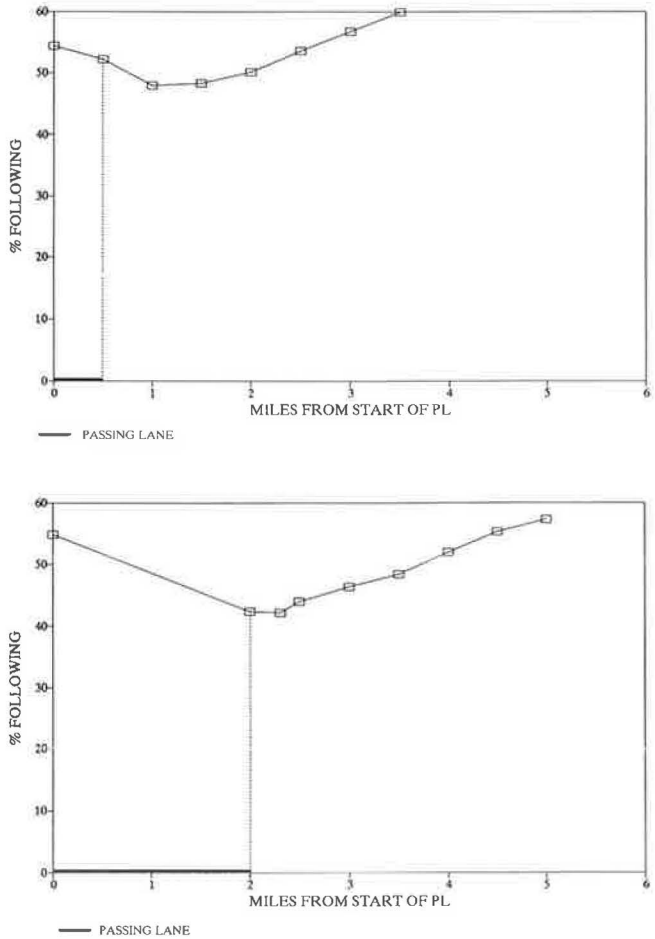

FIGURE 6 SR70: percent time delay downstream.

returns to 54 percent at a distance of 2.0 mi downstream of the end of the passing lane. With the 2.0-mi passing lane, the proportion of vehicles in car-following returns to 54 percent at a distance of 2.1 mi downstream at the end of the passing lane.

Composite results for all passing-lane lengths investigated for each of the three sites are depicted in Figure 7. In the upper diagram, the downstream effective length in miles is plotted as a function of passing-lane length. As expected, this effective distance increases with longer passing lanes but at a decreasing rate. Note that all three curves are quite flat with passing lanes longer than 0.75 mi.

These results are normalized in the lower diagram of Figure 7 by dividing the downstream effective length of the passing-lane length. Results for all sites indicate that short passing lanes are most productive in providing the highest downstream effective length per mile of passing lane.

The results pertaining to effective downstream distances support the conclusions on passing-lane lengths in that both support the desirability of 0.25- to 0.75-mi passing lanes. Passing lanes of such length provide effective downstream distances of 2 to 5 mi depending on downstream design and traffic conditions.

Effect of Flow Level and Vehicle Composition on Passing-Lane Performance

To determine the effect of flow level and vehicle composition, the model was applied to the three calibrated field data sets in which all input data except hourly flow level and percent nonautomobiles were held constant. The findings from the Route 41 site are a typical sample of the results.

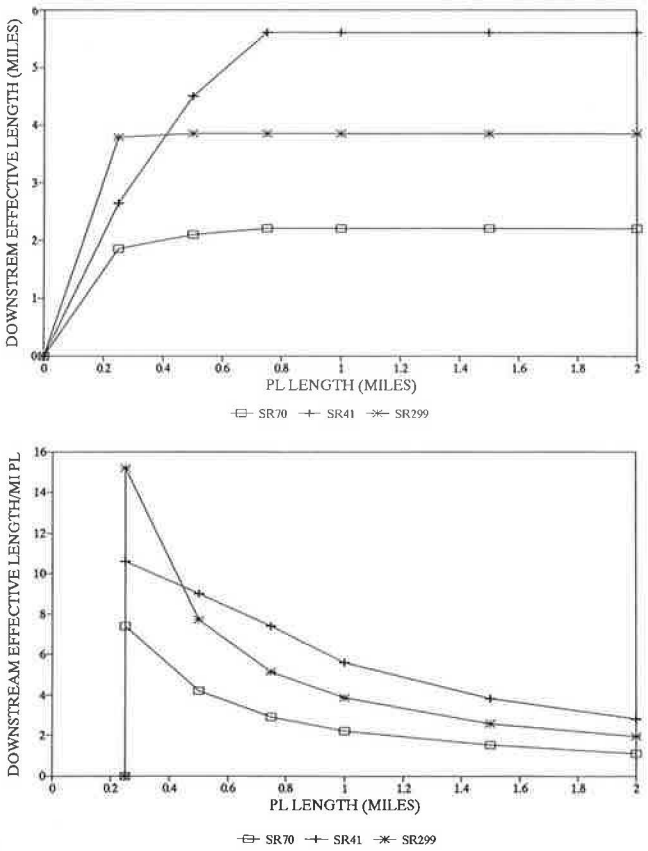

FIGURE 7 Effect of passing-lane length on downstream effective length.

Hourly flow levels varied from 50 to 300 vph in increments of 50 vph; percent nonautomobiles varied from 0 to 40 percent in increments of 10 percent. Three measures of traffic performance were obtained: number of passes per hour, change in percent time delay (exit percent minus entrance percent), and mean journey speed (mph).

The effect of hourly flow level and percent nonautomobiles on number of passes per hour using the Route 41 site data is presented in Figure 8. The curves showing 50, 100, and 150 passes per hour are denoted. As expected, the number of passes per hour increases with hourly flow level and percent nonautomobiles within the ranges studied. It is interesting that the ratio of number of passes in the passing lane to the number of vehicles entering the passing lane is about 50 percent at a nonautomobile percentage of 6 to 8 and increases to a ratio of 67 percent at a nonautomobile percentage of 40.

The effect of hourly flow level and percent nonautomobiles on change in percent time delay using the Route 41 site data is shown in Figure 9. The curves showing +2, 0, −2, −4, −6, −8, −10, and −12 changes in percent time delay are indicated. The detailed pattern is a little irregular but the overall pattern is as expected. The largest reductions in percent time delay occur under low flow levels with a high percentage of nonautomobiles. The smallest reductions (actually an increase) in percent time delay occur under high flow conditions with few nonautomobiles present.

The effect of hourly flow level and percent nonautomobiles on mean journey speeds using the Route 41 site data is presented in Figure 10. The curves showing speeds between 55

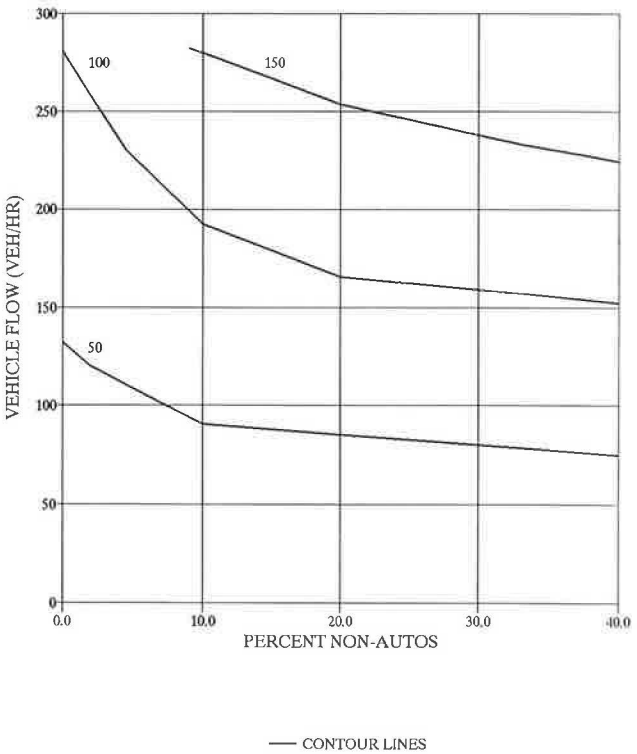

FIGURE 8 SR41: number of passes.

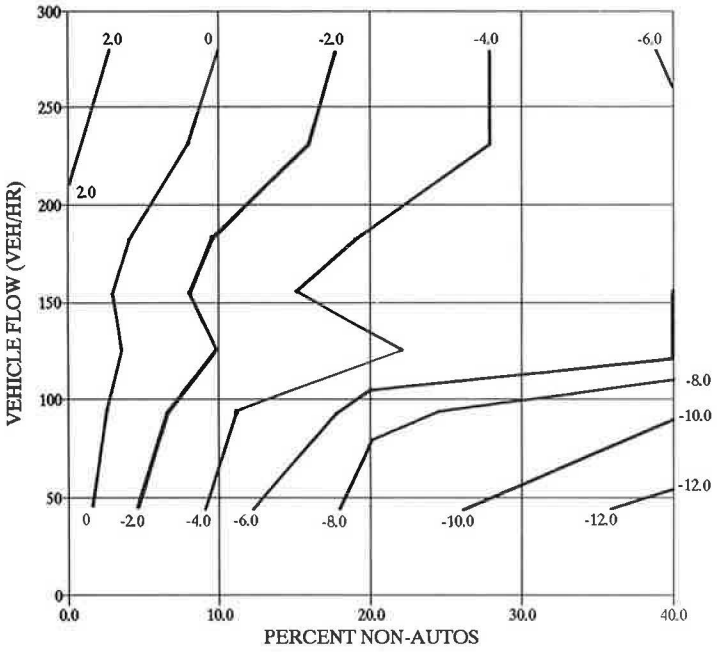

FIGURE 9 SR41: change in percent time delay.

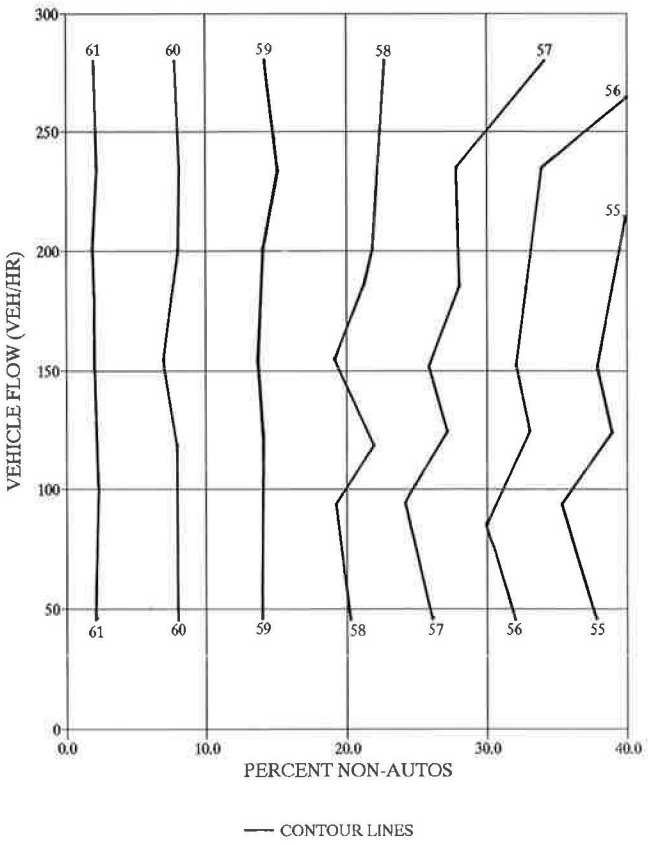

FIGURE 10 SR41: mean journey speed (mph).

and 61 mph in 1-mph increments are indicated. For the range in flow levels considered, the flow level had no effect on mean journey speeds. On the other hand, mean journey speeds decreased from 61 to 55 mph as the proportion of nonautomobiles increased from 0 to 40 percent.

In summary, hourly flow levels and percent nonautomobiles affect to various degrees the number of passes, changes in percent time delay, and mean journey speeds. While number of passes is primarily affected by flow level, changes in percent time delay and mean journey speeds are primarily due to percent nonautomobiles.

SUMMARY

In this study of traffic performance and design of passing lanes on two-lane, two-way rural highways, the four major research emphases were

- Field studies of traffic performance and design of five California passing lanes,
- Before-and-after field study of one of the passing-lane sites to assess two passing-lane entrance designs,
- Field observations of passing maneuvers for five site situations to determine the frequency of passing maneuvers as related to traffic flow levels and vehicle types, and
- Sensitivity analysis through simulation to determine the effect of passing-lane length on traffic performance, the effect of passing-lane length on downstream traffic conditions, and the effect of flow level and vehicle composition on passing-lane performance.

The field studies of traffic performance and design of five California passing lanes provided an operational assessment and raised questions about passing-lane entrance design, the consideration of using number of passes in the passing lane as a measure of performance, and the need for sensitivity analysis through simulation.

The before-and-after field study of two passing-lane entrance designs demonstrated that the modified design significantly increased the proportion of traffic that would enter the passing-lane section in the basic lane. There was no indication of traffic performance improvements, however, using existing measures of effectiveness.

Field observations of passing maneuvers clearly indicated that the number of passes per passing-lane length was a very good measure of effectiveness of passing lanes. Equations were developed for estimating the number of passes as a function of traffic flow level for each of the five data sets. The vehicle-type pattern of passes observed were not randomly distributed; automobiles passing nonautomobiles were much higher than expected, and nonautomobiles passing automobiles were much lower than expected.

The sensitivity analysis through simulation identified that passing lanes of 0.25 to 0.75 mi appeared to be the most effective; spacing of 2 to 5 mi between such passing lanes appeared appropriate depending on downstream roadway and traffic conditions. Estimates of the number of passes that would likely occur at three of the field sites under various traffic flow levels and vehicle composition mixes were determined.

ACKNOWLEDGMENTS

Work described in this paper was made possible with the aid of many individuals. The author wishes to thank all who assisted in selecting field study sites, collecting data, and analyzing data. Special thanks go to Traffic Operations personnel at Caltrans Districts 2, 3, 6, and 10 for field assistance, and to Fred Rooney and Howard Fong of Caltrans Headquarters for their interest, advice, and support throughout the research. Special mention should be given to Doug Harwood, Chris Hoban, and John Morrall for advice and encouragement in the simulation model effort. Finally, and most important, this study could not have been undertaken without the dedicated efforts of four research assistants who worked on various portions of this research: Casey Emoto, Hao Phung, Manual Romana, and Gail Staba.

REFERENCES

1. G. R. Staba, H. O. Phung, and A. D. May. *Development of Comprehensive Passing Lane Guidelines, Volume I: Final Report*. Report UCB-ITS-RR-90-DRAFT, Institute of Transportation Studies, University of California at Berkeley, Aug. 1990.
2. G. R. Staba, H. O. Phung, and A. D. May. *Development of Comprehensive Passing Lane Guidelines, Volume II: Appendix*. Report UCB-ITS-RR-90-DRAFT, Institute of Transportation Studies, University of California at Berkeley, Aug. 1990.
3. A. D. May and T. C. Emoto. *Operational Evaluation of Passing Lanes in Level Terrain*. Working Paper UCB-ITS-WP-88-1, Institute of Transportation Studies, University of California at Berkeley, Feb. 1988.
4. A. D. May and T. C. Emoto. *Operational Evaluation of Passing Lanes in Level Terrain*. Final Report UCB-ITS-RR-88-13, Institute of Transportation Studies, University of California at Berkeley, July 1988.
5. C. J. Hoban, G. J. Fawcett, and G. K. Robinson. *A Model for Simulating Traffic on Two-Lane Rural Roads: User Guide and Manual for TRARR Version 3.0*. ARRB Technical Manual No. 10A and Subsequent Revision, Australian Road Research Board, May 1985.
6. J. F. Morrall, A. Werner, and P. Kilburn. Planning and Design Guidelines for the Development of a System of Passing Lanes for Alberta Highways. *Proc., 13th ARRB—5th REAAA Combined Conference*, Vol. 13, Part 7, Aug. 1986, pp. 58–69.

Publication of this paper sponsored by Committee on Operational Effects of Geometrics.

Safety Considerations for Truck Climbing Lanes on Rural Highways

ANDREW D. ST. JOHN AND DOUGLAS W. HARWOOD

Data on the speed profiles of trucks on sustained upgrades can be combined with safety estimates to quantify the increased accident rates caused by slow-moving trucks and the changes in accident rate with distance up the grade. Truck performance and speed data were taken from recent field measurements and were evaluated using the truck performance equations presented in NCHRP Report 185. The effect of speed differences on accident rate is based on the relationships developed by Solomon. The results show that there is a pronounced increase in accident rates of passenger cars and trucks in the traffic stream only when a sizeable portion of the truck population falls to speeds of 22.5 mph or less. The results indicate that, from a safety standpoint, there is little apparent need for truck climbing lanes on moderate upgrades (2 percent) or in the first portion of steeper upgrades. However, the results must be interpreted cautiously in light of limitations in the Solomon data that were found during the analysis. In particular, the Solomon data do not show how accident involvement rates change within the very important speed range from zero to 22.5 mph, and these data may represent sections with more intersection- and driveway-related accidents than would typically be found on a sustained grade. Further research is needed to quantify relationships between speed differences and accident involvement rates that are specifically applicable to sustained grades.

It has long been recognized that trucks can cause traffic service and safety problems on steep, sustained grades. Current AASHTO criteria for truck climbing lanes address these considerations through the concept of a critical grade (*1*) (one in which the alignment, truck population, and flow rate may cause an unacceptable reduction in the level of traffic service). Current AASHTO criteria (*1*) define a critical grade as one that is long and steep enough to slow a 300-lb/hp truck by at least 10 mph. The AASHTO Green Book recognizes the potential for collisions between slow-moving trucks and faster vehicles overtaking them, but this effect has not been quantified to provide guidance on where truck climbing lanes may be needed.

The relationship of speed differences in the traffic stream to accidents is well known from the work of Solomon (*2*), who demonstrated that the accident involvement rates of vehicles increase as the deviation of the vehicle speed from the mean speed of traffic increases. Figure 1 illustrates the form of the relationships developed by Solomon. Although the Solomon data were not collected specifically for upgrades, Solomon's results suggest that slow-moving trucks on a steep upgrade should have higher accident involvement rates than faster-moving vehicles. Data on the speed profiles of trucks on grade can be combined with the safety estimates developed by Solomon to quantify the increased accident rates of passenger cars and trucks in the traffic stream caused by slow-moving trucks and the changes in accident rate with distance up the grade. The results obtained from this analysis have some obvious limitations but illustrate an approach that could be used to develop safety warrants for truck climbing lanes. This approach could be used to obtain results more directly applicable to truck climbing lanes if future research could identify relationships between accident rates and speed differentials similar to those of Solomon, but specifically for steep grades.

A. D. St. John, 8470 E. Amethyst Place, Tucson, Ariz. 85715. D. W. Harwood, Midwest Research Institute, 425 Volker Blvd., Kansas City, Mo. 64110.

TRUCK PERFORMANCE ON GRADES

Truck performance on grades is influenced by truck acceleration and speed-maintenance capabilities (typically represented by the truck weight-to-power ratio), by aerodynamic drag (represented by the truck weight-to-frontal area), and by the acceleration and speed preferences of drivers.

The truck population used is that documented in a 1979 paper by St. John (*3*), which was the basis for the passenger car equivalency factors for trucks in Chapters 3 and 7 of the 1985 *Highway Capacity Manual* (*4*). The five-axle truck component of the 1979 truck population was updated with speeds measured by the California Department of Transportation in 1983 and 1984 on sustained 4 and 6 percent grades (*5*). Table 1 summarizes the relative proportions of eight typical ranges of truck characteristics that collectively represent the truck population. The table includes the relative proportion of each truck type determined from the cited sources. The horsepower values used in Table 1 represent the installed net horsepower, which is usually about 94 percent of the engine manufacturer's maximum rated net horsepower. The computations assume that no trucks are present in the traffic stream with weight-to-power ratios outside the range of 50 to 400 lb/hp, as represented by the truck population in Table 1.

The performance capabilities of trucks were computed using the performance equations in Appendix C of NCHRP Report 185 (*6*) together with an improved version of the correction for gear shift delays in Appendix D. The aerodynamic drag coefficients were also reduced to values appropriate for modern truck configurations. The truck performance equations in the NCHRP report allow the determination of the maximum speed of a truck at any point on a specified grade, as a function of truck engine, transmission, aerodynamic drag, and driver characteristics.

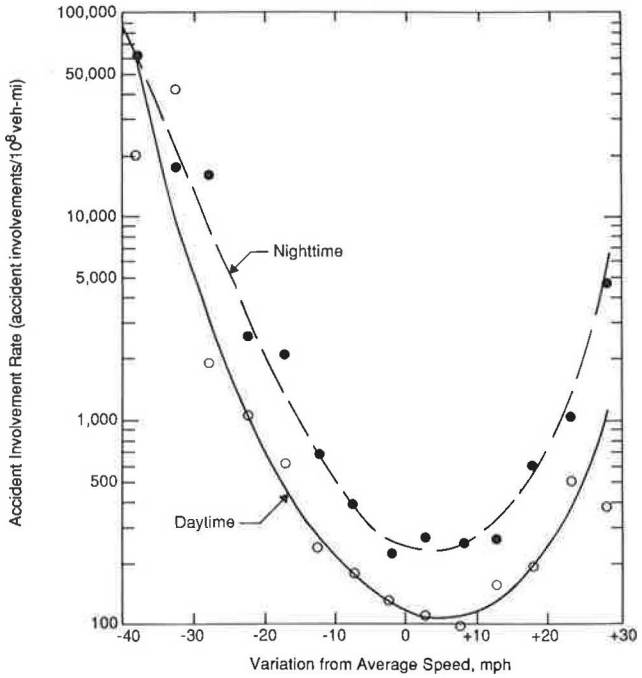

FIGURE 1 Example of U-shaped curves for accident involvement rate versus speed from Solomon (*2*).

DESIRED SPEEDS OF TRUCK DRIVERS

Driver speed preferences (also referred to as desired speeds) will determine truck speeds at any location where the desired speed is less than the truck speed capability. The desired speeds of truck drivers were represented in this investigation by a truncated normal distribution that corresponds well with measurements of free speeds on highways with 55-mph speed limits obtained in NCHRP Project 3-33 (*7*). A range of 43 to 67 mph was used for desired speeds of truck drivers, based on a desired speed distribution with a mean value of 55 mph and a standard deviation of 5 mph suggested by field data (*7*). Table 2 presents eight specific desired speed levels drawn from that distribution, ranging from 2.4 standard deviations below the mean (43 mph) to 2.4 standard deviations above the mean (67 mph), which were used to represent the range of speed preferences of drivers. Since driver speed preferences were assumed to be normally distributed, the percentages of truck drivers in each desired speed stratum shown in Table 2 were determined from tables of the standard normal distribution.

ESTIMATION OF TRUCK SPEED DISTRIBUTIONS ON SPECIFIC GRADES

The truck performance capabilities and truck driver desired speeds can be used together to estimate actual speeds on upgrades. The entrance speed of a truck at the foot of the grade is the lesser of the driver's desired speed and the speed capability of the truck on the approach grade. Trucks with excess performance capabilities are assumed not to exceed the driver's desired speed.

Table 3 shows the joint distribution of truck characteristics and driver speed preferences that results from combining the distributions shown in Tables 1 and 2. Each of the 64 entries in Table 3 represents the relative likelihood of a particular

TABLE 1 CHARACTERISTICS OF TYPICAL TRUCKS

	Range of weight/power ratio (lb/hp)	Range of weight/frontal area ratio (lb/ft²)	Proportion of truck population
Lowest performance trucks	318-400	1161-1460	0.0122
	258-318	942-1161	0.0407
	227-258	829-942	0.0721
	195-227	712-829	0.1050
	161-195	588-712	0.1392
	134-161	489-588	0.1742
Highest performance trucks	105-134	383-489	0.2100
	50-105	183-383	0.2466

TABLE 2 DESIRED SPEEDS OF DRIVERS

	Driver desired speed (mph)	Standard deviations above or below mean speed	Proportion of driver population
Slowest drivers	43-46	-2.4 to -1.8	0.0282
	46-49	-1.8 to -1.2	0.0805
	49-52	-1.2 to -0.6	0.1618
	52-55	-0.6 to 0.0	0.2295
	55-58	0.0 to 0.6	0.2295
	58-61	0.6 to 1.2	0.1618
	61-64	1.2 to 1.8	0.0805
Fastest drivers	64-67	1.8 to 2.4	0.0282

TABLE 3 PROPORTIONS FOR COMBINATIONS OF SPECIFIC TRUCK TYPE AND DESIRED SPEED

Truck weight/power ratio (lb/hp)	Proportion in truck population	Desired speed (mph) 43-46	46-49	49-52	52-55	55-58	58-61	61-64	64-67
		Proportion in driver population 0.0282	0.0805	0.1618	0.2295	0.2295	0.1618	0.0805	0.0282
318-400	0.0122	0.000344	0.000982	0.001974	0.002800	0.002800	0.001974	0.000982	0.000344
258-318	0.0407	0.001148	0.003276	0.006585	0.009341	0.009341	0.006585	0.003276	0.001148
227-258	0.0721	0.002033	0.005804	0.011666	0.016547	0.016547	0.011666	0.005804	0.002033
195-227	0.1050	0.002961	0.008453	0.016989	0.024098	0.024098	0.016989	0.008453	0.002961
161-195	0.1392	0.003925	0.011206	0.022523	0.031946	0.031946	0.022523	0.011206	0.003925
134-161	0.1742	0.004912	0.014023	0.028186	0.039979	0.039979	0.028186	0.014023	0.004912
105-134	0.2100	0.005922	0.016905	0.033978	0.048195	0.048195	0.033978	0.016905	0.005922
50-105	0.2466	0.006954	0.019851	0.039900	0.056595	0.056595	0.039900	0.019851	0.006954

combination of the eight truck performance strata and eight desired speed strata. Because these 64 combinations are assumed to represent all possible truck performance–desired speed combinations, the sum of all entries in Table 3 is 1.0.

Several typical grades were selected for analysis, including sustained 2, 4, and 6 percent upgrades with level (0 percent) approach grades. Truck speeds were calculated on each grade at 200-ft stations until a point on the grade was found where the trucks for all combinations of truck type and desired speed had reached steady speeds. The weight factors in Table 3 were used to assemble a truck speed distribution at each station on each grade using speed strata with a width of 5/3 mph (i.e., 1.67 mph), which was a convenient stratum width for correspondence with the accident data.

If no combinations of truck type and desired speed produced speeds in a particular 5/3-mph speed stratum, but speeds were produced in strata on either side, the proportion of truck speeds in the empty strata was determined by linear interpolation. This smoothing of the cumulative speed distribution curves is logically consistent because each type speed combination calculated (except the lowest one—the 400-lb/hp truck with a desired speed of 43 mph) defines the upper speed bound for some portion of the truck population.

PASSENGER CAR SPEEDS

The passenger car speed distribution at all stations on each grade was assumed to be represented by the desired speed distribution shown in Table 2. This approach neglects the moderate decreases in passenger car speeds that are known to occur on steep grades. This common assumption is also made in the *Highway Capacity Manual* procedures (*4*); that is, passenger car equivalents are not calculated for passenger cars on grades.

SPEED DISTRIBUTIONS FOR MIXED FLOWS

The speed distributions in the mixed passenger car and truck flows at each 200-ft station on each grade were obtained by combining the passenger car and truck speed distributions for four different proportions of trucks in the traffic stream: 5, 10, 15, and 20 percent. These speed distributions are all expressed in terms of the proportion of vehicle speeds in each 5/3-mph speed stratum. The use of explicit speed strata in this way is appropriate because Solomon's results (*2*) can then be used to determine the safety implications of the speed distribution expressed in this form.

ACCIDENT RATES AS A FUNCTION OF SPEED DIFFERENCES

In evaluating the need for truck climbing lanes on rural highways, the primary safety concern is the risk of rear-end or same-direction sideswipe accidents involving slow-moving trucks. Steep, sustained grades generally have less than average roadside development and few intersections and driveways, so there is less concern about the potential for angle or turning accidents than at other locations. Climbing lanes may have the potential to eliminate some head-on or opposite-direction sideswipe accidents, but these accident types have no direct relationship to the internal dynamics of the speed distribution in the uphill traffic. Therefore, the accident rate evaluation has been limited to rear-end and same-direction sideswipe accidents which, for convenience, are referred to as rear-end accidents.

Two methods for estimating the accident rate corresponding to a particular speed distribution can be used with Solomon's data (*2*). These methods are as follows:

- *Method 1:* Use data from Table 5, Table 41, and Figure 18 of Solomon's report to estimate rear-end accident rates for all possible combinations of slower and faster speed strata. For example, the Solomon data can be used to estimate the rear-end accident rate per 10^8 veh-mi for a slower vehicle traveling 25 mph and a faster vehicle traveling 60 mph.
- *Method 2:* Use the data in Tables 5 and 41 of the Solomon report to estimate rear-end involvement accident rates (counting each two-vehicle accident as two separate accident in-

volvements) for specific speed strata. In other words, the Solomon data can be used to estimate the rear-end accident involvement rate for vehicles traveling in a specific speed stratum, assuming that the speed distribution of other vehicles on the road is similar to that observed by Solomon.

It was found that by smoothing Solomon's data, Method 2 could be directly used to determine accident involvement rates. However, the assumption (described above) that the speed distribution on the roadway must be similar to that observed by Solomon seems unrealistic for steep grades, so Method 2 appears to be too simplistic for the proposed application. Method 1 requires the assumption that the distribution of flow rates on the steep grades being analyzed is the same as the distribution of flow rates at Solomon's field sites; otherwise, the accident rates would need to be adjusted for the differences in flow rates. This assumption appears more acceptable than the assumption involving speed distributions that must be made to use Method 2. The derivation of Method 1 suggests that, with other factors held constant, accident rate is proportional to flow rate. It would be desirable to have data from steep grades to confirm or refute this relationship. Method 1 has the advantage that it explicitly accounts for the effects of changes in vehicle mix and grade geometrics. Method 1 can be used to determine accident involvement rates only after recasting Solomon's accident data into slower-vehicle–faster-vehicle cells. The available data and the required iterative procedures cannot provide unique results, but do provide very narrow constraints, which ensure results that follow logically from Solomon's data.

Figures 2 and 3 present overviews of the accident rates derived with Methods 1 and 2. For illustrative purposes, Figure 2 assumes that for each pair of slower and faster vehicle speeds, vehicles with those speeds are present in the traffic stream in equal proportions. (This assumption is necessary to illustrate the accident rates in Figure 2; it is not needed for the analyses that were performed.) The most prominent feature in Figure 2 is the consequence of low vehicle speed, particularly below 40 mph. A vehicle traveling less than 40 mph has a much increased likelihood of involvement as either the faster or slower vehicle in a two-vehicle accident. This compounded effect from slow vehicle speeds leads to nonlinearities in accident-speed relationships and illustrates why it is important to use the Method 1 approach, which avoids assumptions about similarities in the speed distributions between the field data (Solomon's) and the calculated speed distribution on grades. Figure 3 presents the rear-end accident involvement rates based on speed strata alone. The foregoing

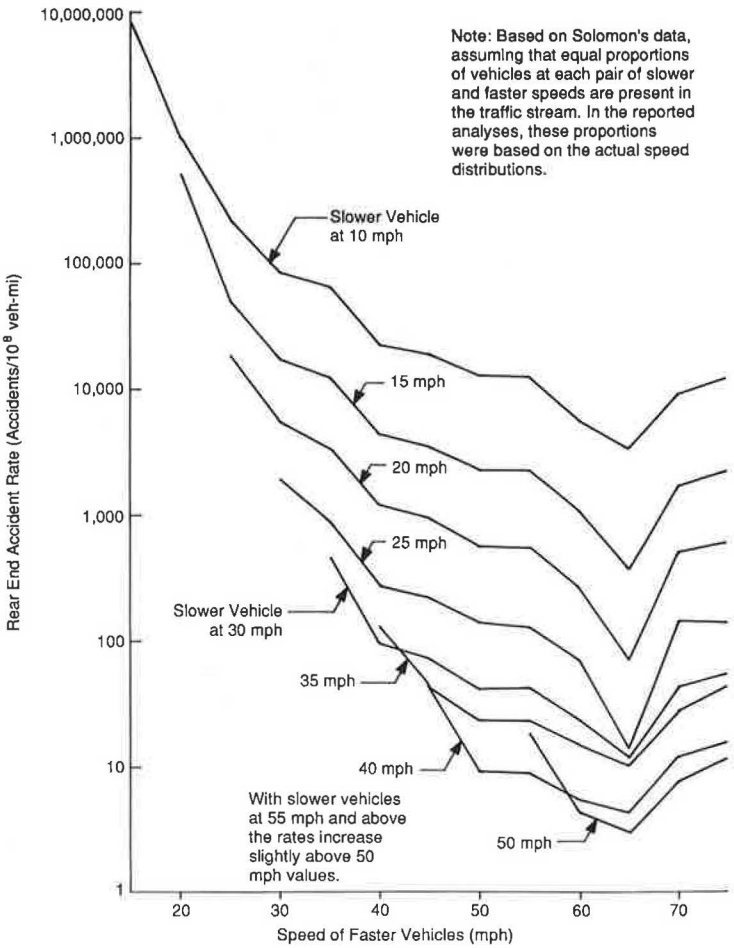

FIGURE 2 Example of rear-end accident rates for specific combinations of slower and faster vehicle speed determined using Method 1.

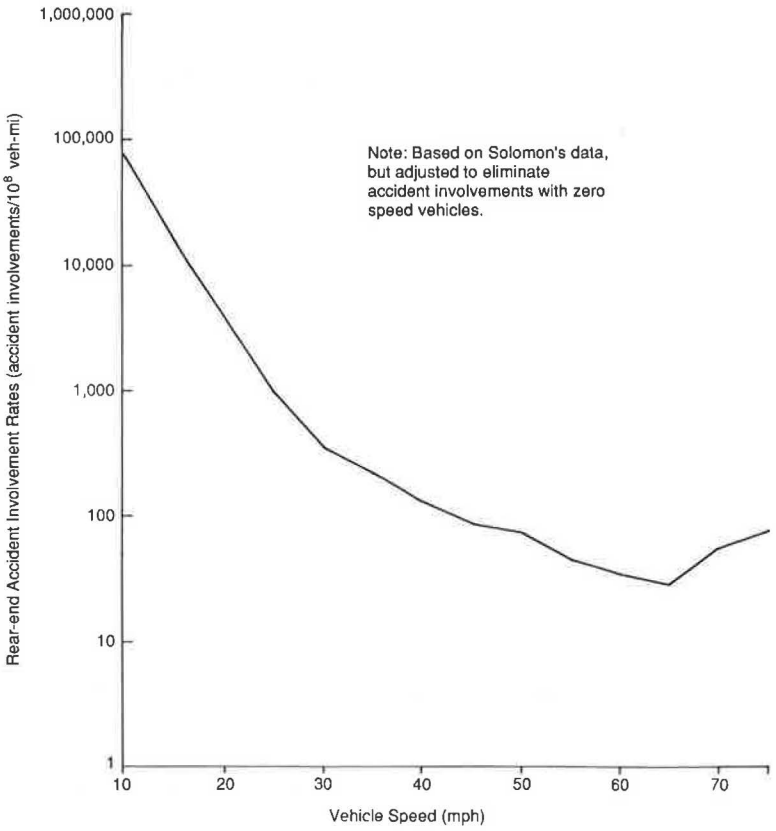

FIGURE 3 Rear-end accident involvement rates as a function of vehicle speed determined from Solomon's data using Method 2.

discussion of Figures 2 and 3 illustrates why Method 1 was found to be more realistic than Method 2, because Method 1 explicitly considers the speed differences in the traffic stream and was used as described below. For simplicity, Solomon's data were combined over roadway types and over day and night.

In Method 1, accident rates were computed for an array in which each cell represented accidents between vehicles in a slower speed stratum (v_i) and a faster speed stratum (v_j).

The accident rate array elements for Method 1 were determined as

$$A_e = \sum_i \sum_j [l_{ij} P_i P_j / 10^4] \quad (1)$$

where

A_e = rear-end and same-direction sideswipe accidents per 10^8 veh-mi,

$l_{ij} = 10^{10}[a_{ij} N]/[T(p_i p_j)]$ (2)

a_{ij} = percent of observed rear-end and same-direction sideswipe, accidents involving the combination of the ith and jth speed strata (Solomon),

N = total number of rear-end and same-direction accidents observed by Solomon = 4,309/2,

P_i = percent of vehicle-miles in ith speed stratum,

P_j = percent of vehicle-miles in jth speed stratum,

T = total vehicle-miles of travel observed by Solomon = 3.671×10^9,

p_i = percent of observed vehicle-miles in the ith speed stratum (from Solomon), and

p_j = percent of observed vehicle-miles in the jth speed stratum (from Solomon).

Method 1 uses the concept that accidents between vehicles in the ith and jth speed strata are proportional to the frequency with which their speed difference brings them into potential conflict. There are 43 vehicle speed strata, each 5/3 mph in width, to which Equation 1 is applied. Thus, there are 903 unique combinations of faster and slower vehicle speeds (i.e., [(43)(43) − 43]/2), and Equation 1 involves the summation of 903 separate terms.

Accident involvements as a function of speed were taken from Table 41 of the Solomon report, with night and day values combined. Accident frequencies were set equal to half of the accident involvement frequencies, assuming that each rear-end accident involved only two vehicles. Speed difference data were obtained from Figure 8 of the Solomon report. Although these data are for passenger cars only, most of the vehicles in the mixed flow considered here are passenger cars as well. The important point is that these data properly incorporate the role of speed differences in accident situations. Thus, Table 41 and Figure 8 from the Solomon report provide the raw data for determining the a_{ij} in Equation 2.

The a_{ij} are not uniquely defined by the available data. However, numerical experience with iterations and adjustments indicates that the overall pattern is strongly constrained. In the derivation of the a_{ij} for 5-mph speed increments, it is clear

that the vehicles in the highest speed stratum must be the faster vehicle in any rear-end accident in which they are involved, and the vehicles in the lowest speed stratum must always be the slower vehicle. Vehicles in other speed strata may be the faster vehicle in some accidents and the slower vehicle in others. However, because all rear-end accidents were assumed to involve only two vehicles, there must be an equal number of faster vehicle and slower vehicle involvements. In addition, the percentage of involvements by speed stratum are known from the data in Solomon's Table 41. Solomon's Figure 8 provides the percentage of accidents within each speed difference. These assumptions and constraints were used to calculate the a_{ij}, within the added constraint that the a_{ij} must vary smoothly between cells. After the l_{ij} were calculated for the 5-mph speed strata, interpolation was used to obtain values at 5/3-mph intervals that matched the speed distribution data derived earlier.

CALCULATED RESULTS

Upgrade of 2 Percent

Figure 4 shows the calculated truck speed distributions at six locations on the sustained 2 percent upgrade with a level approach. The locations selected for illustrative purposes in this figure are the start of the grade, and stations located 800, 1,600, 3,200, 6,400, and 9,600 ft up the grade. As explained earlier, similar speed distributions were determined at 200-ft intervals on each grade. The minimum truck speed on this grade was about 29 mph, but only about 3.6 percent of the truck speeds would fall below 40 mph.

In the mixed flow with 20 percent trucks and 80 percent passenger cars, the estimated speed distributions for trucks and passenger cars correspond to a rear-end accident rate of 26 accidents per 10^8 veh-mi for the final steady-speed conditions on the upper portion of the grade. Thus, although some trucks decelerate to speeds of 29 mph and some passenger cars travel as fast as 67 mph on the upper portion of the grade, accident rates would be expected to increase by only 1 percent above the accident rate in level terrain. The 2 percent upgrade is simply not steep enough to have a major effect on accident rates.

Upgrade of 4 Percent

Figure 5 shows the estimated truck speed distribution curves at various points on the 4 percent upgrade. The figure shows that on the upper portion of the 4 percent upgrade, 40 percent of the trucks travel at speeds of 40 mph or less, and 5 percent of trucks fall to speeds less than 25 mph. The minimum truck speed on this grade is 18 mph.

Figure 6 shows the safety implications of these speed reductions based on Solomon's accident and exposure estimates for strata of slower and faster vehicles. The figure shows that accident rates do not change appreciably until the trucks are about 2,500 ft up the grade; this is where truck speeds start to drop below 22.5 mph. With 5 percent trucks in the flow, accident rates increase only about 4 percent over the length of the grade, but accident rates more than double with 20 percent trucks in the traffic stream. Finally, the figure shows that at about 7,500 ft up the grade, where trucks reach their steady speeds, the accident rates stop increasing.

Upgrade of 6 Percent

Figures 7 and 8 show comparable data for trucks on a sustained 6 percent upgrade. Figure 8 shows that rapid increases in the estimated accident rate begin at about 1,800 ft up the grade and that, as in the 4 percent case, accident rates increase

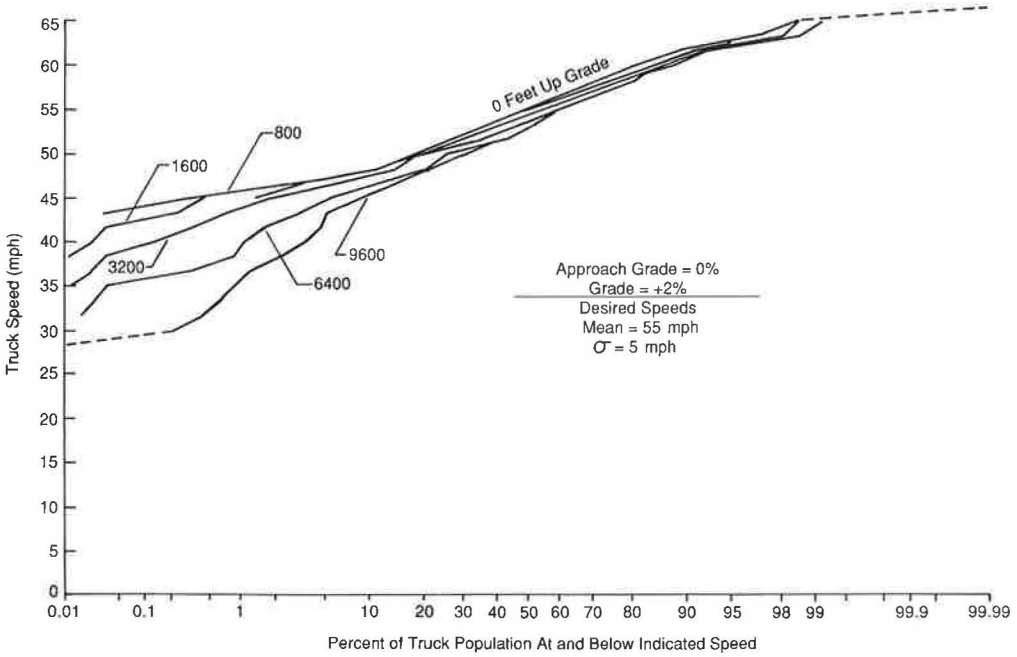

FIGURE 4 Percent of truck population at or below indicated speed on 2 percent upgrade.

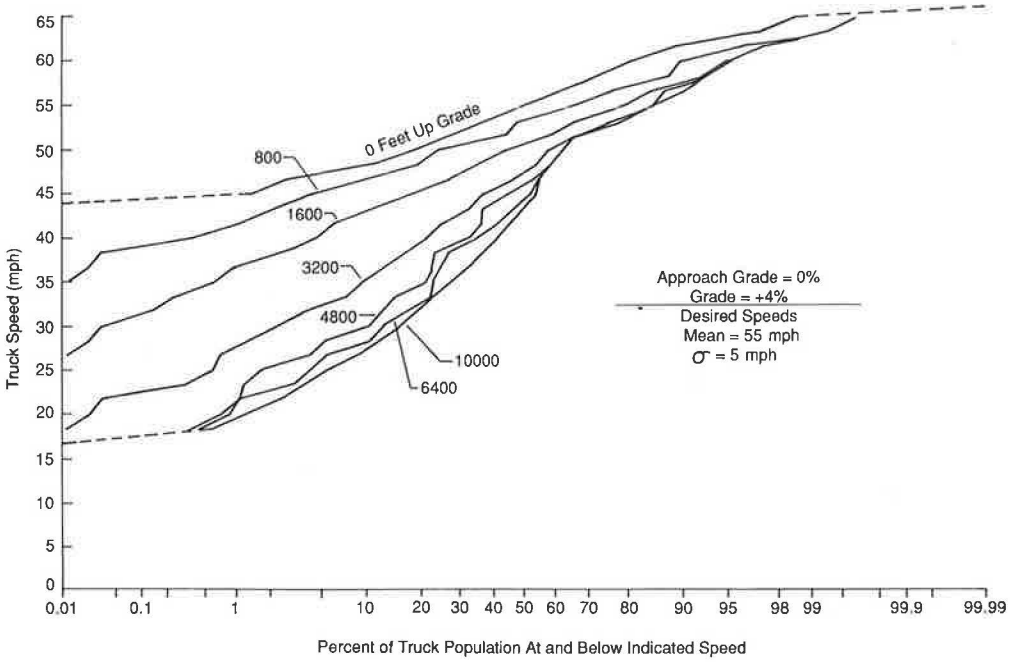

FIGURE 5 Percent of truck population at or below indicated speed on 4 percent upgrade.

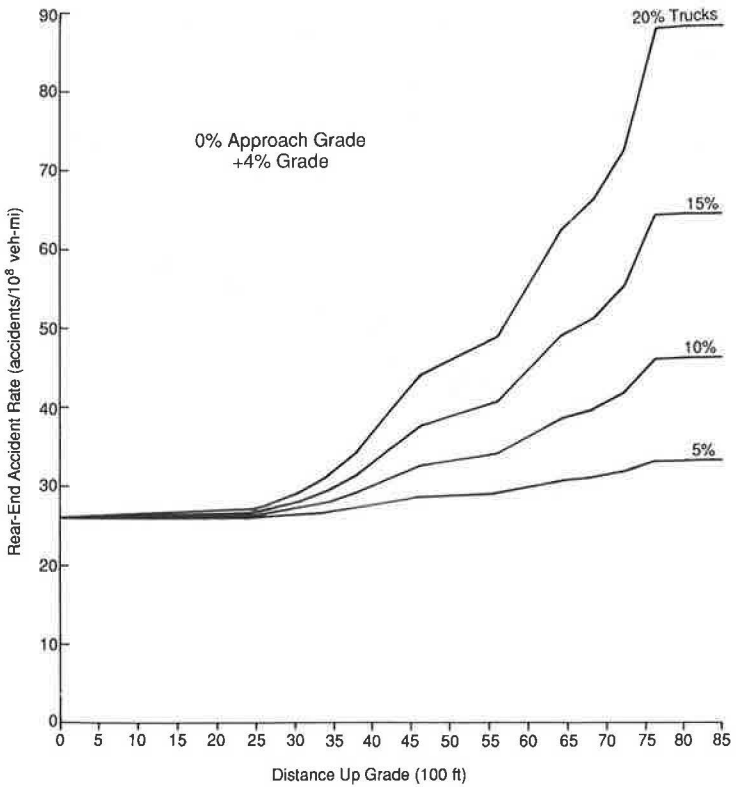

FIGURE 6 Calculated rear-end accident rates on 4 percent upgrade.

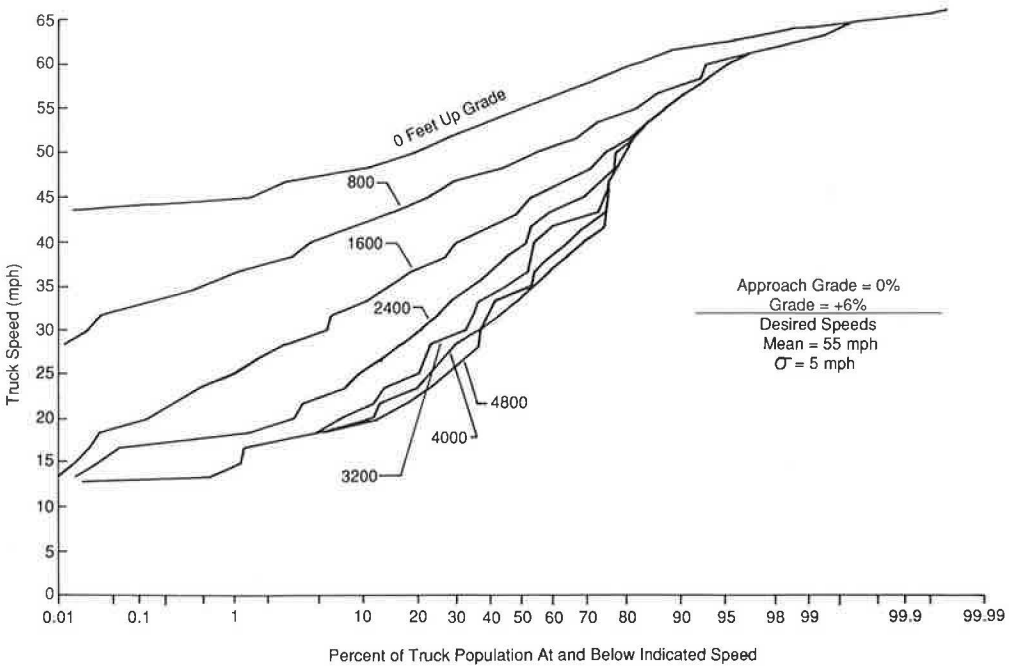

FIGURE 7 Percent of truck population at or below indicated speed on 6 percent upgrade.

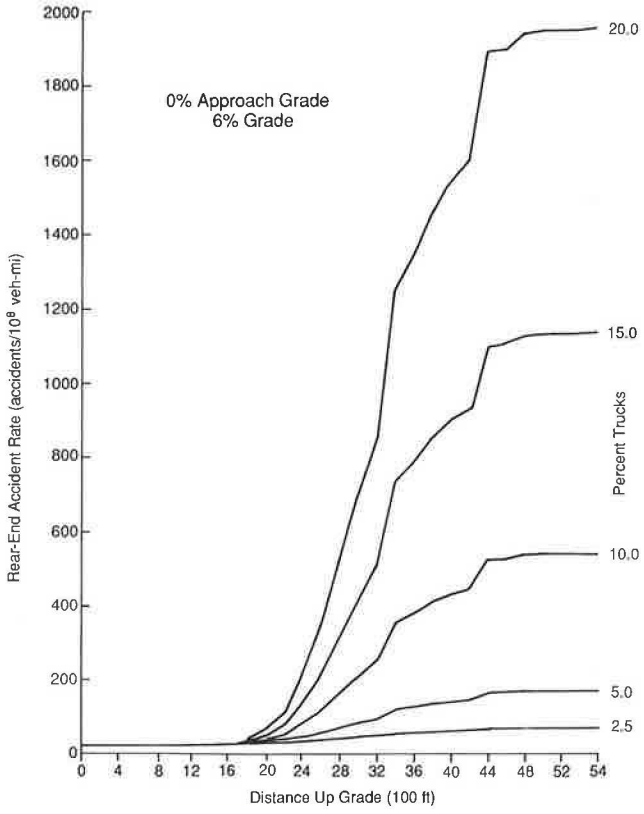

FIGURE 8 Calculated rear-end accident rates on 6 percent upgrade.

nonlinearly with increasing percent trucks. The figure implies that the increase in accident rate with 20 percent trucks will be more than 10 times greater than with 5 percent trucks.

DISCUSSION OF RESULTS

The increases in accident rate on upgrades presented in Figures 4 and 6, relative to the accident rates shown for level terrain, are undoubtedly larger than those observed in the real world. Nevertheless, the results reported here certainly indicate the manner in which conflicts between slow and fast vehicles increase with increasing percent grade and increasing percent trucks. These results should help guide future research.

The results imply that there is a pronounced rise in rear-end accident rates whenever a sizeable portion of the truck population, 0.5 percent or more, falls to speeds below 22.5 mph. However, these results must be interpreted in light of the limitations of the Solomon data. The Solomon data contain a single category for speeds of accident-involved vehicles greater than zero and less than or equal to 22.5 mph. This broad speed range, coupled with the extremely high accident involvement rate for these lower-speed vehicles, makes it very difficult to determine the exact character of the lower-speed accident rates. This is in contrast to the higher-speed strata, which are only 5-mph wide with much better defined accident rates. Other aspects of the data set raise additional questions.

Solomon's data indicate that 12.7 percent of the rear-end accident involvements were vehicles at zero speed (stopped

and presumably waiting for the opportunity to make a turning maneuver). Because the second vehicle in each accident involving a stopped vehicle must be moving, Solomon's data imply that about 25 percent of all rear-end accidents involved a stopped vehicle. This high proportion of zero-speed accidents has not affected the results reported here because all accidents involving a zero-speed vehicle were omitted from the analysis. However, the presence of these zero-speed accidents in Solomon's data implies that the presence of intersections or driveways may be overrepresented in comparison to typical sustained grades. This possibility is reinforced by the accident rates in Figure 2, where two vehicles at generally low speeds are much more likely to be involved with each other than with a higher-speed vehicle.

The concerns discussed about the Solomon data and their applicability to sustained grades occur in the speed range that is most responsible for the large accident rate increases that were calculated for trucks. Thus, the large accident rate increases shown for trucks in Figure 6 and 8 should not be taken too literally. It is likely that they show accident rate increases larger than those that would be observed in the field. Nevertheless, the results have implications that may be useful in deciding where truck climbing lanes are not needed from a safety standpoint.

First, the analysis results show (not surprisingly) that there would be almost no safety benefit to installing a truck climbing lane on a 2 percent grade and that there is little apparent need for truck climbing lanes in the first portion of steeper grades. There are unlikely to be safety benefits from climbing lane installations in the first 2,500 ft of a 4 percent grade or the first 1,800 ft of a 6 percent grade. Thus, it is reasonable to consider introducing the climbing lane on the grade itself, rather than at the foot of the grade.

Second, the potential safety benefits of truck climbing lanes clearly appear to increase with percent grade, length of grade, and percent trucks. Although these findings are not surprising, the nonlinear effect of increasing percent trucks may have important implications. Installation of truck climbing lanes on grades with high truck percentages and high proportions of very low performance trucks may be much more important than is suggested merely by the increased number of trucks. However, these nonlinear effects need to be investigated further to determine whether they are an artifact of the apparent predominance of access-point-related accidents in the Solomon data.

Third, if one accepts the Solomon data as accurate for vehicle speeds above 22.5 mph but potentially misleading for speeds below 22.5 mph, this implies that the current AASHTO truck climbing lane criteria may be overly conservative from a safety standpoint. The truck speed reduction required under AASHTO criteria to warrant a climbing lane was changed in 1984 from 15 to 10 mph on the rationale that the 10-mph criterion was needed for increased safety. However, the data on which Figures 6 and 8 are based clearly imply that there is little, if any, increase in accident rate for vehicles traveling at speeds above 22.5 mph (which is 32.5 mph below the speed limit of most rural highways and the mean speed of trucks on those highways). Thus, it appears that reductions in truck speeds much larger than 10 or 15 mph are needed to produce increases in accident rate large enough to warrant construction of a climbing lane.

With better data on the accident rates actually associated with specific speed differences on grades, it might be possible to develop a formal accident warrant for truck climbing lanes. Thus, there is a need for further research patterned on the Solomon study but focusing on steep grades and with better stratification of the speed range below 22.5 mph.

SUMMARY

In summary, the analyses imply that the Solomon data are not adequate to predict accident rates on steep upgrades, primarily because of the poor definition of accident rates for vehicles traveling at speeds less than 22.5 mph. However, the Solomon data for vehicles traveling faster than 22.5 mph imply that there is little safety justification for truck climbing lanes at locations where essentially all truck speeds remain above 22.5 mph. Of course, traffic service considerations should also enter into the decision to install a truck climbing lane. Furthermore, the truck performance data show that very few trucks would be slowed to speeds of 22.5 mph or below on any 2 percent upgrade, in the first 2,500 ft of a 4 percent upgrade, or in the first 1,800 ft of a 6 percent upgrade. Further research is needed to better quantify the safety effects of vehicle speeds below 22.5 mph, but the Solomon data for this speed range, although flawed, imply that accident rates on steep grades may be more strongly influenced by percent grade, length of grade, and percent trucks than previously thought.

REFERENCES

1. *A Policy on Geometric Design of Highways and Streets*. AASHTO, Washington, D.C., 1990.
2. D. Solomon. *Accidents on Main Rural Highways Related to Speed, Driver, and Vehicle*. FHWA, U.S. Department of Transportation, 1964 (reprinted April 1974).
3. A. D. St. John. *The Truck Population on High-Type Rural Highways*. Midwest Research Institute, Kansas City, Mo., 1979.
4. *Special Report 209: Highway Capacity Manual*. TRB, National Research Council, Washington, D.C., 1985.
5. *Speed Trends of Five-Axle Trucks on Grades in California*. California Department of Transportation, Sacramento, Jan. 1985.
6. A. D. St. John and D. R. Kobett. *NCHRP Report 185: Grade Effects on Traffic Flow Stability and Capacity*. TRB, National Research Council, Washington, D.C., 1978.
7. W. R. Reilly et al. *Capacity and Level of Service Procedures for Multilane Rural and Suburban Highways*. Final Report, NCHRP Project 3-33. TRB, National Research Council, Washington, D.C., May 1989.

Publication of this paper sponsored by Committee on Operational Effects of Geometrics.

Warrants for Passing Lanes

WILLIAM C. TAYLOR AND MUKESH K. JAIN

A two-lane road in rolling and hilly topography may not provide sufficient passing zone length between crests of vertical curves. The use of passing lanes can increase the passing opportunities, alleviating safety and operational problems on two-lane highways in a cost-effective manner. The simulation model TWOPAS was calibrated for different traffic and roadway conditions in Michigan. The calibrated model was used to study the operational benefits of providing passing lanes on two-lane highways. Two parameters, delay reduction and percentage vehicles in platoon, were selected for three configurations of road profiles. Simulation runs were made for different traffic volumes and truck percentages. The magnitude of the accident reduction potential of passing lanes was obtained. The total delay benefits were calculated by using a unit value of time established by AASHTO. The total benefit per year for different truck percentages and roadway conditions and the cost of construction for a passing lane were plotted against different average daily traffic values. The traffic volumes at which the benefits equal the costs of passing lanes for different traffic and roadway conditions were obtained.

There are more than 3 million mi of two-lane rural highways in the United States, composing about 97 percent of the total rural system and 80 percent of all U.S. roadways. More than two-thirds of the two-lane mileage is in mountainous or rolling terrain characterized by steep grades and sharp curves. An estimated 68 percent of rural travel and 30 percent of all travel occur on the rural two-lane system. Many of these roadways experience significant increases in traffic on weekends and during peak vacation periods.

The design of two-lane, two-way roads has some serious safety and operational problems, especially with the rapid increase in the number of trucks on the road. The two-lane road in rolling and hilly topography may not provide sufficient passing zone length between crests of vertical curves. Slow-moving heavy trucks on two-lane roads create operational problems in terms of delay, a reduced level of service, and an increase in passing attempts, aborted passes, and driver frustration. If a large portion of a road consists of no-passing zones, motorists may violate the established passing restriction, thereby increasing the probability of an accident. In these situations the use of passing lanes can increase the passing opportunities and alleviate safety and operational problems.

Accidents and traffic characteristics with and without passing lanes were analyzed to determine the possible benefits of passing relief lanes under various traffic conditions.

The main objectives of the study were

1. To select and calibrate a model to study the behavior of traffic, including the passing maneuver, on two-lane highways in Michigan;
2. To develop information on travel time savings due to passing lanes for different traffic composition and roadway geometry and driver characteristics;
3. To obtain and analyze accident data for two-lane, two-way Michigan highways with and without passing lanes to determine the potential benefits in terms of fewer accidents; and
4. To evaluate passing relief lanes on the basis of benefit-cost analyses for different combinations of traffic composition and geometrics.

College of Engineering, Michigan State University, A349 Engineering Building, East Lansing, Mich. 48824-1226.

The passing maneuver is a complex phenomenon and cannot be described fully through a mathematical model. Computer simulation, on the other hand, has the capability of describing traffic behavior on a vehicle-by-vehicle basis. Different simulation models of the passing maneuver on two-lane, two-way highways were reviewed, and a simulation model called TWOPAS was selected for use in this study. The advantages and disadvantages of different simulation models and the selection criteria for this model are given in the final project report.

To calibrate this model, headway, speed, and traffic composition data were collected on two selected two-lane, two-way roads in Michigan. The simulation model output values were compared with the field values at different locations along the simulated roadway. It was found that the TWOPAS model could be calibrated to accurately depict traffic and roadway conditions in Michigan.

The accident rate (per million vehicle-miles) was calculated for sections of highway in Michigan where passing relief lanes exist. These rates were compared with the accident rates on all sections of rural two-lane roads in Michigan without passing lanes to estimate the accident reduction potential of passing lanes.

Once calibrated, the selected simulation model was run with a wide variety of input values to obtain the average delay. These values were used to determine the sensitivity of delay to different parameters. The costs of the motorist delay and accidents were used to develop warrants for passing relief lane construction.

TWOPAS MODEL

TWOPAS is a microscopic computer model of traffic operations on two-lane, two-way highways. The capability to simulate passing and climbing lanes was validated from field data by Harwood and St. John (*1*). Good agreement was found between model results and field data for traffic platooning and traffic speeds upstream and downstream of passing lanes.

The TWOPAS model simulates traffic operations on two-lane highways by reviewing the position, speed, and accel-

eration of each vehicle on a simulated roadway at 1-sec intervals and advancing the vehicle along the roadway. The model takes into account the effects on traffic operations of road geometrics, traffic control, driver preferences, vehicle size and performance characteristics, and oncoming and same-direction vehicles that are in sight at any given time. The model incorporates realistic passing and pass abort decisions by drivers in two-lane highway passing zones. The model can also simulate traffic operations in added passing and climbing lanes on two-lane highways, including the operation of the addition and lane drop transition areas and lane changing within the passing or climbing lane section. Spot data, space data, vehicle interaction data, and overall travel data are accumulated and processed, and various statistical summaries are printed. The model also gives output at different locations and subsections along the simulated roadway (*2*).

SIMULATION MODEL CALIBRATION

Field Data Collection

Two sections with passing lanes, one on US-37 in Lake County and one on M-115 in Clare County, were selected for extensive field data collection to calibrate the simulation model. The features of these sites are shown in Figures 1 and 2. These sites were selected mainly because they are on the main routes leading toward Traverse City, a widely used recreational area in Michigan.

Special data recording machines (VC-1900), recommended by FHWA, were used to record traffic volume, speed, headway, and vehicle mix. An important feature of these machines is the ability to classify the vehicles in 13 categories on the basis of total number and spacing of axles on a vehicle. Three sets of machines were installed at a location 0.5 mi upstream of the passing lane, and two sets of machines were installed at two locations, 0.5 and 1.5 mi downstream of the passing lane. The setup of machines is shown in Figures 1 and 2 for both the sites. The upstream machines collected speed, headway, and vehicle classification separately, and the downstream machines collected speed and headway data. Data were collected on Friday for 6 hr from noon to 6:00 p.m. in one direction and on Sunday for the same 6 hr in the other direction. The same machine setup, timings, and days of the week were used for both locations.

Speed data were collected in 5-mph intervals and were plotted to get the speed distribution of the vehicles in the field. Mean desired speed and standard deviation of desired speed were obtained from these graphs. Vehicles having a headway of less than 5 sec were counted separately to get the percentage of vehicles in platoon.

For the simulation run, trucks were divided into three categories. The trucks classified by the machine as 5, 6, and 7 were taken as high-performance trucks; trucks classified as 8, 9, and 10 were taken as medium-performance trucks; and trucks classified as 11, 12, and 13 were taken as low-performance trucks. The model accepts three types of trucks and one type of bus. This machine does not distinguish rec-

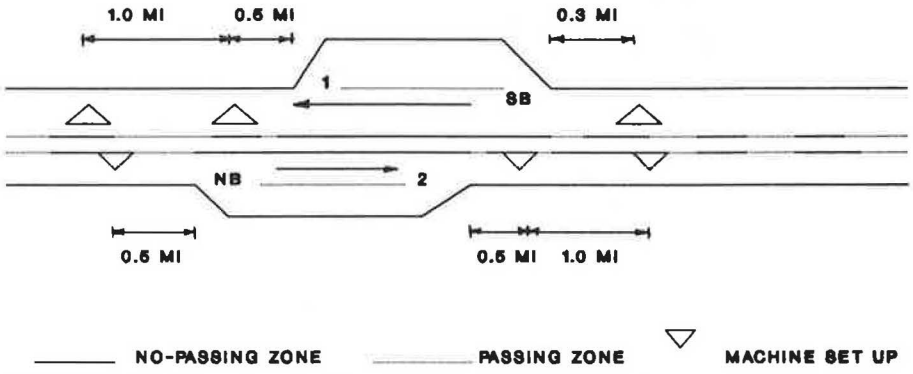

FIGURE 1 Machine setup for data collection at Lake County site.

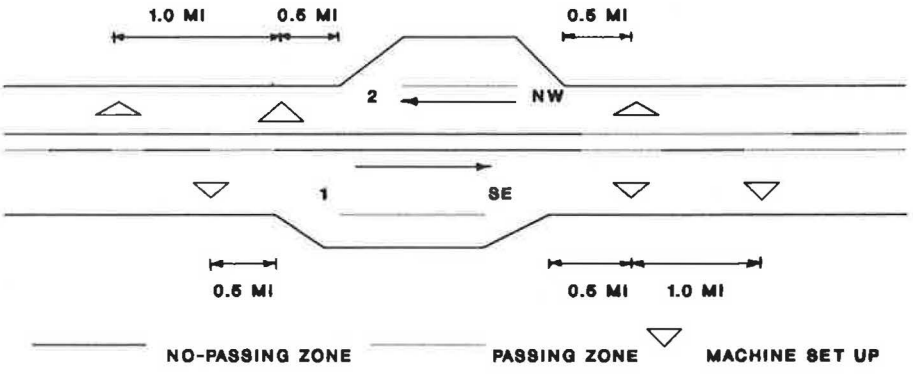

FIGURE 2 Machine setup for data collection at Clare County site.

reational vehicles as a single category, but classifies them as trucks with similar axle spacing. The machine classifies cars and pickup trucks separately. These two categories were taken as two high-performance types of cars in the model. Overall, three types of trucks, one type of bus, and two types of cars/pickups were used to calibrate the model.

Geometric data were collected by using the Michigan Automated Recording System (MARS) vehicle, which gives complete details of the alignment of the road. It measures location and different elements of vertical and horizontal curves as it moves along the road. The location and length of passing zones and no-passing zones and passing lanes were noted from the photolog films of the roads for both directions.

Input Data Required

To run the simulation model, the following input data are required. Most of these data were collected in the field as discussed; a few values were taken directly from the TWOPAS user's guide (*2*) as default values.

- Entering traffic data,
- Geometric data,
- Traffic control data,
- Vehicle characteristics, and
- Driver characteristics.

All vehicle types for which a fraction of the flow is specified for either direction of travel must be defined in terms of performance capabilities. The model takes weight/net horsepower ratio, weight/projected frontal area, a factor correcting horsepower to local elevation, and a factor correcting aerodynamic drag to local elevation to determine performance capabilities of trucks and buses. The performance capabilities of cars were considered in terms of maximum acceleration using maximum available horsepower and limitations on sustained use of maximum horsepower. These values were taken from the manual as default values for calibration of the model.

Mean desired speed and standard deviation of desired speed are required in the model. This speed distribution gives the speed at which drivers are willing to drive under given roadway conditions and indirectly represents the driver characteristics. Figure 3 shows a mean desired speed of 58.0 mph and standard deviation of 6.0 mph for the Clare County site. The model takes 10 types of drivers defined in terms of risk-taking characteristics and car-following sensitivity factors. In car-following models, driver response in a traffic stream can be explained in terms of sensitivity and stimuli. The response represents acceleration (or deceleration) of the following vehicle, and stimuli represent the relative velocity of the lead and following vehicle. The factor that relates response and stimuli in a car-following model is defined as the car-following sensitivity factor. The values recommended in NCHRP Project Report 3-28 A (*3*) were used in this study. These suggested values are 0.43, 0.51, 0.57, 0.65, 0.76, 0.91, 1.13, 1.34, 1.58, and 2.12 and are defined as stochastic driver type factors. The car-following sensitivity factor was taken as 0.8.

The model gives output values at specified locations along the simulation roadway length. These locations were the same locations at which the machines were installed to collect field data, so different output values could be compared with the field values to calibrate the simulation model.

Model Calibration

To calibrate the model, the values of selected parameters given by the simulation model were compared with the field values. The model output includes the percentage of vehicles in platoon, percentage of vehicles at or above the desired speed, average delay at a particular location, and delay for a specified section of simulated roadway. According to the *Highway Capacity Manual* (*4*), level of service on two-lane, two-way highways can be defined in terms of the percentage of vehicles in platoon. The percentage of vehicles in platoon at different locations was obtained to calibrate the model. As mentioned, these locations were 0.5 mi upstream and 0.5 and

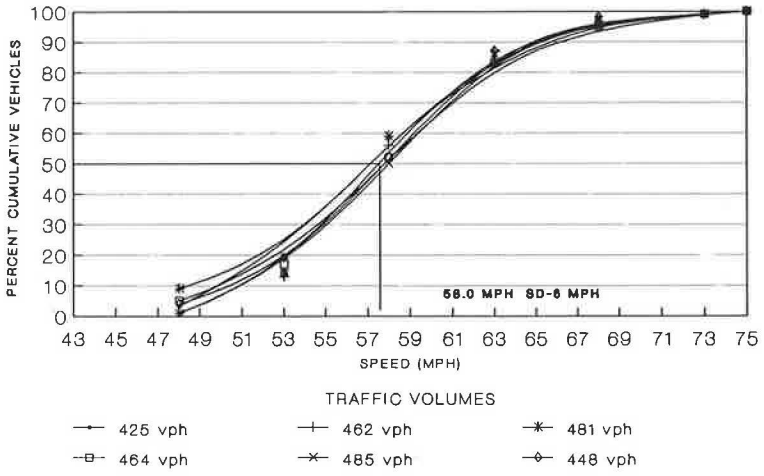

FIGURE 3 Speed distribution for Clare County site (southeast-bound traffic) showing mean desired speed and standard deviation of desired speed.

1.5 mi downstream of the passing lanes. Speed and headway data were collected at these three locations for all four passing lanes.

Simulation runs were made using hourly volumes and traffic mix collected in the field for both directions of flow and for different distributions of desired speeds. Average desired speeds were taken as 88 ft/sec, 92.4 ft/sec, and 95.4 ft/sec, and the standard deviation was taken as 8.58 ft/sec, 10.98 ft/sec, and 12.0 ft/sec for different runs for the Lake County roadway and traffic conditions. Subsequent runs were made using different values of the car-following sensitivity factor with a desired speed of 92.4 ft/sec and a standard deviation of 8.58 ft/sec for Lake County. The values of the sensitivity factor were raised until the model results best fit the field data. A value of 0.5 gave the best results. The simulation and field values of the percentage vehicles in platoon at different locations are given in Table 1. For the same values of desired speed and car-following sensitivity factor, different runs were made for each hourly volume for Clare County roadway conditions. The coding was done in the same way as for the Lake County site. The simulation and field values for the percentage of vehicles in platoon at different locations are given in Table 2.

To calibrate the model, the percentage of vehicles in platoon was taken as the main variable to compare the field values with the simulation values. The field values of percentage of vehicles in platoon were plotted against the values obtained by simulation for both sites, as shown in Figure 4. The field values are close to the simulation values, which indicates that the model is accurately simulating the Michigan roadway environment for the desired speed of 92.4 ft/sec (63.0 mph) with standard deviation of 8.58 ft/sec and a car-following sensitivity factor of 0.5.

TABLE 1 PERCENTAGE OF PLATOONING AT DIFFERENT LOCATIONS FOR DIFFERENT TRAFFIC VOLUMES (LAKE COUNTY SITE)

VOLUME DIR1/DIR2 (VPH)	DESIRED SPEED FT/SEC	MPH	HEADWAY < 5 SEC (BY SIMULATION) AT BEG. OF ROAD DIR 1	DIR 2	AVG. BOTH	AT END OF ROAD DIR 1	DIR 2	AVG. BOTH	AVERAGE** DIR 1	DIR 2	HEADWAY < 5 SEC (FIELD VALUES) DIR-1 AT LOCATIONS* 1	2	DIR-2 AT LOCATIONS* 1	2	AVERAGE** DIR 1	DIR 2
473/270	88.0	60	73	57	67	73	60	68	73	59	65	63	49	43	64	46
	92.4	63	68	52	62	65	55	61	67	53	65	63	49	43	64	46
	95.3	65	74	57	68	74	62	70	74	59	65	63	49	43	64	46
423/196	88.0	60	62	44	60	70	48	62	66	46	62	60	36	32	61	34
	92.4	63	62	39	54	64	35	55	63	37	62	60	36	32	61	34
	95.3	65	68	43	60	71	45	63	69	44	62	60	36	32	61	34
388/268	88.0	60	73	62	62	70	62	67	71	62	60	61	52	48	61	50
	92.4	63	70	58	65	62	57	60	66	57	60	61	52	48	61	50
	95.3	65	73	62	68	69	64	67	71	63	60	61	52	48	61	50
380/180	88.0	60	63	44	57	69	50	62	66	47	55	56	37	39	56	38
	92.4	63	58	40	52	56	39	51	57	39	55	56	37	39	56	38
	95.3	65	64	44	57	67	47	61	65	45	55	56	37	39	56	38
372/191	88.0	60	64	46	61	62	52	60	63	49	59	61	41	38	60	40
	92.4	63	62	44	56	57	48	54	59	46	59	61	41	38	60	40
	95.3	65	67	48	61	69	54	64	67	51	59	61	41	38	60	40
322/178	88.0	60	66	47	59	64	52	59	65	49	52	56	40	38	54	39
	92.4	63	60	41	53	57	47	53	58	44	52	56	40	38	54	39
	95.3	65	65	46	61	65	53	61	65	49	52	56	40	38	54	39

* Location 1__ 0.5 Miles Upstream of Passing Lane
* Location 2__ 0.5 Miles Downstream of Passing Lane
* Location 3__ 1.5 Miles Downstream of Passing Lane
** Average__ Average of Values in the Beginning and End of the Road.

TABLE 2 PERCENTAGE OF PLATOONING AT DIFFERENT LOCATIONS FOR DIFFERENT TRAFFIC VOLUMES (CLARE COUNTY SITE)

VOLUME DIR1/DIR2 (VPH)	DESIRED SPEED FT/SEC	MPH	PERCENTAGE VEHICLES IN PLATOON (HEADWAY <5 SECONDS) (SIMULATION VALUES) AT BEG. OF ROAD DIR 1	DIR 2	AVG. BOTH	AT END OF ROAD DIR 1	DIR 2	AVG. BOTH	AVERAGE DIR 1	DIR 2	(FIELD VALUES) DIR1 AT LOCATIONS* 1	2	3	DIR2 AT LOCATIONS* 1	2	3	AVERAGE DIR 1	DIR 2
415/226	92.4	63	61	32	51	63	45	56	62	38	59	54	53	32	32	35	55	33
458/228	92.4	63	68	39	58	68	40	58	68	39	64	62	60	34	33	35	62	34
461/247	92.4	63	69	39	58	68	43	60	68	41	65	56	57	38	34	38	59	37
447/278	92.4	63	68	44	59	67	52	61	67	48	65	63	61	41	35	37	63	38
469/337	92.4	63	62	50	57	68	55	62	65	52	62	61	59	49	44	39	61	44
432/390	92.4	63	69	51	60	68	62	65	68	56	63	57	56	49	43	47	59	46

* Location 1- 0.5 Miles Upstream of Passing Lane
* Location 2- 0.5 Miles Downstream of Passing Lane
* Location 3- 1.5 Miles Downstream of Passing Lane

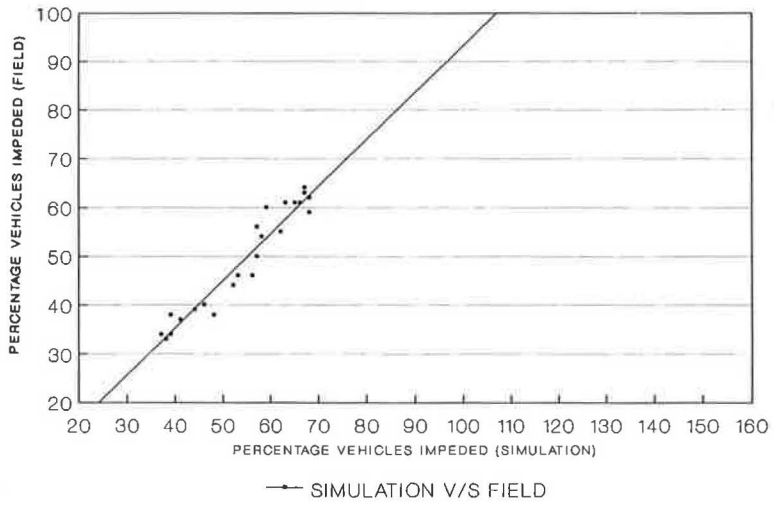

FIGURE 4 Percentage of vehicles impeded for speed of 92.4 ft/sec (simulation versus field values).

Although this calibration did not produce a true orthogonal line, the slope of the line matches the field data. The precise location of the line can be modified by changing the percentage of vehicles in platoon specified at the entry location.

Accident Data Required

Accident data were used to determine the effectiveness of passing lanes in reducing total accidents and severity of accidents on two-lane highways. The accident data were separated from the state data file for those sections having passing lanes on two-lane highways throughout Michigan. These data were separated for 5 years, 1983 to 1987. To compare the accident rates and severity of the accidents within the passing lane and the rest of the road, all the accident data on two-lane highways in Michigan were segregated on the basis of average daily traffic (ADT) levels: less than 5,000, between 5,000 and 10,000, and greater than 10,000. These accident rates by severity on two-lane rural highways in Michigan (with and without passing lanes) are given in Table 3.

CASE STUDIES

The calibrated model was used to study the operational benefits gained by providing a passing lane on two-lane highways. According to the *Highway Capacity Manual* (*4*), the main

TABLE 3 ACCIDENT RATES BY SEVERITY ON TWO-LANE RURAL HIGHWAYS IN MICHIGAN WITH AND WITHOUT PASSING LANES

	WITHOUT PASSING LANES				WITH PASSING LANES			
YEAR	INJURY ACC. RATE	FATAL ACC. RATE	P.D.O. ACC. RATE	TOTAL ACC. RATE	INJURY ACC. RATE	FATAL ACC. RATE	P.D.O. ACC. RATE	TOTAL ACC. RATE
FOR ADT 1-5000								
1983	61.0	2.2	203.1	266.3	49.1	0.0	183.8	232.9
1984	61.8	2.3	221.9	286.0	59.4	0.0	172.4	231.9
1985	60.4	2.3	242.6	305.3	40.6	0.0	283.0	323.7
1986	60.0	2.5	255.6	318.1	46.3	3.0	206.8	256.0
1987	59.5	2.5	259.5	321.5	14.6	0.0	249.4	264.1
FOR ADT 5001-10000								
1983	72.5	2.1	169.1	243.7	63.8	2.5	181.2	246.3
1984	75.7	2.6	172.9	251.2	49.3	0.0	170.5	192.4
1985	79.0	2.6	210.0	291.6	80.9	0.0	183.9	263.3
1986	72.0	2.9	210.1	285.0	45.8	0.0	228.2	272.0
1987	73.1	2.6	204.5	280.2	59.1	0.0	168.6	260.0
FOR ADT 10001-15000								
1983	103.8	1.5	199.6	304.9	27.5	10.5	203.8	241.5
1984	109.4	2.8	217.5	329.7	39.8	0.0	183.0	222.8
1985	97.7	3.0	228.9	329.6	70.5	0.0	157.5	228.0
1986	99.9	2.2	245.4	347.5	63.3	0.0	328.0	391.3
1987	98.9	3.0	223.0	324.9	93.0	0.0	216.5	309.5

NOTE: Rates = Accidents Per 100 Million Vehicle Miles

parameters defining the level of service on two-lane highways are delay and percentage of vehicles in platoon. These two parameters were selected to study the operational benefits of passing lanes. Three configurations of road profiles were used for this study. In the first configuration, two passing lanes (one in each direction) were provided; in the second configuration, one passing lane was provided in Direction 1 only; and in the third configuration, one passing lane was provided in Direction 2 only. The roadway profile and these configurations are shown in Figures 5 and 6.

Runs were made for these three configurations for different traffic volumes and truck percentages. The runs were made for all three cases for volumes of 500, 800, and 1,000 vehicles per hour. The values of delay benefits for each case are given in sec/veh in Table 4.

BENEFIT-COST ANALYSIS

The benefits of a passing lane are reductions in delay and accidents. The road user cost savings associated with these benefits were evaluated over a range of traffic volumes and compared with the cost of constructing and maintaining passing lanes. The reduction in delay provided by a passing lane results in operational cost savings to the road users. Simulation runs were made for different volumes, truck percentages, and geometric conditions; the reduction in delay due to a passing lane was computed as the difference between the average delay in the two directions of flow. The reduction in delay was used to compute the time cost savings.

A value is placed on travel time savings by selecting a unit value of time, usually expressed in dollars per traveler or vehicle hour, and multiplying this unit value by the amount of (traveler or vehicle) time saved. Besides the need for updating such values to current price levels, travel time value is sensitive to trip purpose, travelers' income levels, and the amount of time savings per trip. According to AASHTO (*5*), the time savings is divided into three categories and can be expressed as a function of time saved in a trip and type of trip.

1. Low time savings (0–5 min): For work trips and average trips, the values of time per traveler hour are suggested as $0.48 (6.4 percent of average hourly family income) and $0.21 (2.8 percent of average hourly family income), respectively.
2. Medium time savings (5–15 min): For work trips and average trips, the values of time per traveler hour are suggested as $2.40 (32.2 percent of average hourly family income) and $1.80 (24.4 percent of average hourly family income), respectively.

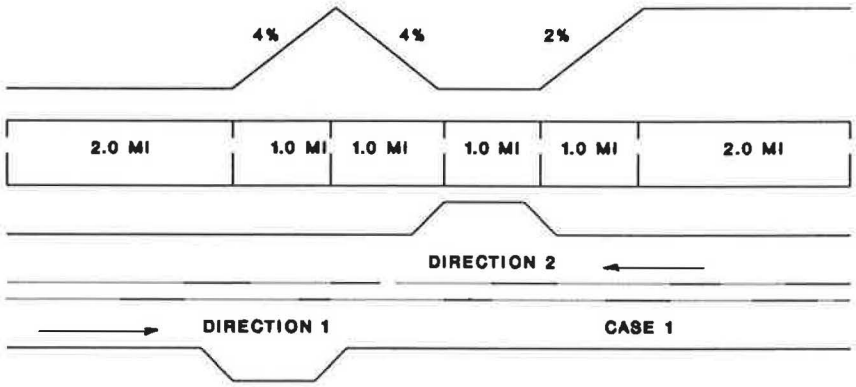

FIGURE 5 Layout of roadway for typical case study with two passing lanes, one in each direction.

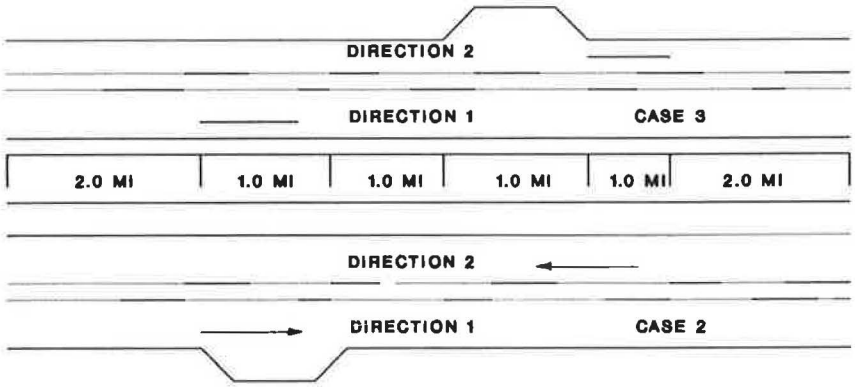

FIGURE 6 Layout of roadway for typical case study with one passing lane in each direction.

TABLE 4 COST BENEFIT DUE TO PASSING LANES FOR TYPICAL CASES

VOLUME VEH/HR BOTH DIRS	ADT	DELAY BENEFIT SEC/VEH (DT)	DELAY BENEFITS FOR AVERAGE TRIPS $/HR	$/YEAR	DELAY BENEFITS FOR WORK TRIPS $/HR	$/YEAR
WITH TWO PASSING LANES ONE IN EACH DIRECTION (CASE 1)						
500	5000	28.88	2.2	8030	5.1	18615
800	8000	32.76	4.0	14600	9.2	33580
1000	10000	37.84	5.8	21170	13.4	48910
WITH ONE PASSING LANE IN DIRECTION 1 (CASE 2)						
500	5000	17.29	1.3	4745	3.0	10950
800	8000	17.56	2.2	8030	5.1	18615
1000	10000	17.91	2.8	10220	6.5	23725
WITH ONE PASSING LANE IN DIRECTION 2 (CASE 3)						
500	5000	14.38	1.1	4015	2.5	9125
800	8000	19.06	2.3	8395	5.3	19345
1000	10000	23.40	3.6	13140	8.3	30295

3. High time savings (over 15 min): For work trips and average trips, the value of time per traveler hour is suggested as \$3.90 (52.3 percent of average hourly family income).

The delay benefits were calculated using the values of travel time for both average trips and work trips. According to 1980 Census data, the average annual family income in Michigan is \$27,000. That gives the average hourly family income as \$13.00, considering 2,080 working hours in a year. For average trips, the value of travel time per traveler hour was taken as \$0.36, which is 2.8 percent of the average hourly income of \$13.00. For work trips, the value of time per traveler hour was taken as \$0.88, which is 6.4 percent of the average hourly income of \$13.00. The average delay benefits were calculated by using Equation 1 in terms of dollars per hour and dollars per year. These values are given in Table 4.

Because the relationship between time savings and volume was not linear, a procedure for converting hourly benefits to annual benefits was required. Using Figure 2-4(a) of the *Highway Capacity Manual* (*4*), the relationship between daily benefits and peak-hour benefits was established as daily benefits equals hourly volumes times the benefits expected at that volume summed over the 24-hr period. The ratio of this sum to the benefits derived during the peak hour was approximately 10. Thus, the estimated daily benefits were taken to be equal to 10 times the peak-hour benefits.

Accident Cost Savings

An analysis of accidents on two-lane highways with and without passing lanes determined the effectiveness of a passing lane in reducing accidents. For the purpose of this analysis, the accident data were obtained from the state file for all two-lane road sections on rural highways throughout Michigan for 5 years, 1983 to 1987. The accident rates (by severity) were calculated, and the values are given in Table 3 for different ADT ranges.

To compare the accident rates within the passing lane and on the rest of the road, the mean accident rates for different ADT ranges were calculated for the sections with and without passing lanes. An average reduction in accidents was computed for each accident type for each ADT range. These values are given in Table 5, which indicates that passing lanes are effective in reducing accidents on two-lane highways.

Accident Costs

One of the most recent studies, by Miller et al. for FHWA (*6*), evaluated various approaches to accident cost estimation. The principal shortcoming of this study is its failure to express accident costs in a form that can be directly used in benefit-

TABLE 5 AVERAGE ACCIDENT BENEFIT (PER MILLION VEHICLE-MILES) DUE TO PASSING LANE

	AVERAGE ACCIDENT BENEFIT DUE TO PASSING LANE FATAL ACC. RATE	PERSON KILLED RATE	INJURY ACC. RATE	PERSON INJURED RATE	PDO ACC. RATE	TOTAL ACC. RATE
ADT < 5000						
WITHOUT PL	2.4	2.9	60.5	96.6	236.5	299.4
WITHIN PL	0.6	0.6	42.0	62.8	219.1	261.7
BENEFIT	1.8	2.3	18.5	33.8	17.4	37.7
5000 < ADT < 10000						
WITHOUT PL	2.6	3.1	74.5	123.3	193.3	270.4
WITHIN PL	0.5	0.5	59.8	94.1	186.5	246.8
BENEFIT	2.1	2.6	14.7	29.2	6.8	23.6
ADT > 10000						
WITHOUT PL	2.5	3.0	101.9	168.7	222.8	327.2
WITHIN PL	2.1	2.1	58.8	94.6	217.8	278.7
BENEFIT	0.4	0.9	43.1	74.1	5.0	48.5

TABLE 6 ACCIDENT COSTS BY AREA AND SEVERITY (1988 DOLLARS)

AREA AND TYPE OF COST	ACCIDENT COST BY SEVERITY FATAL($)	INJURY($)	PDO($)	AVERAGE($)
RURAL				
DIRECT	50654	9542	1600	5424
INDIRECT	1183580	5731	282	21356
TOTAL	1234234	15273	1882	26780
URBAN				
DIRECT	44071	8403	1872	3768
INDIRECT	1111355	4172	330	6364
TOTAL	1155426	12575	2202	10132

cost calculations. Costs are expressed per victim and per vehicle rather than per accident, and are presented in terms of the Maximum Abbreviated Injury Scale (MAIS). However, benefit-cost analyses are often based on accident data, which typically consist of numbers of accidents per year at various accident locations, with injury severities coded on the ABC scale (incapacitating, non-incapacitating, and possible injury) rather than on the MAIS (0, no injury; 1 to 5, least to most severe nonfatal injury; 6, fatality). Hence, costs such as those presented by Miller et al. (*6*) could not be directly applied to this analysis. On the basis of the values presented by Miller et al. (*6*), the accident costs were calculated by using methods previously developed in a study for FHWA (*7,8*). This method gives direct, indirect, and total costs per fatal, injury, and property-damage-only (PDO) accident in rural and urban areas. These values were updated for 1988 dollars and are summarized in Table 6.

Accident Cost Savings Analysis

The accident cost savings provided by passing lanes were computed with the following equation:

$$ACS = (AC)(365)(ARF)(ADT)10^{-8} \quad (1)$$

where

ACS = annual accident cost savings provided by a 1-mi passing lane (dollars per year per mile),
AC = average cost of accidents by severity (values taken from Table 10), and
ARF = average reduction in accidents by severity for different ADT values (per 100 million vehicle-miles).

Equation 1 was used to compute the safety benefits of a passing lane on rural two-lane highways in Michigan. In Equation 1, the values of the average cost of an accident were taken as the total rural accident cost for fatal, injury, and PDO accidents from Table 6. The accident cost benefits for different ADT values were calculated by considering direct costs of an accident.

Previously calculated delay benefit values were plotted and extrapolated for different ADT values. Total benefits were calculated by adding delay and accident benefits for different ADT values.

Equivalent uniform annual cost (EUAC) values were calculated for one passing lane 1 mi long and for two passing lanes each 1 mi long. Previous studies show that it may not be economical to provide passing lanes that are either too long or too short. Based on these studies, the length of passing lane was taken as 1.0 mi for this study. The life of the road was taken as $n = 15$ years. For $i = 5$ and 10, the values of the capital recovery factor were calculated as 0.0964 and 0.1315, respectively.

The values of total benefits for average trips and EUAC for 5 and 10 percent discount rates were plotted in Figure 7. The values of total benefits for work trips and EUAC for 5 and 10 percent discount rates were plotted in Figure 8.

Figures 7 and 8 show the benefit and cost values for average trips and work trips on a typical roadway. For example, using Figure 7, the warrants for a passing lane are met at a 4 percent grade, 10 percent trucks, and average trip type, as the user benefits are greater than construction costs for a passing lane for all ADT values greater than 6,500 for a discount rate of 5 percent. Similarly, for the same value of truck percentage, grade, and trip type, the benefits are greater than construction

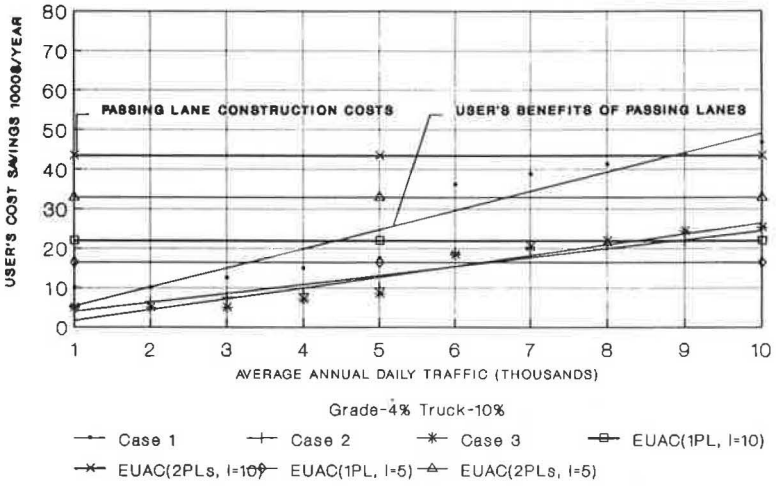

FIGURE 7 Comparison of cost and benefits for 4 percent grade, 10 percent trucks, and average trips on typical road profile.

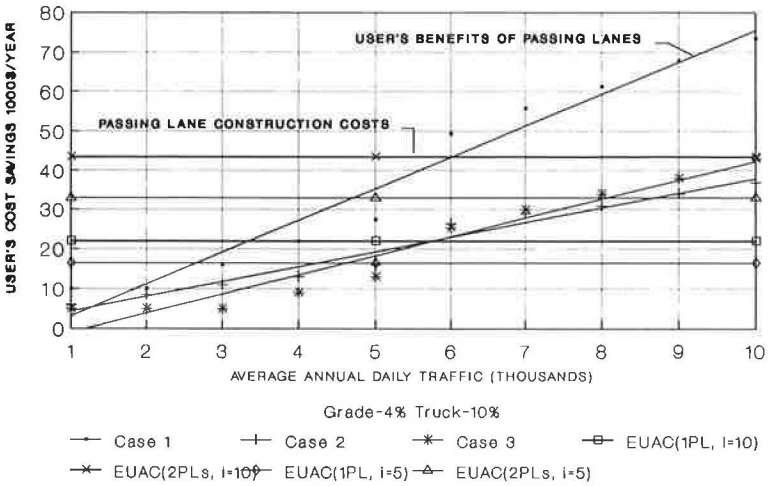

FIGURE 8 Comparison of cost and benefits for 4 percent grade, 10 percent trucks, and work trips on typical road profile.

cost for two passing lanes for ADT values greater than 9,000 for a 10 percent discount rate.

Figure 8 shows that for 4 percent grade, 10 percent trucks, and work trips, warrants for a passing lane are met at an ADT of 4,500 for a 5 percent discount rate. For the same value of truck percentage, grade, and trip type, the benefits are greater than the cost of two passing lanes at 6,000 ADT for a 10 percent discount rate. The values of ADT that warrant passing lanes were obtained for different grades, truck percentages, and percentage no-passing zones, and are documented in the final project report.

This analysis indicates that for a roadway with mild grades, the delay benefits in time savings for an isolated passing lane may be insignificant. However, the value of time savings will increase significantly with the type of trip and the unit value of travel time. Thus, if a series of passing lanes was provided on a single route, the cumulative time savings could reach the high time savings value, which increases the benefits by a factor of 17. The value of the discount rate selected to calculate the EUAC affects the benefit-cost analysis significantly. The analyst must select the unit value of time and discount rate cautiously in determining warrants for passing relief lanes, particularly where the grades are quite mild and the delay benefits are low.

REFERENCES

1. D. W. Harwood, A. D. St. John, and D. L. Warren. Operational and Safety Effectiveness of Passing Lanes on Two-Lane Highways. In *Transportation Research Record 1026*, TRB, National Research Council, Washington, D.C., pp. 31–39.
2. *A User's Guide to TWOPAS—A Microscopic Computer Simulation Model of Traffic on Two-Lane, Two-Way Highways*, FHWA, U.S. Department of Transportation, May 1986.
3. C. J. Messer. *Two-Lane Two-Way Rural Highway Capacity*. Final Report, NCHRP Project 3-28 A, TRB, National Research Council, Washington, D.C., Feb. 1983.
4. *Special Report 209: Highway Capacity Manual*, TRB, National Research Council, Washington, D.C., 1985.
5. *A Manual on User's Benefit Analysis of Highway and Bus-Transit Improvements*. AASHTO, Washington, D.C., 1977.
6. T. R. Miller, K. A. Reinert, and B. E. Whiting. *Alternative Approaches to Accident Cost Concepts: State of the Art.* Report FHWA/RD-83/079. FHWA, U.S. Department of Transportation, 1984, pp. 1–4, 122–130.
7. W. F. McFarland and J. B. Rollins. *Cost Effectiveness Techniques for Highway Safety, Resource Allocation.* Report FHWA/RD-84/011. FHWA, U.S. Department of Transportation, 1985, pp. 1–6, 55–118.
8. J. B. Rollins and W. F. McFarland. Costs of Motor Vehicle Accidents and Injuries. In *Transportation Research Record 1068*, TRB, National Research Council, Washington, D.C., 1986, pp. 1–7.

Publication of this paper sponsored by Committee on Operational Effects of Geometric Design.

Comparison of Safety Effects of Roadside Versus Road Improvements on Two-Lane Rural Highways

RAHIM F. BENEKOHAL AND MICHAEL H. LEE

The cost-effectiveness of roadside improvements was compared with road improvements on two-lane rural highways in Illinois. Accident reductions due to the improvements on 17 resurfacing, restoration, and rehabilitation projects were determined, and the benefits from the accident reductions were compared with the improvement costs. Accident data for 2 years before and 2 years after the improvements were extracted for two categories: (a) fixed-object, off-roadway, single-vehicle (FOS) accidents and (b) related accidents, which include overturned, other noncollision, head-on, and sideswipe accidents in addition to the FOS accidents. The roadside improvement costs were used in a benefit/cost analysis of the FOS accidents, and the road improvement costs were used in a benefit/cost analysis of the related accidents. Benefits, in terms of number of accidents reduced, were computed using the before-and-after study with control site approach. Roadside improvements reduced accidents by 7.02 per year, road improvements by 33.35 accidents per year. On the average, for every $28,471 spent on the roadside improvement, or for every $26,487 spent on the road improvement projects, one accident was reduced. The benefit/cost ratios for roadside improvements were very similar to those for road improvements. The cost-effectiveness approach and benefit/cost analysis indicated that the roadside improvements provided similar benefits to the road improvements. A more comprehensive study with a larger number of sites is suggested to evaluate the cost-effectiveness of highway improvements over a longer period of time.

This study compares the cost-effectiveness of roadside improvements with that of road improvements on two-lane rural highways in Illinois. The distinction between roadside and roadway improvements is made using the AASHTO definition of the terms. According to the AASHTO *Transportation Glossary* (*1*), *roadside* is a general term denoting the area adjoining the outer edge of the roadway; *roadway* is the portion of a highway, including shoulder, for vehicular use. In this study, *road improvement* denotes roadside improvement and roadway improvement.

The types of roadside improvements frequently made in these projects included removal of culvert headwalls and replacement with end sections and grates; removal or relocation of trees, utility poles, posts, and fences; and installation or end treatments of guardrails. Road improvements included these roadside improvements as well as widening the traveled lane and widening or upgrading the shoulder.

A roadside improvement project on a two-lane rural highway in most cases would cost considerably less than a road improvement project. On the other hand, the roadside improvement would yield less accident reduction than the road improvement. Given a limited highway safety improvement budget, are a few roadside improvements more cost-effective than a single road improvement? This study attempted to determine benefit/cost ratios and the cost-effectiveness of roadside and road improvements.

The study identified a sample of highway sites whose roadsides were improved, but whose sideslopes remained practically unchanged. The actual costs of the roadside and road improvements were determined for each project. The cost of each type of improvement was compared with the benefits from the reductions in number of accidents. The approach used for the comparison is a before-and-after study with control site approach. For the improved and control sites, accident data for 7 years were obtained from Illinois Department of Transportation (IDOT): accident data for 2 years before the improvements were compared with accident data for 2 years after the improvements. Benefit/cost analyses were conducted to evaluate the effectiveness of each type of improvement.

R. F. Benekohal, University of Illinois at Urbana-Champaign, 205 N. Mathews Ave., Urbana, Ill. 61801-2397. M. H. Lee, CH2M Hill/Leisch Associates, 1890 Maple Ave., Suite 200, Evanston, Ill. 60201.

BACKGROUND

A review of the literature on roadside safety indicated that the most frequently hit objects or features include utility poles, trees, ditch embankments, signposts, guardrails and fences, drainage facilities, and bridge structures (*2–4*). The highest percentage of fatalities is associated with fixed-object collisions with trees, utility poles, embankments, and culverts (*2,3*). A study of run-off-the-road accidents on two-lane rural roads (*5*) showed that 75 percent of these accidents involved fixed objects and 25 percent were turnover accidents. One-third of the fixed-object accidents and three-fifths of the turnover accidents involved injuries or fatalities. In Illinois from 1980 to 1985, 23,958 accidents per year occurred on two-lane rural highways (*6*). Single-vehicle run-off-the-road (SVROR) accidents constituted about 25 percent of these accidents. About 46 percent of the SVROR accidents were fatal and injury accidents.

A study of the effects of shoulder type on accident frequency (*3*) indicated that shoulder stabilization on two-lane roads was effective in reducing accidents on narrow roadways (20 ft or less), but was virtually ineffective on roads with widths of 24 ft or more. The study found that nearly 47 percent

of the single-vehicle accidents were collisions with fixed objects or roadside features and that nearly 51 percent of these collisions resulted in death or injury. A different study (*7*) showed that increasing pavement width by 1 ft would have the same effect on accident frequency as increasing shoulder width by 1 ft. Another study (*8*) found that the addition of paved shoulder width decreased the frequency and severity of accidents.

Perchonok et al. (*4*) found that accident frequency was higher on curves than on straight roads and higher on downgrade tangents than on upgrade tangents. The frequency was also higher immediately after the curve than farther downstream. The injury rate for accidents on vertical curves was higher than that for level roads. Cleveland et al. (*9*) concluded that average daily traffic (ADT) was the most significant parameter in the frequency of accidents for two-lane rural roads with ADT values ranging from 2,000 to 13,000, followed by driveway and intersection density and geometric parameters. They found that effects of longitudinal alignment parameters were significant in accident prediction for rural two-lane roads with ADT values of 4,000 or less, whereas effects of roadside elements were more significant at higher ADT values.

Vehicle-tree and vehicle-utility pole accidents are common types of fixed-object accidents on rural roads. It was reported (*10*) that of total accidents in Michigan from 1981 to 1985, 2.8 percent were with trees; 11 percent of these accidents were fatal. Another study (*11*) found that accident severity was higher for wooden poles than for the metal ones, mainly because of the frangible bases of the metal types. Zegeer and Cynecki (*12*) conducted a study to determine the different cost-effective treatments for utility pole accidents.

A study by Kohutek and Ross (*13*) concluded that for steep and flat sideslopes, leaving the culvert unprotected in its original position was the most cost-effective alternative for ADT values less than 750 and culvert offset greater than 12 ft. Guardrails were found to be cost-effective for double box culverts with moderate traffic volumes (>2,000 ADT) and for single box culverts with high traffic volumes (>20,000 ADT).

Accident characteristics on the rural Interstate system were studied by Nemeth and Migletz (*14*). After safety upgrading, the accident rates on improved sites were lower than those on control sites. The fatal accident rates were nearly the same, but injury accident rates were higher on the improved sites. They concluded that minor safety upgrading on projects was effective in reducing the injury and total accident rates.

Zegeer et al. (*15,16*) developed relationships between accident and cross-section elements for two-lane roads (mostly rural). They used accident data from a 5-year period (in most cases), collected for 1,362 rural sections in seven states, to develop different prediction models.

The possibility of combining accident data from different states for analysis was studied by Ng and Hauer (*17*). They used the data from seven states (used by Zegeer et al.) and concluded that for similar geometric and traffic conditions, different states had different numbers of accidents per mile-year. Therefore, they recommended that accident data for analysis not be pooled from different states, but that each state develop its own safety standards based on accident experience in that region.

DATA COLLECTION

Site Selection

Resurfacing, restoration, and rehabilitation (3R) projects on two-lane rural highways in Illinois during 1983–1985 were identified. These projects were either resurfacing or widening and resurfacing with some roadside improvements. They had some roadside and roadway improvements, but the sideslopes practically remained unchanged—the sideslope change was either for a very short length compared with the project length or for less than 1 percent. Construction plans for each project were reviewed to identify the type of improvements and to assess suitability of the project for this study.

From a total of 167 such 3R projects, 87 projects with some roadside improvements were selected for further analysis. The remaining projects either did not have roadside improvement or did not have a substantial amount. Projects with more than two lanes and those located mostly in urban areas were deleted because of the scope of this study. An urban area includes locations in or adjacent to a municipality or other urban areas with a population greater than 5,000. Because of these constraints, the number of selected projects was reduced from 87 to 68.

Additional roadway information for the 68 selected projects was obtained from IDOT roadway description records. The information included ADT, lane width, unpaved shoulder width, paved shoulder width, and number of days for which accident data were available for before-and-after improvement conditions. The project length, type of roadway and roadside improvements, amount of improvements, cost for each item of work, and percentage of the project located in rural or urban areas were also recorded. The amount of roadside and roadway improvements for each project was taken from the construction plans—this process was very time-consuming because each page of the construction plan had to be carefully reviewed to determine the type and amount of improvements.

Sixty-eight projects could be used for this study. However, for only 51 were the accident data for 2 years before (1981–1983) and 2 years after (1985–1987) the improvement conditions available. This further limited the number of improved sites to 51.

Traffic Data

The ADT values for improved and control sites were obtained from IDOT roadway description records. Every attempt was made to select projects with uniform ADT values over the entire length or to select portions of a project that had less ADT fluctuation between segments. When ADT values were not the same for different segments of a project, a weighted ADT was computed by dividing vehicle-miles traveled by the project length. The weighted ADT was then compared with ADT values from IDOT maps. Generally, there was very close agreement between the two ADT values.

Traffic growth rate on rural highways in Illinois was determined from IDOT data for 1982–1989. The data showed annual vehicle-miles traveled on rural federal-aid primary routes

and number of miles of rural highways on the system. ADT values and growth rate for the 7-year period were determined from this information. The average annual increase over the 7-year period was about 1.9 percent. This rate is very close to a traffic growth rate of 1.5 percent used by IDOT for long-term traffic projection on two-lane rural highways. ADT for 1987 was adjusted using 1.5 percent growth rate to reflect traffic volumes in the base year and analysis year. The base year is 1984 because most of the construction projects were undertaken from 1983 to 1985. The future year for economic analysis is 1994. The future year used for the analysis is not necessarily the same as the design year for a facility. Because major improvements have a service life of about 20 years, half of the service life was added to the base year to come up with 1994.

Roadway Improvement Data

Roadway improvement included widening the traveled lane and/or widening or upgrading the shoulder. Roadway width before the improvement, roadway width after the improvement, average ADT of the improved site, and average ADT of the control site are summarized in Table 1. The traveled lane was widened by 0 to 3 ft, and accordingly the shoulder was narrowed by 0 to 3 ft for 16 of the 17 projects—the width of the traveled lane in project 99 decreased by 0.5 ft because of restriping of the pavement edge. In resurfacing-only projects (18, 97, and 162), the total width of the traveled lane, and accordingly the total width of the shoulder, remained unchanged.

Accident Data

Accident data for improved and control sites were obtained for a period of 7 years (1981–1987). The accident data were separated into two groups: improved sites and control sites. The improved sites had some roadside or roadway improvement. For each improved site, one or two control sites were located immediately before or after the improved site. Most of the control sites had the same length as the corresponding improved sites.

For the improved and control sites, the accident data were further separated into two categories of accident:

1. Fixed-object, off-roadway, single-vehicle (FOS) accidents and
2. Related accidents.

The accidents included in the FOS category were SVROR accidents involving certain fixed objects for which the first involvement was running off the road and the second involvement was striking one of the following fixed objects: guardrail (excluding bridge guardrail), highway sign, culvert headwall, bridge abutment, guardrail on bridge approach, light standard, advertising sign, fence (excluding median fence), underpass structure, barricade, building, mailbox, water hydrant, impact attentuator, tree, utility pole, ditch or embankment, or delineator post. The non-FOS accidents were not used in this study.

Multivehicle accidents on or off the roadway, overturn accidents, and other noncollision types were excluded from the FOS category. Accidents with the following fixed objects were also excluded: curb or channelizing island curb, concrete median barrier, traffic signal, bridge or bridge guardrail, median fence, machinery, thrown or falling objects, falling load, railroad gate or signal, snow bank, animals, pedestrians, train, parked motor vehicle, and pedalcyclists.

The related accidents included the FOS accidents plus overturn accidents, other noncollision accidents, head-on accidents, and sideswipe accidents in the same or opposite directions.

STUDY APPROACH

A before-and-after study with control site approach was used to evaluate cost and effectiveness of the roadside and road

TABLE 1 LANE AND SHOULDER WIDTH BEFORE AND AFTER IMPROVEMENTS AND AVERAGE DAILY TRAFFIC FOR IMPROVED AND CONTROL SITES

PROJ ID	LANE WIDTH BEF	LANE WIDTH AFT	SHOULDER WIDTH UNPAVED BEF	SHOULDER WIDTH UNPAVED AFT	SHOULDER WIDTH PAVED BEF	SHOULDER WIDTH PAVED AFT	ADT IMPRVD	ADT CONTROL
18	12	12	8	8	0	0	600	1350
27	9	12	11	7	0	1	1450	2200
32	9	11	8	6	0	0	1150	1550
50	9	12	11	8	0	1	1950	2100
59	9	11	4	3	2	1	1950	2700
85	9	11	11	8	0	1	800	1400
91	9	12	11	8	0	0	2400	1700
96	9	11	8	5	0	1	1050	750
97	11	11	10	7	0	3	2950	3000
99	12	11.5	10	10	0	0.5	3050	2600
106	9	12	9.5	7	1.5	1	2600	2350
107	9	11	11	8	0	1	900	600
109	9	11	8	5	0	1	800	850
128	10	12	10	4	0	4	1900	1750
130	8	11	5.5	4	1.5	0	700	600
131	11	13	5	3	0	0	3850	3900
162	11	11	1	1	0	0	3400	4200

improvements. This approach yields more accurate results than a simple before-and-after study when the control sites have characteristics similar to those of the improved sites. Selection of suitable control sites is very important in a before-and-after accident study with control sites (*18*). To increase the accuracy of this experimental design, it was confirmed that the control sites did not have roadside or roadway improvements during the study period. If a control site had roadside or roadway improvements during 1981–1987, the control site was deleted from the list. Although these exercises limited the number of available control sites to one-third the number of improved sites (*17*), they increased the reliability of the results from this analysis.

Selection of Control Sites

Control sites were located immediately in advance of an improved site (Site A) or past the improved site (Site B). These control sites usually had the same length as the corresponding improved sites, but were not improved. For each control site, information about ADT, length, location (urban or rural), number of lanes, lane width, shoulder width, type of traffic control devices used on different segments of a site, location of intersections and bridges, and roadway alignment (curve or tangent) was obtained from IDOT's roadway description records. After the review and comparison of the information from each control site with that of the corresponding improved site, either Site A or Site B was selected when two suitable control sites were available.

Suitability was determined by comparing the control site's roadway and traffic information with that of the corresponding improved site. If control sites had significantly different ADT values than the corresponding improved sites, the control sites were not used. If a control site was located in both urban and rural areas, the urban part was deleted. Some parts of control sites were also deleted if roadway geometry changed from two to four lanes, or if the roadway did not continue. This deletion of parts is not critical when accident frequency on a control site is compared with accident frequency on the adjacent improved site. When comparing accident frequencies (number of accidents divided by the site length) between improved and control sites, equal length requirement is not as critical as it is in comparing the number of accidents. This is because the effect of site length on number of accidents is linear (*6,15,16*). On the other hand, when number of accidents on control sites is used to adjust number of accidents on improved sites, comparable site lengths should be used.

For the 51 improved projects, only 39 corresponding control sites were identified. The remaining 12 projects did not have suitable control sites. Of these 39 control sites, 18 had some roadside or roadway improvements during the study period and were deleted. The remaining 21 control sites did not have roadside or roadway improvements or resurfacing during 1981–1987. Because resurfacing and roadway improvements could affect accident frequency, only those 21 control sites were considered in selecting the final control sites.

Characteristics of Control Sites

ADT values of the 21 remaining control sites were compared with ADT values of the corresponding improved sites. The difference between the ADT of each improved site and the ADT of its corresponding control site was computed. On the basis of the ADT differences, the sites were assigned to four groups—see Tables 2 and 3. The first three groups were those sites with differences less than or equal to 100, 400, or 800. The last group included all 21 sites regardless of ADT differences.

Accident data and number of control sites for different ADT groups are summarized in Tables 2 and 3 for the FOS and related accidents. The tables indicate that for the selected groups of control sites, the total number of accidents [sum of property-damage-only (PDO), injury, and fatal accidents] increased for the after period. Only Group 1 of the FOS accidents showed no increase in total number of accidents for the after condition.

The difference in ADT between a control site and its corresponding improved site was less than 800 vpd for 17 locations; for the last four sites, however, the difference was quite high (a range of 1,350–2,650 vpd). These four sites were considered unsuitable; thus, only 17 control sites were used for the final analysis.

Ideally one would try to find control sites with roadway and traffic conditions identical to those of the corresponding

TABLE 2 NUMBER OF FIXED-OBJECT ACCIDENTS IN BEFORE AND AFTER PERIODS FOR CONTROL SITES

Group	Difference In 1987 ADT	Number of Control Sites	BEFORE				AFTER			
			PDO	INJ	F	Total	PDO	INJ	F	Total
1	$\lvert ADT_{imp} - ADT_{con} \rvert \leq 100$	4	6	1	0	7	5	1	0	6
2	$\lvert ADT_{imp} - ADT_{con} \rvert \leq 400$	10	10	7	0	17	15	6	0	21
3	$\lvert ADT_{imp} - ADT_{con} \rvert \leq 800$	17	14	9	1	24	19	12	0	31
4	Regardless of difference in ADT	21	5	12	1	28	20	13	0	33

ADT_{imp} = is average daily traffic for improved sites

ADT_{con} = is average daily traffic for control sites

PDO = property damage accidents, INJ = injury accidents, F = fatal accidents

TABLE 3 NUMBER OF RELATED ACCIDENTS IN BEFORE AND AFTER PERIODS FOR CONTROL SITES

Group	Difference In 1987 ADT	Number of Control Sites	BEFORE				AFTER			
			PDO	INJ	F	Total	PDO	INJ	F	Total
1	$\lvert ADT_{imp} - ADT_{con} \rvert \leq 100$	4	11	6	0	17	14	11	1	26
2	$\lvert ADT_{imp} - ADT_{con} \rvert \leq 400$	10	20	14	0	34	35	19	2	56
3	$\lvert ADT_{imp} - ADT_{con} \rvert \leq 800$	17	29	21	1	51	45	29	2	76
4	Regardless of difference in ADT	21	33	27	2	62	51	33	2	86

improved sites. However, it is almost impossible to satisfy the ideal experimental design requirements in actual roadway and traffic conditions. Often accident analysis is conducted a few years after the improvements have been completed, as in this study. Furthermore, the improvements are not proposed according to a careful experimental design for statistical analysis, but are proposed by state officials because there is a need for highway improvement. In this project, it was attempted to use a before-and-after study with control site approach to work completed in the past. This situation imposed conditions that were not ideal—using control sites with different ADT values than the corresponding improved sites. Such imperfection in design might introduce minor errors that it was not possible to quantify.

It should be mentioned that using a control site with an ADT identical to that of an adjacent improved site does not mean that the accident frequency for the two sites is considered to be the same. Rather it means that the difference in number of accidents for before-and-after periods for a control site is assumed to be equal to the expected value of the change in number of accidents for an adjacent site (the site planned for future improvement) with a similar ADT, if the adjacent site did not have the roadway or roadside improvements. In other words, the change in the number of accidents for a site with future improvement plan is assumed to be equal to the change in the number of accidents on the corresponding control site with a similar ADT if the improvement was not to occur.

After a review of the ADT difference between control sites and improved sites, it was concluded that for this study the contribution of the errors would be negligible (see Table 1). Of the 17 control sites, three had an ADT difference of 50 vpd. For practical purposes, one may assume that these three control sites had the same ADT as their corresponding improved sites. For half the remaining 14 control sites, ADT values were higher than those of improved sites; for the other half of the control sites, ADT values were lower than those of improved sites. Therefore, it is reasonable to assume that the errors due to volume difference would cancel one another.

Statistical Analyses

The statistical analyses were performed with the data from 17 improved and 17 control sites. Data analyses for 51 sites and different adjustment options are reported elsewhere (*19*).

The analyses were performed to determine whether the changes in accident frequencies were statistically significant. Accident frequencies (accidents per mile) for the FOS and related accidents under before-and-after conditions were computed on the control and improved sites (eight sets)—for example, frequency of the FOS accidents for the improved sites before the improvement, frequency of the FOS accidents for the control sites before the improvement of the adjacent sites, and frequency of the related accidents for the improved sites after the improvement. The accident frequencies are given in Tables 4 and 5.

Four paired *t*-tests were performed to evaluate the change in accident frequency on the control and improved sites. The difference in accident frequencies before and after improvement conditions was computed for the FOS and related accidents on the control and improved sites (four sets)—for example, the difference between frequency of the FOS accidents for the improved sites after the improvement and frequency of the FOS accidents for the improved sites before the improvement and the difference between frequency of the related accidents for the improved sites after the improvement and frequency of the related accidents for the improved sites before the improvement.

A paired *t*-test is normally used for experiments with paired design. Pairing observations (paired design) is a special case of randomized block design, where block size is 2. Blocking should be used to reduce sources of discrepancy, whenever appropriate (*20*). In this study, there are 17 blocks (sites) and each block has two treatments (before and after). By using sites as blocks and finding the difference in accident frequencies for each site, it was possible to obtain a more meaningful comparison of conditions before and after treatment. The *t*-value for the paired *t*-test was computed as

$$t = \frac{X_D - X_O}{S_D/(N_D)^{1/2}}$$

where

X_D = sample mean of the differences,
X_O = sample standard deviation of the differences,
S_D = expected value of treatments difference, and
N_D = number of pairs.

For each set, the mean and variance of the differences were computed and used in running a paired *t*-test (*21*). The summary of computations for these tests is given in Table 6.

TABLE 4 FREQUENCY AND NET REDUCTION IN FOS ACCIDENTS

PROJ ID	IMPROVED SITES LENGTH	ACCIDENT/MILE BEF	AFT	CONTROL SITES LENGTH	ACCIDENT/MILE BEF	AFT	NET RED. PER YEAR
18	9.24	0	0	9.23	0.108	0	-0.054*
27	7.1	0.563	0.282	7.09	0.423	0.846	-0.352
32	8.87	0.451	0.564	8.86	0.226	0.677	0.169
50	7.89	0.253	0.507	7.88	0.381	0	-0.317
59	3.51	0.285	1.140	3.5	0.286	0.286	-0.427
85	6.56	0	0	6.55	0	0	0
91	4.06	0.739	0	4.05	0.247	0.493	0.493
96	8.82	0.113	0.113	3.41	0	0.880	0.440
97	11.95	0.335	0.251	15	0.267	0.2	0.009
99	4.6	0	0	1.98	0	0	0
106	14.19	0.141	0.070	6.37	0.314	0.628	0.192
107	9.8	0.204	0.306	6.99	0	0	-0.051
109	6.42	0.312	0.312	6.41	0.312	0.156	-0.078
128	3.74	0.267	0.535	3.73	0.804	0.536	-0.268
130	3.69	0	0	3.58	0	0	0
131	4.1	1.463	0.732	4.09	0.244	0.489	0.488
162	6.33	0.948	0.474	5.59	0.179	0.179	0.237
TOTAL	120.87			104.3			

* This site is treated as no change in accident frequency

TABLE 5 FREQUENCY AND NET REDUCTION IN RELATED ACCIDENTS

PROJ ID	IMPROVED SITES LENGTH	ACCIDENT/MILE BEF	AFT	CONTROL SITES LENGTH	ACCIDENT/MILE BEF	AFT	NET RED. PER YEAR
18	9.24	0.216	0.108	9.23	0.217	0.000	-0.054
27	7.1	1.972	0.704	7.09	0.846	1.834	1.127
32	8.87	0.789	1.015	8.86	0.451	1.580	0.452
50	7.89	0.887	1.014	7.88	0.888	0.127	-0.444
59	3.51	0.855	1.425	3.50	1.429	0.857	-0.571
85	6.56	0.152	0.152	6.55	0.000	0.000	0.000
91	4.06	2.217	1.232	4.05	0.494	0.494	0.493
96	8.82	0.340	0.567	3.41	0.000	0.880	0.327
97	11.9	1.590	0.753	15	0.733	0.933	0.518
99	4.6	0.000	0.435	1.98	0.505	0.505	-0.217
106	14.1	1.128	1.128	6.37	0.314	1.256	0.471
107	9.8	0.714	0.714	6.99	0.000	0.000	0.000
109	6.42	0.467	0.623	6.41	0.312	0.312	-0.078
128	3.74	2.674	0.535	3.73	1.072	1.072	1.070
130	3.69	0.271	1.084	3.58	0.000	0.838	0.012
131	4.1	2.927	1.951	4.09	0.978	1.711	0.855
162	6.33	3.318	1.896	5.59	0.179	0.179	0.711
TOTAL	120.87 Miles			104.3 Miles			

TABLE 6 SUMMARY OF COMPUTED VALUES FOR PAIRED *t*-TESTS

Condition	N_D	$X_B - X_A = X_D$	S_D
1) Control Sites FOS Accidents	17	-0.09	0.314
2) Control Sites Related Accidents	17	-0.244	0.579
3) Improved Sites FOS Accidents	17	0.046	0.384
4) Improved Sites Related Accidents	17	0.304	0.832

Where:

X_B is sample mean for before improvement condition
X_A is sample mean for after improvement condition
X_D is sample mean differences
S_D is sample standard deviation of differences
N_D is number of differences (number of pairs)

Analyses of Test Results

The first paired *t*-test checked whether the difference in accident frequencies between before and after conditions was significant for the FOS accidents on the control sites. The paired *t*-test indicated that the difference was significant with an 87 percent confidence level (the computed t was -1.195). The 87 percent significance level was relatively low; however, considering the sample size and the type of accidents used (FOS accidents on the control sites), the level of significance was accepted for this test. Thus, with an 87 percent confidence level, there was an increase in the frequency of the FOS

accidents for the control sites during the after-improvement period.

The second paired *t*-test checked whether the difference in the frequencies of the related accidents between conditions on the control sites before and after the treatments on the other sites was significant. Using the values in Table 6, the paired *t*-test indicated with a 94 percent confidence level (computed value of t was -1.745) that the difference was significant. This means the number of the related accidents on the control sites increased during the after-improvement period.

The first and second paired *t*-tests indicated an increase in the number of accidents on the control sites because of some factors other than geometric improvements (perhaps increase in traffic volume, change in driver population or behavior, or other unknown variables). It is reasonable to expect that the same factors will also increase the number of accidents on the improved sites because the improved and control sites are adjacent. Therefore, a before-and-after study with control site approach is used to account for the effects of factors other than geometric improvements. It should be noted that the total length of the control sites is about 17 mi shorter than the total length of the improved site. Thus, the change in the number of accidents on the control sites will be a conservative estimate of the change in the number of accidents on the improved sites.

The values in Table 6 indicate that the number of accidents on the improved sites may have decreased where an increase was expected without the improvements. If the indication is true, it means not only that the number of accidents did not increase but also that the number decreased. The purpose of the third and fourth paired *t*-test is to examine the net change in the number of accidents on the improved sites.

The third paired *t*-test checked whether there was a net reduction in the frequency of the FOS accidents on the improved sites after the roadside improvements. For this test, the hypothesis was that the change in the frequency of the FOS accidents on improved sites was equal to the change in the FOS accidents on the control sites. The test indicated with a 92 perent confidence level that the net difference in the number of accidents for before-and-after conditions was significant. Thus, with a 92 percent confidence level, it can be concluded that the FOS accidents were reduced on the site with some roadside improvements.

The purpose of the fourth paired *t*-test was very similar to that of the third paired *t*-test, except that it dealt with related accidents. The hypothesis was that the number of related accidents on the improved sites decreased after the roadway improvements, considering the increasing trend on the control sites. The test indicated with a 92 percent confidence level that the number of related accidents on the improved sites decreased for the after-improvement period. This reduction is due to the road improvements.

Therefore, the results of the third and fourth paired *t*-tests from the 17 improved sites indicated, with a confidence level of 92 percent, that the number of accidents on the improved sites decreased during the 2-year period after the roadside and roadway improvements; the decrease was for both FOS and related accidents. The number of accident reductions resulting from each type of improvement was computed, and economic analyses for roadside and road improvements were performed.

ECONOMIC ANALYSIS

The actual costs of improving the road and roadside were determined for each project. The benefits from the improvements were determined in terms of the number of accidents reduced because of the improvements. Two types of economic analyses were made: benefit-cost ratio and cost-effectiveness analysis.

Improvement Costs

Improvement costs of various roadside and road improvement works were determined for each project. These costs, along with total annualized cost of improvement for a project, are shown in Table 7. The improvement costs consisted of roadside improvement, widening, shoulder improvement, traffic control and protection, and mobilization. The improvement cost did not include incidental items of work, which could affect the total cost of improvement. For example, trench backfill was incidental to pipe culvert extension and was already included in the latter cost.

Three types of improvement costs were calculated:

1. Roadside improvement cost,
2. Widening and/or shoulder improvement cost, and
3. Road improvement cost.

The roadside improvement cost included the cost of all items of work involving removal, relocation, installation, extension, and reinstallation of fixed objects and features to improve roadside—tree removal, headwall removal, culvert removal, guardrail removal, fire hydrant removal, wall removal, delineator removal, fence relocation, culvert extension with end section and grate, impact attenuators, guardrail installation, sign installation, and delineator installation. The widening and/or shoulder improvement cost included the widening of the traveled lane and the widening or upgrading of the shoulder. The road improvement cost was the total of improvement costs 1 and 2, plus traffic control and protection and mobilization costs.

The roadside improvement cost was used in the benefit-cost analysis of the FOS accidents, and the road improvement cost was used in the benefit-cost analysis of the related accidents. Sometimes it was difficult to split the cost of a certain improvement by the two accident types even though the improvement affects both types of accidents. For instance, culvert extension would affect the FOS accidents and, to some degree, the related accidents. In such improvement items, rather than allocating the cost of items to one of two categories (which would be subjective), all such items were included in the roadside improvement cost category. Thus, culvert extension cost was included in the benefit-cost analysis of the FOS accidents. This study did not perform a sensitivity analysis on including the shared costs in the roadside improvement category. The items included in the roadside improvement cost category and their service life are given in Table 8.

Annual Cost

The improvement cost for each item of a project was determined separately. The quantity of each item of work was

TABLE 7 TOTAL COST FOR EACH IMPROVEMENT ITEM AND TOTAL ANNUALIZED COST FOR EACH PROJECT

PROJ ID	TREE	CULVERT	GUARD RAIL	WALL HYDRANT	SIGN	W&RS	TRAFF/ MOBIL	TOT ANN. ROAD	TOT ANN. RDSIDE
18	3620	39660	42828	0	1444	91643	83447	32803	17054
27	5430	127533	58574	0	2137	563527	46232	82765	27923
32	1193	34535	73739	0	3982	402068	46232	62222	21902
50	2904	142105	0	1119	1698	472241	46956	64101	17404
59	0	27272	15307	0	472	211320	45326	29790	6706
85	1140	1376	10434	0	0	425489	57803	45758	2290
91	488	12051	0	0	0	324351	46956	34917	1522
96	0	40159	8177	0	0	604665	46956	65341	6734
97	7510	117483	20104	5067	849	630105	57803	81476	19605
99	0	76555	0	0	0	68094	43269	18277	8260
106	8542	141221	27999	0	0	1055535	65185	125211	24413
107	7113	37648	7614	0	0	656303	54836	70620	6659
109	0	13993	9952	0	0	334168	51927	38271	3546
128	0	39752	17633	0	0	456434	46956	52335	7060
130	1550	153705	3970	0	0	220007	41618	40419	16888
131	0	13854	13707	0	0	131977	46956	21054	4961
162	646	8105	24613	0	1205	75927	46956	17994	6942
TOTAL ANNUAL COST OF 17 PROJECTS								$883354	$199867

Where:

"TREE" is total cost column for tree removal

"CULVERT" is total cost column for headwall removal, culvert removal, and culvert extension

"GUARDRAIL" is total cost column for guardrail removal, impact attenuator, and guardrail installation

"WALL/HYDRNT" is total cost column for fire hydrant removal, wall removal, and fence relocation

"SIGN" is total cost column for sign installation and delineator removal/installation

"W&RS" is total cost column for widening and resurfacing improvement cost

"TRAFF/MOBIL" is total cost column for traffic control and mobilization

"TOT ANN. ROAD" is total annualized road improvement cost for that project

"TOT ANN. RDSIDE" is total annualized roadside improvement cost for that project

TABLE 8 ITEMS INCLUDED IN ROADSIDE IMPROVEMENT COST CATEGORY AND THEIR SERVICE LIFE

Item	Service Life
1) Tree removal	20
2) Headwall removal	20
3) Culvert removal	20
4) Guardrail removal	20
5) Fence relocation	10
6) Culvert extension including end sections and grates	10
7) Impact attenuator installation	3
8) Guardrail installation and reinstallation	10
9) Highway sign installation	5
10) Delineator installation	4
11) Embankment	15
12) Others, such as, removal of walls, buildings, fire hydrant, delineator	20

obtained from construction plans and/or summaries of quantities for bid items. The quantity was then multiplied by the unit cost to get the total cost of that item. The statewide average cost (average of 1983, 1984, and 1985) for a given item of work was used as the unit cost for that item. When there was a lump sum cost in a project (e.g., mobilization cost), the statewide average cost for that item of work was used.

The maintenance cost was not included in the roadside or road improvement work because it is difficult to quantify and the type of work varies with administrative policies and normal maintenance practices. The salvage value of an improved item was also assumed to be zero because it is generally negligible.

The annual cost of each item of work was computed by multiplying the total cost of the item by a capital recovery factor for that item. The capital recovery factor was calculated on the basis of the service life of that item and an interest rate of 4 percent, which was suggested by IDOT. The an-

nualized costs of all items of work were then added to get the total annualized cost of improvement for a project (see Table 7). For 17 projects, the total annual cost was $199,867 for the roadside improvements and $883,354 for the road improvements in the analysis year.

Estimated Benefits

A highway improvement would have many benefits to the motorists and the communities surrounding the highway. Some of the benefits to road users would be a decrease in travel time, delay, fuel consumption, pollution, and vehicle maintenance cost, and an increase in comfort level and safety (reduced frequency or severity of accidents). This study used only the benefits from a reduction in the number of accidents in the economic analysis. Number of accidents reduced because of the improvements was computed using the before-and-after study with control site approach. The number of accidents reduced was converted to a dollar figure by using either the statewide average cost of an accident in Illinois or the cost suggested by FHWA. The average cost of an accident for the base year (1984) was calculated as the mean of accident costs for 1983, 1984, and 1985. This cost was increased annually by 4 percent to reflect the average cost of an accident in the analysis year (1994). The accident cost was based on National Safety Council costs and Illinois statewide average distribution of different types of accidents: PDO, injury, and fatal. The average cost of an accident in Illinois in 1984 was about $9,400. With the 4 percent interest rate, the computed cost for 1994 was about $15,000. This estimate is very low compared with the $53,700 suggested by FHWA (*21*). These accident costs are used only for illustrative purposes and do not mean an endorsement of one agency over the other.

Accident Reduction

The methodology for computing the number of accidents reduced was discussed with the study approach. The following equation is used to compute the number of accidents reduced. In this equation, the number of accidents (FOS and related) occurred on the improved and control sites before and after the improvements.

$$N = [(n_{Ib} - n_{Ia}) - (n_{cb} - n_{ca})]/2$$

where

N = total number of accidents reduced on 17 improved sites per year,
n_{cb} = total number of accidents occurring on 17 control sites during 2 years before the improvement of corresponding adjacent sites,
n_{ca} = total number of accidents occurring on 17 control sites during 2 years after the improvement of corresponding adjacent sites,
n_{Ib} = total number of accidents occurring on 17 improved sites during 2 years before the improvement, and
n_{Ia} = the total number of accidents occurring on 17 improved sites 2 years after the improvement.

This equation has two main components. The first part $(n_{Ib} - n_{Ia})$ represents the accident change on the improved sites, and the second part $(n_{cb} - n_{ca})$ shows the change in the number of accidents on the control sites. To illustrate, this equation is applied to one of the 17 sites. Project 32 had 0.451, 0.564, 0.226, and 0.667 FOS accidents per mile in the before-and-after-improvement conditions on improved and control sites, respectively. Applying these numbers to the equation, net reduction of FOS accident frequency per year is 0.169 as shown in the Table 4.

Tables 4 and 5 show accident frequencies for 17 improved and control sites. For the FOS accidents, changes in the total accident frequency after the improvement were as follows:

- Seven improved sites had net decrease,
- Six improved sites had net increase, and
- Four improved sites had no change.

It should be noted that in Project 18, the FOS accident frequency decreased on control site but exhibited no change on the corresponding improved site. This case was treated as no change in the total accident frequency after the improvement. For the related accidents, the following changes in the total accident frequency were observed:

- Ten improved sites had net decrease,
- Five improved sites had net increase, and
- Two improved sites had no change.

The changes in traffic volume after an improvement affect the number of accidents during service life of improved sites. To account for this increase, N should be adjusted. This adjustment was determined using the infomation provided by Zegeer et al. (*2*) to adjust the historical accident data for future ADT. Since N already included the effect of ADT increase on the number of accidents for first 5 years (1981–1982 to 1986–1987), the adjustment was required only for the remaining period of the service life. The adjustment factor for the remaining period, K, was 1.17 for the FOS and related accidents (*19*). The adjusted number of accidents reduced in the analysis year was computed by multiplying K by N. The computations are summarized in Table 9. The adjusted number of the FOS accidents reduced was 7.02 per year, and the adjusted number of the related accidents reduced was 33.35 per year.

Benefit/Cost Comparisons

The benefits were calculated by multiplying average number of accidents reduced in the analysis year by the average cost of the accident in that same year. The benefit/cost ratios are given for accident costs of $15,000 and $60,000. The $60,000 value is an accident cost in 1994 comparable with the FHWA figure ($53,700 increased with a rate of 2 percent only because of recency of data). Sensitivity of the benefit/cost ratios to the average cost per accident is illustrated in Table 9. The results clearly show that the benefit/cost ratio is very sensitive to the accident cost, and the accident cost can significantly influence the economic analysis of the improvements.

TABLE 9 BENEFIT/COST ANALYSIS FOR FOS AND RELATED ACCIDENTS

n_{ca}	n_{cb}	n_{la}	n_{lb}	N	N * K	Interest Rate	Annual Cost	B/C[1] Ratio	B/C[2] Ratio
A. FOS ACCIDENTS/ROADSIDE IMPROVEMENTS									
31	24	33	38	6	7.02	4%	$199,867	0.53	2.11
B. RELATED ACCIDENTS/ ROAD IMPROVEMENTS									
76	51	103	135	28.5	33.35	4%	$883,354	0.57	2.27

(1) The B/C ratio is based on average accident cost of $15,000, in 1994.
(2) The B/C ratio is based on average accident cost of $60,000, in 1994.

The benefit/cost ratios changed from 0.53 to 2.11 for the FOS accidents and from 0.57 to 2.27 for the related accidents, depending on the accident cost. This is because FHWA recommends a much higher cost per accident than that given by the National Safety Council. The recommended cost per accident by FHWA includes combined fatal-plus-injury cost (also PDO if available), which reflects the amount individuals are willing to pay to reduce the number and severity of accidents. FHWA encourages the states to use these cost figures in the economic analysis of highway safety projects.

The results from the study indicated that the benefit/cost ratios for the roadside and road improvements were very close (0.53 compared to 0.57, for 2.11 compared to 2.27). Thus, based on these data, the roadside improvements were as cost-effective as the road improvements. It is important to note that this study is based on 17 projects and data for 2 years before and 2 years after the improvements. A more comprehensive study with a larger number of sites is suggested to evaluate the long-term effectiveness of each type of improvement.

Cost-Effectiveness Analysis

An alternative economic analysis is to compare the cost-effectiveness of the roadside improvements with that of the road improvements. To do this, the average cost of an accident reduction is computed. Spending $199,867 on the roadside improvements resulted in 7.02 accident reductions per year. That is, an average of one accident was reduced for every $28,471 spent on the roadside improvement projects. Similarly, spending $883,354 on the road improvement projects reduced the number of related accidents by 33.35 per year. On the average, one accident was reduced for every $26,487 spent on road improvement projects.

The cost-effectiveness approach avoids the argument about the average accident cost that exists in the benefit/cost ratio approach. The cost-effectiveness approach also indicated that the road improvements provided benefits similar to the roadside improvements.

Relationship of Costs, Number of Accidents, and ADT

The relationship of improvement costs, number of accidents, and ADT was also investigated. Roadside costs were plotted against number of the FOS accidents and ADT: roadside costs versus net reduction in the FOS accidents; roadside costs versus frequency of the FOS accidents before the improvement for the improved and control sites; roadside costs versus frequency of the FOS accidents after the improvement for the improved and control sites; roadside costs versus average ADT for the improved and control sites; roadside costs versus ADT before the improvement for the improved and control sites; and roadside costs versus ADT after the improvement for the improved and control sites. Road costs were also plotted against number of the related accidents and ADT.

In addition, values for ADT before and after the improvement were plotted against corresponding number of accidents: ADT versus frequency of the FOS accidents before the improvement for the improved and control sites; ADT versus frequency of the FOS accidents after the improvement for the improved and control sites; ADT versus frequency of the related accidents before the improvement for the improved and control sites; and ADT versus frequency of the related accidents after the improvements for the improved and control sites. A total of 30 plots was drawn, but are not shown here because of limited space.

The linear regression analyses were done on these 30 plots, and the square of the correlation coefficient, R^2, was computed for each plot. The R^2 ranged from 0.00014 to 0.437. Four plots had R^2-values ranging from 0.253 to 0.437; these were plots of ADT versus frequency of accidents. The relationship between ADT and accident frequency is discussed by Benekohal and Hashmi (*19*). The rest of the plots had R^2-values less than 0.2. It was concluded that there is no distinct relationship between the road cost and the related accident frequency/reduction or between the roadside cost and the FOS accident frequency/reduction within the scope of this study. Further investigation did not present any distinct relationship between the improvement costs and ADT.

CONCLUSIONS AND RECOMMENDATIONS

The data indicated that the roadside and road improvements reduced the total number of accidents on the study sites. Roadside and road improvements reduced the number of accidents by 7.02 and 33.35 per year, respectively. The total annual cost of the roadside and road improvements was $199,867 and $883,354, respectively. The benefit/cost ratios for the roadside and road improvements were very similar (0.53 compared with 0.57, or 2.11 compared with 2.27), indicating that the roadside improvements were as economical as the road improvements.

The cost-effectiveness approach was used to compare the roadside improvements with the road improvements. On average, for every $28,471 spent on the roadside improvements, or for every $26,487 spent on the road improvement projects, one accident was reduced. The cost-effectiveness approach also indicated that the road improvements provided similar benefits to the roadside improvements. Because the benefit/cost ratio is very sensitive to the unit cost of the accident, it is recommended that the cost-effectiveness approach be used for economic analysis.

It is important to note that this study was based on 17 projects and data only for 2 years before and 2 years after improvements. A more comprehensive study is suggested to evaluate the long-term effectiveness of a roadside and road improvement program using a larger number of sites. It is recommended that the computerized accident data be kept for more than seven years for a more comprehensive study on the cost-effectiveness of highway improvements.

ACKNOWLEDGMENT

The authors would like to thank the Illinois Department of Transportation and FHWA for supporting this study, particularly John Sanford and John Blair of IDOT for their help in retrieving accident and cost data. The authors also wish to thank Asma M. Hashmi for data collection and analysis.

REFERENCES

1. *Transportation Glossary*. AASHTO, Washington D.C., 1983.
2. S. C. Tignor, C. P. Brinkman, J. M. Mason, and J. M. Mounce. *Synthesis of Safety Research Related to Traffic Control and Roadway Elements—Volume 1*. Report FHWA-TS-82-232, FHWA, U.S. Department of Transportation, 1982.
3. T. J. Foody and M. D. Long. *The Identification of Relationships Between Safety and Roadway Obstructions*. Ohio Department of Transportation, Columbus, 1974.
4. K. Perchonok, T. A. Ranney, A. S. Baum, D. F. Morris, and J. D. Eppich. *Hazardous Effects of Highway Features and Roadside Objects, Volumes 1 and 2*. Reports FHWA-RD-78-201 and FHWA-RD-78-202, FHWA, U.S. Department of Transportation, 1978.
5. D. E. Cleveland and R. Kitmura. Macroscopic Modeling of Two-lane Rural Roadside Accidents. In *Transportation Research Record 681*, TRB, National Research Council, Washington, D.C., 1978.
6. D. E. Boyce, J. J. Hochmuth, C. Meneguzzer, and R. G. Mortimer. *Cost-Effective 3R Roadside Safety Policy for Two-Lane Rural Highways*. Illinois Department of Transportation, Springfield, 1988.
7. M. J. Maierle and M. J. Wolfgram. Rural Two-lane Highway Accidents and Geometrics: A Statistical Analysis. Presented at 67th Annual Meeting, Transportation Research Board, Washington, D.C., 1988.
8. R. O. Rogness, D. B. Fambro, and D. S. Turner. Before-After Accident Analysis for Two Shoulder Upgrading Alternatives. In *Transportation Research Record 855*, TRB, National Research Council, Washington, D.C., 1982.
9. D. E. Cleveland, L. P. Kostyniuk, and K. Ting. Geometric Design Element Groups and High-Volume Two-lane Rural Highway Safety. In *Transportation Research Record 960*, TRB, National Research Council, Washington, D.C., 1984.
10. A. J. Zeigler. Risk of Vehicle-Tree Accidents and Management of Roadside Trees. In *Transportation Research Record 1127*, TRB, National Research Council, Washington, D.C., 1987.
11. C. V. Zegeer and M. R. Parker. Effect of Traffic and Roadway Features on Utility Pole Accidents. In *Transportation Research Record 970*, TRB, National Research Council, Washington, D.C., 1984.
12. C. V. Zegeer and M. J. Cynecki. Determination of Cost-effective Roadway Treatments for Utility Pole Accidents. In *Transportation Research Record 970*, TRB, National Research Council, Washington, D.C., 1984.
13. T. L. Kohutek and H. E. Ross, Jr. *Safety Treatment of Roadside Culverts on Low Volume Roads*. Report FHWA-TX 77-225-1, FHWA, U.S. Department of Transportation, 1978.
14. Z. A. Nemeth and D. J. Migletz. Accident Characteristics Before, During, and After Safety Upgrading Projects on Ohio's Rural Interstate System. In *Transportation Research Record 672*, TRB, National Research Council, Washington, D.C., 1978.
15. C. V. Zegeer, J. Hummer, D. Reinfurt, L. Herf, and W. Hunter. *Safety Effects of Cross-Section Design for Two-lane Roads, Volumes 1 and 2*. Reports FHWA-RD-87/008 and FHWA-RD-87/009, FHWA, U.S. Department of Transportation, 1987.
16. C. V. Zegeer, J. Hummer, L. Herf, D. Reinfurt, and W. Hunter. *Safety Cost-Effectiveness of Incremental Changes in Cross-Section Design–Informational Guide*. Report FHWA/RD-87/094, FHWA, U.S. Department of Transportation, 1987.
17. J. C. N. Ng and E. Hauer. Accidents on Rural Two Lane Roads: Differences Between Seven States. Presented at 68th Annual Meeting, Transportation Research Board, Washington, D.C., 1989.
18. F. M. Council, D. W. Reinfurt, B. J. Campbell, F. L. Roediger, C. L. Carroll, A. K. Dutt, and J. R. Dunham. *Accident Research Manual*. Report FHWA/RD-80/016, FHWA, U.S. Department of Transportation, 1980.
19. R. F. Benekohal, and A. M. Hashmi. *Accident Savings from Roadside Improvements on Two-Lane Rural Highways: Final Report*. Report FHWA/IL/RC-009, FHWA, U.S. Department of Transportation, June 1990.
20. G. E. P. Box, W. G. Hunter, and J. S. Hunter, *Statistics for Experimenters*. Wiley & Sons, New York, 1978.
21. *Motor Vehicle Accident Costs*. FHWA Technical Advisory. FHWA, U.S. Department of Transportation, June 30, 1988.

Publication of this paper sponsored by Committee on Operational Effects of Geometrics.

Gaps Accepted at Stop-Controlled Intersections

KAY FITZPATRICK

Gap-acceptance data are used to determine intersection sight distance, capacity, queue length, and delay at unsignalized intersections. They have also been used to determine the need for a traffic signal, the capacity of a left-turn lane, and warrants for left-turn signal phasing and storage lanes. A field study was performed to determine the gap-acceptance values of truck and passenger car drivers at six intersections. Each intersection was formed by two 2-lane roads; the minor road was controlled by a stop sign. The data obtained in the field were evaluated by three methods: Greenshield, Raff, and logit. The findings from the field studies were summarized into generalized values. Passenger car drivers had a 50 percent probability of accepting a gap of 6.5 sec for both left and right turns and an 85 percent probability of accepting a gap of 8.25 sec at a moderate- to high-volume intersection. A 10.5-sec gap represented the 85 percent probability of accepting a gap at an intersection where accepted gaps were influenced by low volume and the intersection's geometry. Truck drivers' 50 percent probability of accepting a gap was 8.5 sec. At a high-volume location, 85 percent of the truck drivers accepted a 10 sec gap; at a low-volume location, 15.0 sec was the accepted gap value.

A driver at a stop-controlled intersection must observe the gaps in the opposing traffic streams and determine whether the gaps are adequate to complete a crossing or turning maneuver. After accepting a gap, the driver should be able to complete the desired maneuver and comfortably join or cross the major road traffic stream within the length of the gap. The evaluation of available gaps and the decision to carry out a specific maneuver within a particular gap are inherent in the concept of gap acceptance.

Gap-acceptance data are used to determine intersection sight distance, capacity, queue length, and delay at unsignalized intersections (*1–4*). These data have also been used to determine the need for a traffic signal, the capacity of a left-turn lane, and warrants for left-turn signal phasing and storage lanes (*5–9*). These procedures are generally based on the gaps accepted by passenger car drivers. However, in those areas that experience significant truck traffic, gaps accepted by truck drivers should be considered. Gaps accepted by truck drivers are typically longer than gaps accepted by passenger car drivers because trucks have different vehicle characteristics (e.g., slower acceleration rates and longer vehicle lengths).

Relatively few studies have determined the difference in gaps accepted by truck drivers and those accepted by passenger car drivers. This field study was performed to determine the gap-acceptance values of truck drivers and passenger car drivers.

Pennsylvania Transportation Institute, Pennsylvania State University, University Park, Pa. 16802. *Current affiliation*: Texas Transportation Institute, Texas A&M University, College Station, Tex. 77843.

PREVIOUS RESEARCH

Several gap-acceptance studies have been conducted at intersections with stop control on the minor road. The findings from the major gap-acceptance studies are listed in Tables 1 and 2. Gap values used in the *Highway Capacity Manual* (*2*) and the *Swedish Capacity Manual* (*3*) are listed in Table 3. Two U.S. studies determined critical gap values for vehicles turning right after stopping. The values were 6.73 sec for Radwan et al. (*13*) and 7.36 sec for Solberg and Oppenlander (*16*). Polus (*14*) in Israel found 7.47 sec as the critical gap. The capacity manuals have lower gap values, ranging from 5.5 and 6.5 sec for the *Highway Capacity Manual* (*2*), and from 5.5 to 7.2 sec for the *Swedish Capacity Manual* (*3*), depending on the speed of vehicles on the major road.

The left-turn maneuver in the United Kingdom is similar to the U.S. right-turn maneuver in that the turning vehicle merges with cross traffic in the near lane. The results from studies in the United Kingdom are generally lower than those from U.S. studies. Cooper et al. (*18*) associated gaps with the approach speed of the vehicle on the major road and found the median accepted gap to range from 5.35 to 6.69 sec. (The gap size did not increase with the higher approach speed; rather, the smallest gap size was associated with the highest approach speed.) Darzentas et al. (*19*) related gap size to light condition, reporting the median accepted gaps as 6.58 sec for daylight conditions and 5.62 sec for dark conditions.

Wennell and Cooper (*20*) collected gap data at four locations in the United Kingdom. They reported gap values that are 2 sec lower than other United Kingdom studies and more than 3 sec lower than the U.S. studies. They filmed during moderate to heavy commuter traffic when the volume for the major road approach lane was between 660 and 890 vehicles per hour (vph). The turning volume on the minor road approach was also high, between 140 and 205 vph. Their study focused on three issues: associating the vehicle's maneuver time with accepted gap size, the difference in gap sizes accepted by men and women drivers, and the effects of passengers on gaps accepted. Their literature review concentrated on other researchers' findings of the presence of differences rather than the value of the differences. Wennell and Cooper did not compare their median gap accepted values with values from previous research.

Results from studies on left-turning vehicles also produced a range of gap-acceptance values. Solberg and Oppenlander

TABLE 1 GAP VALUES FROM MAJOR GAP-ACCEPTANCE STUDIES

Study (Analysis Method)	Measured	Gap
Greenshield, 1947 (10) (Greenshield Method)	Crossing	Average minimum acceptable time gap = 6.1 sec
Raff, 1950 (11) (Raff Method)	Crossing	Critical lag = 5.9 sec Critical gap = 6.1 sec
Bissell, 1960 (12) 2 intersections (Bissell Method)	Crossing	Critical gap = 5.8 sec

Radwan et al., 1980 (13) multilane, divided highways, 6 intersections (Logit Method)		Gap accepted by 50 percent of drivers
	Right Turn	6.73 sec
	Through, one maneuver	7.90 sec
	Through, two maneuvers	7.20 sec
	Left Turn, one maneuver	6.32 sec
	Left Turn, two maneuvers	6.60 sec
	Trucks, all maneuvers	8.40 sec

Polus, 1983 (14) 2 intersections in Israel (Raff Method)		Critical Gap	Critical Lag
	Right Turn from minor to major, Yield	5.20 sec	5.10 sec
	Right Turn from minor to major, Stop	7.47 sec	7.55 sec

Adebisi and Sama, 1989 (15) 2 intersections in Nigeria, Africa left turns, (CHOMP computer program)

Duration Stop Delay (sec)	Mean Delay for Group (sec)	Number of Samples	Mean Critical Gap (sec)
< 5.0	3.23	91	20.99
5.1-10.0	7.46	209	18.77
10.1-15.0	12.01	91	17.58
15.1-20.0	16.52	61	16.31
20.1-25.0	21.65	104	9.87
25.1-30.0	27.53	66	10.46
30.1-35.0	32.74	76	8.62
35.1-40.0	36.78	48	8.29
40.1-60.0	46.66	42	6.78
>60.0	75.85	16	5.32

(*16*) reported 7.82 sec, and Radwan et al. (*13*) reported 6.32 sec when the minor road vehicle crossed a multilane divided highway in one maneuver. Adebisi and Sama (*15*), in Nigeria, Africa, reported mean critical gaps ranging from 20.99 sec, when the minor road vehicle had been stopped for less than 5 sec, to 5.32 sec, when the vehicle had been stopped for more than 60 sec. The *Swedish Capacity Manual* (*3*) lists values of 6.0 to 7.5 sec for left turns, and the *Highway Capacity Manual* (*2*) lists values of 6.5 to 8.0 sec, depending on the major road vehicle's approach speed. A United Kingdom study of right turns (similar to U.S. left turns) had results that were several seconds less than those of comparable U.S. studies. Cooper and McDowell (*17*) studied the effect of police presence on gaps, finding the values to range from 5.9 sec with police activity to 4.6 sec without police activity.

The findings from studies on crossing maneuvers were more consistent than those for turning maneuvers. Greenshield et al. (*10*), Raff and Hart (*11*), and Bissell (*21*) found values of 6.1, 6.1, and 5.8 sec, respectively. The *Swedish Capacity Manual* (*3*) lists 5.8 to 7.0 sec, and the *Highway Capacity Manual* (*2*) lists 6.0 to 7.5 sec. Solberg and Oppenlander (*16*) had a 7.18-sec result for the crossing maneuver, which agrees with the higher values from the capacity manuals.

Other relevant studies on gap acceptance include observations of the effects of the major street speed, type of sign control, length of stop delay, and the behavior of individual drivers. In 1971, Sinha and Tomiak (*22*) reported that the major street speed significantly affected the size of a gap acceptable to a driver on the minor street. In 1983, Polus (*14*) found that the mean gaps and lags accepted may be influenced by the type of sign control (yield versus stop). Adebisi and Sama (*15*) in 1989 found that for mean stop delays shorter than 25 sec, the mean critical gaps were larger than the value obtained from the aggregated data; for mean delays longer than 30 sec, the mean critical gaps were smaller. Ashworth and Bottom (*23*) concluded in 1975 that the gap acceptance behavior of individual drivers is closer to an "inconsistent behavior" model (each driver has a variable critical gap) than to a "consistent behavior" model (each driver has a fixed critical gap).

FIELD STUDY

Six intersections with similar geometric characteristics were selected for the field study. Table 4 summarizes the intersec-

TABLE 2 MEDIAN ACCEPTED GAP VALUES FROM MAJOR GAP-ACCEPTANCE STUDIES USING PROBIT ANALYSIS

Study	Measured	Median Accepted Gap
Solberg & Oppenlander, 1966 (16) 4 intersections	Right Turn Left Turn Through	7.36 sec 7.82 sec 7.18 sec
Cooper & McDowell, 1977 (17) effects of police presence and police activity (warning signs or police motorcycle parked in view) at 3 intersections	Right Turn (UK) from minor road and merging with major road	4.6 sec w/o police 5.7 sec with police 5.3 sec w/o police activity 5.9 sec with police activity
Cooper, Smith, Broadie, 1976 (18) 1 intersection	Left Turn (UK) from minor road and merging with the nearside stream	Approach Speed (mi/h) / Median Accepted Gap (sec) (ft) 17.5 5.86 150 22.5 6.69 221 27.4 5.95 240 32.5 6.34 302 37.4 5.35 294 D = 38' + 5 V where D is in ft and V is in f/sec
Darzentas, Holms, McDowell, 1980 (19) 1 intersection, 10 evenings	Left Turn (UK)	6.58 sec daylight 6.32 sec twilight 5.62 sec darkness
Wennell and Cooper, 1981 (20) 4 intersections	Left Turn (UK)	Left Turn Site / Cars (sec) / Goods (sec) 1 3.91 4.63 3 3.66 5.33 4 4.31 4.99 5 4.41 4.91

tion characteristics. Four intersections had predominately passenger car traffic; one intersection had a high percentage of truck traffic on the minor approach from an industrial park. The minor road approaches for the other two intersections were the driveway of an asphalt and aggregate plant (Central Valley Asphalt) and a truck stop exit (Truck Stop 64). The asphalt and aggregate plant is a few miles outside of a small town, and the truck stop is in a rural area less than 1,000 ft from an Interstate exit. The approach from the asphalt and aggregate plant has primarily three- and four-axle trucks; the truck stop and industrial park approaches have five-axle trucks.

A video camera was placed along the minor road approach at each intersection. The position of the camera maximized the length of the road that could be filmed without jeopardizing the resolution of the vehicles on the videotape. Figure 1 shows a typical setup. An internal clock was started when videotaping began. As a vehicle crossed the center of the minor road approach (the reference line), a hand-held flag was raised. The flagging of a vehicle determined its position as it crossed the reference line and provided a permanent record on the videotape for the data reduction process. The times that each minor road vehicle arrived at and left the intersection and the times that relevant major road vehicles crossed the reference line were recorded from the videotapes. These times were used to calculate the gaps rejected and accepted by the minor road drivers.

DETERMINATION OF GAP-ACCEPTANCE VALUES

The quantity of the proposed data to be collected for the gap-acceptance analysis was a compromise between a reasonable, realistic data collection effort and the need for adequate data for numerical analysis. Several combinations of vehicles (passenger cars, five-axle trucks, or trucks with fewer than five axles) and maneuvers (left, right, or through) at an intersection had less than the goal of 50 data points. An analysis was conducted for combinations with data from a minimum of 15 minor road vehicles.

Several difficulties and biases arose in the measurement of the critical gap. For example, the actual critical gap of an observed single driver cannot be measured. The actual value lies somewhere between the length of the largest gap that the driver rejected and the gap that was eventually accepted. Drivers may react differently to a lag (interval from the arrival

TABLE 3 GAP VALUES USED IN CAPACITY MANUALS

Manual	Gap				
Swedish Capacity Manual, 1977 (3)			Secondary Approach Stream		
based on 18 intersections	Speed (mi/h)	Sign	Right (sec)	Straight (sec)	Left (sec)
	31	Yield	4.8	5.2	5.3
		Stop	5.5	5.8	6.0
	43	Yield	6.0	6.0	6.2
		Stop	6.5	6.5	6.8
	56	Stop	7.2	7.0	7.5

Highway Capacity Manual, 1985 (2)	Average running speed, major road (mi/h)			
	30		55	
	Number of lanes on major road			
	2	4	2	4
Right - Stop (sec)	5.5	5.5	6.5	6.5
Right - Yield (sec)	5.0	5.0	5.5	5.5
Left - Stop (sec)	6.5	7.0	8.0	8.5
Left - Yield (sec)	6.0	6.5	7.0	7.5
Cross - Stop (sec)	6.0	6.5	7.5	8.0
Cross - Yield (sec)	5.5	6.0	6.5	7.0

Adjustments and modifications to critical gap (sec):

Right from minor street: curb radius > 50 ft or turn angle < 60 degree = -0.5 sec
Right from minor street: acceleration lane provided = -1.0 sec
All movements: population > 250,00 = -0.5 sec
Restricted sight distance = up to + 1.0 sec

TABLE 4 SELECTED INTERSECTION'S CHARACTERISTICS

Intersection			ADT Volume[a]		Percent Trucks[a]		Speed Limit[b] (mi/h)	85th %-ile Speed[b] (mi/h)
Major Road	Minor Road	City in Penn.	Major Road	Minor Road	Major Road	Minor Road		
RT 26	Central Valley Asphalt Plant	Pleasant Gap	14,000	175	15	90	45	47
RT 64	Truck Stop 64	Lamar	7,000	500	20	95	40	51
Trindle	Railroad	Harrisburg	20,000	2,000	20	25	40	40
Whitehall	Research	State College	5,900	650	2	4	45	--[c]
College	Cato	State College	11,400	1,025	4	5	45	--
Easterly	Pugh	State College	7,600	2,100	2	2	35	--

[a]Values are unadjusted count volumes obtained during the study.
[b]Major roadway approach.
[c]Approach speeds not measured.

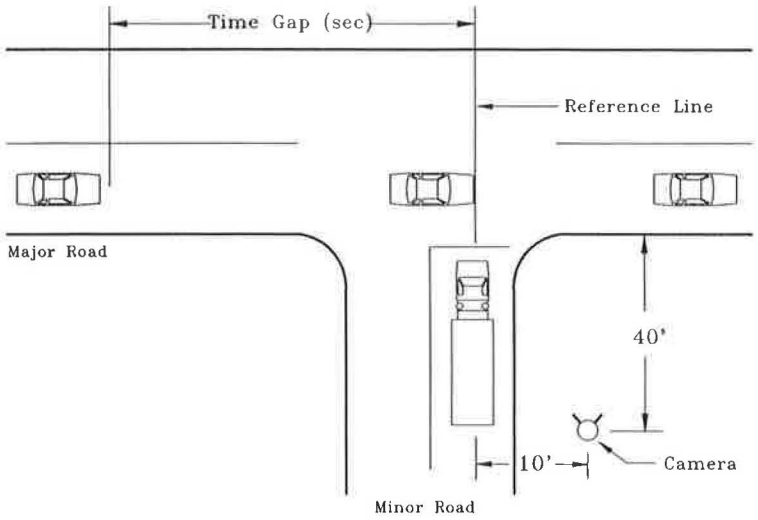

FIGURE 1 Typical setup for data collection.

of a side-street vehicle at the intersection to the arrival of the next main-street vehicle) than they do to a gap (interval from the arrival of one main-street vehicle at the intersection to the arrival of the next main-street vehicle). This problem can be avoided only by using data pertaining to lags. Unfortunately, using these data results in the loss of valuable information and may introduce bias in estimates of the critical gap/lag distribution. Identifying the start time of the lag presents other practical problems.

As a result of such difficulties, many methods of measuring the critical gap have been developed (*24*). Three methods were selected to evaluate the gap data obtained in this field study: Greenshield, Raff, and logit.

Greenshield Method

The classical Greenshield method was selected for its simplicity in performing gap-acceptance analyses. Greenshield et al. (*10*) used histograms to represent the time gaps accepted and rejected by minor-road drivers. The vertical axis represents the number of gaps accepted or rejected per time gap, which is the horizontal axis. Greenshield et al. defined the "average minimum acceptable time gap" as the minimum time gap that is accepted by more than 50 percent of the drivers. Figure 2 illustrates an example of the Greenshield method (*10*) for five-axle, right-turning trucks at the Trindle and Railroad intersection. In the example, the average minimum acceptable time gap occurs at 8.25 sec (three drivers accepted and three drivers rejected the gaps between 8.0 and 8.5 sec).

Raff Method

Raff and Hart (*11*) defined the critical lag, L, as the size lag for which the number of accepted lags shorter than L is the same as the number of rejected lags longer than L. Raff and

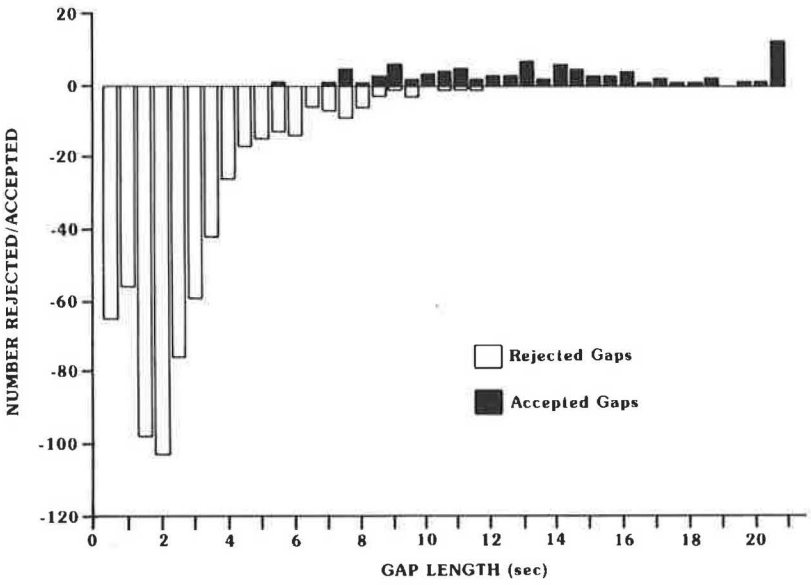

FIGURE 2 Greenshield method plot for a sample vehicle.

Hart did not include gaps in the study, arguing that one driver will only accept a gap of a particular size, but another driver may reject several gaps of the same size. More recent studies indicate that the acceptance of lags is not significantly different from the acceptance of gaps and that the lag and gap data can be combined (*12,16*). Therefore, the lag and gap data for each vehicle-maneuver combination were merged in this study. An example of the Raff graphical method is illustrated in Figure 3. The critical gap value for five-axle trucks turning right at the Trindle and Railroad intersection occurs at 8.5 sec.

Logit Method

When the dependent variable is an indicator variable (i.e., either the acceptance or rejection of a gap), the shape of the response function will frequently be curvilinear and can be approximated using a logistic function (*25*). One property of a logistic function is that it can be easily linearized. The transformation is called the logistic, or logit, transformation. The simple, dichotomous choice logistic function is

$$P = \frac{1}{1 + \exp\left[-(\beta_0 + \beta_1 X)\right]} \tag{1}$$

where

P = probability of accepting a gap,
X = variable related to the gap acceptance decision, gap length, and
β_0,β_1 = regression coefficients.

The mean response is a probability when the dependent variable is a 0 or 1 (accept or reject) indicator variable. The logistic function can be easily linearized with the following transformation:

$$P' = \log_e \frac{P}{1 - P} = \beta_0 + \beta_1 X \tag{2}$$

where P' equals the transformed probability.

A sample logistic curve and equation for five-axle trucks turning right at Trindle and Railroad are shown in Figure 4. The probability of accepting a gap is determined by solving Equation 2 for a particular time value. The time gap for a 50 percent probability can be determined by substituting 0.5 for P in Equation 2:

$$\log_e \frac{0.5}{1 - 0.5} = -9.58 + 1.12 X_{50\%}$$

$$X_{50\%} = 8.52 \text{ sec} \tag{3}$$

Fifty percent of the truck drivers at Trindle and Railroad accepted a gap of 8.52 sec, and 85 percent accepted a gap of 10.06 sec.

Findings

Tables 5 and 6 contain the results for passenger cars and trucks from these methods. In general, the methods yielded critical gap values within a 2.0-sec range.

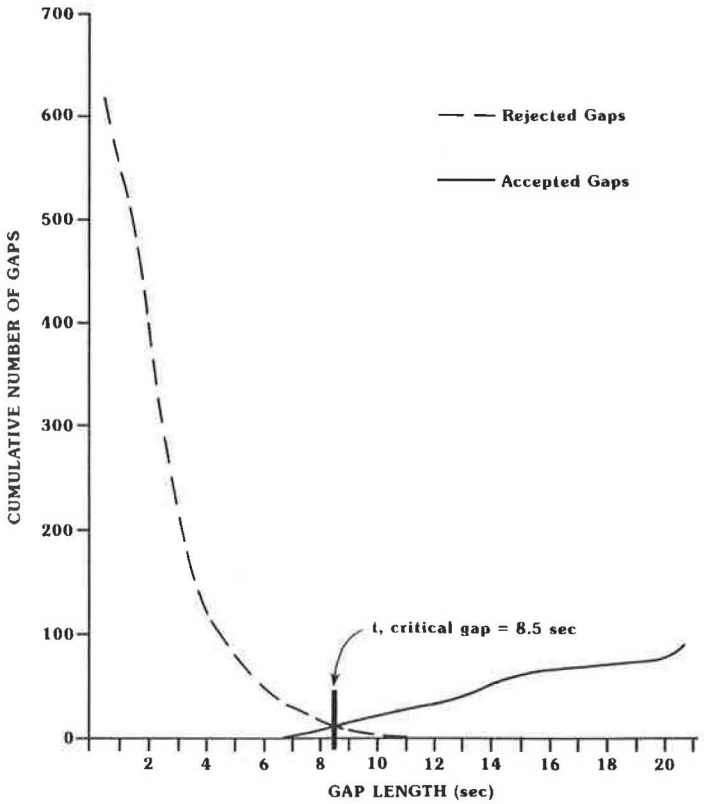

FIGURE 3 Raff method plot for a sample vehicle.

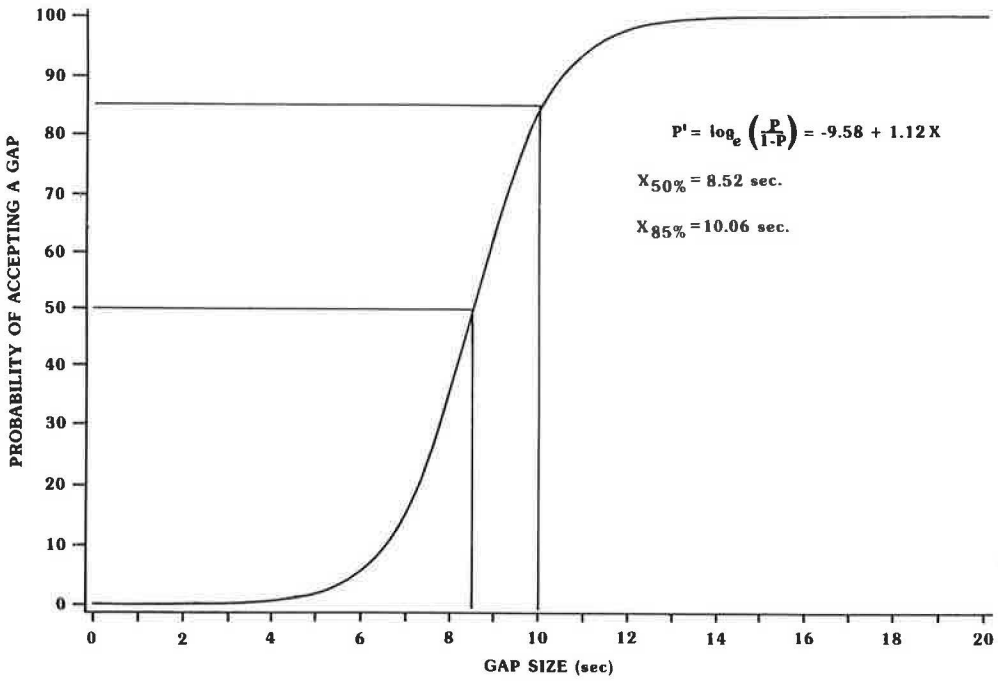

FIGURE 4 Logit method plot for a sample vehicle.

TABLE 5 FINDINGS FROM GAP ACCEPTANCE ANALYSIS FOR PASSENGER CARS

Intersection	Data Sets	Greenshield	Raff	Logit at 50 Percent	Logit at 85 Percent
LEFT-TURNING PASSENGER CARS					
Trindle & Railroad	128	6.00	6.25	6.19	7.49
Whitehall & Research	124	6.00	6.00	5.75	8.14
College & Cato	38	7.50	7.00	7.20	9.27
Easterly & NB Pugh	11	Insufficient Data*	Insufficient Data*	Insufficient Data*	Insufficient Data*
Easterly & SB Pugh	27	5.00	7.75	8.08	10.44
RIGHT-TURNING PASSENGER CARS					
Trindle & Railroad	149	6.00	5.75	6.03	7.47
Whitehall & Research	27	4.50	6.25	6.33	8.12
College & Cato	122	6.00	6.00	5.94	7.19
Easterly & NB Pugh	10	Insufficient Data*	Insufficient Data*	Insufficient Data*	Insufficient Data*
Easterly & SB Pugh	36	6.50	6.55	7.49	10.23
THROUGH PASSENGER CARS					
Easterly & NB Pugh	76	7.50	7.25	7.83	10.41
Easterly & SB Pugh	65	6.00	7.25	7.80	10.41

* Analyses were not performed for data sets containing less than 15 accepted gaps (i.e., 15 minor road vehicles).

TABLE 6 FINDINGS FROM GAP ACCEPTANCE ANALYSIS FOR TRUCKS

Intersection	Data Sets	Greenshield	Raff	Logit at 50 Percent	Logit at 85 Percent
LEFT-TURNING 5-AXLE TRUCKS					
Central Valley Asphalt	1	Insufficient Data*	Insufficient Data*	Insufficient Data*	Insufficient Data*
Truck Stop 64	5	Insufficient Data*	Insufficient Data*	Insufficient Data*	Insufficient Data*
Trindle & Railroad	16	7.25	8.25	8.27	9.84
RIGHT-TURNING 5-AXLE TRUCKS					
Central Valley Asphalt	0	Insufficient Data*	Insufficient Data*	Insufficient Data*	Insufficient Data*
Truck Stop 64	134	10.75	12.50	12.43	14.78
Trindle & Railroad	91	8.25	8.50	8.52	10.06
LEFT-TURNING LESS-THAN-5-AXLE TRUCKS					
Central Valley Asphalt	58	10.25	10.50	11.16	13.89
Truck Stop 64	2	Insufficient Data*	Insufficient Data*	Insufficient Data*	Insufficient Data*
Trindle & Railroad	8	Insufficient Data*	Insufficient Data*	Insufficient Data*	Insufficient Data*
RIGHT-TURNING LESS-THAN-5-AXLE TRUCKS					
Central Valley Asphalt	23	10.75	12.50	13.17	15.86
Truck Stop 64	7	Insufficient Data*	Insufficient Data*	Insufficient Data*	Insufficient Data*
Trindle & Railroad	26	6.25	6.50	7.25	8.87

* Analyses were not performed for data sets containing less than 15 accepted gaps (i.e., 15 minor road vehicles).

COMPARISON OF FINDINGS

Different Methods of Measuring Critical Gap

The Greenshield analyses for several of the combinations were questionable because of limited data. For example, only three of 23 trucks with fewer than five axles turning right at Central Valley Asphalt accepted gaps of less than 20 sec. The smallest gap accepted (10.75 sec) became the minimum accepted gap according to Greenshield's method because only one rejected gap occurred at the same time value. The Raff and logit methods produced higher critical gap values of 12.50 and 13.17 sec.

The Greenshield method had a critical gap more than 1.0 sec smaller than that of either the Raff or logit methods in four vehicle/maneuver/intersection combinations. Because the Greenshield method involves inspecting the gap accepted at isolated times, it does not consider the number of gaps accepted or rejected at other time gaps. Because the Raff method considers cumulative distributions and the logit method considers the probability of accepting different size gaps, the results are influenced by the several accepted gaps of more than 20 sec. Other combinations produced results within a 1.0-sec range from all three methods.

Because of these limitations in the Greenshield method and the more general acceptance of the logit method over the Raff method, the logit method results were used in the comparison with the literature findings and for the generalization of the field study findings. The logit method is also appropriate for a situation in which subjects (drivers) have a series of opportunities (gaps) in which one of two discrete choices (acceptance or rejection) is made.

Findings for Passenger Car Intersections

Because the findings at the Easterly and Pugh intersection were typically between 1.0 and 2.0 sec greater than the findings at the other passenger car intersections, investigations into potential causes were conducted. The average daily traffic (ADT) volumes (see Table 4) for Easterly and Pugh are not the lowest volumes for the four passenger car intersections. However, the speed limit for the major road was the lowest (35 mph rather than 40 or 45 mph). Additional inspection of the intersection geometrics revealed that even though the roads intersect at 90 degrees, the minor road approaches are offset by approximately 5 ft and Easterly begins curving just east of the intersection. Elimination of the Easterly and Pugh data was considered, but the findings were included to illustrate the influence that roadway and traffic characteristics have on gap acceptance. However, the results from this intersection must be used with caution because of these influences.

Findings from the logit method at the 50 percent gap-acceptance level for right-turning passenger cars at the Trindle and Railroad, Whitehall and Research, and College and Cato intersections were within 0.5 sec (5.94 sec to 6.33 sec). Findings for left-turning passenger cars at the Trindle and Railroad intersection and Whitehall and Research intersection (each included data for more than 120 minor road vehicles) were also within 0.5 sec (5.75 sec to 6.19 sec) for the logit method 50 percent gap acceptance. After inspection of the results, the gap-acceptance values were generalized as 6.5 sec for both right and left turns.

The logit method 85 percent probability was generalized as 8.25 sec for right and left turns. All combinations except those at the College and Cato intersection, which had a small data set, had 85 percent probability gap-acceptance values of less than 8.25 sec.

The 50 percent probability of accepting a gap for passenger car crossing maneuvers, which were measured only at the Easterly and Pugh intersection and therefore should be used with caution, was 7.8 sec. The 85 percent probability for all movements at Easterly and Pugh was less than 10.5 sec.

Findings for Truck Intersections

The critical gap accepted findings at the Central Valley Asphalt plant appear large when compared with those of other high-volume intersections. The Central Valley Asphalt intersection has unique qualities that may explain the differences. The intersection is 2,000 ft north of a signalized intersection. Drivers turning right noticeably waited for the end of a platoon that formed at the signal. Also, the vehicles leaving the plant were fully loaded, three- or four-axle aggregate or asphalt trucks with low acceleration capabilities.

The ADT on the major road at Truck Stop 64 is 7,000. Very large gaps were available at this low volume, and several truck drivers waited for these large gaps (defined in this study as greater than 20 sec). Almost all of the trucks turning right out of Truck Stop 64 entered one of the Interstate entrance ramps located 500 ft and 1,000 ft from the truck stop exit. Truck drivers may have accepted larger gaps than usual because they would be accelerating for only a short distance before slowing to make the turn onto an entrance ramp.

The truck drivers at the Trindle and Railroad intersection were pressured to accept smaller gaps than those accepted at the other sites. The frequency of gaps greater than 20 sec was small, and long queues occasionally formed on the minor road behind the truck. The five-axle trucks typically encroached into the far lane of the major road to complete the turn maneuver.

Findings at the 50 percent gap-acceptance level for left- and right-turning five-axle trucks at the high-volume Trindle and Railroad intersection were similar. Left-turning trucks accepted an 8.27-sec gap, whereas right-turning trucks accepted an 8.52-sec gap.

Right-turning trucks with fewer than five axles at the Trindle and Railroad intersection accepted a 7.25-sec gap, which is more than 1.0 sec less than the gap accepted by larger trucks. Left-turning trucks with fewer than five axles, loaded with asphalt and aggregate at Central Valley Asphalt, accepted an 11.16-sec gap.

The 85 percent probability of accepting a gap at the high-volume Trindle and Railroad intersection was generalized as 10.0 sec. The turning trucks had values near (10.06) or less (9.84 and 8.87 sec).

Comparison of Findings with the Literature

The study most similar in data collection and analysis procedures to this field study was performed by Solberg and Oppenlander (*16*). Their results for left and right turns (7.82 sec and 7.36 sec) were approximately 1.0 sec greater than the results listed in Table 4. Solberg and Oppenlander's intersections had an average major road volume of 330 to 590 vph, whereas the passenger car intersections in this study had major road volumes of 580 to 2,000 vph. Solberg and Oppenlander's result for through movement (7.18 sec) was 0.6 sec less than that found at Easterly and Pugh (7.80 sec), but data from Easterly and Pugh were influenced by the geometry of the intersection.

Radwan et al. (*13*) conducted field studies on minor-road drivers crossing or merging with four-lane, divided major road traffic at stop-controlled intersections. As expected, the ADT on the four-lane roads in the Radwan et al. study was greater than the ADT in this study. Also, their findings were for vehicles crossing or turning onto a four-lane divided highway rather than a two-lane highway. However, the number of minor road vehicle data sets used by Radwan et al. was comparable with the number used in this study, and the study methodologies were similar. Therefore, some comparisons between the findings of the two studies were reasonable. The gap accepted by left-turning vehicles in the study by Radwan et al. (6.32 sec) was similar to the gaps accepted in this study (5.75 to 6.19 sec). Right-turning vehicles accepted a slightly larger gap in the study by Radwan et al. (6.73 sec) than in this study (5.94 to 6.33 sec).

Radwan et al. combined the truck data for all maneuvers (right, through, and left) because the number of data points was small: 34, 75, and 43, respectively. This study's findings at the high-volume Trindle and Railroad intersection for five-axle trucks (8.27 and 8.52 sec) were similar to Radwan's findings for all truck maneuvers (8.4 sec). The similar methodologies of the two studies and the results of Radwan et al. support the findings in this study.

SUMMARY AND RECOMMENDATIONS

Gap acceptance is the act of safely joining or crossing the major road traffic stream within the length of the accepted gap. Gap-acceptance data are used in designing intersections and in evaluating operations at intersections. Truck drivers' gap-acceptance values should be considered at intersections with significant truck traffic.

Passenger car drivers' 50 percent probability of accepting a gap was generalized as 6.5 sec for both left and right turns and as 8.25 sec for the 85 percent probability of accepting a gap at a moderate- to high-volume intersection. A 10.5-sec gap represents the 85 percent probability of accepting a gap at an intersection where the accepted gaps were influenced by low volume and the intersection geometry. Truck drivers'

50 percent probability of accepting a gap was generalized as 8.5 sec. In general, at a high-volume location, 85 percent of the truck drivers accepted a 10.0 sec gap; at a low-volume location, 15.0 sec was the accepted gap value.

The data collection and reduction procedures were tedious and required several hours to film the operations of the intersections and view the videotapes to acquire the needed gap times. Alternative procedures for obtaining the gap data should be investigated.

Some of the critical gap values determined at several of the intersections were influenced by geometric or traffic characteristics, such as offset approaches and low traffic volumes. Additional research is necessary to determine the extent to which different characteristics (e.g., intersection configuration, rural versus urban location, and high versus low volume) affect gap-acceptance values. These findings could be incorporated into a gap-acceptance procedure adopted by an agency.

ACKNOWLEDGMENT

Portions of the work reported in this paper were sponsored by FHWA, U.S. Department of Transportation.

REFERENCES

1. D. W. Harwood, J. M. Mason, Jr., W. D. Glauz, B. T. Kulakowski, and K. Fitzpatrick. *Truck Characteristics for Use in Highway Design and Operation, Volume II: Appendices*. Report FHWA-RD-89-227. FHWA, U.S. Department of Transportation, 1989.
2. *Special Report 209: Highway Capacity Manual*. TRB, National Research Council, Washington, D.C., 1985.
3. A. Hansson, R. C. Blumenthal, J. A. Hutter, and A. A. Carter. Swedish Capacity Manual, Part 2, Capacity of Unsignalized Intersections. In *Transportation Research Record 667*, TRB, National Research Council, Washington, D.C., 1978, pp. 4–7.
4. D. E. Blumenfeld and G. H. Weiss. The Effects of Gap Acceptance Criteria on Merging Delay and Capacity at an Uncontrolled Junction. *Traffic Engineering and Control*, Vol. 20, No. 1, Jan. 1979, pp. 16–20.
5. L. G. Neudorff. Gap-Based Criteria for Traffic Signal Warrants. *ITE Compendium of Technical Papers*, Washington, D.C., 1984.
6. P. G. Michalopulos, J. O'Connor, and S. M. Novoa. Estimation of Left-Turn Saturation Flows. In *Transportation Research Record 667*, TRB, National Research Council, Washington, D.C., 1978, pp. 35–41.
7. K. R. Agent and R. C. Deen. Warrants for Left-Turn Signal Phasing. In *Transportation Research Record 737*, TRB, National Research Council, Washington, D.C., 1979, pp. 1–10.
8. K. R. Agent. Warrants for Left-Turn Lanes. *Transportation Quarterly*, Vol. 37, No. 1, 1983, pp. 99–114.
9. H. Lin and R. B. Machamehl. Developmental Study of Implementation Guidelines for Left-Turn Treatments. In *Transportation Research Record 905*, TRB, National Research Council, Washington, D.C., 1983, pp. 96–104.
10. B. D. Greenshield, D. Schapiro, and E. L. Ericksen. *Traffic Performance at Urban Intersections*. Technical Report No. 1. Yale Bureau of Highway Traffic Engineering, Eno Foundation for Highway Traffic Control, Westport, Conn., 1947.
11. M. S. Raff and J. W. Hart. *A Volume Warrant for Urban Stop Signs*. The Eno Foundation for Highway Traffic Control, Westport, Conn., 1950.
12. A. E. Radwan, K. C. Sinha, and H. L. Michael. *Development and Use of a Computer Simulation Model for the Evaluation of Design and Control Alternatives for Intersections of Minor Roads with Multi-lane Rural Highways: Selection of the Simulation Model*. Report FHWA-IN-79-8. FHWA, U.S. Department of Transportation, July 1979.
13. A. E. Radwan, K. C. Sinha, and H. L. Michael. *Development and Use of a Computer Simulation Model for the Evaluation of Design and Control Alternatives for Intersections of Minor Roads with Multi-lane Rural Highways: Field Studies and Model Validation*. Report FHWA-IN-79-9. FHWA, U.S. Department of Transportation, 1979.
14. A. Polus. Gap Acceptance Characteristics at Unsignalized Urban Intersections. *Traffic Engineering and Control*, Vol. 24, No. 5, May 1983, pp. 255–258.
15. O. Adebisi and G. N. Sama. Influence of Stopped Delay on Driver Gap Acceptance Behavior. *Journal of Transportation Engineering*, Vol. 115, No. 3, May 1989.
16. P. Solberg and J. C. Oppenlander. Lag and Gap Acceptance at Stop-Controlled Intersections. In *Highway Research Record 118*, HRB, National Research Council, Washington, D.C., 1966, pp. 48–67.
17. D. F. Cooper and M. R. C. McDowell. Police Effects on Accident Risks at T-Junctions. *Traffic Engineering and Control*, Vol. 18, No. 10, Oct. 1977, pp. 486–491.
18. D. F. Cooper, W. Smith, and V. Broadie. Traffic Studies at T-Junctions, 1. The Effect of Approach Speed on Merging Gap Acceptance. *Traffic Engineering and Control*, Vol. 17, No. 6, June 1976, pp. 256–257.
19. J. Darzentas, V. Holms, and M. R. C. McDowell. Driver Behavior at T-Junction in Daylight and Darkness. *Traffic Engineering and Control*, Vol. 21, No. 4, April 1980, pp. 186–189.
20. J. Wennell and D. F. Cooper. Vehicle and Driver Effects on Junction Gap Acceptance. *Traffic Engineering and Control*, Vol. 22, No. 12, Dec. 1981, pp. 628–632.
21. H. H. Bissell. *Traffic Gap Acceptance at Stop Signs*. Institute of Transportation and Traffic Engineering, University of California, Berkeley, 1960.
22. K. C. Sinha and W. W. Tomiak. Section Gap Acceptance Phenomenon at Stop-Controlled Intersections. *Traffic Engineering*, April 1971.
23. R. Ashworth and C. G. Bottom. Some Observations of Driver Gap-Acceptance Behavior at a Priority Intersection. *Transportation Engineering*, Vol. 18, No. 2, Dec. 1977, pp. 569–571.
24. R. H. Hewitt. A Comparison Between Some Methods of Measuring Critical Gap. *Traffic Engineering and Control*, Vol. 26, No. 1, Jan. 1985, pp. 13–22.
25. J. Neter, W. Wasserman, and M. Kutner. *Applied Linear Statistical Models*, 2nd ed. Irwin, Homewood, Ill., 1985.

Publication of this paper sponsored by Committee on Operational Effects of Geometrics.

Some Traffic Parameters for the Evaluation of the Single-Point Diamond Interchange

MARK JAMES POPPE, A. ESSAM RADWAN, AND JUDSON S. MATTHIAS

The single-point diamond interchange (SPDI) has received a great deal of attention in recent years. Various analyses have been performed to evaluate the operation of the SPDI, but little field data has been collected to substantiate the input parameters used in these analyses. Research was performed to determine the saturation flow rate for the through and left-turn movements at the SPDI, and to determine the lost time per phase for the SPDI. Data were collected on 10 approaches at three interchanges in the Phoenix metropolitan area. More than 3,500 headways were measured. Mean saturation flow rates of approximately 2,000 passenger cars per hour green per lane were observed for both the through and the left-turn movements at the three SPDIs studied. Mean start-up lost times between 1.5 and 2 sec per phase were measured. Clearance lost time tended to be approximately 2.5 to 3 sec per phase less than the length of the clearance interval. Total lost time varied from 20 to 24 sec per cycle. The data indicate that the large turning radii found at the SPDI tend to cause the left-turn movement to operate much like a through movement in terms of capacity. The study also indicates that long clearance intervals translate directly into increased lost time per cycle.

Recent innovations in the design and operation of signalized diamond interchanges have created some uncertainty and controversy regarding the selection of the most appropriate interchange design. This uncertainty is mostly due to the advent of the diamond interchange configuration first introduced (by Greiner Engineering) in the early 1970s. This configuration has come to be known by a variety of names: the urban interchange, the single-signal interchange, the single-point urban interchange, and the single-point diamond interchange. The name used in this research is single-point diamond interchange (SPDI).

The SPDI (Figure 1) has received a great deal of attention in recent years (*1–3*) as a workable and even superior alternative to the conventional diamond interchange (CDI, Figure 1). The operational and geometric characteristics of the two interchange forms are essentially identical with respect to the freeway. The two forms differ considerably, however, with respect to operation on the cross street. The CDI is characterized by two closely spaced intersections, three-phase control at each intersection, and tight turning radii. The SPDI operates as one large three-phase controlled intersection with large turning radii. These major differences between the two configurations affect operation of the interchange on the cross street. Other differences with respect to geometrics, bridge design, right-of-way requirements, construction costs, and flexibility for future reconstruction further cloud the decision as to which design is the most appropriate for any given situation (*4*). The greatest confusion, however, lies in the area of the relative operational efficiency of the two competing configurations.

M. J. Poppe, Lee Engineering, 2701 E. Camelback Ave., Phoenix, Ariz. 85016. A. E. Radwan, Department of Civil and Environmental Engineering, University of Central Florida, Orlando, Fla. 32816-0450. J. S. Matthias, Department of Civil Engineering, Arizona State University, Tempe, Ariz. 85287-5306.

STUDY SCOPE AND OBJECTIVES

The Problem

The following statements provide some indication as to the range of opinions regarding the relative merits of the two configurations. Brown and Walters (*1*) write:

> By reducing the number of conflicts, and thus reducing the number of phases, the single-signal interchange can offer at least 10% more capacity than a diamond interchange. The advantage can be as much as 50% in cases where the left-turn volumes on the off-ramps are balanced and relatively high compared to the approach volumes on the minor street.

Leisch et al. (*4*) state:

> The analyses presented make it evident that applications are limited for the single-point diamond. Generally speaking, the compressed diamond is less costly, has similar right-of-way requirements, and is more efficient.

Warner (*5*) finds that

> the urban interchange is more efficient in distributing traffic between the freeway and the arterial, and vice-versa, whereas the diamond interchange is more efficient for through traffic on the arterial under the conditions studied.

A great deal of the confusion and lack of consensus among traffic engineers concerning the operational efficiency of the SPDI is due to the fact that very little is known about the operational characteristics of the SPDI. Because the SPDI operates as a single intersection, the methodology found in Chapter 9 of the *Highway Capacity Manual* (*6*) has been applied to evaluate the operation of the SPDI.

The two characteristics of the SPDI that distinguish it from the high type intersection are the large turning radii for the

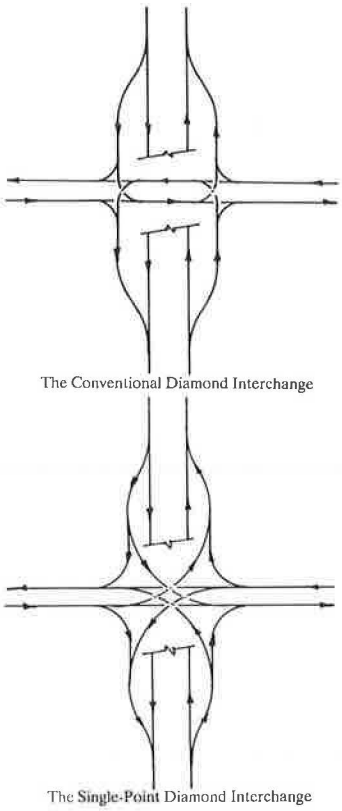

FIGURE 1 Interchange types.

left-turn movements and the large distance between stop bars. These two characteristics should be acknowledged in the analysis.

The large turning radii provided for the left-turn movements constitute one of the positive aspects of the SPDI configuration. However, there are currently very little data that quantify this advantage. Do the large turning radii provided by the SPDI configuration substantially affect the saturation flow rate for the left-turn movements?

The large land area required for the SPDI (and the long clearance intervals required as a consequence of the large area) is identified as one of the negative aspects of the SPDI. The hypothesis is that the lost time is directly proportional to the length of the clearance interval. There are no data, however, that quantify the lost time associated with long clearance intervals like those found at the SPDI. How much lost time per phase is generated by the long clearance intervals required by the SPDI?

Research Objectives

The focus of this research is the collection of data on various key parameters for the analysis of the SPDI. Current techniques for the operational analysis of the SPDI are based on the operational characteristics of the typical high type signalized intersection. The traffic parameters used in these analyses are based on data collected at typical high type intersections.

The primary objectives of the research are as follows:

1. To determine the saturation flow rates for the through and left-turn movements at the SPDI, and
2. To determine the lost time per phase for the SPDI.

Completion of the first objective will provide information that may be used to evaluate the influence of the SPDI's large turning radii. Completion of the second objective will provide information that may be used to evaluate the influence of the SPDI's long clearance intervals.

BACKGROUND INFORMATION AND LITERATURE REVIEW

Interrupted Traffic Flow Theory

The number of vehicles that may pass through a signalized intersection during one green indication is controlled by two factors: (a) the effective length of the green indication, and (b) the rate at which vehicles pass through the intersection, or the flow rate. The operation of a traffic signal also entails the periodic stoppage of traffic, at which time a queue of vehicles is formed. Therefore, the dynamics of starting a standing queue and stopping a steady flow of vehicles must also be considered.

When a traffic signal changes to green, time will elapse before the driver reacts and accelerates the vehicle into the intersection. This elapsed time, from beginning of green to the time the first queued vehicle enters the intersection, is called the first headway (h_1), measured in seconds per vehicle. The second headway (h_2) is elapsed time between entry of the first vehicle into the intersection and the entry of the second vehicle. The second driver must also react to the green indication and accelerate into the intersection; however, part of this reaction and acceleration time will occur during the first headway. Therefore, the second headway will be less than the first. The third, fourth, and fifth vehicles proceed through the intersection in a similar fashion, each with a slightly shorter headway than the previous vehicle. At some vehicle position, the headway between vehicles stabilizes at some relatively constant headway (h).

The saturation flow rate is defined as the rate of flow per lane at which vehicles pass through the intersection under the condition of stable headways (*6*, p. 1–8). The saturation flow rate is computed as

$$s = 3600/h, \tag{1}$$

where s is the saturation flow rate, in vehicles per hour green per lane (vphgpl), and h is the saturation headway (sec).

The start-up lost time associated with the first vehicle (l_{s1}) is computed as

$$l_{s1} = h_1 - h \tag{2}$$

where l_{s1} is the first vehicle start-up lost time (sec), and h_1 is the first vehicle headway (sec).

If the nth + 1 vehicle is the first in the queue with a headway equal to h, then the total start-up lost time (l_s) is computed as

$$l_s = \Sigma_{i=1 \text{ to } n} (h_i - h) \tag{3}$$

The start-up lost time (l_s) must be subtracted from the green time in order to account for the dynamics of starting a standing queue.

The dynamics of stopping a steady stream of vehicles is another source of lost time at signalized intersections. When the movement of vehicles on a particular approach is terminated, some time must be provided to allow all vehicles to safely clear the intersection. Immediately following a green indication, some combination of yellow and all-red indication is provided as a clearance interval. Therefore, the time actually allocated to the movement is the green time (G) and the clearance interval ($Y + R$). Experience attests to the fact that a portion of the clearance interval is used by motorists. This portion of the clearance interval (the time from beginning of yellow to the time the last vehicle enters the intersection) is, essentially, an extension of the green time. The clearance lost time (l_c) is the portion of the clearance interval that is not used by the motorists. It is measured as the time elapsed from when the last vehicle entered the intersection to the end of the clearance interval (i.e., the beginning of the green indication for the next conflicting movement).

The number of vehicles that may pass through a signalized intersection during one green indication is controlled by two factors: (a) the effective length of the green indication, and (b) the saturation flow rate. However, as discussed, the effective green time is not necessarily the length of the green indication. The effective green time available to any given movement is the length of the green indication (G) plus the length of the clearance interval ($Y + R$) minus the start-up and clearance lost times.

With respect to this research, two questions must be answered through a review of the literature:

1. What are the key factors that should be analyzed in establishing values for saturation flow rates and lost times per phase at signalized facilities?
2. What is the best method for the collection of field data on the parameters of saturation flow rate and lost time at signalized facilities?

Saturation Flow Rate

The saturation flow rate at a signalized intersection is related to a number of geometric, traffic, and signalization conditions. The *Highway Capacity Manual* established a default value of 1,800 passenger cars per hour green per lane (pcphgpl) as the ideal or maximum rate of flow for vehicles passing through a signalized intersection (*6*, pp. 2–27). This value is called the ideal saturation flow rate because it represents the rate of flow expected under ideal traffic, geometric, and operational conditions. This value of 1,800 pcphgpl is based on research by a number of individuals and the observation of many intersections throughout the United States. It is an average value, not necessarily an absolute maximum.

The *Highway Capacity Manual* (*6*) notes that, irrespective of improved vehicle design or driver response, headways have remained relatively constant over time. Research performed by Johnsen and Matthias (*7*), however, indicates possible regional variations in saturation flow rates.

A number of factors affect the saturation flow rate at a signalized intersection. Tables and equations are given in the *Highway Capacity Manual* (*6*) to determine the value for each factor given the prevailing conditions. The *Highway Capacity Manual* identifies eight factors that influence the saturation flow rates at signalized intersections:

- Lane width,
- Vehicle type,
- Grade,
- Parking conditions,
- Bus blockage,
- Area type,
- Right turn, and
- Left turn.

The left-turn factor (f_{lt}) is of particular importance to this research. All existing SPDIs in the Phoenix metropolitan area operate under protected left-turn phasing, with double exclusive left-turn lanes on all approaches. The *Highway Capacity Manual* (*6*) adjustment factor for double exclusive left-turn lanes under protected phasing is 0.92. This adjustment factor converts to a saturation flow rate of 1,656 vphgpl. The *Highway Capacity Manual* adjustment factor for single exclusive left-turn lanes under protected phasing is 0.95, or a saturation flow rate of 1,710 vphgpl.

This smaller f_{lt} for dual left-turn approaches is partially attributed to research by Capelle and Pinnell (*8*) on the operational characteristics of the CDI. Capelle and Pinnell concluded from the data that the dual left-turn configuration reduced the carrying capacity of the inside lane. They attributed this reduction to a tendency by motorists in both lanes to stagger their position in making the double left-turn movement.

Lost Time

The lost time at signalized intersections is related to a number of geometric, traffic, and signalization conditions. The *Highway Capacity Manual* (*6*) establishes a default value of 4 sec lost time per phase, 2 sec each for start-up and clearance interval lost times. The *Highway Capacity Manual* does not provide a procedure for calculating the lost time as a function of the factors that may influence lost time at signalized intersections.

Agent and Crabtree (*9*) identified a number of factors that influence lost time at signalized intersections:

- City size,
- Location in city,
- Cycle length and length of green time,
- Speed limit,
- Gradient,
- Vehicle type and turning maneuver,
- Turning radius,
- Length of yellow, and
- Lane type.

Agent and Crabtree (*9*) observed a strong relationship between start-up lost time and cycle length. Start-up lost time tended to be lower for longer cycle lengths. They also observed lower start-up lost times for right-turn maneuvers over

left-turn maneuvers. This is attributed more to the shorter saturation flow headways for the left-turn movement than to any actual advantage for the right-turn movement. An investigation of the effect of turning radius on the start-up lost time for the right-turn maneuver indicates lost time is less for shorter turning radii. Again, this is more a function of the saturation flow headways than any difference in the start-up time headways.

The effect of shorter saturation flow headways on start-up lost time is illustrated using the data collected by Capelle and Pinnell (*8*) as shown in Table 1. Capelle and Pinnell identified the first two vehicles in the queue as those contributing to the total start-up lost time at a signalized intersection. The starting delay values shown in Table 1 are the sum of the headways for the first two vehicles. The starting delay defined by Capelle and Pinnell should not be confused with the start-up lost time previously defined. The starting delay is actually the time required for the first two vehicles to enter the intersection and should, more properly, be called the start-up time.

The start-up lost time is calculated as

$$l_s = h_1 + h_2 - 2h \quad (4)$$

where

l_s = total start-up lost time (sec),
h_2 = second vehicle headway (sec), and
h = saturation flow headway (sec).

The inside and outside lanes, for two abreast type turns, have identical start-up times. However, the smaller saturation headway value for the outside lane increases the amount of lost time calculated for the outside lane. This relationship between start-up lost time and saturation flow rate should not be taken lightly. The general (though not universal) relationship exhibited here is that the higher the saturation flow rate the larger the start-up lost time.

Data Collection

The main issue with regard to data collection for this research was the selection of an appropriate intersection screen line and vehicle reference point for measuring time headways. The *Highway Capacity Manual* describes a procedure for the direct measurement of prevailing saturation flow rates (*6, pp. 9–74*). The selection of the reference screen line is largely left to the observer: "Choose a reference point, usually the crosswalk or stop line." The prescribed vehicle reference is the rear axle.

The curb line (extension of the cross street face of curb) is the screen line recommended by Berry (*10*), particularly when measuring headways for calculating lost time. Berry also recommends using the front of the vehicles, rather than the rear axle, as the vehicle reference point.

Agent and Crabtree (*11*) used the rear wheels of the vehicle as the vehicle reference point and the stop bar as the roadway screen line. It was believed this method would provide the best and most consistent results because of cross road offsets and angled intersections.

METHOD OF STUDY

For this study, each movement was classified by number, as shown in Figure 2. This classification of movements is in basic conformance with the classification of movements used in PASSER III-88 (*12*) for the numbering of movements at the CDI. PASSER III is a macroscopic computer model used to evaluate and optimize signal timing at CDIs. Movements 5 and 12, not shown in Figure 2, are the ramp or frontage road through movements in PASSER III. This particular SPDI configuration does not provide for these movements. PASSER III also classifies movements 15, 16, 17, and 18, which are the interior movements at the CDI. These movements are not applicable to the SPDI.

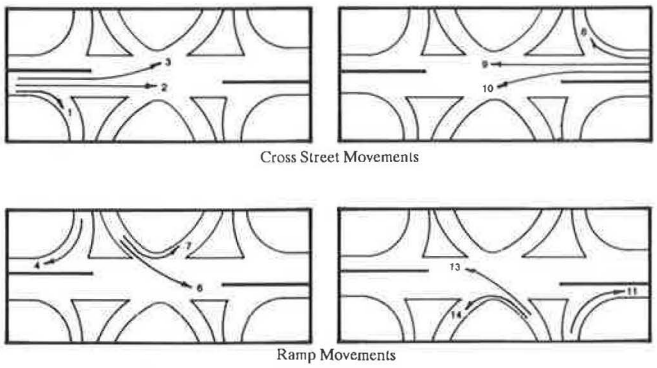

FIGURE 2 Classification of movements.

TABLE 1 CAPELLE AND PINNELL RESULTS FOR START-UP LOST TIME

Type of Movement	Starting Delay:h_1+h_2 (sec)	Average Headway:h (sec)	Start-up Lost Time (sec)
Through	5.8	2.1	1.6
Single left turn	5.8	2.1	1.6
Single right turn	5.8	2.1	1.6
Two-abreast turns:			
Inside lane	6.5	2.4	1.7
Outside lane	6.5	2.2	2.1

Note: Start-up lost time was not a reported parameter in the original source, but calculated by the authors of this research for illustrative purposes.

Site Selection

Five SPDI locations in the Phoenix metropolitan area could be used for data collection at this time:

- Hohokam Expressway (SR-143) and University Drive,
- Squaw Peak Parkway (SR-51) and Indian School Road,
- Squaw Peak Parkway and McDowell Road,
- Papago Inner Loop (I-10) and 7th Street, and
- Papago Inner Loop and 7th Avenue.

Based on the field observations made at the five sites the following three interchanges were selected for this study:

- Interchange A: Hohokam and University Drive (Figure 3),
- Interchange B: Squaw Peak and Indian School Road (Figure 4), and
- Interchange C: Papago Inner Loop and 7th Avenue (Figure 5).

Three criteria were used to select these three interchanges and the movements to be observed at each interchange. The first and most important criterion was length of queue. Long queues are important for collection of valid saturation flow rates and the evaluation of clearance lost time. The second criterion was variety of roadway geometry and signalization. The interchanges at 7th Street and 7th Avenue are nearly

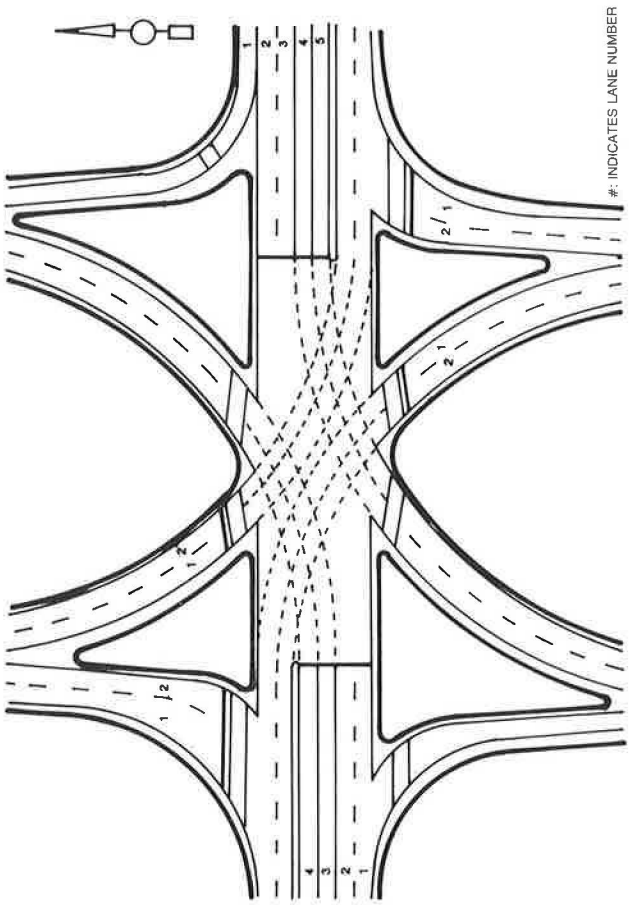

FIGURE 3 Interchange A layout.

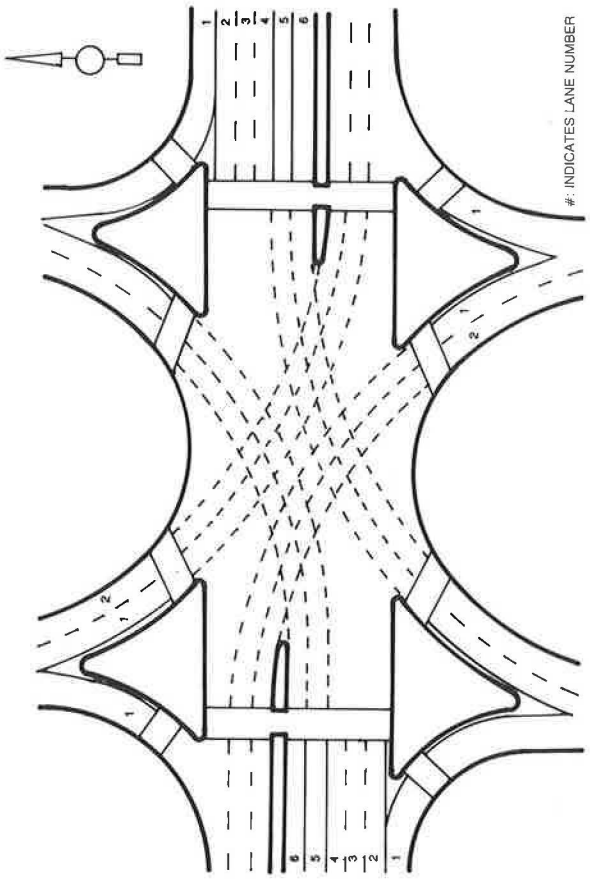

FIGURE 4 Interchange B layout.

identical with respect to geometry and signalization; therefore, the location with the most favorable traffic conditions was selected. The interchanges at Indian School Road and at McDowell Road are also quite similar; therefore, only one of these two interchanges was selected. The third criterion used to select the most appropriate interchanges for this study was location of adjacent intersections and the influence they could have on traffic flow through the interchange. Four movements were selected at Interchange A for data collection: movements 2, 6, 10, and 13. Three movements were selected at Interchange B: movements 2, 10, and 13. Three movements were selected at Interchange C: movements 3, 6, and 9.

Geometric, Signalization, and Traffic Conditions

Information concerning geometric and signalization conditions at the three sites was obtained from the Arizona Department of Transportation (ADOT) and the city of Phoenix. Geometric conditions at the three interchanges were determined by means of as-built drawings and field inspections. The geometric conditions recorded include the number of lanes per movement, lane widths, approach grades, lane configuration, length of turning lane storage bays, left-turn movement radii, parking conditions, stop line separation, and distance to adjacent signalized intersections. Stop line separation is defined as the distance between the stop line and the point

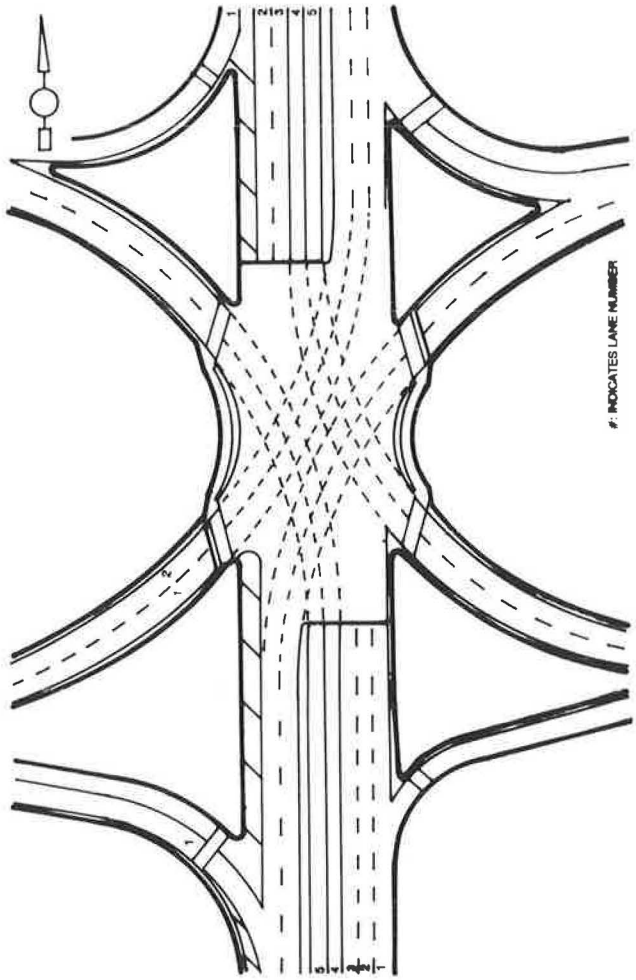

FIGURE 5 Interchange C layout.

beyond the path of conflicting movements. A summary of the geometric conditions for the three interchanges is presented in Table 2. Signalization information was obtained from ADOT documentation and through interviews with ADOT and city of Phoenix personnel. Signal timing was verified in the field using a stop watch. The signalization information recorded includes the cycle length, maximum and minimum green times, yellow and all red clearance interval times, type of operation (actuated or pretimed), pedestrian push-button actuation, minimum pedestrian green times, and the phasing plan. The phasing patterns used at each interchange are shown in Figure 6. Traffic conditions at the three interchanges were evaluated by means of field inspection. The traffic conditions recorded include a qualitative evaluation of the volume for each movement, the length of the queue for each movement with heavy traffic volumes, and the extent to which drivers tend to stop with the front wheels of the vehicle behind the stop line.

Data Collection

Data collection for this research involved the direct measurement of headways relative to changes in the signal head indication. It was important to measure headways relative to the changes in signal head indications in order to evaluate starting and clearance lost times. Data were collected on a per-lane basis for the ten lane groups studied. For this study, the rear wheels of the vehicle were considered the vehicle reference point and the stop line was the roadway screen line. Given the unusual geometry of the SPDI, it was believed that this method would provide the best and most consistent results.

The data collection method selected for this research involved the use of a portable computer and a Turbo Basic program. The computer's real time internal clock measured elapsed time. Keys were programmed to record, when pressed by an observer, the times for changes in signal aspect and the times as each vehicle crossed the stop line. Two observers were used in the data collection process, both working from the same keyboard. The first observer recorded the changes in signal aspect. The second observer recorded the passage of vehicles across the stop line. The second observer was also responsible for identifying the last vehicle in queue at the time the signal changed to green.

ANALYSIS

The first step in data reduction was to determine how average headways varied with position in queue. All data for a particular lane were pooled into a single spreadsheet. All vehicles not in queue at the onset of green were eliminated from the data base. All cycles with oversized vehicles were eliminated from this portion of the data reduction. A mean value for each position in queue was then calculated. A series of plots, like the one shown in Figure 7, were generated to determine the number of queued vehicles that must be counted before the beginning of saturation flow. The plots indicate that headways become fairly constant after the third vehicle. Therefore, the fourth through the last queued vehicle were those used to calculate the mean saturation flow rate. This is consistent with the procedure outlined in the *Highway Capacity Manual* (*6*) for the measurement of prevailing saturation flow rates.

Saturation Flow Rate

The data were analyzed on a per-lane basis in order to evaluate any difference between lanes on a multilane approach. The cross street through movement data do seem to indicate that saturation flow rates tend to be higher for the inside lanes and lower for the curb lane. The data are mixed with regard to changes in saturation flow rates with changes in lane position for the left-turn movements. Five of the seven left-turn lane groups examined recorded higher saturation flow rates in the inside lane. There does not appear to be a strong relationship between lane position and saturation flow rate for the left-turn movements at the SPDI.

A mean saturation headway value was calculated for each lane group studied. A sample standard deviation for the mean saturation headway was also calculated. Only those vehicles in queue at the onset of green were used in the analysis. All oversized vehicles were eliminated from the analysis. The results are shown in Table 3. A mean and a range for the saturation flow rate were calculated using Equation 1. The range is based on the values that represent a 95-percent con-

TABLE 2 INTERCHANGE GEOMETRY

Movement Number	Turning Radius (ft)	Stop Line Separation (ft)	Number of Lanes	Lane Number	Lane Width (ft)
Interchange A:					
2	---a	260	2	1	12
				2	12
6	270	190	2	1	12
				2	12
10	280	165	2	4	12
				5	12
13	270	190	2	1	12
				2	12
Interchange B:					
2	---a	310	3	2	11
				3	11
				4	11
10	280	235	2	5	10
				6	12
13	280	235	2	1	12
				2	12
Interchange C:					
3	310	200	2	5	11
				6	11
6	360	210	2	1	14
				2	14
9	---a	240	2	2	11
				3	11

a. Not applicable

fidence interval for the mean headway. The results of this calculation are shown in Table 4.

The mean saturation flow rate for the combined movements 6 and 13 at Interchange A is approximately 2,050 pcphgpl. The left-turn radii for movements 6 and 13 at Interchange A are 270 ft. The mean saturation flow rate recorded for movement 13 at Interchange B is also approximately 2,050 pcphgpl. The radius for this movement is 280 ft. Interchange C produced a substantially higher saturation flow rate for the ramp to cross street left-turn movement. A saturation flow rate of approximately 2,170 pcphgpl was recorded at Interchange C for movement 6. The left-turn radius for movement 6 at Interchange C is 360 ft. The data for this movement were collected under generally saturated conditions. The data for the ramp to cross street left-turn maneuver at Interchange C were collected under slightly different conditions than that found at the other two interchanges. Due to the closure of the west approach ramps at Interchange C there was no side friction with the opposing left-turn movement.

The saturation flow rate for the cross street to ramp left-turn movement 10 at Interchange A is approximately 2,025 pcphgpl. The turning radius for movement 10 at Interchange A is 280 ft. The saturation flow rate for movement 10 at Interchange B is substantially lower at 1,835 pcphgpl. But the combination of a small sample size and a large sample standard deviation raises a question as to the statistical significance of this mean value. This is reflected in the large range calculated for the mean saturation flow rate for movement 10 at Interchange B. The turning radius for this movement is also 280 ft. The saturation flow rate for the cross street left-turn movement at Interchange C is the highest flow rate recorded for any lane group in this study. The saturation flow rate for movement 3 at Interchange C is 2,225 pcphgpl. Virtually every cycle observed for this movement was operating under saturated conditions. The left-turn radius for movement 3 at Interchange C is 310 ft. However, there was, again, no side friction with opposing left turns for this movement.

Start-up Lost Time

A mean start-up lost time was calculated for each lane group studied. A sample standard deviation for the mean start-up lost time was also calculated. Start-up lost time was calculated using Equation 3 with n equal to 3 and h equal to the mean headway values shown in Table 3 for the lane group of interest. Only those cycles with three or more vehicles in queue at the onset of green were used in the analysis. All cycles with an oversized vehicle in position 1, 2, or 3 in the queue were eliminated from the analysis. The results of this calculation are shown in Table 5.

The mean start-up lost times as calculated on a per-lane group basis generally fall between 1.5 and 2 sec per phase.

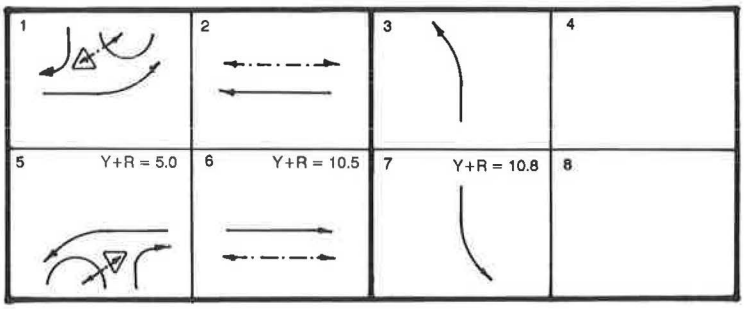

Interchange A

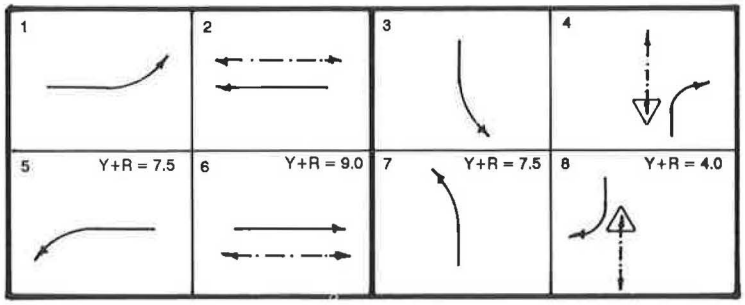

Interchange B

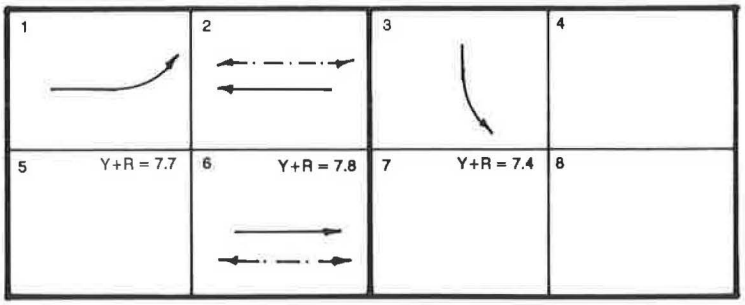

Interchange C

: INDICATES VEHICULAR MOVEMENT

: INDICATES PEDESTRIAN MOVEMENT

FIGURE 6 NEMA phasing.

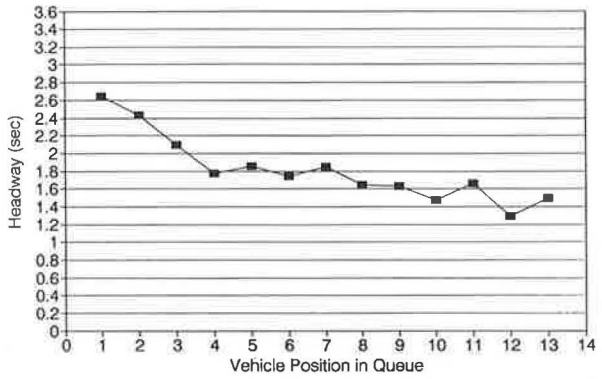

FIGURE 7 Mean headway versus vehicle position in queue.

TABLE 3 STUDY LANE GROUP WEIGHTED MEAN SATURATION HEADWAYS

Movement	Sample Size	Mean Headway (sec)	Sample Standard Deviation	95% Confidence Interval
Interchange A:				
2	229	1.81	0.68	1.72-1.90
6	216	1.79	0.76	1.69-1.89
10	169	1.78	0.76	1.66-1.89
13	298	1.73	0.45	1.68-1.78
6 & 13	514	1.75	0.60	1.70-1.81
Interchange B:				
2	505	1.76	0.50	1.72-1.80
10	76	1.96	0.81	1.78-2.14
13	74	1.76	0.44	1.66-1.86
Interchange C:				
3	354	1.62	0.48	1.57-1.67
6	255	1.66	0.44	1.60-1.71
9	226	1.94	0.55	1.87-2.01

TABLE 4 STUDY LANE GROUP WEIGHTED MEAN SATURATION FLOW RATE

Movement	Sample Size	Saturation Flow Rate (pcphgpl)	Range
Interchange A:			
2	229	1986	1894-2088
6	216	2009	1902-2129
10	169	2026	1904-2164
13	298	2085	2025-2148
6 & 13	514	2052	1994-2115
Interchange B:			
2	505	2044	1995-2096
10	76	1835	1679-2023
13	74	2047	1937-2171
Interchange C:			
3	354	2225	2159-2296
6	255	2172	2103-2246
9	226	1859	1793-1930

TABLE 5 STUDY LANE GROUP MEAN START-UP LOST TIME

Movement	Sample Size	Start-up Lost Time (sec)	Sample Standard Deviation	95% Confidence Interval
Interchange A:				
2	19	1.69	1.09	1.16-2.21
6	32	1.95	1.06	1.58-2.31
10	18	1.58	0.75	1.21-1.96
13	34	1.75	0.91	1.45-2.06
6 & 13	66	1.86	1.00	1.62-2.10
Interchange B:				
2	33	1.69	0.92	1.38-2.01
10	47	0.98	1.06	0.68-1.28
13	16	1.83	1.04	1.28-2.39
Interchange C:				
3	23	1.72	1.00	1.28-2.15
6	16	2.07	0.75	1.67-2.47
9	26	1.56	0.78	1.25-1.88

Two study lane groups were exceptions to this rule. Movement 10 at Interchange B recorded a mean start-up lost time of 0.98 sec. The mean saturation headway for this movement is 1.96 sec (Table 3), which is the largest saturation headway value recorded for the ten lane groups studied. Movement 6 at Interchange C recorded a mean start-up lost time of 2.07 sec. The mean saturation headway value recorded for this movement is 1.66 sec (Table 3), which is the second smallest mean saturation headway value recorded for the ten lane groups studied.

Clearance Lost Time

Clearance lost time was calculated as the difference between the clearance interval time ($Y + R$) and the green extension time. The green extension time was calculated as the elapsed time from the onset of the yellow indication to the time the last vehicle crossed the stop line. A mean green extension time was calculated for each lane group studied and then used to calculate the clearance lost time. A standard deviation for the clearance lost time was also calculated. Only those cycles that were saturated are included in the analysis. The results of the analysis are shown in Tables 6 and 7.

Large variations in clearance lost time may be observed for the various lane groups. This finding is largely a function of the length of the clearance interval ($Y + R$) provided for each movement. To evaluate the correlation between the clearance lost time and the length of the clearance interval, a plot was generated showing the amount of clearance lost time versus the length of the clearance interval. The plot, shown in Figure 8, indicates a near linear relationship between length of the clearance interval and the clearance lost time. Figure 8 indicates that a large portion of the clearance interval contributes to clearance lost time for long clearance intervals.

CONCLUSIONS AND RECOMMENDATIONS

The primary objectives of the research were to

1. Determine the saturation flow rates for the through and the left-turn movements at the SPDI, and
2. Determine the lost time per phase for the SPDI.

On the basis of the data collected it appears that 2,000 pcphgpl is a suitable base value for the saturation flow rate for both the through and the left-turn movements at the SPDI. The data do indicate that higher saturation flow rates may be in order for left-turn movements with radii greater than 300 ft. However, further study of the effects of side friction due to opposing movements should first be assessed.

Start-up lost time does not tend to vary a great deal by type of movement. Most movements recorded start-up lost times between 1.5 and 2 sec per phase. Start-up lost time is calculated as a function of the mean saturation headway. As saturation headways decrease, the start-up lost time tends to increase. Therefore, in those cases where higher saturation flow rates are used, higher start-up lost time values should also be applied.

The clearance lost time per phase is closely tied to the length of the clearance interval. If long clearance intervals are required then higher clearance lost time values should be applied. The clearance lost time is generally 2.5 to 3 sec less per phase than the clearance interval time for the phase.

The values for saturation flow rate and lost time reported in this study may be used to provide a more accurate evaluation of the SPDI operation. These values may be used as input parameters to determine the capacity of the SPDI and when using computer models to simulate the operation of the SPDI for the conditions studied.

These values are based on data that were collected at a limited number of approaches, all in the same geographi-

TABLE 6 STUDY LANE GROUP MEAN CLEARANCE LOST TIME

Movement	Sample Size	Clearance Lost Time (sec)	Sample Standard Deviation	95% Confidence Interval
Interchange A:				
2	5	8.19	0.54	7.52-8.86
6	4	7.94	1.57	5.45-10.44
10	9	2.61	0.70	2.07-3.15
13	5	7.69	1.02	6.42-8.96
6 & 13	9	7.80	1.21	6.87-8.73
Interchange B:				
2	12	6.31	0.55	5.97-6.66
10	0	---a	---a	--------a
13	0	---a	---a	--------a
Interchange C:				
3	21	5.33	0.89	4.93-5.73
6	16	4.37	0.63	3.73-5.00
9	1	4.74	---b	--------b

a :No data collected due to traffic conditions
b :Insufficient data collected due to traffic conditions

TABLE 7 CLEARANCE LOST TIME AS A PERCENT OF CLEARANCE INTERVAL TIME

Movement	Clearance Interval (sec)	Mean Clearance Lost Time (sec)	Difference (sec)	Percent
Interchange A:				
2	10.5	8.19	2.31	78%
6	10.8	7.94	2.86	74%
10	5.0	2.61	2.39	52%
13	10.8	7.69	3.11	71%
6 & 13	10.8	7.80	3.00	72%
Interchange B:				
2	9.0	6.31	2.69	70%
Interchange C:				
3	7.7	5.33	2.37	69%
6	7.4	4.37	3.03	59%
9	7.8	4.74	3.06	61%

cal location. They do not represent a comprehensive evaluation of all the factors affecting saturation flow rates or total lost time at the SPDI. A more comprehensive study is required to evaluate all the factors that may influence saturation flow rates and total lost time at the SPDI, for all possible conditions.

The values presented in this research are based on 3,500 recorded headways on a total of ten approaches. More data would provide much tighter confidence intervals for start-up and clearance lost times.

Interchange C was half operational at the time data were collected. Further study of this interchange should be performed when it becomes fully operational. Further studies of this interchange could be used in conjunction with the data collected in this study to measure the effects of opposing traffic on the left-turn movements at the SPDI.

New striping and signal design plans are being considered to reduce the clearance interval time at Interchange A. Further study of this interchange could add insight into the relationship between clearance lost time and the length of the clearance interval.

Finally, it should be noted that traffic engineering is not solely concerned with capacity analysis and signal operations. Many safety issues regarding the operation of the SPDI should

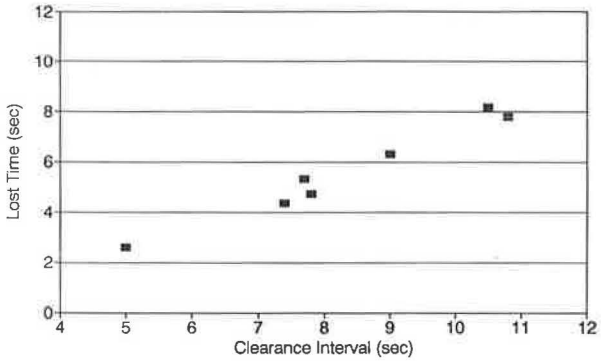

FIGURE 8 Clearance lost time versus clearance interval time.

be addressed. A number of vehicular and pedestrian traffic violations were observed during the course of data collection, most of which indicate road-user confusion. A comprehensive study of the potential safety problems associated with the operation of the SPDI should be conducted.

REFERENCES

1. S. J. Brown and G. Walters. The Single Signal Interchange. *Compendium of Technical Papers*, ITE, Washington D.C., 1988, pp. 180–184.
2. T. Darnell. Gridlock. *American City and Country*, Vol. 102, No. 8, Aug. 1987, pp. 20–28.
3. J. M. Witkowski. Benefit Analysis for Grade Separated Interchanges. *Journal of Transportation Engineering*, Vol. 114, No. 1, Jan. 1988, pp. 93–107.
4. J. P. Leisch, T. Urbanik, and J. P. Oxley. A Comparison of Two Interchange Forms in Urban Areas. *ITE Journal*, Vol. 59, No. 5, May 1989, pp. 21–26.
5. J. H. Warner. *Traffic Engineering Study of the Urban Interchange*. Arizona Department of Transportation, Traffic Engineering Section, Phoenix, Ariz., Aug. 1988, pp. 17–18.
6. *Special Report 209: Highway Capacity Manual*. TRB, National Research Council, Washington, D.C., 1988.
7. R. R. Johnsen and J. S. Matthias. Investigation to Determine the Capacity of Protected Left-turn Movements. In *Transportation Research Record 453*, TRB, National Research Council, Washington D.C., 1973, pp. 49–55.
8. D. G. Capelle and C. Pinnell. Capacity Study of Signalized Diamond Interchanges. *Highway Research Board Bulletin 291*, HRB, National Research Council, Washington D.C., 1961, pp. 1–25.
9. K. R. Agent and J. D. Crabtree. *Analysis of Lost Time at Signalized Intersections*. Report UKTRP-83-3. Kentucky Transportation Research Program, University of Kentucky, Lexington, 1983.
10. D. S. Berry. Discussion of King and Wilkinson. In *Transportation Research Record 615*, TRB, National Research Council, Washington D.C., 1976, pp. 42–43.
11. K. R. Agent and J. D. Crabtree. *Analysis of Saturation Flow at Signalized Intersections*. Report UKTRP-82-2. Kentucky Transportation Research Program, University of Kentucky, Lexington, 1982.
12. D. B. Fambro, N. A. Chaudhary, C. J. Messer, and R. U. Garza. *A Report on the User's Manual for the Microcomputer Version of PASSER III-88*. Texas Transportation Institute, Texas A&M University, College Station, 1988, p. 18.

Publication of this paper sponsored by Committee on Operational Effects of Geometrics.